

**Transition-Metal Complexes Catalyzed Hydrogen  
Atom Transfer: Kinetic Study and Applications to  
Radical Cyclizations**

**Gang Li**

Submitted in partial fulfillment of the requirements for  
the degree of Doctor of Philosophy  
in the Graduate School of Arts and Sciences

**COLUMBIA UNIVERSITY**

**2015**

© 2015

Gang Li

All Rights Reserved



## ABSTRACT

### **Transition-Metal Complexes Catalyzed Hydrogen Atom Transfer: Kinetic Study and Applications to Radical Cyclizations**

Gang Li

Radical cyclizations have been proven to be extremely important in organic synthesis. However, their reliance on toxic trialkyltin hydrides has precluded their practical applications in pharmaceutical manufacturing. Many tin hydride substitutes have been suggested but none of them are adequate alternates to the traditional tin reagent.

Transition-metal hydrides have been shown to catalyze the hydrogenation and hydroformylation of unsaturated carbon-carbon bonds. These reactions begin with a Hydrogen Atom Transfer (HAT) from a metal to an olefin, generating a carbon-centered radical. The cyclization of that radical is an effective route to five- and six-membered rings. The HAT will be fastest if the M–H bond is weak. However, making the reaction catalytic will require that the hydride can be regenerated with H<sub>2</sub>. HCr(CO)<sub>3</sub>Cp has proven to be a good catalyst for such cyclizations, but it suffers from air sensitivity. The yield of the cyclization product depends on how the rate of radical cyclization compares with the rates of side reactions (hydrogenation and isomerization), so special substituents on a substrate are best installed to increase the cyclization rate.

In attempting to improve the efficiency of radical cyclization I have studied the effect of substituents on the target double bond on the rate of cyclization. A single phenyl

substituent has proven to stabilize a radical better than two phenyls. This stabilization leads to faster cyclizations and a higher cyclization yield.

I also have found that  $\text{Co}(\text{dmgBF}_2)\text{L}_2$  ( $\text{L} = \text{THF}, \text{H}_2\text{O}, \text{MeOH}\dots$ ) under  $\text{H}_2$  is an effective  $\text{H}\bullet$  donor. I have monitored by NMR the catalysis by the system of the hydrogenation of stable radicals (trityl radical and TEMPO radical) and found the rate-determining step to be the activation of hydrogen gas by  $\text{Co}^{\text{II}}$ . The reactive form of the complex is five-coordinated cobalt complex  $\text{Co}(\text{dmgBF}_2)_2\text{L}$ .

The  $\text{Co}/\text{H}_2$  system can also transfer  $\text{H}\bullet$  to  $\text{C}=\text{C}$  bonds, thus initiate radical cyclizations. The resting state of the cobalt is the  $\text{Co}^{\text{II}}$  metalloradical, so a *cycloisomerization* is obtained. Such a reaction neither loses nor adds any atom and has 100% atom economy.

# TABLE OF CONTENTS

List of Schemes .....	iv
List of Tables .....	vi
List of Figures .....	vii
Acknowledgements .....	ix
<b>Chapter 1: Introduction to Radical Cyclization in Organic Synthesis</b> .....	<b>1</b>
1.1 Radical Cyclization in Organic Chemistry .....	1
1.2 Mechanism of Radical Cyclization .....	2
1.2.1 Generation of Radicals .....	2
1.2.2 5-exo vs 6-endo .....	3
1.3 Disadvantages of Radical Cyclization Reactions Using Tin Hydrides .....	4
1.4 Application of Transition Metal Hydrides in Radical Chemistry .....	5
1.4.1 Hydrogen Atom Transfer (HAT) from Transition Metal Hydrides to Unsaturated bonds .....	6
1.4.2 Hydrogen Atom Transfer (HAT) from Transition Metal Hydrides to Organic Radicals .....	11
1.4.3 Application of Hydrogen Atom Transfer (HAT) from Transition Metal Hydrides in Radical Cyclization .....	13
1.5 References .....	21
<b>Chapter 2: Chromium-Catalyzed Radical Cyclizations: Effect of Double-Bond Substituents</b> .....	<b>27</b>
2.1 Strategies for Increasing the Yield of Cr-Catalyzed Radical Cyclization .....	27

<b>2.2 Synthesis and Radical Cyclization of Diene Substrates with <math>\text{HCr}(\text{CO})_3\text{Cp}</math></b>	28
<b>2.2.1 Synthesis of Diene Substrates</b>	28
<b>2.2.1 Radical Cyclization of Diene Substrates with Stoichiometric <math>\text{HCr}(\text{CO})_3\text{Cp}</math></b>	28
<b>2.3 Why Does the Monophenyl Radical Cyclize More Rapidly than the <math>\text{Ph}_2</math> and <math>\text{Ph}(\text{Me})</math> Radicals?</b>	32
<b>2.4 Experimental Details</b>	37
<b>2.5 References</b>	44
<b>Chapter 3: Kinetics of Cobaloxime-Catalyzed Hydrogen Atom Transfer</b>	47
<b>3.1 Cobaloximes under <math>\text{H}_2</math> as New Hydrogen Atom Source for Hydrogen Atom Transfer (HAT)</b>	47
<b>3.2 Kinetic Study of Hydrogen Atom Transfer (HAT) from Cobaloximes under <math>\text{H}_2</math> to Organic Radicals</b>	49
<b>3.3 Axial Ligand Effect on Hydrogen Atom Transfer (HAT) from Cobaloximes under <math>\text{H}_2</math> to Organic Radicals</b>	53
<b>3.3.1 Structures of cobaloximes</b>	54
<b>3.3.2 Kinetics of HAT from Cobaloximes under <math>\text{H}_2</math> to Trityl Radical</b>	56
<b>3.4 Mechanism of Dihydrogen Activation by Cobaloxime</b>	62
<b>3.5 Revisit to the Initially Reported Cobaloxime Hydride</b>	66
<b>3.6 Experiment Details</b>	69
<b>3.7 References</b>	72

## **Chapter 4: Cobalt-Catalyzed Radical Reactions Initiated by Hydrogen Atom**

<b>Transfer</b> .....	79
<b>4.1</b> Cobaloxime-Catalyzed Radical Cyclizations .....	79
<b>4.2</b> Cyclization vs Cycloisomerization .....	81
<b>4.3</b> Substrate Scope for Radical Cycloisomerization .....	83
<b>4.3.1</b> Cycloisomerization via 5-exo Cyclization .....	83
<b>4.3.2</b> Attempts at 6-endo and 7-endo .....	86
<b>4.4</b> Cobaloxime-Catalyzed Isomerizations of Olefins .....	86
<b>4.5</b> Experiment Details .....	86
<b>4.5.1</b> Synthesis of Diene Substrates .....	88
<b>4.5.2</b> Cobaloxime-Catalyzed Radical Cyclizations and Cycloisomerizations of Diene Substrates .....	101
<b>4.6</b> References .....	106
<b>Appendix I: Relevant Spectral Data for Chapter 2</b> .....	109
<b>Appendix II: Crystallographic Data and Kinetic Profiles for Chapter 3</b> .....	119
<b>Appendix III: Relevant Spectral Data for Chapter 4</b> .....	148

## List of Schemes

1.1. Natural Product Synthesized via Radical Cyclization .....	1
1.2. General Mechanism for Radical Chain Cyclizations .....	3
1.3. Orbital Interaction in Radical Cyclization .....	4
1.4. Hydrogenation of Anthracene under Syngas Catalyzed by $\text{Co}_2(\text{CO})_8$ .....	6
1.5. Hydroformylation of Styrene Catalyzed by $\text{HCo}(\text{CO})_4$ .....	7
1.6. Radical Cyclization Mediated by Schwartz Reagent .....	14
1.7. Mechanism for Epoxide Opening Catalyzed by Wilkinson's Catalyst .....	15
1.8. Radical Cyclization of <b>1.22</b> by $\text{HCr}(\text{CO})_3\text{Cp}$ .....	17
1.9. Conformers of the $\alpha$ -Alkoxy Radical from HAT .....	19
1.10. Reaction Pathways for <b>1.29</b> and $\text{M-H}$ ( $\text{M} = \text{Cr}(\text{CO})_3\text{Cp}$ or $\text{V}(\text{CO})_4\text{dppe}$ ) .....	20
2.1. Structures of Cyclized Radicals .....	33
2.2. Definition of "Twist Angle" for One of the Phenyl Rings in Benzophenone .....	33
2.3. Twisting between Two Phenyl Substituents on a Radical Center .....	34
2.4. Two views of the transition state for cyclization by radicals <b>2.15</b> and <b>2.18</b> .....	35
3.1. Mechanism of Cobaloxime-Mediated Formation of <b>3.5</b> from <b>1.13</b> .....	52
3.2. Revised Mechanism of Cobaloxime-Mediated Formation of <b>3.5</b> .....	58
3.3. Homolytic Pathway of Dihydrogen Activation by $\bullet\text{Cr}(\text{CO})_3\text{Cp}$ .....	64
3.4. Heterolytic Pathway of Dihydrogen Activation by $\bullet\text{Cr}(\text{CO})_3\text{Cp}$ .....	65
3.5. Heterolytic Pathway of Dihydrogen Activation by $\text{Co}(\text{dmgBF}_2)_2\text{L}_2$ .....	65
3.6. Structure of Paramagnetic Cobalt Trimer .....	69
4.1. How Byproducts Are Formed During Cyclization Reactions .....	80
4.2. Mechanism for the Formation of <b>4.7</b> and <b>2.30</b> from <b>2.9</b> .....	82

<b>4.3. Steric Effect in Cyclized Radical for H• Abstracting</b> .....	82
<b>4.4. Comparison of Cr and Co Catalysts for Cyclization of 4.9</b> .....	83
<b>4.5. Synthesis of 4.9</b> .....	88
<b>4.6. Synthesis of 4.12</b> .....	91
<b>4.7. Synthesis of 4.14</b> .....	92
<b>4.8. Synthesis of 4.16</b> .....	96
<b>4.9. Synthesis of 4.18</b> .....	97
<b>4.10. Synthesis of 4.20</b> .....	98

## List of Tables

<b>1.1</b> Rate Constant for $k_H$ for HAT from $\text{HCr(CO)}_3\text{Cp}$ to Various Olefins at 323 K	9
<b>1.2.</b> Relationship between Bond Dissociation Energy of M–H Bond and Rates of HAT to Styrene at 285 K	10
<b>1.3.</b> Relationship between Bond Dissociation Energy of M–H Bond and Rates of HAT to tris( <i>p</i> - <i>tert</i> -butylphenyl)methyl radical at 298 K	12
<b>2.1.</b> NMR Yields of the Products from Treatment of Diene Substrates with Stoichiometric $\text{HCr(CO)}_3\text{Cp}$	29
<b>2.2.</b> Calculated Average Rate Constant (Gaussian 03, B3LYP, and 6-311++G**) for Cyclization of $\alpha$ -Carbomethoxy Radical at 298K	30
<b>2.3.</b> Isolated Yields of Cyclization Products from Treatment of Diene Substrates with Catalytic Amounts of $\text{HCr(CO)}_3\text{Cp}$ under $\text{H}_2$	31
<b>3.1.</b> Selected bond lengths of $\text{Co(dmgBF}_2)_2\text{L}_2$	55
<b>3.2.</b> Equilibrium Constant $K$ and Rate Constants $k$ and $k_{11}$ with Different Axial Ligands and M-L bond distances	59
<b>3.3.</b> Activation Parameters from Earlier Kinetics Studies of the Reactions of Metalloradicals with $\text{H}_2$	63
<b>4.1.</b> Scope of Cycloisomerizations	85



## List of Figures

<b>3.1</b> Structures of Cobaloxime Hydrides .....	48
<b>3.2.</b> Cobaloxime-Mediated Formation of <b>3.5</b> from <b>1.13</b> under 2.4 atm H <sub>2</sub> in C <sub>6</sub> D <sub>6</sub> at 295 K (eq 3.4). ([ <b>3.1</b> ] = 7.60 × 10 <sup>-4</sup> M, [ <b>1.13</b> ] <sub>0</sub> = 1.02 × 10 <sup>-2</sup> M) .....	50
<b>3.3.</b> Plot of d[ <b>3.5</b> ]/dt vs [ <b>1.13</b> ] <sub>0</sub> : Rate of HAT with different [ <b>1.13</b> ] <sub>0</sub> under the same reaction conditions ([ <b>3.1</b> ] = 7.60 × 10 <sup>-4</sup> mol·L <sup>-1</sup> ; H <sub>2</sub> : 3.0 atm; C <sub>6</sub> D <sub>6</sub> ) .....	50
<b>3.4.</b> Rate d[ <b>3.5</b> ]/dt of eq 3.4 vs [H <sub>2</sub> ] at 295 K in C <sub>6</sub> D <sub>6</sub> .....	51
<b>3.5.</b> Rate d[ <b>3.5</b> ]/dt of eq 3.4 vs [ <b>3.1</b> ] at 295 K in C <sub>6</sub> D <sub>6</sub> .....	51
<b>3.6.</b> Rate d[ <b>3.6</b> ]/dt of eq 3.8 vs [ <b>3.1</b> ] at 295 K in C <sub>6</sub> D <sub>6</sub> .....	53
<b>3.7.</b> Molecular structure of Co(dmgbF <sub>2</sub> ) <sub>2</sub> (CH <sub>3</sub> CN) <sub>2</sub> ( <b>3.9</b> , 50% ellipsoids, hydrogen atoms omitted for clarity) .....	54
<b>3.8.</b> Molecular structure of Co(dmgbF <sub>2</sub> ) <sub>2</sub> (THF) <sub>2</sub> ( <b>3.10</b> , 50% ellipsoids, hydrogen atoms omitted for clarity) .....	55
<b>3.9.</b> Co(dmgbF <sub>2</sub> ) <sub>2</sub> (THF) <sub>2</sub> -Mediated Formation of <b>3.5</b> under 2.4 atm H <sub>2</sub> in C <sub>6</sub> D <sub>6</sub> at 295 K (eq 3.9) ([ <b>3.10</b> ] = 3.80 × 10 <sup>-4</sup> M and [ <b>1.13</b> ] <sub>0</sub> = 1.02 × 10 <sup>-2</sup> M) .....	56
<b>3.10.</b> Rate d[ <b>3.5</b> ]/dt of eq 3.9 vs [H <sub>2</sub> ] at 295 K in C <sub>6</sub> D <sub>6</sub> .....	57
<b>3.11.</b> Rate d[ <b>3.5</b> ]/dt of eq 3.9 vs [Co <sub>Tot</sub> ] at 295 K in C <sub>6</sub> D <sub>6</sub> .....	57
<b>3.12.</b> Rate d[ <b>3.5</b> ]/dt of eq 3.9 vs [THF] at 295 K in C <sub>6</sub> D <sub>6</sub> .....	58
<b>3.13.</b> UV-Vis study of Co + PPh <sub>3</sub> system in CH <sub>2</sub> Cl <sub>2</sub> .....	60
<b>3.14.</b> Job Plot of Co + PPh <sub>3</sub> system in CH <sub>2</sub> Cl <sub>2</sub> .....	60
<b>3.15.</b> <b>3.1</b> /PPh <sub>3</sub> -Mediated Formation of <b>3.5</b> under 3 atm H <sub>2</sub> in C <sub>6</sub> D <sub>6</sub> at 323 K (eq 3.13) ([ <b>3.1</b> ] = 7.60 × 10 <sup>-4</sup> M, [ <b>1.13</b> ] <sub>0</sub> = 1.02 × 10 <sup>-2</sup> M and [PPh <sub>3</sub> ] = 5.73 × 10 <sup>-3</sup> M) .....	61

**3.16.** Rate  $d[\mathbf{3.5}]/dt$  of eq 3.13 vs  $[\text{PPh}_3]$  under 3 atm of  $\text{H}_2$  in  $\text{C}_6\text{D}_6$  at 323 K (The initial concentration of **3.1** and of **3.10** is  $3.80 \times 10^{-4}$  M,  $[\mathbf{1.13}]_0 = 1.02 \times 10^{-2}$  M) .....61

## Acknowledgements

First, I would like to give my greatest thank to my advisor Professor Jack Norton for taking me as graduate student five years ago and for being so supportive in my Ph.D study. With his sincerity, patience and immense knowledge, Jack has guided my growth as a chemist. I couldn't have hoped for a better boss for my Ph.D. Jack has given me the biggest freedom to chase my own interest and work on my own pace. I also appreciate the countless opportunities Jack has given me to expose myself in the chemistry community, which helps me make up my mind to join the research club. Besides chemistry, I would also thank Jack for giving me the chance to become his lunch partner. I really enjoyed our conversation on politics, history and so on over the lunch. Not many people in the world have such a chance to have lunch with a world-leading scientist almost every day!

I am also very grateful for my graduate committee members Professor Colin Nuckolls and Professor Tristan Lambert who were kindness enough to read my second year report, original research proposal and this thesis. I appreciate the support and guidance provided by them over the five years.

Many thanks to Professor John Sowa and Professor Andreas Zavitsas for spending the time to sit on my defense committee and read my thesis. I would like to show special thanks to Professor John Sowa. We have been friends for 8 years and John tried very hard to persuade me to join Columbia five years ago. I really appreciate him for helping me make the smartest decision I've ever made so far.

I am deeply grateful for all the Norton group alumni and current members I have the fortune to work with: Dr. John Hartung, Dr. Jason Polisar, Dr. Deven Estes, Dr. Yue Hu, Dr. Shuo Liu, Jim Yang, Michael Eberhart, Travis Valadez, Jonathan Kuo and Arthur Han, who have made my lab life wonderful. Especially I would like to thank the “Team Radical” Dr. John Hartung, Dr. Deven Estes, Jonathan Kuo and Arthur Han. John and Deven spent quite some time to train me when I first joined the lab. Jonathan (whom I always call Jonny) is a brilliant labmate who always comes up with cool ideas for our projects. I really enjoy our discussions on both chemistry and not. As an undergraduate, Arthur worked with me for 3 years and we’ve co-authored many papers. Part of his work is also included in this thesis. I’m very grateful for his help.

Thanks to Professor Ged Parkin and the Parkin group members who have helped with my chemistry and with the crystallography, especially Dr. Wes Sattler, Dr. Aaron Sattler and Serge Ruccolo.

I also thank my fellow classmates whom I joined at Columbia with for their continuous friendship. Special thanks to Dr. Stephen Ho, Dr. Qishui (Tracy) Chen and Dr. Lu Wei, they know why.

Professor Aiwen Lei (Wuhan University) and Professor Qiang Liu (Tsinghua University) were my mentors when I was undergraduate at Wuhan University in China. I thank them for bringing me into the wonderland of chemistry and for their continuous support even after I graduated from Wuhan University.

Last but not least, I would like to thank my mother Zongkui Zhang, and my father Shihua Li, without whom I can’t finish the thesis. They have supported me spiritually throughout my Ph.D study, and my life in general.

*For mom and dad*

*“Felix qui potuit rerum cognoscere causas”*

*Publius Vergilius Maro*

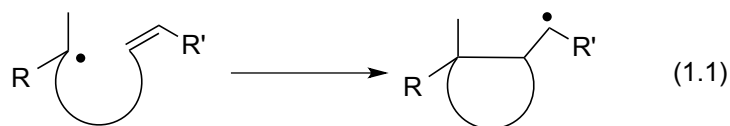
*“Georgicon”*

*ll. 490*

# **CHAPTER 1: INTRODUCTION TO RADICAL CYCLIZATION IN ORGANIC SYNTHESIS**

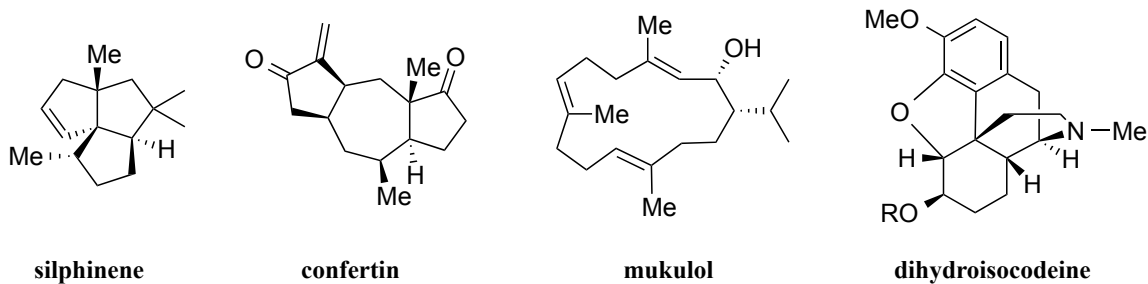
## **1.1 Radical Cyclization in Organic Chemistry**

Since Moses Gomberg reported the first free radical “triphenylmethyl” in 1900,<sup>1</sup> radical chemistry has been on the cutting edge of chemical research and has advanced tremendously. Especially since 1970s, radical chemistry has been proven to be extremely important in synthetic organic chemistry.<sup>2</sup> Among all radical-based reactions that have been reported so far, radical cyclization (eq 1.1) is arguably the most important one since it provides a convenient way to generate a cyclic structure.



Radical cyclization generally occurs under mild conditions, and doesn't require the use of protecting groups.<sup>3</sup> It has very good functional group tolerance as well as good regio- and stereoselectivity.<sup>4</sup> Hence this method has been widely applied in laboratory for the synthesis of natural products.<sup>5</sup> Scheme 1.1 shows four natural products that have been made using radical cyclization.<sup>6-9</sup>

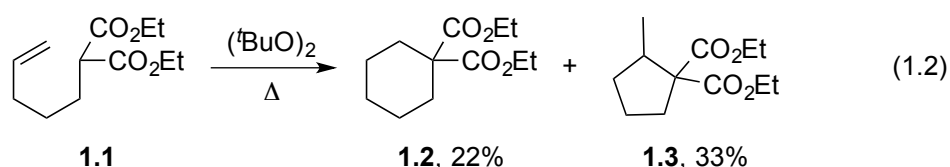
**Scheme 1.1.** Natural Products Synthesized via Radical Cyclization



## 1.2 Mechanism of Radical Cyclization

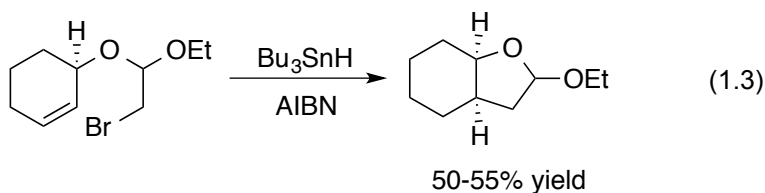
### 1.2.1 Generation of Radicals

As noted in eq 1.1, the key in a radical cyclization is the cyclization of the initial radical onto an unsaturated bond to generate a cyclized radical intermediate. To generate the starting radical and initiate the reaction, atom abstraction is the most commonly used method. One of the early examples of radical cyclization used atom abstraction as the initiation step before intramolecular malonate addition of the radical (eq 1.2).



In this reaction, the *tert*-butoxyl radical generated from homolytic cleavage of the O–O bond of (*t*BuO)<sub>2</sub> abstracts the H• from the malonate CH of **1.1** due to the weakness of the C–H bond strength. The resulting radical cyclizes into the unsaturated C=C bond to give a mixture of 6-*endo* and 5-*exo* cyclized radical intermediates, which give 6-*endo* and 5-*exo* cyclization products (**1.2** and **1.3**, respectively) with a combined yield of 55%. However, cyclizations like eq 1.2 require substrates with weak C–H bonds, which limits the substrate scope and synthetic applications.

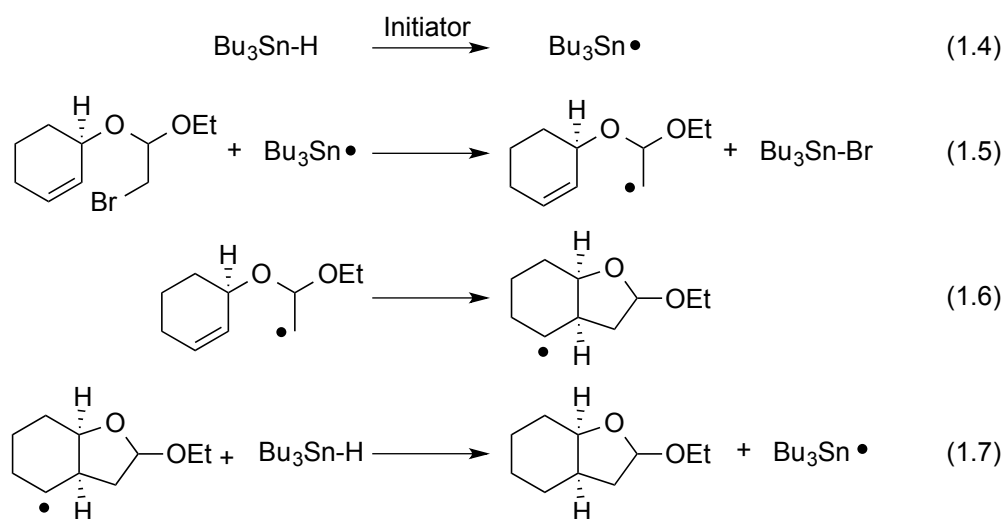
Heavy atom abstraction is another commonly used strategy for generating radicals. In this method, tributyltin hydride is widely used. A typical example is Stork's synthesis of bicyclic acetals and lactones from bromoacetals (eq 1.3).<sup>10</sup>





A detailed mechanism is shown in Scheme 1.2. In the presence of a radical initiator (usually benzoyl peroxide or azobisisobutyronitrile, AIBN), the Sn–H bond (BDE = 78 kcal/mol)<sup>11</sup> can be easily cleaved to generate a tin radical (eq 1.4). This tin radical then abstracts a heavy atom (usually Br, I, S, Se, or, in this case, eq 1.5, Br) to yield an alkyl radical, which will further cyclize to form the cyclic structure (eq 1.6). Another equivalent of tributyltin hydride will transfer H• to the cyclized radical, giving the product and regenerating the tin radical to continue the chain reaction (eq 1.4).

**Scheme 1.2.** General Mechanism for Radical Chain Cyclizations



The overall reaction is driven by the formation of a relatively strong Sn–X bond (85 kcal/mol when X = Br)<sup>12</sup> and C–H bond. The large driving force enables the formation of nearly any desired radical if the substrate contains a heavy atom. For this reason, tributyltin hydride has been extensively used.

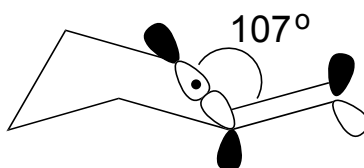
### 1.2.2 5-*exo* vs 6-*endo*

From eq 1.2, although both products are observed, it is clear that the cyclization of 5-hexenyl radicals favors 5-*exo* (33%) over 6-*endo* (22%). The result implies that radical

cyclization is not under thermodynamic control because the *6-endo* product (secondary radical) is more thermodynamically stable than the *5-exo* product (primary radical). In fact, Ingold and Beckwith have reported that at 25 °C, the rate of *5-exo* cyclization ( $2.3 \times 10^5 \text{ s}^{-1}$ )<sup>13-15</sup> is around 60 times faster than that of *6-endo* cyclization ( $4.1 \times 10^3 \text{ s}^{-1}$ )<sup>15, 16</sup> for the 5-hexenyl radical itself.

It has been shown by Beckwith<sup>15, 16</sup> and Houk<sup>17</sup> that the angle of approach of the radical to the C=C bond must be around 107° (similar to the Burgi-Dunitz angle<sup>18</sup> that is required for nucleophilic attack on a carbonyl) to make the SOMO of radical overlap better with the C=C  $\pi^*$  orbital. This strain resulting from this requirement favors a *5-exo* transition state over a *6-endo* mode (Scheme 1.3).

**Scheme 1.3.** Orbital Interaction in Radical Cyclization



### 1.3 Disadvantages of Radical Cyclization Reactions Using Tin Hydrides

As described above, the use of alkyltin hydrides has made radical cyclization an invaluable synthetic method in the laboratory. However, the reliance on alkyltin hydrides has prevented radical cyclizations from being used on an industrial scale.<sup>3, 19</sup> Organotin compounds are well-known for their acute toxicity toward the skin, nervous system and liver.<sup>20</sup> The use of alkyltin hydrides is low in atom economy. In a typical reaction, 2 equivalents of alkyltin hydride will be consumed and 2 equivalents of a tin halide will be produced as waste.<sup>21, 22</sup> Removal of the tin compounds requires special procedures;

standard purification techniques often leaves levels of tin in the product that are still toxic.

Because of the above-mentioned drawbacks, researchers have spent a considerably amount of funds and time searching for tin replacements. There are reports of radical cyclization reactions that are mediated by other main group hydrides, such as Si,<sup>23</sup> Ga,<sup>24</sup> Ge,<sup>25</sup> and In.<sup>26</sup> However, none of them has proven to be as good as a tin hydride in synthetic applications, mainly due to this stronger M–H bonds than Sn–H.<sup>27–29</sup> Efforts have also been made to make Sn–H reactions catalytic in tin by adding reducing reagents.<sup>30</sup> However, these methods still suffer from limitations of substrate scope. More recently, new separation techniques have been invented to make the removal of residual tin easier.<sup>31, 32</sup> But they still fail to decrease the amount of residual tin to a safe level. In fact, to the best of our knowledge, none of those above-described methods are adequate alternates to tin reagents.

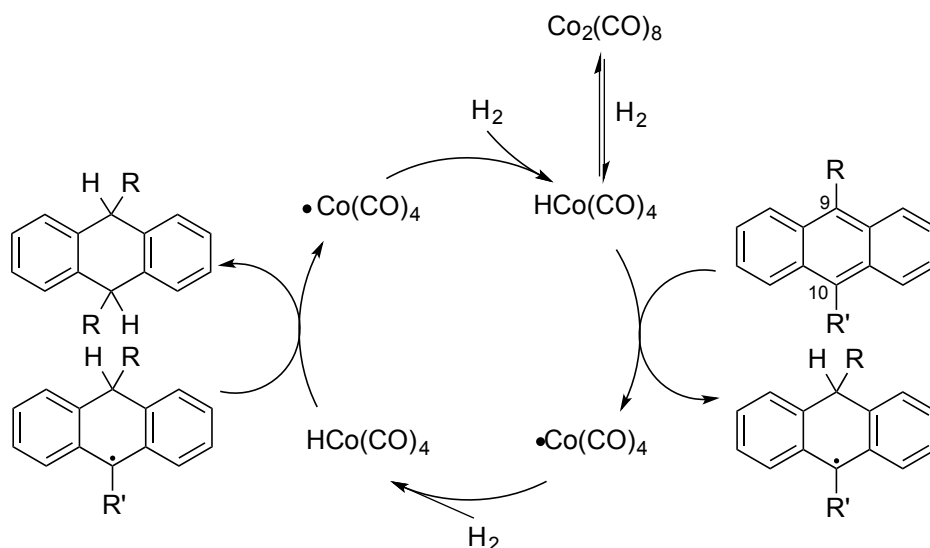
#### **1.4 Application of Transition Metal Hydrides in Radical Chemistry**

Recently, transition metal hydrides have attracted the attention of radical chemists. Hydrides such as HCo(CO)<sub>4</sub> and HMn(CO)<sub>5</sub> (*vide infra*), are known to transfer H• to organic substrates. In many cases it is also possible to regenerate the M–H by activating H<sub>2</sub>, which completes a catalytic cycle. These hydrides thus have the potential to produce a tin-free radical cyclization.

### 1.4.1 Hydrogen Atom Transfer (HAT) from Transition Metal Hydrides to Unsaturated Bonds

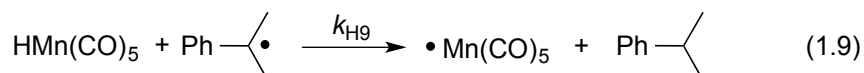
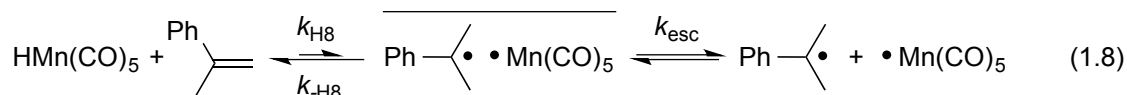
In 1975, Feder and Halpern studied the hydrogenation of anthracene under CO/H<sub>2</sub> (syngas) catalyzed by Co<sub>2</sub>(CO)<sub>8</sub> and concluded that the reaction probably proceeds through a radical mechanism rather than the originally proposed *syn* Co-H addition (Scheme 1.4).<sup>33</sup> The radical mechanism accounts for the following observations: 1) When anthracene is treated with DCo(CO)<sub>4</sub>, H/D exchange is faster than hydrogenation (an addition mechanism won't lead to H/D exchange); 2) 9,10-Substituted anthracenes are hydrogenated more readily, which can be attributed to the generation of a more stabilized radical.

**Scheme 1.4.** Hydrogenation of Anthracene under Syngas Catalyzed by Co<sub>2</sub>(CO)<sub>8</sub>

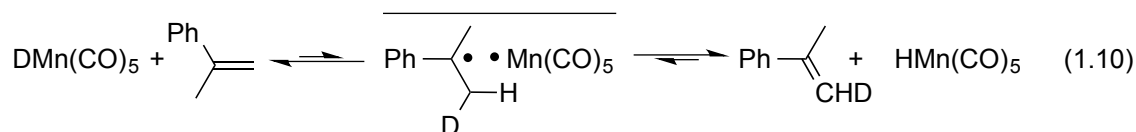


Sweany and Halpern reported in 1977 the hydrogenation of  $\alpha$ -methylstyrene by HMn(CO)<sub>5</sub>. Kinetic studies showed *first-order* dependence on both olefin and hydride but *zero order* dependence on CO. They proposed a reversible HAT process from Mn–H to olefin (eq 1.8) followed by a fast HAT from Mn–H to the radical (eq 1.9).<sup>34</sup> The

mechanism is supported by the observation of Chemically Induced Dynamic Nuclear Polarization (CIDNP) when the reaction was monitored in a magnetic field, which indicates a caged radical pair must be formed and the rate of escaping from the cage ( $k_{\text{esc}}$  in eq 1.8) competes with the rate of recombination ( $k_{\text{H8}}$  in eq 1.8).

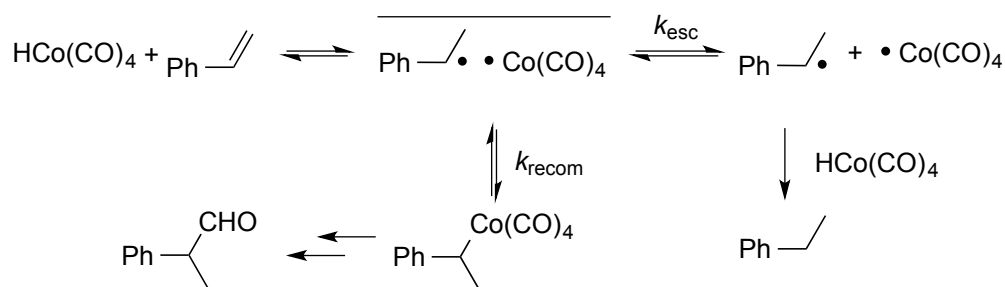


The mechanism was further supported by the observation of isotope exchange. When  $\text{DMn(CO)}_5$  was treated with  $\alpha$ -methylstyrene, deuterium incorporation was observed in the vinyl position (eq 1.10). Such observation can be rationalized by the reversibility of the HAT process in the first step.

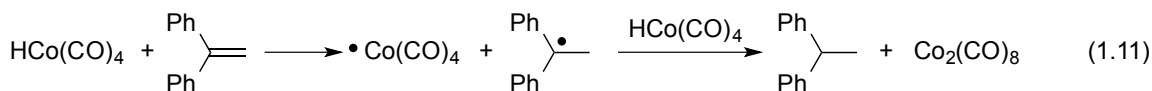


Solvent viscosity also affects the reaction. Ungvary found that during hydrogenation of styrene by  $\text{HCo(CO)}_4$ , changing the solvent from octane to Nujol shifted the major product from hydrogenation to hydroformylation (Scheme 1.5).<sup>35, 36</sup> This is consistent with a radical pair mechanism.

**Scheme 1.5.** Hydroformylation of Styrene Catalyzed by  $\text{HCo(CO)}_4$

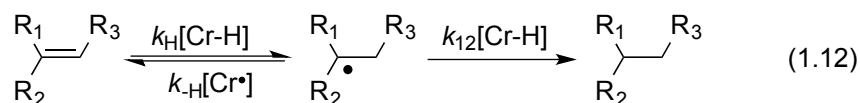


Roth reported that CO pressure *did not* affect the hydrogenation of 1,1-diphenylethylene by  $\text{HCo}(\text{CO})_4$  (eq 1.11).<sup>37</sup> The hydrogenation did not require that the substrate displace a coordinated CO on cobalt, which implied that the HAT process was an “outer-sphere” transfer.



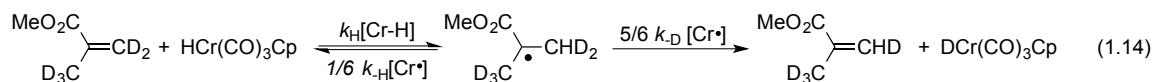
More hydrogenation cases of HAT from transition-metal hydrides to unsaturated substrates were reported later, all proposed to occur via a HAT process.<sup>38-50</sup>

The Norton group has previously studied the kinetics of HAT from  $\text{HCr}(\text{CO})_3\text{Cp}$  to various olefins (eq 2.1).<sup>51, 52</sup> They have used two different methods to obtain the rate constant ( $k_{\text{H}}$ ) for HAT to olefins. If only hydrogenation occurs ( $k_{\text{H}} \ll k_{12}$  in eq 1.12), then  $k_{\text{H}}$  can be determined by eq 1.13 from the *pseudo-first-order* rate constant  $k_{\text{obs}}$ .



$$k_{\text{obs}} = 2k_{\text{H}}[\text{olefin}] \quad (1.13)$$

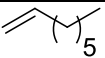
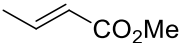
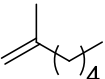
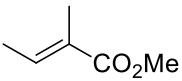
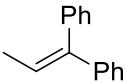
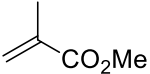
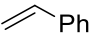
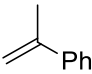
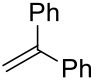
If only H/D exchange is observed ( $k_{\text{H}} \gg k_{12}$  in eq 1.12, as is the case for methyl methacrylate, MMA), then  $k_{\text{H}}$  can be measured by the exchange of  $\text{CpCr}(\text{CO})_3\text{H}$  with excess deuterated olefin (eq 1.14 and 1.15, S is a statistical correction for the reabstraction of H versus D).



$$k_{\text{H}} = S k_{\text{obs}}, \text{ where } S = \frac{\frac{5}{6} k_{\text{D}}[\text{Cr}^\bullet]}{\frac{1}{6} k_{\text{H}}[\text{Cr}^\bullet] + \frac{5}{6} k_{\text{D}}[\text{Cr}^\bullet]} = \frac{5}{5 + \frac{k_{\text{H}}}{k_{\text{D}}}} \text{ for MMA} \quad (1.15)$$

The measured rate constants are listed in Table 1.1. Apparently, olefins with phenyl substituents on the incipient radical center generally accept H• more readily ( $R_1$  or  $R_2 = \text{Ph}$  in eq 1.12). Moreover,  $k_H$  can be further increased if a methyl or a second phenyl substituent is installed on the same carbon, presumably because the resulting radical is a more stable tertiary radical (**1.9** and **1.10**). Steric inhibition also affects  $k_H$ . If there is a methyl substituent on the other carbon,  $k_H$  is suppressed significantly (compare **1.8** to **1.10**).

**Table 1.1** Rate Constant for  $k_H$  for HAT from  $\text{HCr}(\text{CO})_3\text{Cp}$  to Various Olefins at 323 K

Compound	Structure	$k_H (\times 10^{-3}) (\text{M}^{-1}\text{s}^{-1})$	Relative Rate
<b>1.4</b>		$\leq 1.1 \times 10^{-4}$	1
<b>1.5</b>		$\leq 3.2 \times 10^{-4}$	3
<b>1.6</b>		$\leq 3.2 \times 10^{-3}$	29
<b>1.7</b>		$(0.8 \text{ to } 1.6) \times 10^{-2}$	73 to 146
<b>1.8</b>		0.59(2)	5400
<b>MMA</b>		14(3)	$1.3 \times 10^5$
<b>Styrene</b>		15.8(6)	$1.4 \times 10^5$
<b>1.9</b>		79(3)	$7.2 \times 10^5$
<b>1.10</b>		460(60)	$4.2 \times 10^6$

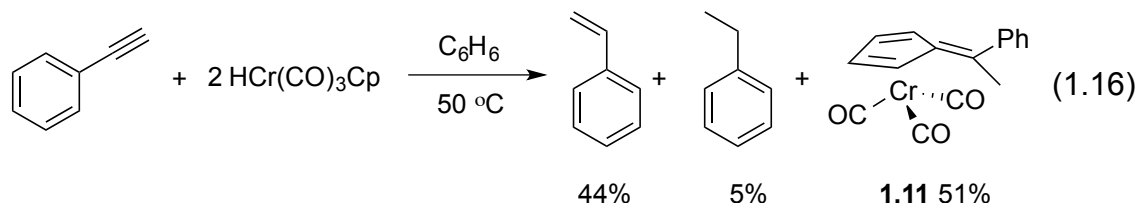
The Norton Group has also studied HAT from transition-metal hydrides with much weaker M–H bonds, namely  $\text{HV}(\text{CO})_4(\text{P-P})$  (where  $\text{P-P} = \text{PPh}_2(\text{CH}_2)_n\text{PPh}_2$ ,  $n = 1-4$ ), to styrene, and has compared these  $k_H$  with those obtained from  $\text{HCr}(\text{CO})_3\text{Cp}$  (Table 1.2).<sup>53</sup>

It's clear that, due to their weaker M–H bonds, vanadium hydrides undergo HAT to styrene much faster than does  $\text{HCr(CO)}_3\text{Cp}$ . On the other hand, the rate of HAT doesn't increase as much as one would expect from large change in the bond strength. One possible explanation is the steric effect of the bulky chelating phosphine ligand. The bulkier the phosphine chelate is (as indicated by the number of methylene groups in the backbone of the chelate), the slower  $k_{\text{H}}$  becomes, even though the V–H bonds become weaker. The steric effect of the chelating ligand appears to overwhelm the effect of the weaker M–H bond.

**Table 1.2.** Relationship between Bond Dissociation Energy of M–H Bond and Rates of HAT to Styrene at 285 K

Hydrides	BDE (kcal/mol)	$k_{\text{H}} (\times 10^{-3}) (\text{M}^{-1}\text{s}^{-1})$
$\text{HV(CO)}_4\text{dppm}$	57.9	$\geq 17.0$
$\text{HV(CO)}_4\text{dppe}$	57.5	$\geq 9.0$
$\text{HV(CO)}_4\text{dppp}$	56.0	7.0
$\text{HV(CO)}_4\text{dppb}$	54.9	5.7
$\text{HCr(CO)}_3\text{Cp}$	62.2	0.85

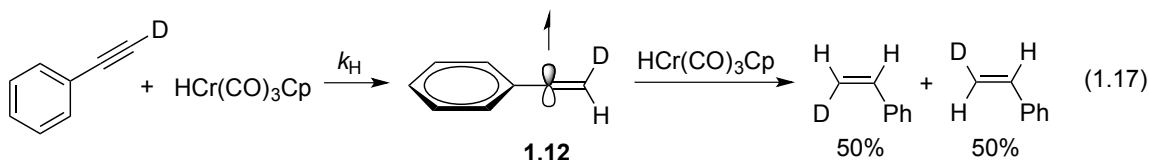
Very recently the Norton group has also reported HAT from  $\text{HCr(CO)}_3\text{Cp}$  to alkyne.<sup>54</sup> When the electron-rich alkyne phenylacetylene was treated with  $\text{HCr(CO)}_3\text{Cp}$ , styrene, ethylbenzene and a Cr-complex **1.11** were observed (eq 1.16).



The formation of **1.11** raises the issue of whether the mechanism is HAT or not. In order to clarify the mechanism, the Norton group treated phenylacetylene- $d_1$  with  $\text{HCr(CO)}_3\text{Cp}$  and observed a 1:1 ratio of *cis*- and *trans*-styrene- $d_1$ . This observation is a



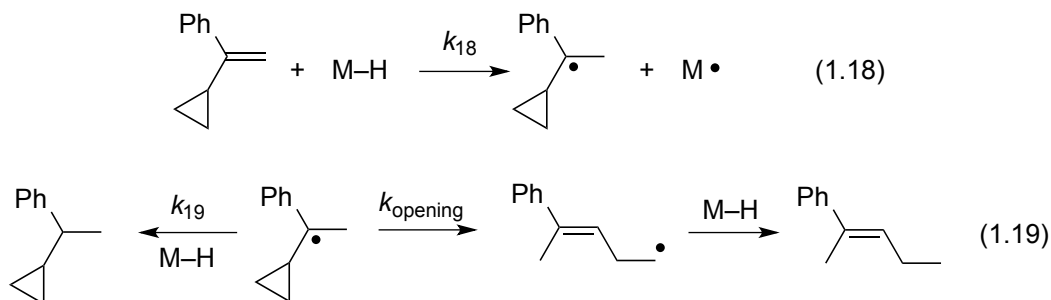
solid evidence for the linear vinyl radical intermediate **1.12** that would result from HAT (eq 1.17).



#### 1.4.2 Hydrogen Atom Transfer (HAT) from Transition Metal Hydrides to Organic Radicals

As mentioned in the previous section, in hydrogenation reactions that proceed through HAT, the rate-determining step is the initial HAT, which transfers  $H^\bullet$  from transition-metal hydrides to unsaturated bonds. Therefore, less is known of the second HAT step involving transferring  $H^\bullet$  to organic radicals, such as reaction 1.9.

Bullock has studied the hydrogenation of  $\alpha$ -cyclopropylstyrene by several transition metal hydrides (eq 1.18 and 1.19).<sup>49</sup> They determined the rate constant  $k_{18}$  for the  $H^\bullet$  transfer in eq 1.18 from the overall rate of hydrogenation, and used the rearrangement of the cyclopropylbenzyl radicals as a clock to determine the rate of HAT to the cyclopropylbenzyl radical,  $k_{19}$ , in eq 1.19.



Bullock's method provides an indirect way to measure the rate constant for HAT to organic radicals. If one would like to directly measure that rate constant, a stable radical

substrate must be employed. Gomberg's triphenylmethyl radical was the first reported stable radical. Unfortunately, it undergoes head-to-tail dimerization. Therefore, the tris(*p*-*tert*-butylphenyl)methyl radical (**1.13** in eq 1.20) is interesting to consider since the head-to-tail dimerization is prevented by its *p*-*tert*-butyl substituents. Thus, it is always monomeric in solution and a better radical to study.<sup>55</sup>

The Norton Group has studied rates of HAT from various transition-metal hydrides to **1.13** (eq 1.20).<sup>56-58</sup> Some representative results are listed in Table 1.3.

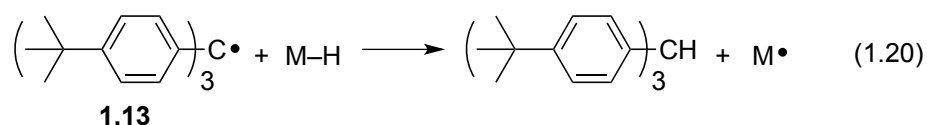


**Table 1.3.** Relationship between Bond Dissociation Energy of M–H Bond and Rates of HAT to tris(*p*-*tert*-butylphenyl)methyl radical at 298 K

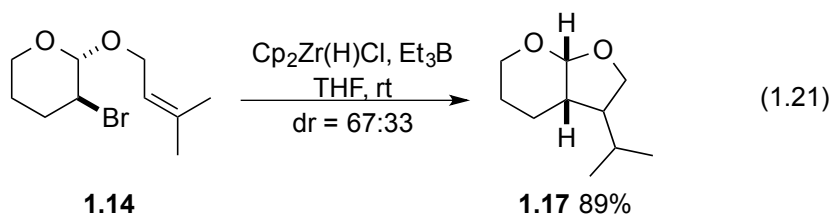
Hydrides	BDE (kcal/mol)	$k_{\text{H}}$ (M <sup>-1</sup> s <sup>-1</sup> )
HFe(CO) <sub>2</sub> Cp	58	$1.2(4) \times 10^4$
HCr(CO) <sub>3</sub> Cp	62	335(2)
HRu(CO) <sub>2</sub> Cp	65	$1.03(3) \times 10^3$
HCo(CO) <sub>4</sub>	67	$1.6(9) \times 10^3$
HMn(CO) <sub>5</sub>	68	741(8)
HMo(CO) <sub>3</sub> Cp	69	514(2)
HMo(CO) <sub>3</sub> Cp*	70	13.9(5)
HWCO) <sub>3</sub> Cp	73	91(1)
H <sub>2</sub> Os(CO) <sub>4</sub>	78	15.7(7)

From the results, it is clear that the rates of HAT generally decrease as the M–H bonds get stronger. However, steric factors can also be important. The Mo–H bond of HMo(CO)<sub>3</sub>Cp is only 1 kcal/mol weaker than that of HMo(CO)<sub>3</sub>Cp\*, but HAT from HMo(CO)<sub>3</sub>Cp\* is almost 40 times slower than HAT from HMo(CO)<sub>3</sub>Cp.

### 1.4.3 Application of Hydrogen Atom Transfer (HAT) from Transition Metal Hydrides in Radical Cyclization

As discussed in section 1.2.1, after initiation, a tin radical will be generated. The tin radical will abstract a heavy atom from the substrate to generate an organic radical. This is one of the key roles of a tin reagent in radical reactions. New methods have been reported to replace tin radical for this purpose, including the famous  $\text{Et}_3\text{B}/\text{O}_2$  system<sup>59</sup> and the  $\text{Cp}_2\text{TiCl}$  system (generated *in situ* by reducing  $\text{Cp}_2\text{TiCl}_2$ ).<sup>60, 61</sup> Although these new methods do replace tin at generating organic radicals, they are unable to finish a radical reaction by transferring  $\text{H}\bullet$  to the product organic radical (see eq 1.7). From the discussion in last section, HAT from transition-metal hydrides to organic radicals has been well established. So transition-metal hydrides are promising termination reagents for radical cyclizations and have the potential to be regenerated by  $\text{H}_2$ .

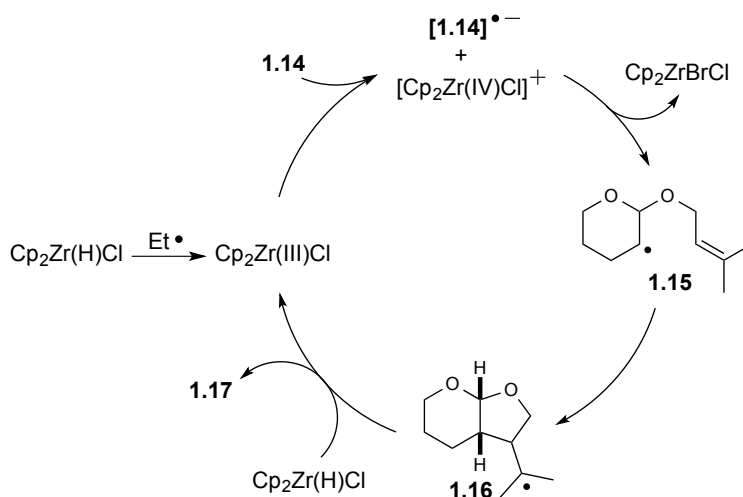
Oshima reported in 2001 the first example of transition-metal hydride catalyzed radical cyclization using the Schwartz reagent  $\text{Cp}_2\text{Zr(H)Cl}$  (eq 1.21).<sup>62</sup>



The proposed mechanism is different from that of tin-hydride mediated radical reaction (Scheme 1.6). In the presence of  $\text{Et}_3\text{B}$ ,  $\text{Cp}_2\text{Zr(H)Cl}$  transfers  $\text{H}\bullet$  to an ethyl radical to generate  $\text{Cp}_2\text{ZrCl}$ , which will transfer a single electron to the bromide **1.14** to give the radical anion of **1.14** and  $[\text{Cp}_2\text{Zr(IV)Cl}]^+$ . Then  $\text{Cp}_2\text{ZrClBr}$  is liberated along with radical **1.15**, which cyclizes to give radical **1.16**. Another equivalent of  $\text{Cp}_2\text{Zr(H)Cl}$

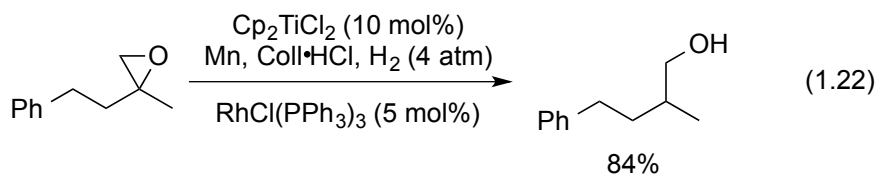
will convert the radical **1.16** into the product **1.17**, while  $\text{Cp}_2\text{ZrCl}$  is regenerated to continue the reaction.

**Scheme 1.6.** Radical Cyclization Mediated by Schwartz Reagent



It's clear that there is room for improvement in this reaction since the Schwartz reagent is used stoichiometrically. Therefore, modifying this reaction so it can be performed under catalytic conditions is a worthwhile endeavor.

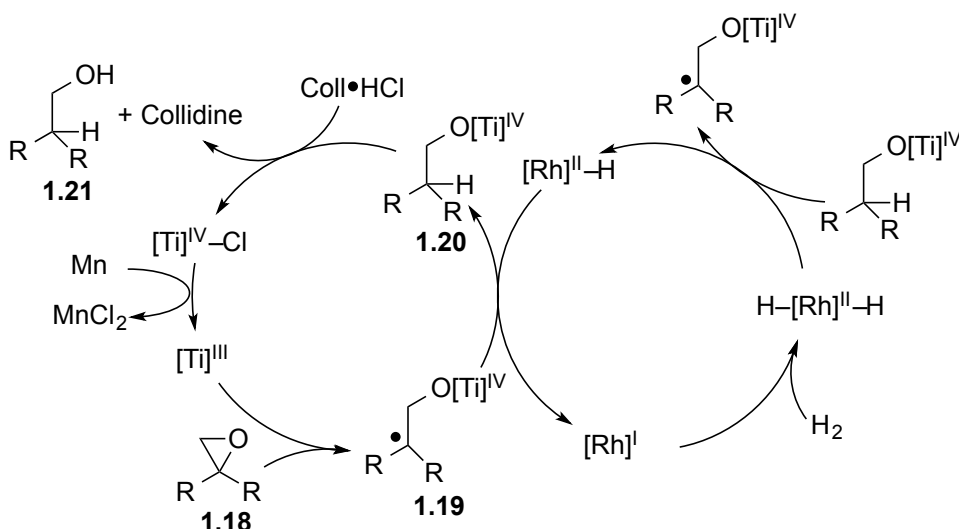
Gansäuer recently used  $\text{RhCl}(\text{PPh}_3)_3$  (Wilkinson's catalyst) with  $\text{Cp}_2\text{TiCl}_2/\text{Mn}$  to achieve a catalytic reduction of certain epoxides under  $\text{H}_2$  (eq 1.22,  $\text{Coll}\cdot\text{HCl}$  = 2,4,6-collidine hydrochloride).<sup>63</sup>



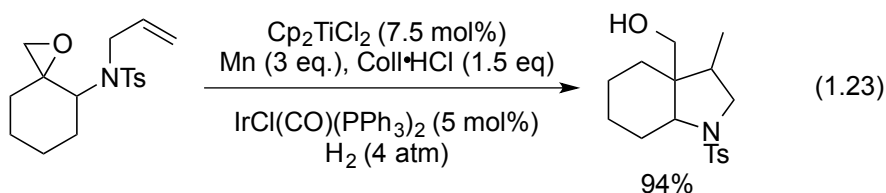
The reaction is initiated by a single electron transfer (SET) from  $\text{Cp}_2\text{TiCl}$  to **1.18** to generate the radical **1.19**. That intermediate is then terminated by HAT from a rhodium hydride species to give **1.20**; the  $[\text{Ti}]^{\text{IV}}\text{-O}$  is cleaved by the weak acid collidine

hydrochloride to yield the desired product **1.21**. The Rh–H bond can be regenerated under H<sub>2</sub> from Wilkinson’s catalyst, making the overall reaction catalytic (Scheme 1.7)

**Scheme 1.7.** Mechanism for Epoxide Opening Catalyzed by Wilkinson’s Catalyst



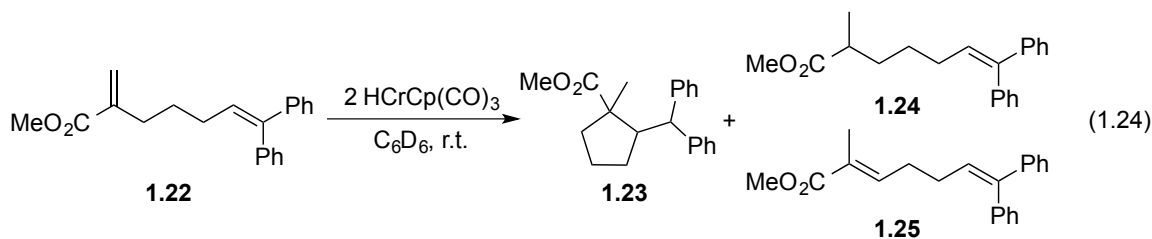
The same group later reported that IrCl(CO)[P(C<sub>6</sub>H<sub>5</sub>)<sub>3</sub>]<sub>2</sub> (Vaska’s Complex) allowed cyclization of the radical intermediate onto an unsaturated carbon-carbon bond and thus achieved a catalytic radical cyclization under same mechanism (eq 1.23).<sup>64</sup>



Although the above reaction works nicely, it still involves three metals (one very expensive, Ir) and stoichiometric amount of a weak acid. It would be ideal if a radical cyclization could be both initiated (HAT to unsaturated bonds) and terminated (HAT to organic radicals) by transition-metal hydrides under catalytic condition.

The Norton group has long been interested in developing a new method for radical cyclization. From measured rates of HAT to olefins (see Table 1.1), the Norton group

developed a radical cyclization method using  $\text{HCr}(\text{CO})_3\text{Cp}$ .<sup>65</sup> A typical substrate can be considered as a combination of **1.8** and methyl methacrylate (MMA) (**1.22** in eq 1.24).

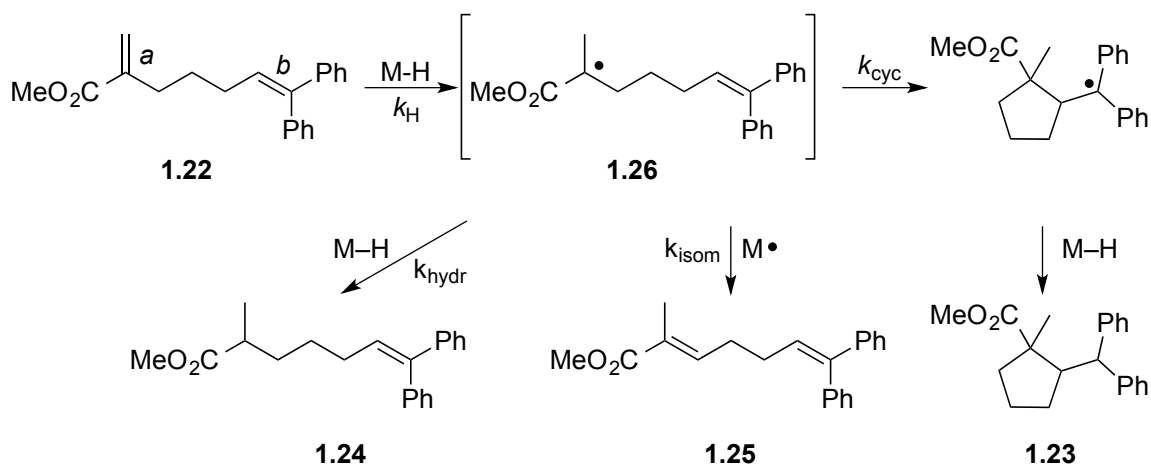


When **1.22** was treated with two equivalents of  $\text{HCr}(\text{CO})_3\text{Cp}$ , a 5-*exo* cyclization product **1.23** was observed with a yield of 34%. A hydrogenated byproduct and an isomerized byproduct were also observed in yields of 11% and 6%, respectively. The reaction left 49% unreacted diene substrate.

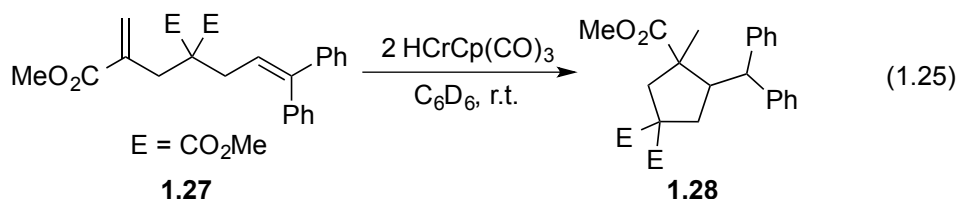
The incomplete reaction (eq 1.24) occurs because the rate-determining step is the HAT from the transition-metal hydride to olefin. So, this suggests that a transition-metal hydride with a weaker M–H bond will increase the yield of cyclization product by increasing the conversion of substrate. This is shown to be true. When **1.22** is treated with two equivalents of  $\text{HV}(\text{CO})_4\text{dppe}$  (BDE (V–H) = 57.5 kcal/mol, in comparison, BDE (Cr–H) = 62.2 kcal/mol in  $\text{HCr}(\text{CO})_3\text{Cp}$ , see Table 1.2.), the cyclized product is obtained with a yield of 77%.<sup>53</sup>

The above observations suggest a mechanism which is shown in Scheme 1.8. The acrylate double bond (double bond *a* in **1.22**) is the kinetic site for HAT on the basis of the  $k_{\text{H}}$  measurements in Table 1.1. The radical (**1.26**) generated from HAT can react in three ways: cyclization, hydrogenation and isomerization. The ratio of the three products will depend on the rate constants for cyclization ( $k_{\text{cyc}}$ ), isomerization ( $k_{\text{iso}}[\text{Cr}\cdot]$ ) and hydrogenation ( $k_{\text{hyd}}[\text{Cr–H}]$ ).

**Scheme 1.8.** Radical Cyclization of **1.22** by  $\text{HCr}(\text{CO})_3\text{Cp}$



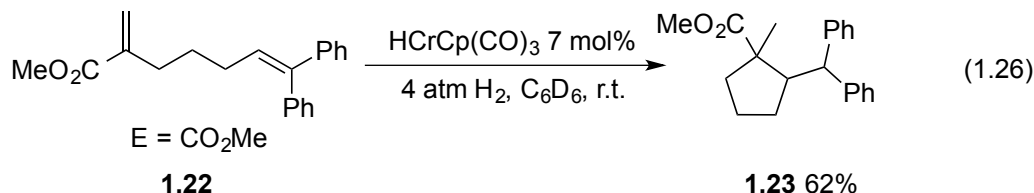
Increasing the cyclization yield requires increasing the cyclization rate. One possibility is the well-known Thorpe-Ingold effect. Adding two substituents to the same carbon in the backbone of **1.22** increases the rate of any cyclization reaction.<sup>66, 67</sup> The new diene substrate **1.27**, when treated with 2 equivalents of  $\text{HCr}(\text{CO})_3\text{Cp}$ , gives a cyclized product **1.28** in 65% yield, which is almost twice as much as that of **1.22** (eq 1.25).<sup>65</sup>



The other way to achieve higher cyclization yields is to decrease the rates of hydrogenation and isomerization. Hydrogenation occurs by HAT from  $\text{M-H}$  to the organic radical. As discussed in section 1.4.2, this process is controlled by steric factors as well as the strength of the  $\text{M-H}$  bond. It is possible to decrease  $k_{\text{hydr}}$  by an appropriate choice of transition-metal hydride.

Decreasing the rate of isomerization is more complicated, since  $k_{\text{iso}}$  has not been extensively studied. However, the formation of the isomerization product can be regulated by the concentration of  $\text{M}^\bullet$ . The formation of the hydrogenated product is regulated by the concentration of  $\text{M-H}$ . So both side reactions can be controlled by controlling the concentration of the two forms of  $\text{M-H}$ .

These cyclization reactions can be carried out catalytically if the hydride can be regenerated from the metalloradical. Fischer reported many years ago that  $\text{HCr(CO)}_3\text{Cp}$  could be regenerated from  $\bullet\text{Cr(CO)}_3\text{Cp}$  by reaction with  $\text{H}_2$ .<sup>68</sup> The cyclization of **1.22** proved possible with a catalytic amount of  $\text{HCr(CO)}_3\text{Cp}$  under  $\text{H}_2$  (eq 1.26). Indeed, a much improved cyclization yield was obtained.<sup>65</sup>

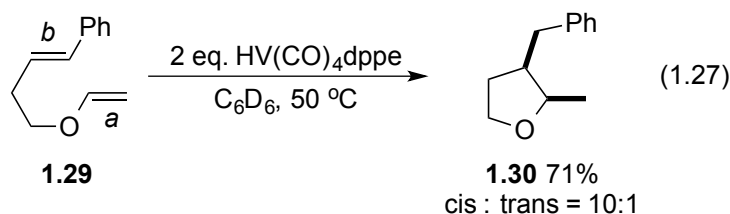


Attempts to cyclize **1.22** with various vanadium hydrides under catalytic conditions were unsuccessful even with higher temperature and  $\text{H}_2$  pressure.<sup>53</sup> A vanadium hydride cannot be regenerated from  $\text{V}^\bullet$  with  $\text{H}_2$ . There are two possible reasons for this difficulty. One is that the  $\text{V-H}$  bond is too weak to activate  $\text{H}_2$  because of the lack of driving force (the BDE of the  $\text{H-H}$  bond is 104 kcal/mol, while the BDEs of vanadium hydride complexes are 54-57 kcal/mol). The other is the steric congestion around  $\text{V}^\bullet$ , which may make it hard for  $\text{H}_2$  to approach the vanadium center.

Vanadium hydrides are good  $\text{H}^\bullet$  donors in the generation of oxygen-substituted radicals. The study of HAT from  $\text{HCr(CO)}_3\text{Cp}$  to various olefins shows that the enol ether double bonds are ideal  $\text{H}^\bullet$  acceptors since the radical generated will be stabilized by

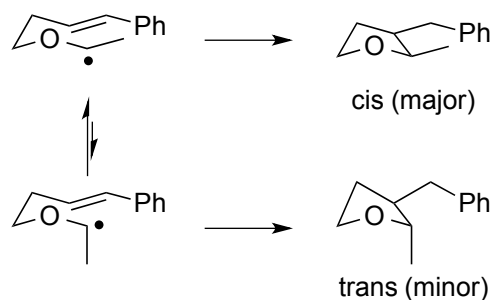


the oxygen substituents via conjugative delocalization of the radical and the non-bonding electron pairs of the adjacent heteroatom<sup>69</sup> and they are sterically unhindered. The Norton group showed in early 2015 the cyclization of enol ether dienes by vanadium hydrides occurs quite efficiently (eq 1.27).<sup>70</sup>



The reaction gives high diastereoselectivity, presumably due to the 1,3-diaxial interactions in the transition state (Scheme 1.9); the *cis* conformer is preferred to the *trans*. An oxygen in the backbone enhances the 1,3-diaxial interaction by shortening the bond lengths (a C–O bond is generally shorter than a C–C bond by about 0.15 Å).

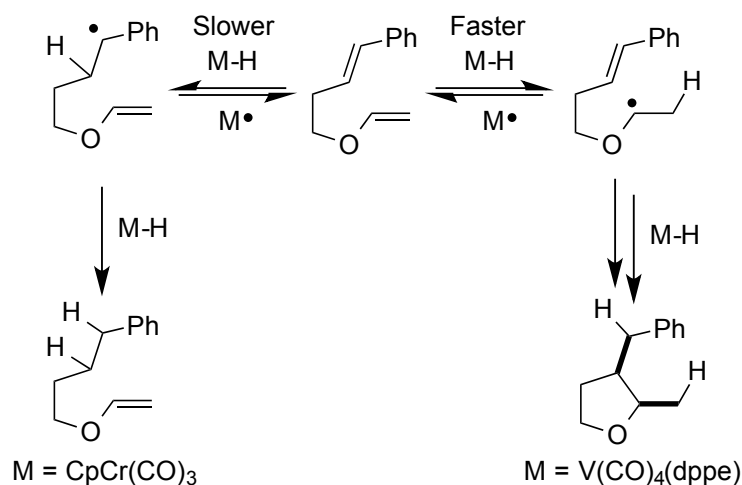
**Scheme 1.9.** Conformers of the  $\alpha$ -Alkoxy Radical from HAT



It is noteworthy that the cyclization of enol ethers only works with vanadium hydrides. Use of  $\text{HCr(CO)}_3\text{Cp}$  results only in hydrogenation of the *b* double bond. This is surprising as the *a* double bond should be the kinetic site. An experiment with  $\text{DCr(CO)}_3\text{Cp}$  shows that fast H/D exchange does occur on the *a* double bond, which implies that HAT to double bond *a* is slower than the reverse reaction and no cyclization occurs. HAT to double bond *b* is slower but more thermodynamically favored because a

more stable radical is formed, such that the double bond becomes hydrogenated. The use of a vanadium hydride, with its weaker M–H bond, makes HAT to an enol ether faster than the reverse reaction and results in cyclization (Scheme 1.10).

**Scheme 1.10.** Reaction Pathways for **1.29** and M–H (M = Cr(CO)<sub>3</sub>Cp or V(CO)<sub>4</sub>dppe)



From the above discussion, four conclusions can be drawn as to how to achieve a high yield of cyclized product in a reaction catalyzed by a transition-metal hydride: 1) the hydride catalyst must have a reasonable M–H bond strength (a BDE between 58 to 62 kcal/mol is best) to permit the regeneration of M–H from M• under H<sub>2</sub>, and allow HAT to the substrate olefin to occur at an appreciable rate; 2) the radical generated from the HAT must cyclize rapidly (high rate of cyclization  $k_{\text{cyc}}$ ); 3) the rate of hydrogenation ( $k_{\text{hydr}}$ ) by M–H must be slow to avoid the hydrogenation side reaction; 4) the rate of isomerization ( $k_{\text{isom}}$ ) by M• must be slow to avoid the isomerization side reaction. These rules will guide both new catalyst design and substrate synthesis during the remainder of this thesis.

## 1.5 References

1. Gomberg, M., An Instance of Trivalent Carbon: Triphenylmethyl. *J. Am. Chem. Soc.* **1900**, *22*, 757-771.
2. Renaud, P.; Sibi, M. P., *Radicals in Organic Synthesis*, 1st ed.; Wiley-VCH Verlag GmbH: Weinheim, Germany, 2001.
3. Baguley, P. A.; Walton, J. C., Flight from the Tyranny of Tin: The Quest for Practical Radical Sources Free from Metal Encumbrances. *Angew. Chem. Int. Ed.* **1998**, *37*, 3073-3082.
4. Curran, D. P.; Porter, N. A.; Giese, B., *Stereochemistry of Radical Reactions: Concepts, Guidelines, and Synthetic Applications*. VCH Publisher: New York, 1996.
5. Curran, D. P., Radical Cyclization and Sequential Radical Reactions. In *Comprehensive Organic Synthesis*, Trost, B. M.; Fleming, I.; Semmelhack, M. F., Eds. Pergamon Press: Oxford, 1991; Vol. 4, pp 779-831.
6. Rao, Y. K.; Nagarajan, M., Formal Total Synthesis of (±)-Silphinene via Radical Cyclization. *J. Org. Chem.* **1989**, *54*, 5678-5683.
7. Ohtsuka, M.; Takekawa, Y.; Shishido, K., Novel and General Entry into Pseudoguaianolides. Formal and Enantioselective Synthesis of (+)-Confertin. *Tetrahedron Lett.* **1998**, *39*, 5803-5806.
8. Cox, N. J. G.; Pattenden, G.; Mills, S. D., Radical Macrocyclizations in Synthesis. A New Approach to Mukulol and Marine Cembranolide Lactones. *Tetrahedron Lett.* **1989**, *30*, 621-624.
9. Parker, K. A.; Fokas, D., Convergent Synthesis of (±)-Dihydroisocodeine in 11 Steps by the Tandem Radical Cyclization Strategy. A Formal Total Synthesis of (±)-Morphine. *J. Am. Chem. Soc.* **1992**, *114*, 9688-9689.
10. Stork, G.; Sher, P. M.; Chen, H. L., Radical Cyclization-Trapping in the Synthesis of Natural Products. A Simple, Stereocontrolled Route to Prostaglandin F<sub>2</sub>α. *J. Am. Chem. Soc.* **1986**, *108*, 6384-6385.
11. Laarhoven, L. J. J.; Mulder, P.; Wayner, D. D. M., Determination of Bond Dissociation Enthalpies in Solution by Photoacoustic Calorimetry. *Acc. Chem. Res.* **1999**, *32*, 342-349.
12. Davies, J. V.; Skinner, H. A.; Pope, A. E., Thermochemistry of Metallic Alkyls. Part 10—Heats of Combustion of Some Tetra-Alkyls of Tin. *Trans. Faraday Soc.* **1963**, *59*, 2233-2242.

13. Chatgililoglu, C.; Ingold, K. U.; Scaiano, J. C., Rate Constants and Arrhenius Parameters for the Reactions of Primary, Secondary, and Tertiary Alkyl Radicals with Tri-*n*-butyltin Hydride. *J. Am. Chem. Soc.* **1981**, *103*, 7739-7742.
14. Beckwith, A. L. J.; Easton, C. J.; Lawrence, T.; Serelis, A. K., Reactions of Methyl-Substituted Hex-5-Enyl and Pent-4-Enyl Radicals. *Aust. J. Chem.* **1983**, *36*, 545-556.
15. Beckwith, A. L. J.; Schiesser, C. H., Regio- and Stereo-Selectivity of Alkenyl Radical Ring Closure: A Theoretical Study. *Tetrahedron* **1985**, *41*, 3925-3941.
16. Beckwith, A. L. J.; Schiesser, C. H., A Force-Field Study of Alkenyl Radical Ring Closure. *Tetrahedron Lett.* **1985**, *26*, 373-376.
17. Spellmeyer, D. C.; Houk, K. N., A Force-Field Model for Intramolecular Radical Additions. *J. Org. Chem.* **1987**, *52*, 959-974.
18. Burgi, H. B.; Dunitz, J. D.; Lehn, J. M.; Wipff, G., Stereochemistry of Reaction Paths at Carbonyl Centers. *Tetrahedron* **1974**, *30*, 1563-1572.
19. Parsons, A., A Race Against Tin. *Chem. Br.* **2002**, *38*, 42-44.
20. Magos, L., Tin. In *Handbook on the Toxicology of Metals*, 2 ed.; Friberg, L.; Nordberg, G. F.; Vouk, V., Eds. Elsevier: New York, 1986; pp 568-593.
21. Trost, B. M., The Atom Economy - A Search for Synthetic Efficiency. *Science* **1991**, *254*, 1471-1477.
22. Trost, B. M., Atom Economy - A Challenge for Organic-Synthesis: Homogeneous Catalysis Leads the Way. *Angew. Chem., Int. Ed. Engl.* **1995**, *34*, 259-281.
23. Chatgililoglu, C., Organosilanes as Radical-Based Reducing Agents in Synthesis. *Acc. Chem. Res.* **1992**, *25*, 188-194.
24. Mikami, S.; Fujita, K.; Nakamura, T.; Yorimitsu, H.; Shinokubo, H.; Matsubara, S.; Oshima, K., Triethylborane-Induced Radical Reactions with Gallium Hydride Reagent HGaCl<sub>2</sub>. *Org. Lett.* **2001**, *3*, 1853-1855.
25. Bowman, W. R.; Krintel, S. L.; Schilling, M. B., Tributylgermanium Hydride as a Replacement for Tributyltin Hydride in Radical Reactions. *Org. Biomol. Chem.* **2004**, *2*, 585-592.
26. Inoue, K.; Sawada, A.; Shibata, I.; Baba, A., Indium(III) Chloride-Sodium Borohydride System: A Convenient Radical Reagent for an Alternative to Tributyltin Hydride System. *J. Am. Chem. Soc.* **2002**, *124*, 906-907.

27. Studer, A.; Amrein, S., Tin hydride Substitutes in Reductive Radical Chain Reactions. *Synthesis-Stuttgart* **2002**, 835-849.
28. Corey, E. J.; Suggs, J. W., Method for Catalytic Dehalogenations via Trialkyltin Hydrides. *J. Org. Chem.* **1975**, *40*, 2554-2555.
29. Stork, G.; Sher, P. M., A Catalytic Tin System for Trapping of Radicals from Cyclization Reactions. Regio- and Stereocontrolled Formation of Two Adjacent Chiral Centers. *J. Am. Chem. Soc.* **1986**, *108*, 303-304.
30. Kuivila, H. G.; Menapace, L. W., Reduction of Alkyl Halides by Organotin Hydrides. *J. Org. Chem.* **1963**, *28*, 2165-2167.
31. Curran, D. P.; Hadida, S.; Kim, S. Y.; Luo, Z. Y., Fluorous Tin Hydrides: A New Family of Reagents for Use and Reuse in Radical Reactions. *J. Am. Chem. Soc.* **1999**, *121*, 6607-6615.
32. Curran, D. P.; Yang, F. L.; Cheong, J. H., Relative Rates and Approximate Rate Constants for Inter- and Intramolecular Hydrogen Transfer Reactions of Polymer-Bound Radicals. *J. Am. Chem. Soc.* **2002**, *124*, 14993-15000.
33. Feder, H. M.; Halpern, J., Mechanism of Cobalt Carbonyl-Catalyzed Homogeneous Hydrogenation of Aromatic Hydrocarbons. *J. Am. Chem. Soc.* **1975**, *97*, 7186-7188.
34. Sweany, R. L.; Halpern, J., Hydrogenation of  $\alpha$ -Methylstyrene by Hydridopentacarbonylmanganese(I). Evidence for a Free-Radical Mechanism. *J. Am. Chem. Soc.* **1977**, *99*, 8335-8337.
35. Ungváry, F.; Markó, L., Reaction of  $\text{HCo}(\text{CO})_4$  and CO with Styrene. Mechanism of ( $\alpha$ -Phenylpropionyl)cobalt and ( $\beta$ -Phenylpropionyl)cobalt Tetracarbonyl Formation. *Organometallics* **1982**, *1*, 1120-1125.
36. Ungvary, F.; Marko, L., Effect of Solvent Viscosity on the Reaction of Styrenes with  $\text{HCo}(\text{CO})_4$  and CO. *J. Organomet. Chem.* **1983**, *249*, 411-414.
37. Roth, J. A.; Orchin, M., Stoichiometric Hydrogenation of 1,1-Diphenylethylene with Hydridocobalt Tetracarbonyl; Differences from the Hydroformylation Reaction. *J. Organomet. Chem.* **1979**, *182*, 299-311.
38. Nalesnik, T. E.; Orchin, M., The Stoichiometric Hydrogenation of 9-Methylidene fluorene and Related-Compounds with Hydridocobalt Tetracarbonyl. *J. Organomet. Chem.* **1980**, *199*, 265-269.

39. Roth, J. A.; Wiseman, P., The Stoichiometric Hydrogenation of Substituted Phenyl Alkenes by Hydridocobalt Tetracarbonyl. *J. Organomet. Chem.* **1981**, *217*, 231-234.
40. Sweany, R.; Butler, S. C.; Halpern, J., The Hydrogenation of 9,10-Dimethylanthracene by Hydridopentacarbonylmanganese(I). Evidence for a Free-Radical Mechanism. *J. Organomet. Chem.* **1981**, *213*, 487-492.
41. Sweany, R. L.; Comberrel, D. S.; Dombourian, M. F.; Peters, N. A., The Hydrogenation of  $\alpha$ -Methylstyrene by Tricarbonyl(Cyclopentadienyl)Hydride Compounds of Tungsten and Molybdenum; Support for a Radical Mechanism. *J. Organomet. Chem.* **1981**, *216*, 57-63.
42. Nalesnik, T. E.; Orchin, M., Free-Radical Reactions of  $\text{HCo}(\text{CO})_4$ . *Organometallics* **1982**, *1*, 222-223.
43. Connolly, J. W., Reaction between Hydridotetracarbonyl(trichlorosilyl)Iron,  $\text{HFe}(\text{CO})_4\text{SiCl}_3$ , and Conjugated Dienes. Evidence for a Free-Radical Mechanism. *Organometallics* **1984**, *3*, 1333-1337.
44. Bockman, T. M.; Garst, J. F.; King, R. B.; Markó, L.; Ungváry, F., CIDNP Evidence for Radical Intermediates in the Hydroformylation and Reduction of Styrene by  $\text{HCo}(\text{CO})_4/\text{CO}$ . *J. Organomet. Chem.* **1985**, *279*, 165-169.
45. Jacobsen, E. N.; Bergman, R. G., Synthesis and Chemistry of a Bridging Vinylidenedicobalt Complex. Evidence for a Nonchain Radical Mechanism in Its Reaction with Metal-Hydrides to Give Heteronuclear Clusters. *J. Am. Chem. Soc.* **1985**, *107*, 2023-2032.
46. Thomas, M. J.; Shackleton, T. A.; Wright, S. C.; Gillis, D. J.; Colpa, J. P.; Baird, M. C., Evidence for the Radical Pair Mechanism in Insertion Reactions of Transition-Metal Hydrides with Conjugated Dienes. *J. Chem. Soc., Chem. Comm.* **1986**, 312-314.
47. Wassink, B.; Thomas, M. J.; Wright, S. C.; Gillis, D. J.; Baird, M. C., Mechanisms of the Hydrometalation (Insertion) and Stoichiometric Hydrogenation Reactions of Conjugated Dienes Effected by Manganese Pentacarbonyl Hydride: Processes Involving the Radical Pair Mechanism. *J. Am. Chem. Soc.* **1987**, *109*, 1995-2002.
48. Shackleton, T. A.; Baird, M. C., The Radical Pair Mechanism in Hydrometalation and Stoichiometric Hydrogenation Reactions of  $\eta^5\text{-C}_5\text{H}_5\text{Fe}(\text{CO})_2\text{H}$  with Conjugated Dienes. *Organometallics* **1989**, *8*, 2225-2232.
49. Bullock, R. M.; Samsel, E. G., Hydrogen Atom Transfer-Reactions of Transition-Metal Hydrides. Kinetics and Mechanism of the Hydrogenation of  $\alpha$ -Cyclopropylstyrene by Metal-Carbonyl Hydrides. *J. Am. Chem. Soc.* **1990**, *112*, 6886-6898.

50. Bockman, T. M.; Garst, J. F.; Ungváry, F., Reaction of Cobalt Tetracarbonyl Hydride with Phenylacetylene. *J. Organomet. Chem.* **1999**, *586*, 41-47.
51. Tang, L. H.; Papish, E. T.; Abramo, G. P.; Norton, J. R.; Baik, M. H.; Friesner, R. A.; Rappe, A., Kinetics and Thermodynamics of H• Transfer from ( $\eta^5$ -C<sub>5</sub>R<sub>5</sub>)Cr(CO)<sub>3</sub>H (R = Ph, Me, H) to Methyl Methacrylate and Styrene. *J. Am. Chem. Soc.* **2003**, *125*, 10093-10102; revised: *J. Am. Chem. Soc.*, **2006**, *128*, 11314.
52. Choi, J.; Tang, L. H.; Norton, J. R., Kinetics of Hydrogen Atom Transfer from ( $\eta^5$ -C<sub>5</sub>H<sub>5</sub>)Cr(CO)<sub>3</sub>H to Various Olefins: Influence of Olefin Structure. *J. Am. Chem. Soc.* **2007**, *129*, 234-240.
53. Choi, J.; Pulling, M. E.; Smith, D. M.; Norton, J. R., Unusually Weak Metal-Hydrogen Bonds in HV(CO)<sub>4</sub>(P-P) and Their Effectiveness as H• Donors. *J. Am. Chem. Soc.* **2008**, *130*, 4250-4252.
54. Estes, D. P.; Norton, J. R.; Jockusch, S.; Sattler, W., Mechanisms by which Alkynes React with CpCr(CO)<sub>3</sub>H. Application to Radical Cyclization. *J. Am. Chem. Soc.* **2012**, *134*, 15512-15518.
55. Colle, T. H.; Lewis, E. S., Hydrogen Atom Transfers from Thiophenols to Triarylmethyl Radicals. Rates, Substituent Effects, and Tunnel Effects. *J. Am. Chem. Soc.* **1979**, *101*, 1810-1814.
56. Eisenberg, D. C.; Lawrie, C. J. C.; Moody, A. E.; Norton, J. R., Relative Rates of H. Transfer from Transition-Metal Hydrides to Trityl Radicals. *J. Am. Chem. Soc.* **1991**, *113*, 4888-4895.
57. Eisenberg, D. C.; Norton, J. R., Hydrogen-Atom Transfer Reactions of Transition-Metal Hydrides. *Isr. J. Chem.* **1991**, *31*, 55-66.
58. Rodkin, M. A.; Abramo, G. P.; Darula, K. E.; Ramage, D. L.; Santora, B. P.; Norton, J. R., Isotope Effects on Hydrogen Atom Transfer from Transition Metals to Carbon. *Organometallics* **1999**, *18*, 1106-1109.
59. Ollivier, C.; Renaud, P., Organoboranes as a Source of Radicals. *Chem. Rev.* **2001**, *101*, 3415-3434.
60. Handa, Y.; Inanaga, J., A Highly Stereoselective Pinacolization of Aromatic and  $\alpha,\beta$ -Unsaturated Aldehydes Mediated by Titanium(III)-Magnesium(II) Complex. *Tetrahedron Lett.* **1987**, *28*, 5717-5718.
61. Rajanbabu, T. V.; Nugent, W. A., Selective Generation of Free Radicals from Epoxides Using a Transition-Metal Radical. A Powerful New Tool for Organic Synthesis. *J. Am. Chem. Soc.* **1994**, *116*, 986-997.

62. Fujita, K.; Nakamura, T.; Yorimitsu, H.; Oshima, K., Triethylborane-Induced Radical Reaction with Schwartz Reagent. *J. Am. Chem. Soc.* **2001**, *123*, 3137-3138.
63. Gansäuer, A.; Fan, C. A.; Piestert, F., Sustainable Radical Reduction through Catalytic Hydrogen Atom Transfer. *J. Am. Chem. Soc.* **2008**, *130*, 6916-6917.
64. Gansauer, A.; Otte, M.; Shi, L., Radical Cyclizations Terminated by Ir-Catalyzed Hydrogen Atom Transfer. *J. Am. Chem. Soc.* **2011**, *133*, 416-417.
65. Smith, D. M.; Pulling, M. E.; Norton, J. R., Tin-free and Catalytic Radical Cyclizations. *J. Am. Chem. Soc.* **2007**, *129*, 770-771.
66. Beesley, R. M.; Ingold, C. K.; Thorpe, J. F., CXIX.-The Formation and Stability of Spiro-compounds. Part I. spiro-Compounds from Cyclohexane. *J. Chem. Soc., Trans.* **1915**, *107*, 1080-1106.
67. Kaneti, J.; Kirby, A. J.; Koedjikov, A. H.; Pojarlieff, I. G., Thorpe-Ingold Effects in Cyclizations to Five-membered and Six-membered Rings Containing Planar Segments. The Rearrangement of N(1)-alkyl-substituted Dihydroorotic Acids to Hydantoinacetic Acids in Base. *Org. Biomol. Chem.* **2004**, *2*, 1098-1103.
68. Fischer, E. O.; Hafner, W.; Stahl, H. O., Über Cyclopentadienyl-metall-carbonyl-wasserstoffe des Chroms, Molybdäns und Wolframs. *Z. Anorg. Allg. Chem.* **1955**, *282*, 47-62.
69. Gregory, A. R.; Malatesta, V., Stereochemistry of Tetrahydropyran-2-yl Ions, Radicals, and Related Species. Conjugative and Inductive Effects. *J. Org. Chem.* **1980**, *45*, 122-125.
70. Kuo, J. L.; Hartung, J.; Han, A.; Norton, J. R., Direct Generation of Oxygen-Stabilized Radicals by H• Transfer from Transition Metal Hydrides. *J. Am. Chem. Soc.* **2015**, *137*, 1036-1039.



## **CHAPTER 2: CHROMIUM-CATALYZED RADICAL**

### **CYCLIZATIONS: EFFECT OF DOUBLE-BOND SUBSTITUENTS<sup>a</sup>**

#### **2.1 Strategies for Increasing the Yield of Cr-Catalyzed Radical Cyclization**

In light of the discussion in Chapter 1, there are two ways to maximize the yield of cyclized product:

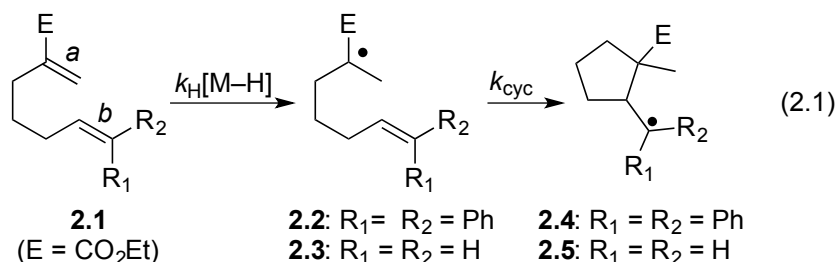
- 1) To decrease the concentration of the two forms of transition-metal hydrides, namely,  $M-H$  and  $M\bullet$  to suppress side reactions (hydrogenation and isomerization). The Norton Group has thus developed a catalytic system using  $HCr(CO)_3Cp$  as a catalyst to achieve radical cyclizations with respectable yields;
- 2) To increase the rate of cyclization by installing substituents on the backbone of the substrate. The Norton Group has used the Thorpe-Ingold effect to accelerate the rate of cyclization resulting in significantly improved yields of cyclization product.<sup>1</sup>

It is, in fact, possible to increase the rate of cyclization ( $k_{cyc}$ ) by varying the substituents on double bond  $b$  of diene substrates like **2.1** (eq 2.1). For example, Newcomb and co-workers reported experimental rate constants for the cyclization of the related ( $E = CO_2Et$ ) radicals **2.2** and **2.3** to the corresponding radicals **2.4** and **2.5** (eq 2.1) and noticed a decrease in  $k_{cyc}$  from **2.2** ( $3.3 \times 10^5 s^{-1}$  at  $20\text{ }^\circ C$ )<sup>2</sup> to **2.3** ( $1 \times 10^4 s^{-1}$  at  $25\text{ }^\circ C$ )<sup>3</sup>. The change in  $k_{cyc}$  is presumably due to a change in the stability of the resulting cyclized radical. Phillips and Yang's theoretical studies on similar radicals (with a variety

---

<sup>a</sup> This part of the work was largely done by an undergraduate student under my supervision, Arthur Han, and has been partly published in Han, A.; Spataru, T.; Hartung, J.; Li, G.; Norton, J. R., Effect of Double-Bond Substituents on the Rate of Cyclization of  $\alpha$ -Carbomethoxyhex-5-enyl Radicals. *J. Org. Chem.* **2014**, 79, 1938-1946. Arthur synthesized and cyclized substrates **2.6-2.9** and **2.11**; I synthesized and cyclized substrate **2.10** and drafted the manuscript.

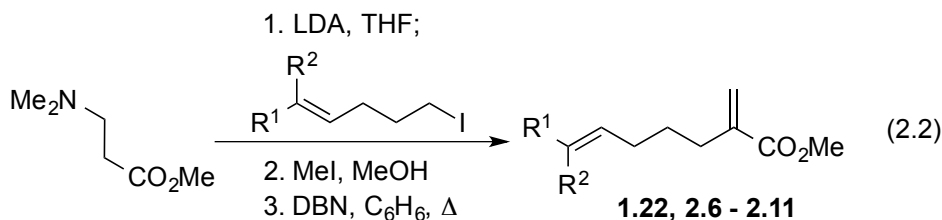
of substituents E and R) also suggest the influence of substituents on  $k_{\text{cyc}}$ .<sup>4, 5</sup> It is essential to understand the effect of substituents on double bond *b* on the rates of radical cyclization to guide the design of substrates.



## 2.2 Synthesis and Radical Cyclization of Diene Substrates with HCr(CO)<sub>3</sub>Cp

### 2.2.1 Synthesis of Diene Substrates

Diene substrates **2.11** to **2.17** were prepared by the method that had previously been used for compound **1.22** (eq 2.2).<sup>1</sup>



### 2.2.2 Radical Cyclization of Diene Substrates with Stoichiometric HCr(CO)<sub>3</sub>Cp

These diene substrates were treated with a stoichiometric amount of HCr(CO)<sub>3</sub>Cp under standard conditions (C<sub>6</sub>D<sub>6</sub>, 323 K) and the products were quantified by <sup>1</sup>H NMR. From substrates without methyl substituents on the *b* double bond (**1.22**, **2.6**, **2.9** and **2.10**), cyclization products like **1.22** were obtained (eq 2.3). However, from substrates bearing methyl groups on the *b* double bond (**2.7**, **2.8** and **2.11**) unsaturated products like **2.11** were obtained (eq 2.4), presumably the result of H• abstraction from the methyl of

the cyclized radical (and of the congestion around the radical center). The conversion of **2.11** to **2.12** involves neither the gain nor the loss of hydrogen atoms and is thus a *cycloisomerization*.<sup>6, 7</sup>

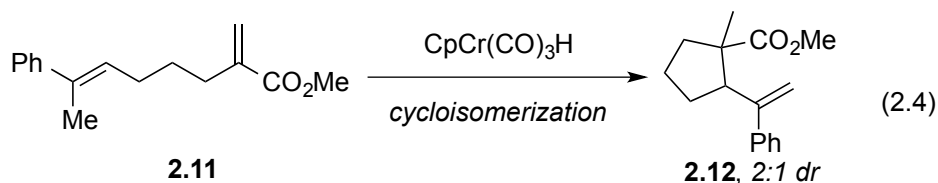
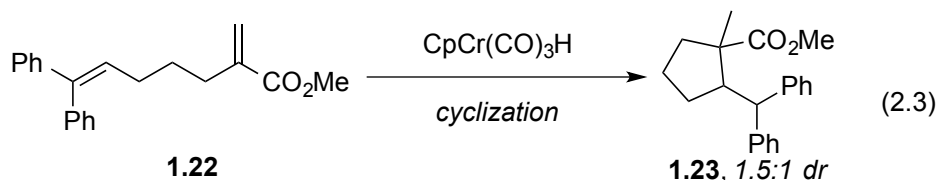
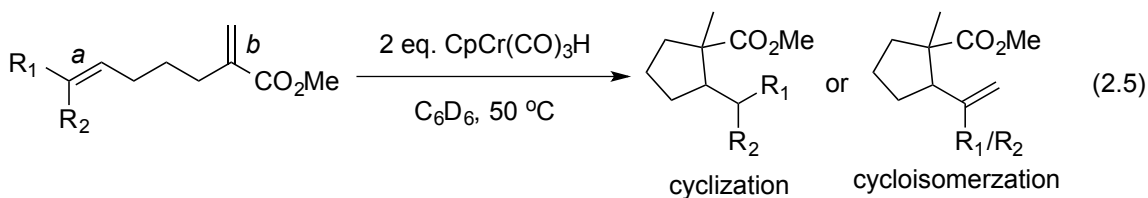


Table 2.1 gives the yields for the products from the stoichiometric reaction.

**Table 2.1.** NMR Yields of the Products from Treatment of Diene Substrates with Stoichiometric  $\text{HCr(CO)}_3\text{Cp}$



compound	R <sub>1</sub>	R <sub>2</sub>	cyclization	cycloisomerization	hydrogenation	isomerization
<b>2.6</b>	H	H	5	0	76	19
<b>2.7</b>	Me	H	0	16	56	28
<b>2.8</b>	Me	Me	0	18	51	31
<b>2.9</b>	Ph	H	52	0	37	11
<b>2.10</b>	H	Ph	53	0	38	9
<b>2.11</b>	Ph	Me	0	41	49	10
<b>1.22</b>	Ph	Ph	27	0	55	18

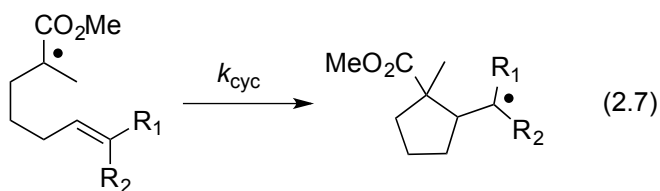
It is obvious that the rate of hydrogenation ( $k_{\text{hydr}}[\text{HCr(CO)}_3\text{Cp}]$ ) will be little affected by the substituents on the *b* double bond (Scheme 2.1). For a particular substrate, with a

given concentration of  $\text{HCr(CO)}_3\text{Cp}$ , the relative rates of cyclization and hydrogenation will be determined by  $k_{\text{cyc}}$ , as implied in eq 2.6 (see also in Scheme 1.8).

$$\frac{k_{\text{cyc}}}{k_{\text{hyd}}[\text{HCr(CO)}_3\text{Cp}]} = \frac{\text{rate of formation of the cyclized product}}{\text{rate of formation of the hydrogenation product}} \quad (2.6)$$

In order to clarify the results in Table 2.1, it is necessary to obtain some cyclization rate constants. Houk<sup>8-11</sup> and others<sup>12-17</sup> have shown that DFT, in particular with the B3LYP functional, is useful in predicting the rate constants of various radical reactions, including cyclizations and retrocyclizations. We therefore calculated  $k_{\text{cyc}}$  for the above diene substrates with the assistance of Dr. Tudor Spataru (Table 2.2).

**Table 2.2.** Calculated Average Rate Constant (Gaussian 03, B3LYP, and 6-311++G\*\*) for Cyclization of  $\alpha$ -Carbomethoxy Radical at 298K



compound	R <sub>1</sub>	R <sub>2</sub>	Average calculated $k_{\text{cyc}} (\text{s}^{-1})^b$
<b>2.12</b>	H	H	$2.33 \times 10^2$
<b>2.13</b>	Me	H	$1.01 \times 10^3$
<b>2.14</b>	Me	Me	$1.18 \times 10^3$
<b>2.15</b>	Ph	H	$2.02 \times 10^5$
<b>2.16</b>	H	Ph	$6.11 \times 10^4$
<b>2.17</b>	Ph	Me	$1.58 \times 10^4$
<b>2.18.</b>	Ph	Ph	$2.31 \times 10^4$

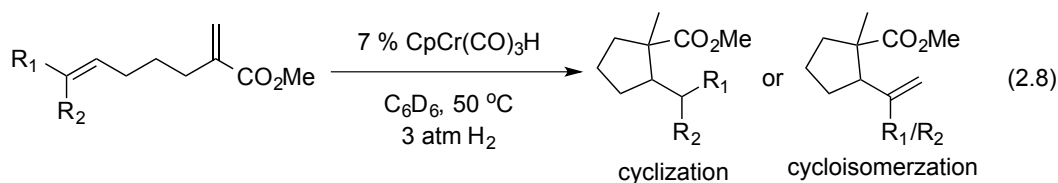
Indeed, the cyclization yields for the various substrates in Table 2.1 are approximately what we expect from the calculated  $k_{\text{cyc}}$  in Table 2.2. For example, the

<sup>b</sup> The rate constants are the average of the calculated  $k_{\text{cyc}}$  of two conformations of  $\alpha$ -carbomethoxy radical. Details can be obtained from Han, A.; Spataru, T.; Hartung, J.; Li, G.; Norton, J. R., Effect of Double-Bond Substituents on the Rate of Cyclization of  $\alpha$ -Carbomethoxyhex-5-enyl Radicals. *J. Org. Chem.* **2014**, 79, 1938-1946.

yield of cyclization product increases, relative to the yield of the hydrogenation product, as the calculated  $k_{\text{cyc}}$  increases, in the order **2.6** < **2.7** < **2.8**. Of course, the concentration of  $\text{HCr(CO)}_3\text{Cp}$ , and thus the rate of hydrogenation, decreases in the course of a stoichiometric cyclization.

In the course of a catalytic reaction (eq 2.8), the concentration of  $\text{HCr(CO)}_3\text{Cp}$  will remain approximately constant and lower in concentration than during the stoichiometric reactions in Table 2.1. (Although the hydrogen in a catalytic reaction keeps most of the Cr in the form of  $\text{HCr(CO)}_3\text{Cp}$ , only 7 mol % of Cr is present.) We thus expect higher yields of the cyclization products under catalytic conditions, and these are apparent in Table 2.3. The relative yields in Table 2.3 from the various substrates show a pattern like that in Table 2.1, approximately what we would expect from the calculated rate constants in Table 2.2.

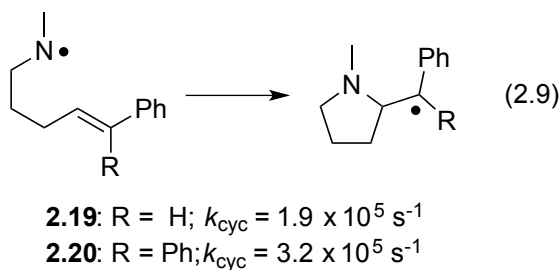
**Table 2.3.** Isolated Yields of Cyclization Products from Treatment of Diene Substrates with Catalytic Amounts of  $\text{HCr(CO)}_3\text{Cp}$  under  $\text{H}_2$



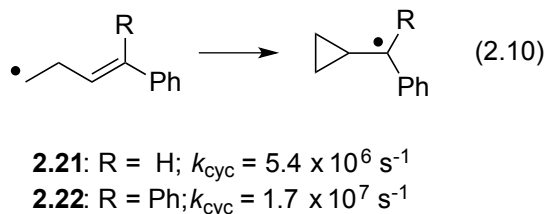
compound	R <sub>1</sub>	R <sub>2</sub>	cyclization	cycloisomerization
<b>2.6</b>	H	H	10	0
<b>2.7</b>	Me	H	0	42
<b>2.8</b>	Me	Me	0	45
<b>2.9</b>	Ph	H	97	0
<b>2.10</b>	H	Ph	92	0
<b>2.11</b>	Ph	Me	0	74
<b>1.22</b>	Ph	Ph	71	0

### 2.3 Why Does the Monophenyl Radical Cyclize More Rapidly than the Ph<sub>2</sub> and Ph(Me) Radicals?

In general, the addition of radicals to RCH=CPh<sub>2</sub> is faster than the addition of the same radicals to RCH=CHPh, although the effect is smaller than would be expected if the substituent effects were additive. For the cyclization of **2.19**,  $k_{\text{cyc}}$  at 20 °C is  $1.9 \times 10^5 \text{ s}^{-1}$ , whereas for **2.20** it is  $3.2 \times 10^5 \text{ s}^{-1}$  (eq 2.9).<sup>18</sup>

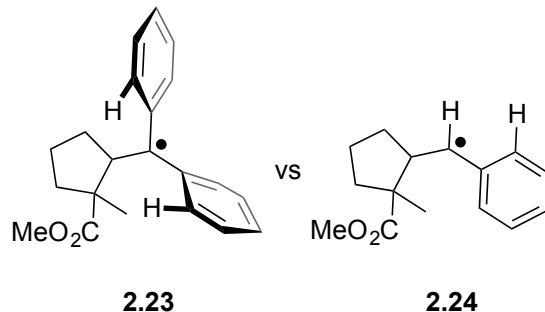


For the cyclization of **2.21**,  $k_{\text{cyc}}$  at 20 °C is  $5.4 \times 10^6 \text{ s}^{-1}$ , whereas for **2.22** it is  $1.7 \times 10^7 \text{ s}^{-1}$  (eq 2.10).<sup>19</sup>



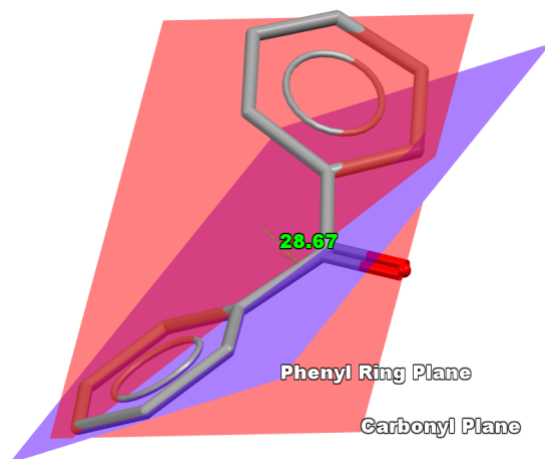
However, the yield of the cyclized product in Tables 2.1 and 2.3 is higher with one Ph substituent (substrates **2.9**, **2.10**) than with two (substrate **1.22**), in agreement with the calculated  $k_{\text{cyc}}$  values in Table 2.2 for **2.15** and **2.16** vs **2.18**. The higher yields suggest faster  $k_{\text{cyc}}$ , consistent with the implications of our DFT calculations. The lack of substituent additivity in all these reactions presumably arises from the gearing of two phenyls on the same carbon. For example, neither phenyl is coplanar with the radical center in the cyclized radical **2.23**, whereas planarity and stabilization are easily achieved by the single phenyl substituent in **2.24** (Scheme 2.1).

### Scheme 2.1. Structures of Cyclized Radicals



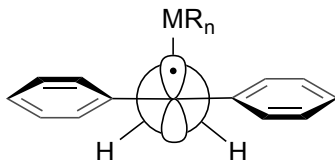
The interaction of two phenyl rings attached to the same  $sp^2$  carbon is illustrated by the X-ray structures of  $\text{Ph}_2\text{CO}$  and  $\text{Ph}_2\text{C}=\text{CH}_2$  and their derivatives. Benzophenone (which exists in two different crystalline forms) shows an average twist angle of  $33^\circ$ .<sup>20</sup> (We define the “twist angle” as the angle between the normal to the purple phenyl ring plane and the normal to the pink “carbonyl plane” in Scheme 2.2.) Various para-substituted derivatives of 1,1-diphenylethylene show twist angles averaging  $39^\circ$ .<sup>21</sup> The diphenylethylene derivatives have larger twist angles because of repulsion between the ethylenic hydrogens and the ortho hydrogens on the phenyl rings. These precedents suggest a considerable twist of the two phenyl substituents in our substrate **1.22**, which our DFT calculations confirm ( $k_{\text{cyc}} = 2.31 \times 10^4 \text{ s}^{-1}$ ).

### Scheme 2.2. Definition of "Twist Angle" for One of the Phenyl Rings in Benzophenone

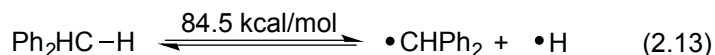
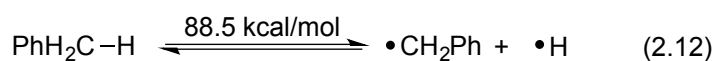
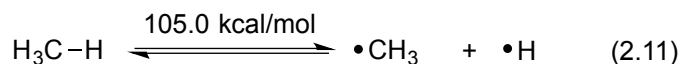


Such twisting has also been found using EPR for two phenyl substituents on a radical center, i.e., for 1,1-diphenylethyl radicals like the one in Scheme 2.3 (M = a variety of group 4 elements).<sup>22</sup> (At low temperatures the H's pictured are inequivalent.) A twist angle of 22° was obtained for benzophenone ketyl by early ab initio calculations.<sup>23</sup>

**Scheme 2.3.** Twisting between Two Phenyl Substituents on a Radical Center



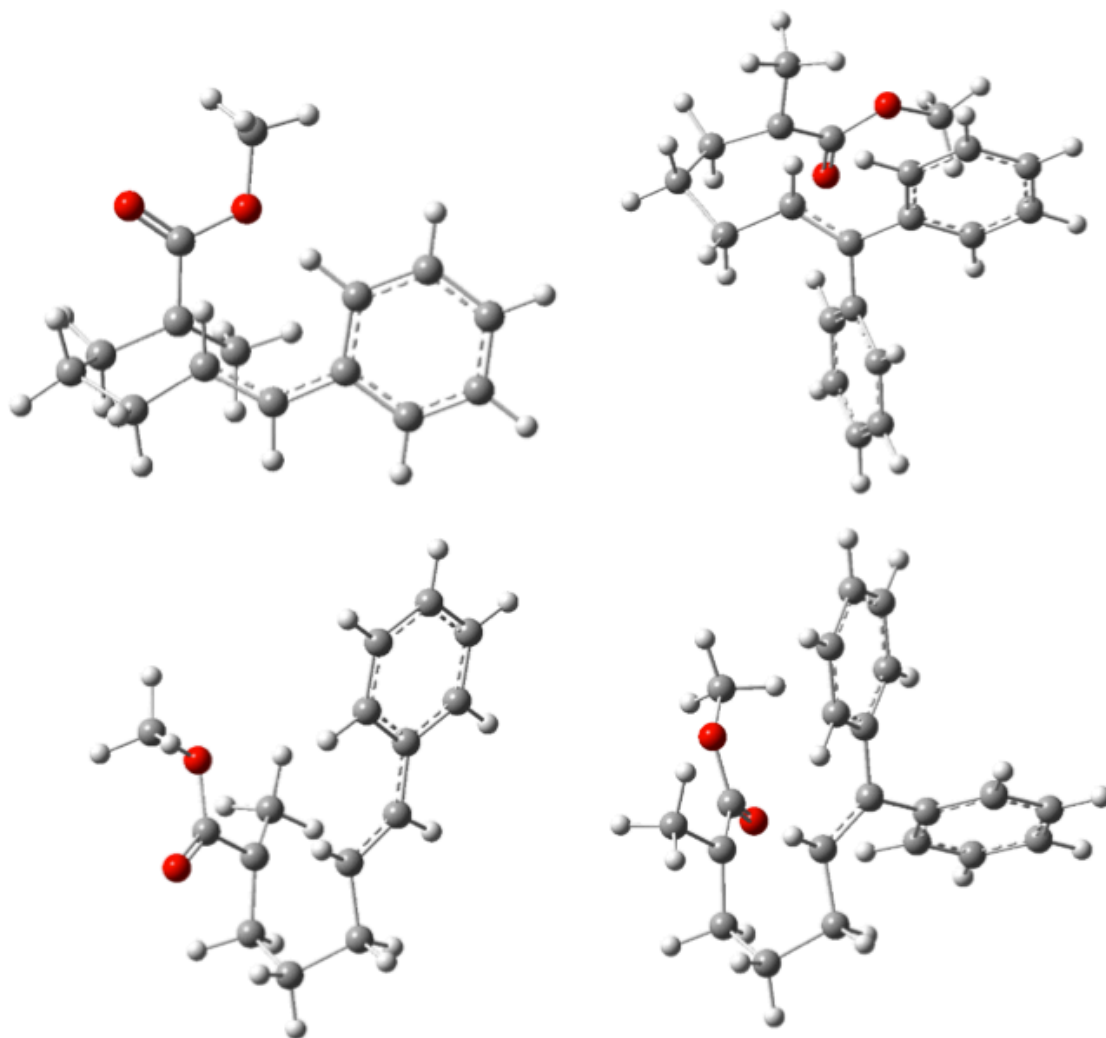
The twisting of two phenyl substituents on a radical center is responsible for the decrease between the effect of the first phenyl substituent and the effect of the second on the C–H bond strengths below (eqs 2.11, 2.12 and 2.13).<sup>24</sup> Halgren, Roberts, Newcomb and coworkers have also noted the differential effect of Ph substitution on C–H bond strengths.<sup>19</sup>



With our radicals (for example, **2.15** and **2.18**) we expect twisting to decrease as cyclization begins and the C5–C6 bond lengthens; it should, however, remain substantial. Our calculations predict a large twist angle in **2.18** itself (an average of 51.9° for the two phenyls), which decreases as cyclization begins (and C5–C6 lengthens) but remains substantial in the transition state in Scheme 2.4 (an average of 41.3°) and in the cyclized radical **2.23** (an average of 36.1°).

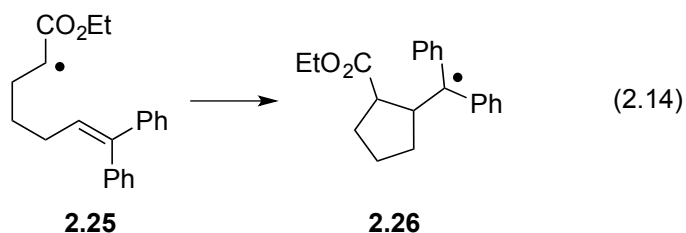


**Scheme 2.4.** Two views of the transition state for cyclization by radicals **2.15** (left) and **2.18** (right)<sup>a</sup>



<sup>a</sup>oxygen atoms are red, C1, C5, and C6 are blue. In the transition state for **2.15** the C1–C5 distance is 2.22 Å and the C5–C6 distance is 1.39 Å; in that for **2.18** C1–C5 is 2.22 Å and C5–C6 is 1.40 Å.

Similar but smaller twists are found in the transition state for the cyclization of the 6,6-diphenyl carboxy-substituted hexenyl radical **2.25**, the subject of DFT calculations by Phillips et al. (eq 2.14).<sup>4</sup> From their results, we compute an average twist angle for the two phenyls of 46.7° in the initial radical, an average angle of 40.4° in the transition state, and an average angle of 31.9° in the cyclized radical **2.26**. (They considered only cases with two phenyl substituents on C6.)



Why is the Ph<sub>2</sub>/Ph(H) effect so large in our cyclizations that Ph(H) (**2.15**, **2.16**) is now faster than Ph<sub>2</sub> (**2.18**)? The Newcomb aminyl radicals **2.19** and **2.20** resemble secondary carbon radicals, the Newcomb radicals (**2.21** and **2.22**) are primary, and the radicals in the Fischer–Radom table<sup>12</sup> are secondary and primary. The radicals in our case (**2.12**–**2.18**) are tertiary and thus more sensitive (when forming the C1–C5 bond) to repulsion by twisted phenyl substituents on C6. The C1–C5 distance in the transition state for the cyclization is 0.10 Å longer for the Ph<sub>2</sub> case (**2.18**) than for the H<sub>2</sub> (**2.12**) and Me<sub>2</sub> (**2.14**) cases. Note that the Ph twist is smaller (previous paragraph) in the transition state for the cyclization of the Newcomb/Phillips/Yang secondary hexenyl radical **2.25** than for the cyclization of the tertiary radical **2.18**.

Twists are also found when C6 bears a methyl along with a phenyl substituent. In the transition state for the cyclization of **2.17** the phenyl is twisted by an average of 34°.

A single phenyl substituent, however, is flat in the substrates **2.9** (E) and **2.10** (Z) and remains so as **2.15** and **2.16** cyclize. It stabilizes the transition state substantially, and increases the rate constant for cyclization. A similar acceleration is to be expected for any single aryl substituent.

## 2.4 Experimental Details

All reactions were carried out under an atmosphere of argon in glassware that had been flame-dried under vacuum and backfilled with argon. High-pressure reactions were

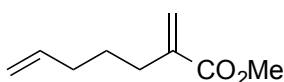
carried out in a Fisher–Porter bottle equipped with a pressure gauge, gas inlet, and pressure release valve. Hexamethylphosphoramide (HMPA) was distilled from  $\text{CaH}_2$ . Deuterated benzene ( $\text{C}_6\text{D}_6$ ) was purified by vacuum transfer from  $\text{CaH}_2$ . THF and benzene ( $\text{C}_6\text{H}_6$ ) were distilled from sodium-benzophenone ketyl.  $\text{Et}_2\text{O}$  and  $\text{CH}_2\text{Cl}_2$  were dried by filtration through alumina.  $\text{HCr}(\text{CO})_3\text{Cp}$  was synthesized according to known procedures<sup>25</sup> and manipulated in an inert argon atmosphere glovebox ( $\text{O}_2 < 1$  ppm). Reaction mixtures involving  $\text{HCr}(\text{CO})_3\text{Cp}$  were all prepared in the glovebox.  $^1\text{H}$  NMR and  $^{13}\text{C}$  NMR spectra were recorded at ambient temperature (298 K) at 500, 400, or 300 MHz and 125, 100, or 75 MHz, respectively. High-resolution mass spectra were acquired (after ionization by EI) by peak matching on a double-focusing magnetic sector instrument.

**General Method for the Synthesis of Diene Substrates (1.22, 2.6-2.11).** The synthesis of substrates followed a known procedure (eq 5).<sup>1</sup> To a solution of LDA in THF was added methyl-3-(dimethylamino)propionate (1.1 mmol) dropwise at  $-78^\circ\text{C}$ . The mixture was stirred for 0.5 h<sup>c</sup> before the addition of a solution of alkyl halide (1 mmol) in THF and freshly distilled HMPA (1 mmol). The mixture was then warmed to room temperature, stirred for 48 h, quenched with saturated  $\text{NH}_4\text{Cl}$ , and extracted with  $\text{Et}_2\text{O}$ . The extract was dried over  $\text{MgSO}_4$ , filtered, concentrated, and taken up in 5 mL MeOH, and excess MeI (13 mmol) was added; the flask was wrapped in foil and the mixture stirred overnight (16-18 h). After concentration *in vacuo*, the residue was washed with  $\text{Et}_2\text{O}$  three times; removal of the remaining solvent afforded the ammonium iodide salt as a bright yellow solid. Benzene (20 mL) was then added, along with excess

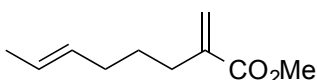
---

<sup>c</sup> It is probably better to run the reaction for a longer time; see Chapter 4.

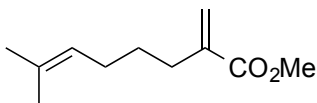
1,5-diazabicyclo[4.3.0]non-5-ene (DBN, 2 mL), and the bright yellow mixture was stirred at reflux for 4 h. After being cooled to room temperature, the solution was washed with 1 N HCl, and Et<sub>2</sub>O was added. The collected organic layers were washed with brine, dried over MgSO<sub>4</sub>, filtered, and concentrated. Flash chromatography (10% EtOAc/hexanes) on silica gel afforded the desired 1,6-diene.



*Methyl 2-Methylenehept-6-enoate (2.6).* Compound **2.6** was prepared in 28% yield (43 mg) over three steps from 1 mmol of 5-iodopent-1-ene as a bright yellow oil. Spectroscopic data matched the literature.<sup>26</sup>

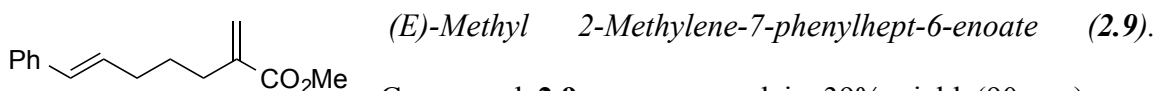


*Methyl 2-Methyleneoct-6-enoate (2.7).* Compound **2.7** was prepared in 55% yield (91 mg) over three steps from 1 mmol of (*E*)-6-iodohex-2-ene<sup>27</sup> as a golden yellow oil: <sup>1</sup>H NMR (400 MHz, CDCl<sub>3</sub>) δ 6.13 (s, 1 H), 5.52 (s, 1 H), 5.43 (d, *J* = 3.9 Hz, 2 H), 3.75 (s, 3 H), 2.30 (t, *J* = 7.6 Hz, 2H), 2.06-1.93 (m, 2 H), 1.65 (s, 3 H), 1.56-1.48 (m, 2 H); <sup>13</sup>C NMR (100 MHz, CDCl<sub>3</sub>) δ 167.8, 140.7, 130.9, 125.3, 124.6, 51.8, 32.1, 31.4, 28.3, 17.9; IR (neat) 2932, 2859, 1725, 1632 cm<sup>-1</sup>; HRMS (FAB<sup>+</sup>) calcd for C<sub>10</sub>H<sub>16</sub>O<sub>2</sub> [M]<sup>+</sup> 168.1150, found 168.1149.

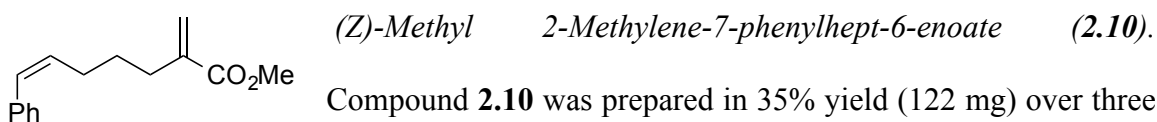


*Methyl 7-Methyl-2-methyleneoct-6-enoate (2.8).* Compound **2.8** was prepared in 65% yield (59 mg) over three steps from 0.5 mmol of 6-iodo-2-methylhex-2-ene<sup>28</sup> as a golden yellow oil: <sup>1</sup>H NMR (500MHz, CDCl<sub>3</sub>) δ 6.15 (s, 1H), 5.55 (s, 1H), 5.14 (t, *J* = 7.0 Hz, 1H), 3.77 (s, 3H), 2.32 (t, 2H), 2.03 (q, *J* = 7.2 Hz, 2H), 1.71 (s, 3H), 1.62 (s, 3H), 1.57-1.48 (m, 2H); <sup>13</sup>C NMR (125

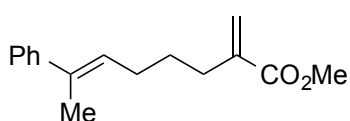
MHz, CDCl<sub>3</sub>)  $\delta$  167.9, 140.8, 131.8, 124.5, 124.2, 64.5, 51.7, 31.5, 28.6, 27.6, 25.7; IR (neat) 2927, 2858, 1725, 1630 cm<sup>-1</sup>; HRMS (FAB<sup>+</sup>) calcd for C<sub>11</sub>H<sub>18</sub>O<sub>2</sub> [M]<sup>+</sup> 182.1307, found 182.1315.



Compound **2.9** was prepared in 39% yield (90 mg) over three steps from 1 mmol of (*E*)-(5-iodopent-1-en-1-yl)benzene<sup>29</sup> as a cloudy pale yellow oil: <sup>1</sup>H NMR (500 MHz, CDCl<sub>3</sub>)  $\delta$  7.34-7.17 (m, 5H), 6.39 (d, *J* = 15.8 Hz, 1H), 6.27-6.17 (m, 1H), 6.16 (s, 1H), 5.55 (s, 1H), 3.74 (s, 3H), 2.36 (t, *J* = 7.3 Hz, 2H), 2.24 (q, *J* = 13.6, 6.6 Hz, 2H), 1.67-1.64 (m, 2H); <sup>13</sup>C NMR (125 MHz, CDCl<sub>3</sub>)  $\delta$  167.7, 140.4, 137.8, 130.34, 130.31, 128.5, 126.9, 126.0, 124.9, 51.8, 32.5, 31.5, 28.1; IR (neat) 3082, 3060, 3026, 2962, 2853, 1723, 1631, 1495 cm<sup>-1</sup>; HRMS (FAB<sup>+</sup>) calcd for C<sub>15</sub>H<sub>18</sub>O<sub>2</sub> [M]<sup>+</sup> 230.1307, found 230.1314.



Compound **2.10** was prepared in 35% yield (122 mg) over three steps from 1.5 mmol of (*Z*)-(5-iodopent-1-en-1-yl)benzene<sup>30</sup> as a golden yellow oil: <sup>1</sup>H NMR (400 MHz, CDCl<sub>3</sub>)  $\delta$  7.35-7.19 (m, 5H), 6.43 (dt, *J*<sub>1</sub> = 11.8 Hz, *J*<sub>2</sub> = 1.9 Hz, 1H), 6.11 (d, *J* = 1.5 Hz, 1H), 5.66 (dt, *J*<sub>1</sub> = 11.7 Hz, *J*<sub>2</sub> = 7.3 Hz, 1H), 5.48 (q, *J* = 1.4 Hz, 1H), 3.74 (s, 3H), 2.41-2.29 (m, 4H), 1.69-1.57 (m, 2H); <sup>13</sup>C NMR (125 MHz, CDCl<sub>3</sub>)  $\delta$  167.7, 140.3, 137.6, 132.3, 129.3, 128.7, 128.1, 126.5, 124.9, 51.8, 31.5, 28.6, 28.0; IR (neat) 3082, 3060, 3026, 2962, 2853, 1723, 1631, 1495 cm<sup>-1</sup>. HRMS (FAB<sup>+</sup>) calcd for C<sub>15</sub>H<sub>18</sub>O<sub>2</sub> [M]<sup>+</sup> 230.1307, found 230.1314.



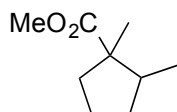
(*E*)-Methyl 2-Methylene-7-phenyloct-6-enoate (**2.11**).

Compound **2.11** was prepared in 36% yield (89 mg) over three steps from 1 mmol of (*E*)-(6-iodohex-2-en-2-yl)benzene as a bright yellow oil:  $^1\text{H}$  NMR (300 MHz,  $\text{CDCl}_3$ )  $\delta$  7.41-7.17 (m, 5H), 6.16-6.15 (m, 1H), 5.77 (td,  $J_1 = 7.2$  Hz,  $J_2 = 1.4$  Hz, 1H), 5.55 (q,  $J = 1.4$  Hz, 1H), 3.76 (s, 3H), 2.38 (t,  $J = 7.5$  Hz, 2H), 2.23 (q,  $J = 7.3$  Hz, 2H), 2.03 (dd,  $J_1 = 2.1$  Hz,  $J_2 = 0.8$  Hz, 3H), 1.65-1.43 (m, 2H);  $^{13}\text{C}$  NMR (100 MHz,  $\text{CDCl}_3$ )  $\delta$  167.8, 143.9, 140.5, 135.1, 128.2, 127.9, 126.5, 125.6, 124.8, 51.8, 31.6, 28.3, 28.3, 15.9; IR (neat) 2919, 2853, 1722, 1630, 1494  $\text{cm}^{-1}$ ; HRMS (FAB $^+$ ) calcd for  $\text{C}_{16}\text{H}_{20}\text{O}_2$   $[\text{M}]^+$  244.1463, found 244.1470.

**General Method for Stoichiometric Cyclizations.** To a J. Young tube were added  $\text{HCr}(\text{CO})_3\text{Cp}$  (50 mg, 0.13 mmol) and a  $\text{C}_6\text{D}_6$  (0.6 mL) solution of the substrate (0.06 mmol). The bright green reaction mixture was then kept overnight (16-18 h) at 50  $^\circ\text{C}$  before product yields were determined by  $^1\text{H}$  NMR.

**General Method for Catalytic Cyclizations.** To a Fisher-Porter pressure apparatus were added  $\text{HCr}(\text{CO})_3\text{Cp}$  and a  $\text{C}_6\text{H}_6$  solution of the substrate (0.1 M) before the apparatus was thoroughly purged with  $\text{H}_2$  and pressurized to 3 atm. The bright green reaction mixture was kept for 16 h at 50  $^\circ\text{C}$  and the reaction examined by  $^1\text{H}$  NMR before being cooled to room temperature and quenched with  $\text{O}_2$ . The resulting dark green reaction mixture was filtered, concentrated, and purified by flash chromatography on silica gel (0-10% EtOAc/hexanes), affording the cyclized product (always a clear oil) as a mixture of two inseparable diastereomers.

The structures of the isolated major and minor diastereomers of cyclization product **2.31** were confirmed by 2D NMR as previously reported by Pulling, Smith, and Norton.<sup>1</sup> The stereochemistries of the cyclization products agree with those predicted by the Beckwith<sup>31</sup>-Houk<sup>32</sup> model.



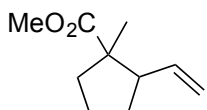
**2.27**

*Methyl 1,2-Dimethylcyclopentanecarboxylate (2.27).* Compound **2.27**

was isolated as a mixture of diastereomers (61:39) in 10% yield (5 mg)

from 0.3 mmol **2.6**. The spectroscopic data matched those in the

literature.<sup>33</sup>



**2.28**

*Methyl 1-Methyl-2-vinylcyclopentanecarboxylate (2.28).* Compound

**2.28** was isolated as a mixture of diastereomers (57:43) in 42% yield

(21 mg) from 0.3 mmol of **2.7**: <sup>1</sup>H NMR (500 MHz, CDCl<sub>3</sub>) δ major:

5.77 (p, *J* = 10 Hz, 1H), 5.44 (m, 1H), 5.02 (dd, *J* = 6 Hz, 1H), 3.68 (s, 3 H), 2.88 (q, *J* =

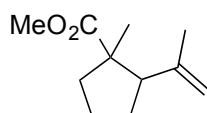
10 Hz, 1H), 2.2-2.10 (m, 2H), 1.89-1.49 (m, 4H), 1.07 (s, 3 H); minor: 5.69 (p, *J* = 10 Hz,

1H), 5.44 (m, 1H), 4.99 (dd, *J* = 6 Hz, 1H), 3.62 (s, 3 H), 2.51 (q, *J* = 10 Hz, 1H), 2.2-

2.10 (m, 2H), 1.89-1.49 (m, 4H), 1.25 (s, 3 H); <sup>13</sup>C NMR (125 MHz, CDCl<sub>3</sub>) δ major:

178.3, 138.2, 115.5, 51.7, 51.1, 38.2, 31.4, 28.7, 23.9, 18.4; HRMS (FAB<sup>+</sup>) calcd for

C<sub>10</sub>H<sub>16</sub>O<sub>2</sub> [M]<sup>+</sup> 168.1150, found 168.1155.



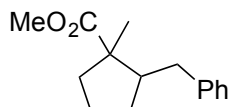
**2.29**

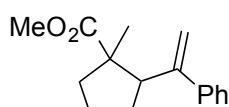
*Methyl 1-Methyl-2-(prop-1-en-2-yl)cyclopentanecarboxylate (2.29).*

Compound **2.29** was isolated as a mixture of diastereomers (59:41) in

45% yield (33 mg) from 0.4 mmol of **2.8**: <sup>1</sup>H NMR (500 MHz, CDCl<sub>3</sub>)

$\delta$  major: 4.86 (s, 1 H), 4.70 (s, 1 H), 4.11, (t,  $J$  = 6.5 Hz, 1 H), 3.72 (s, 3 H), 2.35 (q,  $J$  = 10 Hz, 1H) 1.65 (d,  $J$  = 5 Hz, 3H); minor: 4.80 (s, 1 H), 4.73 (s, 1 H), 4.00 (t,  $J$  = 6.5 Hz, 1 H), 3.62 (s, 3 H), 2.50 (q,  $J$  = 10 Hz, 1H), 1.73 (d,  $J$  = 5 Hz, 3H);  $^{13}\text{C}$  NMR (125 MHz,  $\text{CDCl}_3$ )  $\delta$  major: 179.3, 142.3, 111.6, 53.1, 30.8, 29.0, 27.0, 25.6, 23.2, 19.3, 12.4; HRMS ( $\text{FAB}^+$ ) calcd for  $\text{C}_{11}\text{H}_{18}\text{O}_2$   $[\text{M}]^+$  182.1307, found 182.1310.

 *Methyl 2-Benzyl-1-methylcyclopentanecarboxylate (2.30).*  
**2.30** Compound **2.30** was isolated as a mixture of diastereomers (52:48) in 97% yield (44 mg) from 0.2 mmol of **2.9**:  $^1\text{H}$  NMR (400 MHz,  $\text{CDCl}_3$ )  $\delta$  major: 7.19-7.13 (m, 5H), 3.70 (s, 3H), 2.83-2.77 (m, 2H), 2.61-2.07 (m, 3H), 1.94-1.47 (m, 4H), 1.30 (s, 3H); minor: 7.19-7.13 (m, 5H), 3.58 (s, 3H), 2.61-2.07 (m, 5H), 1.94-1.47 (m, 4H), 1.17 (s, 3H);  $^{13}\text{C}$  NMR (125 MHz,  $\text{CDCl}_3$ )  $\delta$  major: 177.5, 141.6, 128.8, 128.2, 125.8, 53.6, 52.4, 51.3, 38.8, 37.4, 30.8, 22.5, 17.5; minor: 178.5, 141.5, 128.8, 128.2, 125.7, 51.7, 51.2, 49.1, 37.3, 36.8, 30.0, 24.3, 21.9; IR (neat) 3026, 2926, 2871, 2855, 1725, 1603, 1496  $\text{cm}^{-1}$ ; HRMS ( $\text{FAB}^+$ ) calcd for  $\text{C}_{15}\text{H}_{21}\text{O}_2$   $[\text{M}+\text{H}]^+$  233.1542, found 233.1555.

 *Methyl 1-Methyl-2-(1-phenylvinyl)cyclopentanecarboxylate (2.31).*  
**2.31** Compound **2.31** was isolated as a mixture of diastereomers (67:33) in 74% yield (36 mg) from 0.2 mmol of **2.11**:  $^1\text{H}$  NMR (400 MHz,  $\text{CDCl}_3$ )  $\delta$  major: 7.29-7.19 (m, 5H), 5.19 (s, 1H), 5.08 (s, 1H), 3.63-3.59 (m, 1H), 3.15 (s, 3H), 2.24-2.21 (m, 1H), 2.00-1.79 (m, 3H), 1.61-1.54 (m, 2H), 0.94 (s, 3H); minor: 7.29-7.21 (m, 5H), 5.14 (s, 1H), 5.04 (s, 1H), 3.48 (s, 3H), 2.98-2.94 (m, 1H), 2.38-2.34



(m, 1H), 2.00-1.79 (m, 5H), 1.06 (s, 3H);  $^{13}\text{C}$  NMR (125 MHz,  $\text{CDCl}_3$ )  $\delta$  major: 178.5, 149.0, 142.7, 128.0, 127.9, 127.2, 127.1, 127.0, 114.3, 55.4, 52.4, 51.3, 40.1, 29.3, 22.6, 18.9; minor: 176.7, 150.1, 143.9, 128.0, 127.9, 127.2, 127.1, 127.0, 113.4, 53.9, 51.0, 50.2, 37.8, 31.8, 25.6, 22.9; IR (neat) 3082, 3057, 3024, 2951, 2874, 1733, 1627, 1600, 1575, 1495  $\text{cm}^{-1}$ ; HRMS ( $\text{FAB}^+$ ) calcd for  $\text{C}_{16}\text{H}_{20}\text{O}_2$   $[\text{M}]^+$  244.1442, found 244.1466

## 2.5 References

1. Smith, D. M.; Pulling, M. E.; Norton, J. R., Tin-free and Catalytic Radical Cyclizations. *J. Am. Chem. Soc.* **2007**, *129*, 770-771.
2. Newcomb, M.; Horner, J. H.; Filipkowski, M. A.; Ha, C.; Park, S. U., Absolute Rate Constants for Reactions of  $\alpha$ -Carbethoxy and  $\alpha$ -Cyano Radicals. *J. Am. Chem. Soc.* **1995**, *117*, 3674-3684.
3. Newcomb, M.; Filipkowski, M. A.; Johnson, C. C.,  $\alpha$ -Ethoxycarbonyl and  $\alpha$ -Methoxy Substituted Radical Clocks. *Tetrahedron Lett.* **1995**, *36*, 3643-3646.
4. Guan, X. G.; Phillips, D. L.; Yang, D., A Density Functional Theory Study of the 5-*exo* Cyclization Reactions of  $\alpha$ -Substituted 6,6-Diphenyl-5-hexenyl Radicals. *J. Org. Chem.* **2006**, *71*, 1984-1988.
5. Guan, X. G.; Phillips, D. L., A Density Functional Theory Study of the Cyclization and Ring Opening Reactions of Selected 2,2-Diphenyl-cyclopropyl Radicals. *J. Mol. Struct. Theochem* **2007**, *811*, 135-140.
6. Trost, B. M., Palladium-Catalyzed Cycloisomerizations of Enynes and Related Reactions. *Acc. Chem. Res.* **1990**, *23*, 34-42.
7. Widenhoefer, R. A., Synthetic and Mechanistic Studies of the Cycloisomerization and Cyclization/hydrosilylation of Functionalized Dienes Catalyzed by Cationic Palladium(II) Complexes. *Acc. Chem. Res.* **2002**, *35*, 905-913.
8. Leach, A. G.; Wang, R. X.; Wohlhieter, G. E.; Khan, S. I.; Jung, M. E.; Houk, K. N., Theoretical Elucidation of Kinetic and Thermodynamic Control of Radical Addition Regioselectivity. *J. Am. Chem. Soc.* **2003**, *125*, 4271-4278.
9. Luft, J. A. R.; Winkler, T.; Kessabi, F. M.; Houk, K. N., Substituent Effects on the Rearrangements of Cyclohexyl to Cyclopentyl Radicals Involving Avermectin-Related Radicals. *J. Org. Chem.* **2008**, *73*, 8175-8181.
10. Krenske, E. H.; Pryor, W. A.; Houk, K. N., Mechanism of S<sub>H</sub>2 Reactions of Disulfides: Frontside vs Backside, Stepwise vs Concerted. *J. Org. Chem.* **2009**, *74*, 5356-5360.
11. Krenske, E. H.; Agopcan, S.; Ayiyente, V.; Houk, K. N.; Johnson, B. A.; Holmes, A. B., Causation in a Cascade: The Origins of Selectivities in Intramolecular Nitrone Cycloadditions. *J. Am. Chem. Soc.* **2012**, *134*, 12010-12015.

12. Fischer, H.; Radom, L., Factors Controlling the Addition of Carbon-Centered Radicals to Alkenes - An Experimental and Theoretical Perspective. *Angew. Chem. Int. Ed.* **2001**, *40*, 1340-1371.
13. Sung, K. S.; Wang, Y. Y., Mn(III)-Based Oxidative Free-radical Cyclizations of Substituted Allyl  $\alpha$ -methyl- $\beta$ -ketoesters: Syntheses, DFT Calculations, and Mechanistic Studies. *J. Org. Chem.* **2003**, *68*, 2771-2778.
14. Shanks, D.; Berlin, S.; Besev, M.; Ottosson, H.; Engman, L., On the Origin of cis Selectivity in the Cyclization of N-Protected 2-Substituted 3-Aza-5-hexenyl Radicals: A Density Functional Study. *J. Org. Chem.* **2004**, *69*, 1487-1491.
15. Pinter, B.; De Proft, F.; Van Speybroeck, V.; Hemelsoet, K.; Waroquier, M.; Chamorro, E.; Veszpremi, T.; Geerlings, P., Spin-Polarized Conceptual Density Functional Theory Study of the Regioselectivity in Ring Closures of Radicals. *J. Org. Chem.* **2007**, *72*, 348-356.
16. Yu, Y. Y.; Fu, Y.; Xie, M.; Liu, L.; Guo, Q. X., Controlling Regioselectivity in Cyclization of Unsaturated Amidyl Radicals: 5-Exo versus 6-Endo. *J. Org. Chem.* **2007**, *72*, 8025-8032.
17. Sandhiya, L.; Kolandaivel, P.; Senthilkumar, K., Reaction Mechanism and Kinetics of the Atmospheric Oxidation of 1,4-Thioxane by NO<sub>3</sub> — A Theoretical Study. *Can. J. Chem.* **2012**, *90*, 384-394.
18. Musa, O. M.; Horner, J. H.; Shahin, H.; Newcomb, M., A Kinetic Scale for Dialkylaminyl Radical Reactions. *J. Am. Chem. Soc.* **1996**, *118*, 3862-3868.
19. Halgren, T. A.; Roberts, J. D.; Horner, J. H.; Martinez, F. N.; Tronche, C.; Newcomb, M., Kinetics and Equilibrium Constants for Reactions of  $\alpha$ -Phenyl-substituted Cyclopropylcarbinyl Radicals. *J. Am. Chem. Soc.* **2000**, *122*, 2988-2994.
20. Allen, F. H. K., O., 3D Search and Research Using the Cambridge Structural Database. *Chem. Design Automation News* **1993**, *8*, 1 & 31-37.
21. Wei, Y. Y.; Tinant, B.; Declercq, J. P.; Van Meerssche, M., Structures of 4 Para-substituted 1,1-diphenylethylene Derivatives - 4,4'-ethylenedibenzonitrile (i) - 4,4'-ethylenedianisole (ii) - Para-(1-phenylethylene)anisole (iii) and N,N-dimethyl-4-(1-para-nitrophenylethylene)aniline (iv). *Acta Crystallogr. Sect. C: Cryst. Struct. Commun.* **1987**, *43*, 86-89.
22. Leardini, R.; Tundo, A.; Zanardi, G.; Pedulli, G. F., An Electron Spin Resonance Investigation of  $\beta$ -Substituted 1,1-Diphenylethyl Radicals. *J. Chem. Soc., Perkin Trans. 2* **1983**, 285-290.

23. Bernardi, F.; Guerra, M.; Pedulli, G. F., Theoretical Interpretation of Rotational Barrier in Benzophenone Ketyl. *J. Phys. Chem.* **1974**, *78*, 2144-2148.
24. Luo, Y.-R., *Handbook of Bond Dissociation Energies in Organic Compounds*. CRC Press LLC: Boca Raton, 2003; p 31.
25. Choi, J.; Tang, L. H.; Norton, J. R., Kinetics of Hydrogen Atom Transfer from ( $\eta^5$ -C<sub>5</sub>H<sub>5</sub>)Cr(CO)<sub>3</sub>H to Various Olefins: Influence of Olefin Structure. *J. Am. Chem. Soc.* **2007**, *129*, 234-240.
26. Tsimelzon, A.; Braslau, R., Radical [n+1] Annulations with Sulfur Dioxide. *J. Org. Chem.* **2005**, *70*, 10854-10859.
27. Bullock, R. M.; Rappoli, B. J., Preparation and Reactions of Mn<sub>2</sub>(CO)<sub>9</sub>( $\eta^1$ -aldehyde) Complexes. *J. Am. Chem. Soc.* **1991**, *113*, 1659-1669.
28. Wallace, G. A.; Heathcock, C. H., Further Studies of the Daphniphyllum Alkaloid Polycyclization Cascade. *J. Org. Chem.* **2001**, *66*, 450-454.
29. Curran, D. P.; Liu, H., 4+1 Radical Annulations with Isonitriles: A Simple Route to Cyclopenta-fused Quinolines. *J. Am. Chem. Soc.* **1991**, *113*, 2127-2132.
30. Thornton, A. R.; Martin, V. I.; Blakey, S. B.,  $\pi$ -Nucleophile Traps for Metallonitrene/Alkyne Cascade Reactions: A Versatile Process for the Synthesis of  $\alpha$ -Aminocyclopropanes and  $\beta$ -Aminostyrenes. *J. Am. Chem. Soc.* **2009**, *131*, 2434-2435.
31. Beckwith, A. L. J.; Schiesser, C. H., Regio- and Stereo-Selectivity of Alkenyl Radical Ring Closure: A Theoretical Study. *Tetrahedron* **1985**, *41*, 3925-3941.
32. Spellmeyer, D. C.; Houk, K. N., A Force-Field Model for Intramolecular Radical Additions. *J. Org. Chem.* **1987**, *52*, 959-974.
33. Jorgenson, M. J.; Brattesani, A. J.; Thacher, A. F., Stereochemical Studies in Substituted Cyclopentanecarboxylates. *J. Org. Chem.* **1969**, *34*, 1103-1105.

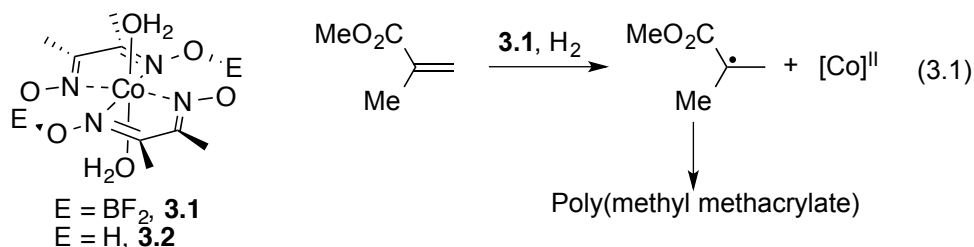
## CHAPTER 3: KINETICS OF COBALOXIME-CATALYZED

### HYDROGEN ATOM TRANSFER<sup>1</sup>

#### 3.1 Cobaloximes under H<sub>2</sub> as a New Hydrogen Atom Source for Hydrogen Atom Transfer (HAT)

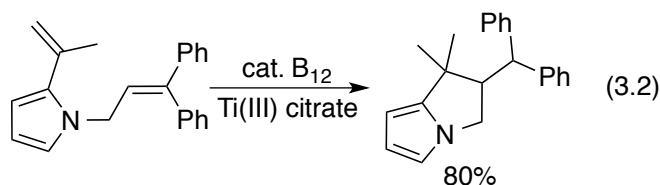
In light of the discussion in Chapter 1, it is important to find new hydrogen atom sources that are suitable for hydrogen atom transfer (HAT) and can thus replace tin hydrides in synthesis. As was noted in Chapter 1 and Chapter 2, HCr(CO)<sub>3</sub>Cp and HV(CO)<sub>4</sub>(P-P) have proven to be good hydrogen atom sources for HAT<sup>1-3</sup> and have been shown to carry out radical cyclizations.<sup>3-7</sup> With HCr(CO)<sub>3</sub>Cp, the reaction is catalytic, as HCr(CO)<sub>3</sub>Cp can be regenerated from •Cr(CO)<sub>3</sub>Cp with H<sub>2</sub>,<sup>8,9</sup> but HAT is relatively slow. With HV(CO)<sub>4</sub>(P-P), HAT is faster, but cyclizations can be effected only stoichiometrically because the V-H bond is too weak for •V(CO)<sub>4</sub>(P-P) to cleave H<sub>2</sub>. Both the Cr and V hydrides are air-sensitive and thermally unstable.

The possibility that Co complexes might catalyze the generation of radicals from H<sub>2</sub> was suggested by the 2006 report<sup>10</sup> that the macrocyclic Co<sup>II</sup> complex (H<sub>2</sub>O)<sub>2</sub>Co(dmgBF<sub>2</sub>)<sub>2</sub> (**3.1**) (dmg = dimethylglyoximate) could initiate the polymerization of acrylates under H<sub>2</sub> gas (eq 3.1).

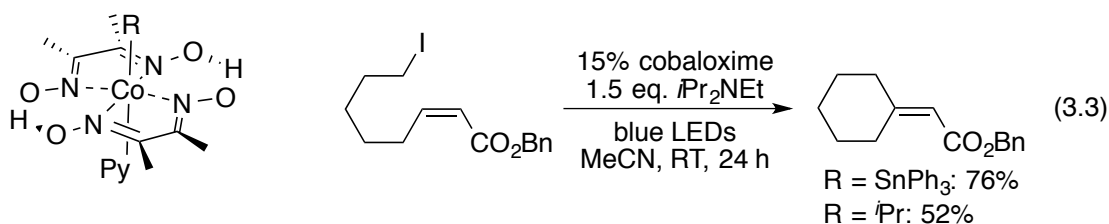


<sup>1</sup> Part of this work has been published in Li, G.; Han, A.; Pulling, M. E.; Estes, D. P.; Norton, J. R., Evidence for Formation of a Co-H Bond from (H<sub>2</sub>O)<sub>2</sub>Co(dmgBF<sub>2</sub>)<sub>2</sub> under H<sub>2</sub>: Application to Radical Cyclizations. *J. Am. Chem. Soc.* **2012**, *134*, 14662-14665 and Li, G.; Estes, D. P.; Norton, J. R.; Ruccolo, S.; Sattler, A.; Sattler, W., Dihydrogen Activation by Cobaloximes with Various Axial Ligands. *Inorg. Chem.* **2014**, *53*, 10743-10747.

Such “cobaloximes” are air- and moisture-stable solids that are widely accepted as models for vitamin B<sub>12</sub>. Indeed, van der Donk has shown that vitamin B<sub>12</sub> itself can catalyze radical cyclizations with Ti<sup>III</sup> as the stoichiometric reductant (eq 3.2).<sup>11</sup>



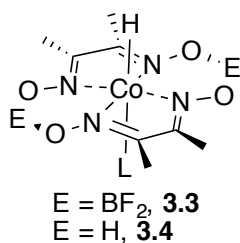
Carreira has shown that photolysis of cobaloxime complexes generates a catalyst for the cyclization of unsaturated alkyl iodides (eq 3.3).<sup>12</sup>



A Co<sup>III</sup> hydride is probably formed in all three of these reactions: in reaction 3.1 from H<sub>2</sub>, in reaction 3.2 by protonation of the Co<sup>I</sup> vitamin B<sub>12</sub> anion, and in reaction 3.3 from an alkyl–Co<sup>III</sup> intermediate.

Cobaloxime hydrides (**3.3** and **3.4**, Figure 3.1), and the hydrides of similar tetraazamacrocyclic complexes, have been proposed as intermediates in the operation of Co catalysts for H<sub>2</sub> evolution. Important recent work in this area has come from Gray,<sup>13-16</sup> Peters,<sup>16-20</sup> Eisenberg,<sup>21, 22</sup> Fontecave,<sup>23, 24</sup> Sun,<sup>24-28</sup> Alberto,<sup>29-32</sup> Bakac,<sup>33</sup> and Tiede.<sup>34</sup>

**Figure 3.1** Structures of Cobaloxime Hydrides

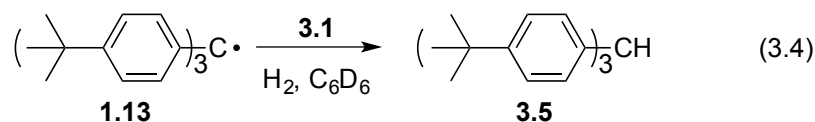


Schrauzer and co-workers reported a reaction between cobaloxime **3.2** and H<sub>2</sub>,<sup>35</sup> and there were subsequent studies of the kinetics of H<sub>2</sub> uptake by **3.2** in the presence of various acceptors, including Schiff bases,<sup>36, 37</sup> the dmgH ligand itself,<sup>38-41</sup> and styrene.<sup>42</sup> However, no spectroscopic data were reported for the dmgBF<sub>2</sub> hydridocobaloxime **3.3** with L = H<sub>2</sub>O until 2010, when Szajna-Fuller and Bakac assigned a peak at 608 nm to **3.3** in water.<sup>33</sup> This peak is close to, but less intense than, the peak at 610 nm assigned to [Co<sup>I</sup>(dmgBF<sub>2</sub>)<sub>2</sub>]<sup>-</sup>.<sup>33</sup> In order to confirm that cobaloxime hydride **3.3** is generated under H<sub>2</sub> we set out to trap it from the reaction of cobaloxime **3.1** with H<sub>2</sub>.

### 3.2 Kinetic Study of Hydrogen Atom Transfer (HAT) from Cobaloximes under H<sub>2</sub> to Organic Radicals

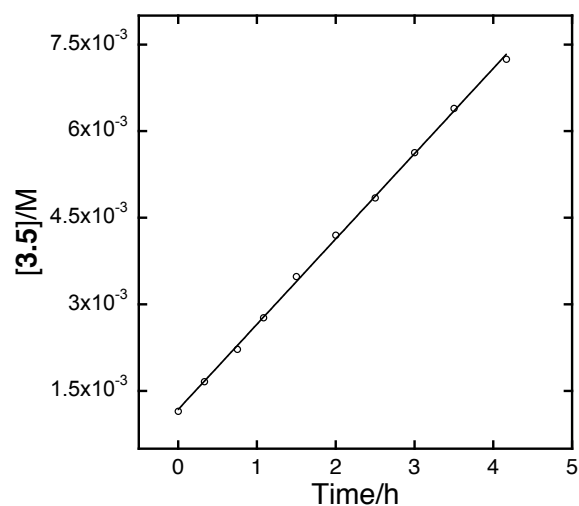
As noted in Chapter 1, the tris(*p*-*tert*-butylphenyl)methyl radical (trityl radical **1.13**) is good to study rates of HAT from various transition-metal hydrides,<sup>43-46</sup> and thus was used in the present case.

Indeed, **1.13** was converted to tris(*p*-*tert*-butylphenyl)methane (**3.5**) in the presence of **3.1** and H<sub>2</sub> (eq 3.4). No **3.5** was observed unless both **3.1** and H<sub>2</sub> were present.



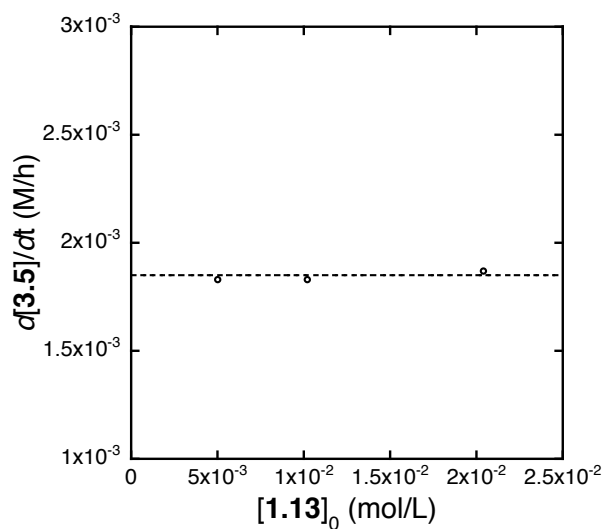
The cobaloxime **3.1** catalyzes the reaction between trityl radical **1.13** and H<sub>2</sub>, presumably via cobalt hydride **3.3**. When reaction 3.4 was monitored by NMR spectroscopy under constant H<sub>2</sub> pressure, the rate of formation of **3.5** did not change with time (Figure 3.2); the reaction is thus *zero order* in **1.13**.

**Figure 3.2.** Cobaloxime-Mediated Formation of **3.5** from **1.13** under 2.4 atm H<sub>2</sub> in C<sub>6</sub>D<sub>6</sub> at 295 K (eq 3.4) ([**3.1**] = 7.60 × 10<sup>-4</sup> M, [**1.13**]<sub>0</sub> = 1.02 × 10<sup>-2</sup> M)



We confirmed this by showing that the rate  $d[\mathbf{3.5}]/dt$  was independent of the initial concentration of **1.13** (Figure 3.3).

**Figure 3.3.** Plot of  $d[\mathbf{3.5}]/dt$  vs [**1.13**]<sub>0</sub>: Rate of HAT with different [**1.13**]<sub>0</sub> under the same reaction conditions ([**3.1**] = 7.60 × 10<sup>-4</sup> mol•L<sup>-1</sup>; H<sub>2</sub>: 3.0 atm; C<sub>6</sub>D<sub>6</sub>)





We then studied reaction 3.4 at various  $H_2$  pressures and various concentrations of **3.1**.<sup>2</sup> During a given reaction,  $[H_2]$  remained constant because it was present in substantial excess, and **[3.1]** remained constant because it was regenerated. The reaction proved to be *first order* in  $H_2$  (Figure 3.4) and *second order* in cobalt (Figure 3.5).

**Figure 3.4.** Rate  $d[\mathbf{3.5}]/dt$  of eq 3.4 vs  $[H_2]$  at 295 K in  $C_6D_6$

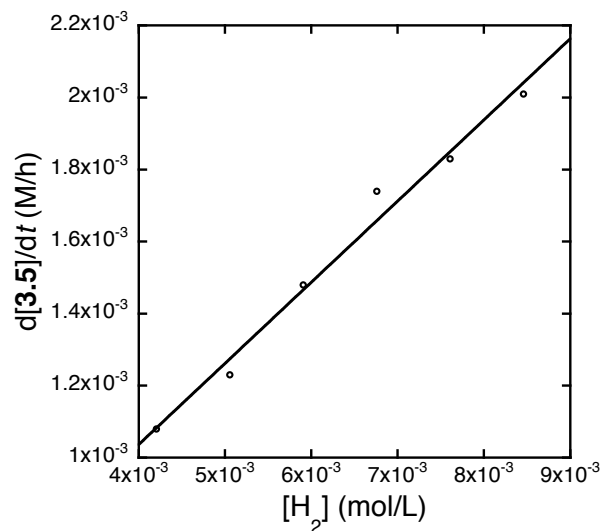
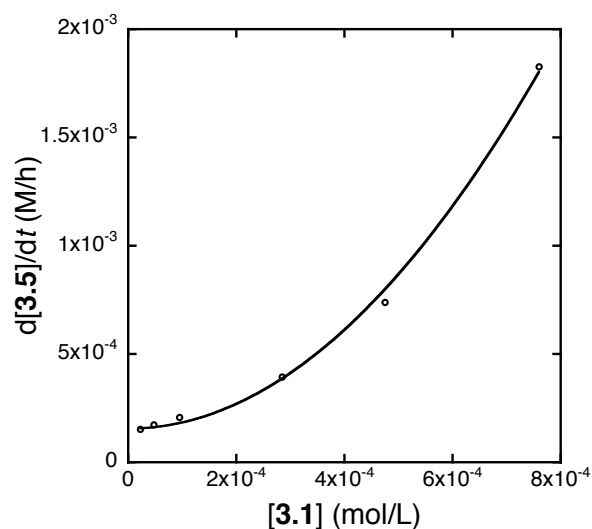


**Figure 3.5.** Rate  $d[\mathbf{3.5}]/dt$  of eq 3.4 vs **[3.1]** at 295 K in  $C_6D_6$



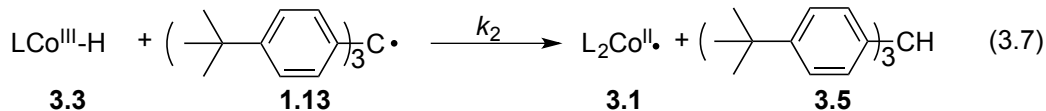
<sup>2</sup> See Appendix II for details of kinetic measurements.

These results suggest efficient trapping of hydride **3.3** by trityl radical **1.13** and rate-limiting activation of H<sub>2</sub> by **3.1**, that is, the rate law in eq 3.5, which is the same as the rate law reported earlier for catalysis of H<sub>2</sub> uptake by **3.2**.<sup>39, 41, 42, 47</sup>

$$\frac{d[\mathbf{3.5}]}{dt} = k[\mathbf{3.1}]^2[\text{H}_2] \quad (3.5)$$

This rate law suggests the mechanism in Scheme 3.1 with large  $k_2$  and small  $k_1$ .

**Scheme 3.1.** Mechanism of Cobaloxime-Mediated Formation of **3.5** from **1.13**



From Figure 3.4 and the value of  $[\mathbf{3.1}]^2$  we obtain a  $k_1$  value of 108(7) M<sup>-2</sup> s<sup>-1</sup> (Appendix II), and from Figure 3.5 and the value of  $[\text{H}_2]$ <sup>48, 49</sup> we obtain a  $k_1$  value of 104(3) M<sup>-2</sup> s<sup>-1</sup> (Appendix II), implying that  $k_1$  is 106(3) M<sup>-2</sup> s<sup>-1</sup> at 295 K.<sup>3</sup> The first step, eq 3.6 in Scheme 3.1, is analogous to those for the activation of H<sub>2</sub> by other metalloradicals, such as •Co(CN)<sub>5</sub><sup>3-</sup> (Halpern),<sup>50</sup> •Rh(TMP) (Wayland, TMP = tetramesitylporphyrin),<sup>51</sup> •Cr(CO)<sub>3</sub>Cp\* (Hoff),<sup>52</sup> •Cr(CO)<sub>3</sub>Cp (Franz),<sup>9</sup> and •W(CO)<sub>2</sub>(NHC)Cp (Bullock).<sup>53, 54</sup>

Of course the value of  $k_1$  should be independent of the nature as well as the concentration of the trapping radical. We therefore replaced **1.13** by TEMPO radical (2,2,6,6-tetramethylpiperidine N-oxyl radical, **3.6**), giving eq 3.8. We examined the rate of eq 3.8 with  $[\mathbf{3.1}] = 7.60 \times 10^{-4}$  M and P<sub>H<sub>2</sub></sub> = 3.0 atm (Figure 3.6).

<sup>3</sup> The concentration of hydrogen was calculated by Henry's law from its pressure; the Henry's constant at 295K was calculated to be 399.6 atm/M by extrapolation from numbers reported at other temperatures, see refs 48 and 49

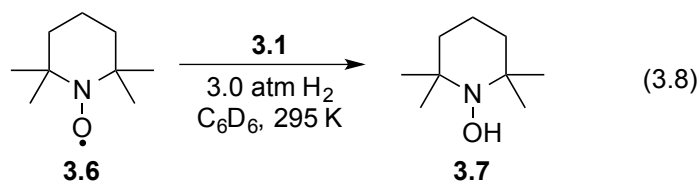
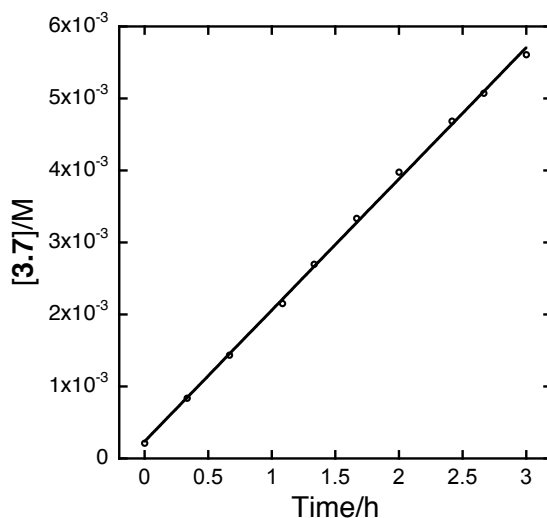


**Figure 3.6.** Rate  $d[3.6]/dt$  of eq 3.8 vs  $[3.1]$  at 295 K in  $C_6D_6$



With  $[3.6] = 0.116$  M, the rate  $d[3.7]/dt$  was found to be  $1.82(2) \times 10^{-3}$  M/h, implying a  $k_1$  value of  $115(1) \text{ M}^{-2} \text{ s}^{-1}$ , almost the same as that found with various concentrations of **1.13**. This result is consistent with the mechanism in Scheme 3.1.

### 3.3 Axial Ligand Effect on Hydrogen Atom Transfer (HAT) from Cobaloximes under $H_2$ to Organic Radicals

It has been suggested that the ability of cobaloximes to catalyze the production of  $H_2$  from protons is substantially affected by the nature of their axial ligands.<sup>25, 55</sup> It is reasonable to suggest that HAT from cobaloximes under  $H_2$  to organic radicals is also affected by the axial ligands. We have thus examined the effect of axial ligands on the ability of cobaloximes to catalyze hydrogenations like the one in reaction 3.4.

### 3.3.1 Structures of cobaloximes

In both solution and solid state, cobaloximes exist as planar macrocyclic complexes with axial ligands L,  $\text{Co}(\text{dmgE})_2\text{L}_n$  ( $\text{E} = \text{BF}_2$  or H,  $n = 1, 2$ ). When L is a coordinating solvent molecule, the  $\text{L} = 2$  form  $\text{Co}(\text{dmgE})_2\text{L}_2$  dominates and the axial ligands are easily exchanged. However,  $\text{Co}(\text{dmgH})_2\text{L}_2$  suffers decomposition from the hydrogenation of dmgligand,<sup>36, 38</sup> thus only cobaloximes with  $\text{BF}_2$  will be discussed in this section.

$\text{Co}(\text{dmgBF}_2)_2(\text{MeOH})_2$  (**3.8**) and its X-ray structure have been reported,<sup>56</sup> and  $\text{Co}(\text{dmgBF}_2)_2(\text{MeCN})_2$  (**3.9**) has been characterized by UV-vis spectroscopy in  $\text{CH}_3\text{CN}$  solution.<sup>18</sup> We have also prepared crystals of  $\text{Co}(\text{dmgBF}_2)_2(\text{MeCN})_2$  and  $\text{Co}(\text{dmgBF}_2)_2(\text{THF})_2$  (**3.10**) and have confirmed by X-ray diffraction that they have the structures below (Figure 3.7 and Figure 3.8), with the two ligands L coordinated axially as in the MeOH complex. Selected bond distances for the MeOH, THF, and  $\text{CH}_3\text{CN}$  complexes are shown in Table 3.1. The preparation of  $\text{Co}(\text{dmgBF}_2)_2(\text{H}_2\text{O})_2$  (**3.1**) was unsuccessful due to the low solubility of the cobaloxime in water.

**Figure 3.7.** Molecular structure of  $\text{Co}(\text{dmgBF}_2)_2(\text{CH}_3\text{CN})_2$  (**3.9**, 50% ellipsoids, hydrogen atoms omitted for clarity)

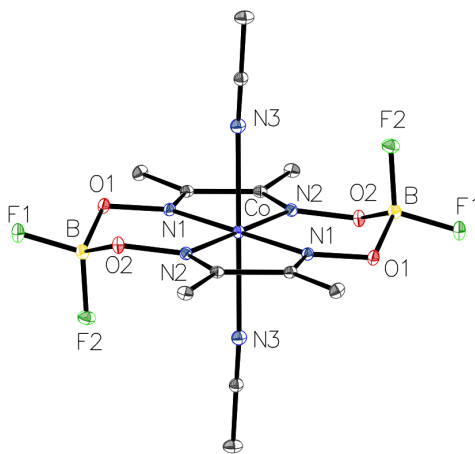


**Figure 3.8.** Molecular structure of  $\text{Co}(\text{dmgBF}_2)_2(\text{THF})_2$  (**3.10**, 50% ellipsoids, hydrogen atoms omitted for clarity)

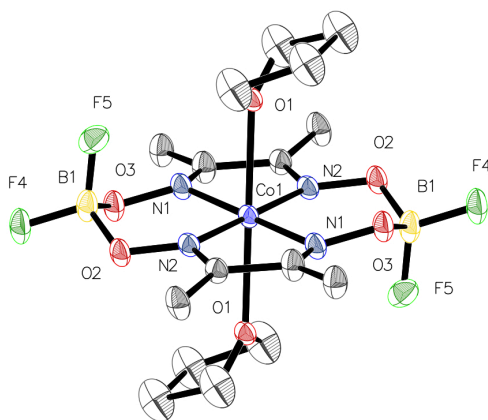


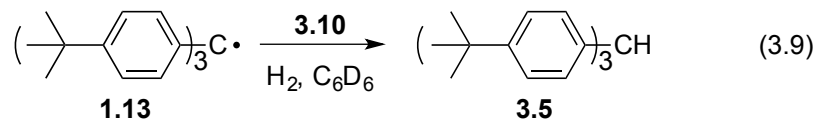
**Table 3.1.** Selected bond lengths of  $\text{Co}(\text{dmgBF}_2)_2\text{L}_2$

compounds	M–L (Å)	M–N (Å)	N=C (Å)	C–C (Å)	ref
$\text{Co}(\text{dmgBF}_2)_2(\text{MeCN})_2$ <b>3.9</b>	2.260	1.878	1.297	1.479	this work
$\text{Co}(\text{dmgBF}_2)_2(\text{MeOH})_2$ <b>3.8</b>	2.264	1.877	1.270	1.473	56
$\text{Co}(\text{dmgBF}_2)_2(\text{THF})_2$ <b>3.10</b>	2.324	1.890	1.299	1.483	this work

EPR studies have shown that stronger  $\sigma$ -donor ligands (e.g.,  $\text{Ph}_3\text{P}$ , pyridine) form cobaloxime complexes with only a single axial ligand ( $L = 1$ ).<sup>57</sup> In toluene/ $\text{CH}_2\text{Cl}_2$   $\text{Co}(\text{dmgBF}_2)_2(\text{py})_2$  is only formed in the presence of a 10-fold excess of py,<sup>57</sup> although EPR has shown that  $\text{Co}(\text{dmgBF}_2)_2(\text{py})_2$  is also formed when a frozen matrix of  $\text{Co}(\text{dmgBF}_2)_2$  is allowed to warm to room temperature.<sup>58</sup>

### 3.3.2 Kinetics of HAT from Cobaloximes under H<sub>2</sub> to Trityl Radical

I first examined the kinetics of the hydrogenation of trityl radical **1.13** in benzene with Co(dmgbF<sub>2</sub>)<sub>2</sub>(THF)<sub>2</sub> (**3.10**) as a catalyst (eq 3.9).



The rate is once again independent of [**1.13**] (Figure 3.9), first-order (Figure 3.10) in [H<sub>2</sub>], and second-order (Figure 3.11) in [Co<sub>Tot</sub>], where [Co<sub>Tot</sub>] is the concentration of **3.10** initially added.

**Figure 3.9.** Co(dmgbF<sub>2</sub>)<sub>2</sub>(THF)<sub>2</sub>-Mediated Formation of **3.5** under 2.4 atm H<sub>2</sub> in C<sub>6</sub>D<sub>6</sub> at 295 K (eq 3.9) ([**3.10**] = 3.80 × 10<sup>-4</sup> M and [**1.13**]<sub>0</sub> = 1.02 × 10<sup>-2</sup> M)

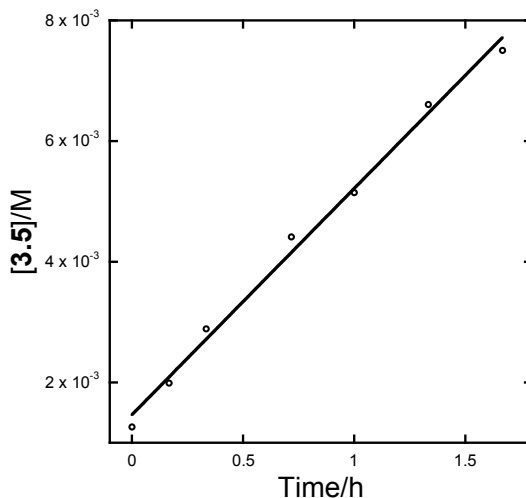


**Figure 3.10.** Rate  $d[3.5]/dt$  of eq 3.9 vs  $[H_2]$  at 295 K in  $C_6D_6$

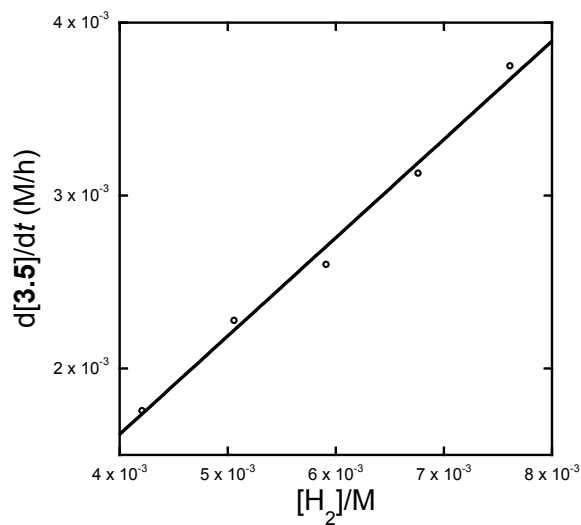
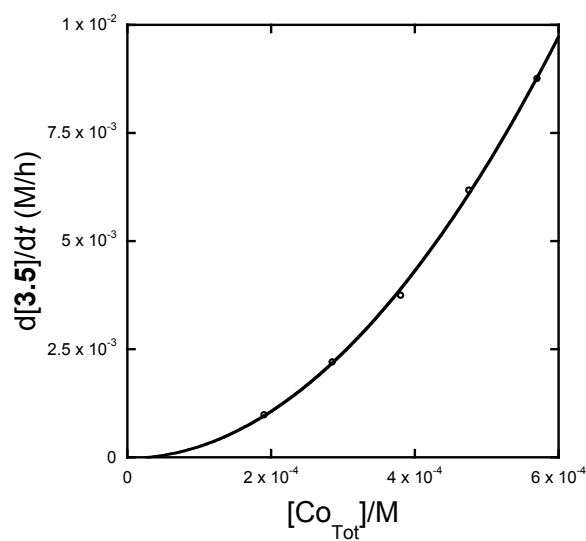


**Figure 3.11.** Rate  $d[3.5]/dt$  of eq 3.9 vs  $[Co_{Tot}]$  at 295 K in  $C_6D_6$



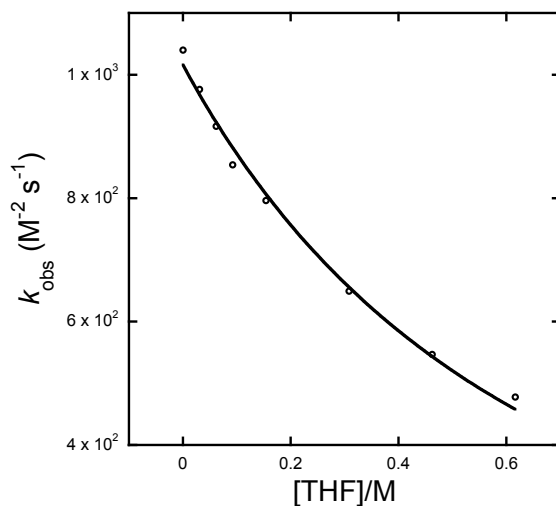
From the above kinetic studies the rate law in eq 3.10 can be obtained.

$$\frac{d[3.5]}{dt} = k[Co_{Tot}]^2[H_2] \quad (3.10)$$

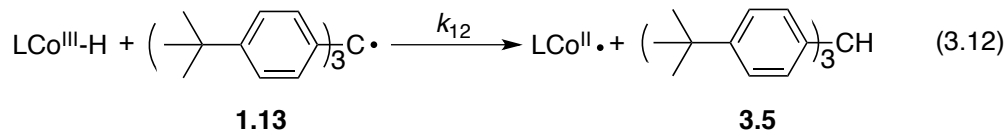
The data in Figure 3.10 and Figure 3.11 give a third-order rate constant  $k$  (defined in eq 3.10) of  $1.04(6) \times 10^3 M^{-2} s^{-1}$ . Experiments in  $C_6D_6$  with different concentrations of added THF (Figure 3.12) show that the reaction is inhibited by that ligand, suggesting a dissociative pre-equilibrium (with equilibrium constant  $K$ ) similar to that that shown in

Scheme 3.2. Subsequent H<sub>2</sub> activation and H• transfer steps, similar to those found in the previous section (Scheme 3.1) with Co(dmgBF<sub>2</sub>)<sub>2</sub>(H<sub>2</sub>O)<sub>2</sub> (**3.1**), complete a plausible mechanism.

**Figure 3.12.** Rate d[**3.5**]/dt of eq 3.9 vs [THF] at 295 K in C<sub>6</sub>D<sub>6</sub>



**Scheme 3.2.** Revised Mechanism of Cobaloxime-Mediated Formation of **3.5**



The data with added THF fit the rate law in eq 3.13 if  $k_{11}$  is  $1.02(1) \times 10^3 \text{ M}^{-2} \text{ s}^{-1}$  and  $K$  is 1.26(6) M. The results of similar experiments with MeOH in C<sub>6</sub>D<sub>6</sub> fit the same rate law if  $k_{11}$  is  $346(7) \text{ M}^{-2} \text{ s}^{-1}$  and  $K$  is 0.128(6) M, respectively (see Appendix III). The larger dissociation constant  $K$  for L = THF does correlate with the longer M–O distance in the THF adduct (see Table 3.1). In neither case is there any evidence for dissociation of the second ligand.



$$\frac{d[\mathbf{3.5}]}{dt} = k_{11} \left( \frac{K[\text{Co}_{\text{Tot}}]}{K + [\text{L}]} \right)^2 [\text{H}_2] \quad (3.13)$$

It is clear that the nature and concentration of free axial ligand L affect both  $K$  and  $k_{11}$  (see Table 3.2). It is, unfortunately, impractical to determine these constants for other ligands from the kinetics of the formation of **3.5**. For example, with  $\text{L} = \text{CH}_3\text{CN}$ , the rate of the reaction with  $\text{H}_2$  is negligible; with  $\text{L} = \text{H}_2\text{O}$  the low solubility of water in benzene makes the determination of  $K$  impractical.

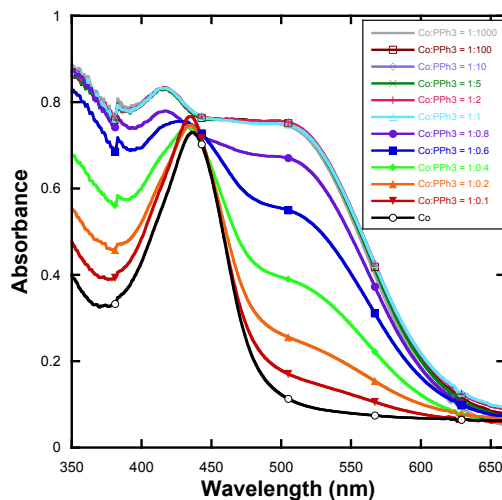
**Table 3.2.** Equilibrium Constant  $K$  and Rate Constants  $k$  and  $k_{11}$  with Different Axial Ligands and M-L bond distances<sup>a</sup>

Ligand	THF	MeOH	$\text{PPh}_3^b$	$\text{H}_2\text{O}$	MeCN
$k_{11}(\text{M}^{-2} \text{s}^{-1})$	$1.02(1) \times 10^3$	346(7)	37(5)	–	–
$k(\text{M}^{-2} \text{s}^{-1})^a$	$1.04(6) \times 10^3$	343(7)	37(5)	106(3)	<16 <sup>c</sup>
$K(\text{M})$	1.26(6)	0.128(6)	–	–	–
M–L (Å)	2.324	2.264	–	–	2.260

<sup>a</sup>For each axial ligand the cobaloxime concentrations used in the measurement of  $k$  are given in Appendix III. For all axial ligands other than  $\text{PPh}_3$  and  $\text{CH}_3\text{CN}$  the rate and equilibrium constants were measured at 295 K in  $\text{C}_6\text{D}_6$ . <sup>b</sup>These rate constants ( $k$  and  $k_{11}$ ) do not differ for  $\text{PPh}_3$  as there is no coordination of a sixth ligand, *vide infra* were extrapolated from measurements between 45 and 60 °C. <sup>c</sup>Conversion is less than 5% after 48 h at either 295 K or 323 K.

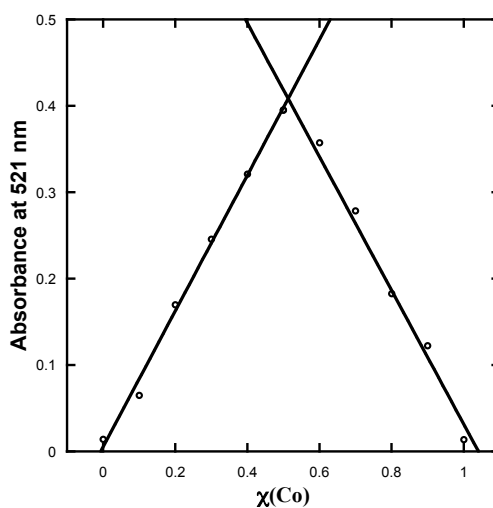
In order to compare  $k_{11}$  for THF and MeOH with the rate constant for a stronger  $\sigma$  donor, the formation of **3.5** was monitored with  $\text{Co}(\text{dmgBF}_2)_2(\text{PPh}_3)$  as the catalyst. However, after many attempts, it was not possible to isolate  $\text{Co}(\text{dmgBF}_2)_2(\text{PPh}_3)$ . Nevertheless, it has been confirmed that a 1:1 adduct is formed in  $\text{CH}_2\text{Cl}_2$  solution – the same conclusion reached in toluene/ $\text{CH}_2\text{Cl}_2$  by the EPR study.<sup>57</sup> The addition of  $\text{PPh}_3$  to a solution of  $\text{Co}(\text{dmgBF}_2)_2(\text{H}_2\text{O})_2$  (**3.1**) changes the UV-Vis spectrum (Figure 3.13), but there are no further changes after 1 equiv of  $\text{PPh}_3$  has been added.

**Figure 3.13.** UV-Vis study of Co + PPh<sub>3</sub> system in CH<sub>2</sub>Cl<sub>2</sub>



A Job plot (Figure 3.14) of the absorbance at 521 nm further confirms the 1:1 stoichiometry.

**Figure 3.14.** Job Plot of Co + PPh<sub>3</sub> system in CH<sub>2</sub>Cl<sub>2</sub>



At 295 K the catalysis of HAT to **1.13** by **3.1**/PPh<sub>3</sub> proved too slow for convenient kinetic measurements, so the reaction was examined at higher temperatures. At 323 K, the reaction (eq 9) was again *zero order* in trityl radical **1.13** (Figure 3.15) but not inhibited by additional Ph<sub>3</sub>P (Figure 3.16).

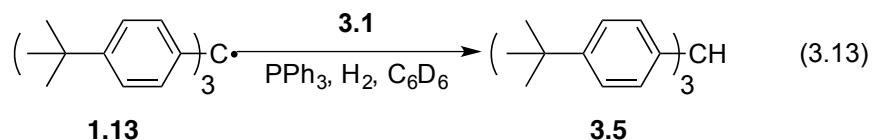


**Figure 3.15.** **3.1**/PPh<sub>3</sub>-Mediated Formation of **3.5** under 3 atm H<sub>2</sub> in C<sub>6</sub>D<sub>6</sub> at 323 K (eq 3.13) ([**3.1**] = 7.60 × 10<sup>-4</sup> M, [**1.13**]<sub>0</sub> = 1.02 × 10<sup>-2</sup> M and [PPh<sub>3</sub>] = 5.73 × 10<sup>-3</sup> M)

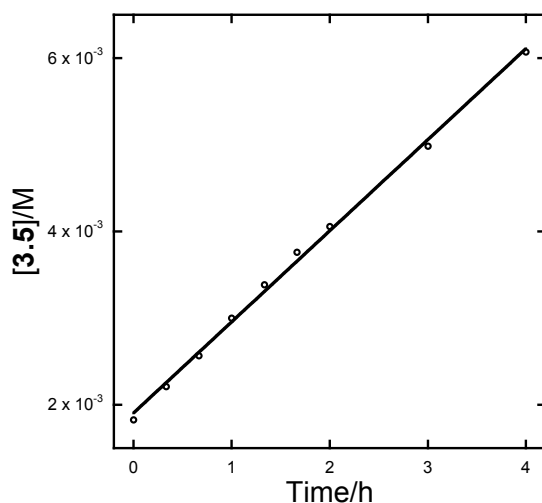
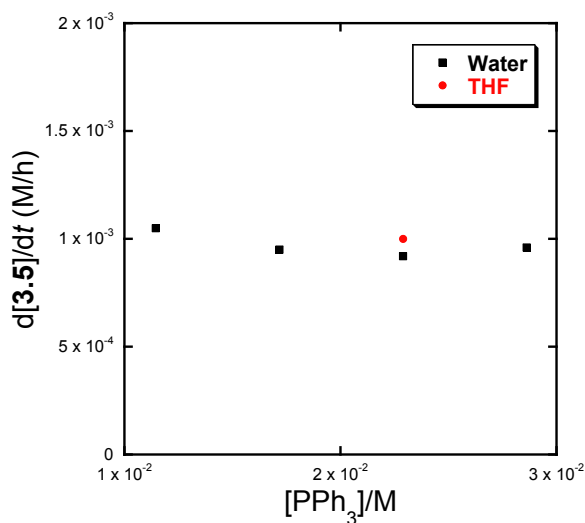


**Figure 3.16.** Rate d[**3.5**]/dt of eq 3.13 vs [PPh<sub>3</sub>] under 3 atm of H<sub>2</sub> in C<sub>6</sub>D<sub>6</sub> at 323 K (The initial concentration of **3.1** and of **3.10** is 3.80 × 10<sup>-4</sup> M, [**1.13**]<sub>0</sub> = 1.02 × 10<sup>-2</sup> M)



The rate constants between 318 and 333 K gave a  $\Delta H^\ddagger$  of 8(1) kcal/mol and a  $\Delta S^\ddagger$  of -23(2) cal mol<sup>-1</sup> K<sup>-1</sup>, similar to the near-zero  $\Delta H^\ddagger$  and negative  $\Delta S^\ddagger$  reported for the activation of H<sub>2</sub> by [Co(CN)<sub>5</sub>]<sup>3-</sup>,<sup>50</sup> Rh(II)(TMP),<sup>51</sup> Cp\*Cr(CO)<sub>3</sub>,<sup>52</sup> and CpCr(CO)<sub>3</sub>.<sup>9</sup>

The extrapolation to 295 K of  $k_{11}$  for  $\text{Co}(\text{dmgBF}_2)_2(\text{PPh}_3)$  gives the value in Table 2 (*vide supra*), showing that  $k_{11}(\text{THF}) > k_{11}(\text{MeOH}) > k_{11}(\text{PPh}_3)$ . The slowness of  $\text{Co}(\text{dmgBF}_2)_2(\text{PPh}_3)$  may be partly the result of its “bowl-shaped” structure, as calculated by Niklas et al.,<sup>57</sup> which will make more difficult a reaction (like eq 3.11) that is *second order* in cobalt. It has been suggested that there is steric hindrance to the approach of a similar phosphine ligand,  $\text{P}(n\text{-Bu})_3$ , to a five-coordinate alkylcobaloxime.<sup>59</sup> Overall it is apparent that  $\text{H}_2$  is best activated by five-coordinate cobalt, with a single axial ligand:  $\text{Co}(\text{dmgBF}_2)_2(\text{THF})$ ,  $\text{Co}(\text{dmgBF}_2)_2(\text{MeOH})$ , or  $\text{Co}(\text{dmgBF}_2)_2(\text{PPh}_3)$ . The  $\text{H}_2$ /cobaloxime reaction is the reverse of the bimolecular mechanism that has been suggested<sup>60</sup> for the evolution of  $\text{H}_2$  from hydrides  $\text{HCo}(\text{dmgBF}_2)_2\text{L}$ .

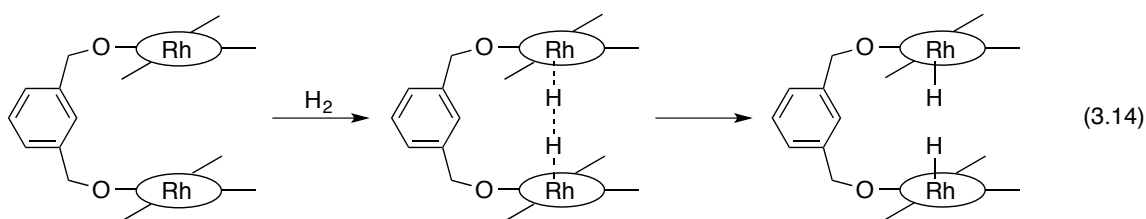
### 3.4 Mechanism of Dihydrogen Activation by Cobaloxime

Although the kinetic study in the above section showed that dihydrogen activation by a cobaloxime is the rate-determining step in eq 3.9, these results did not indicate how cobaloximes cleave  $\text{H}_2$ . The rate law in eq 3.13 suggests that the H–H bond is cleaved by two metal centers, which may involve homolytic or heterolytic mechanisms of  $\text{H}_2$  cleavage (*vide infra*).<sup>61</sup> Kinetic studies of dihydrogen activations by other metalloradicals ( $[\bullet\text{Co}(\text{CN})_5]^{3-}$ ,<sup>50</sup>  $\bullet\text{Rh}(\text{TMP})$ ,<sup>51</sup>  $\bullet\text{Cr}(\text{CO})_3\text{Cp}^*$ ,<sup>52</sup> and  $\bullet\text{Cr}(\text{CO})_3\text{Cp}^9$ ) have given the activation parameters listed in Table 3.3. All of these reactions have relatively large negative activation entropies and small activation enthalpies.

**Table 3.3.** Activation Parameters from Earlier Kinetics Studies of the Reactions of Metalloradicals with H<sub>2</sub>

Metalloradicals	$\Delta H^\ddagger$ (kcal/mol)	$\Delta S^\ddagger$ (cal mol <sup>-1</sup> K <sup>-1</sup> )	Reference
(•Co(CN) <sub>5</sub> ) <sup>3-</sup>	-0.7(5)	-55(5)	50
Rh(TMP)	5(1)	-40(5)	51
•Cr(CO) <sub>3</sub> Cp*	0(1)	-47(3)	52
•Cr(CO) <sub>3</sub> Cp	8	-25	9
Co(dmgbF <sub>2</sub> ) <sub>2</sub> (PPh <sub>3</sub> )	8(1)	-23(2)	this work

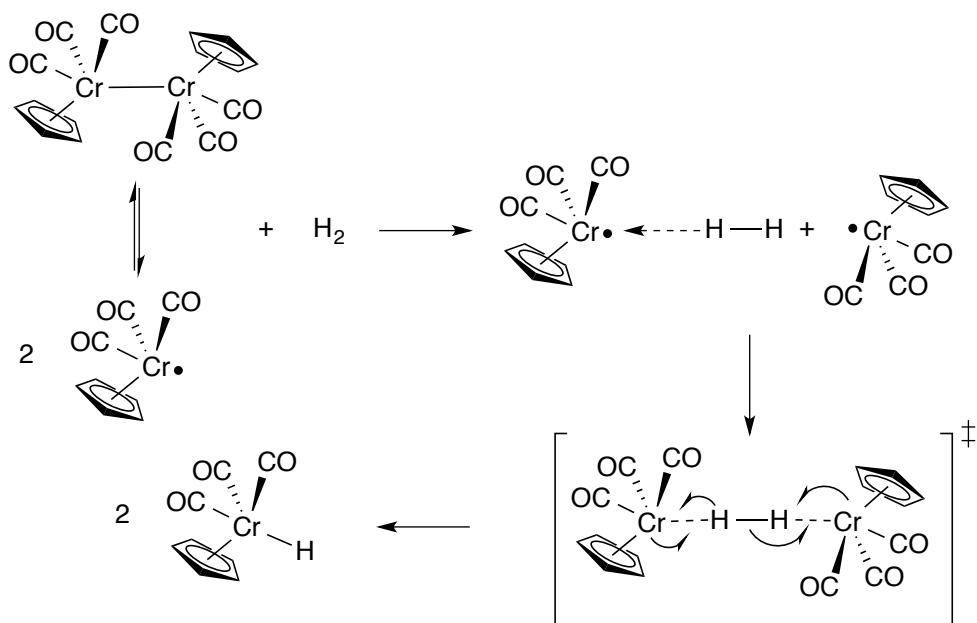
These large negative activation entropies and small activation enthalpies strongly suggest that the H<sub>2</sub> cleavage is entropically controlled, which is consistent with organizing three molecules into a transition state. Wayland has thus proposed an *end-on* transition state (Rh···H···H···Rh) for dihydrogen activation homolytically by Rh(TMP) radical.<sup>51</sup> The Wayland group recently studied dihydrogen activation by a linked Rh porphyrin bimetalloradical system and observed a large H<sub>2</sub> activation rate enhancement (40(6) M<sup>-2</sup> s<sup>-1</sup> at 296 K) when compared to Rh(TMP) (2.7 M<sup>-2</sup> s<sup>-1</sup> at 296 K). These results support the *end-on* transition state (eq 3.14).<sup>62</sup>



However, a heterolytic pathway cannot be simply ruled out by the measured activation parameters. The Norton group (and the late Dr. Jim Franz at PNNL and Dr. Tudor Spataru) studied the mechanism of dihydrogen activation by •Cr(CO)<sub>3</sub>Cp. The •Cr(CO)<sub>3</sub>Cp species is in rapid equilibrium with its dimer Cp(CO)<sub>3</sub>Cr–Cr(CO)<sub>3</sub>Cp. DFT

calculations suggest both homolytic and heterolytic cleavage of H<sub>2</sub> are plausible, although the homolytic pathway is slightly favored.<sup>9</sup> The homolytic pathway involves an *end-on* intermediate and an *end-on* transition state (Scheme 3.3).

**Scheme 3.3.** Homolytic Pathway of Dihydrogen Activation by •Cr(CO)<sub>3</sub>Cp

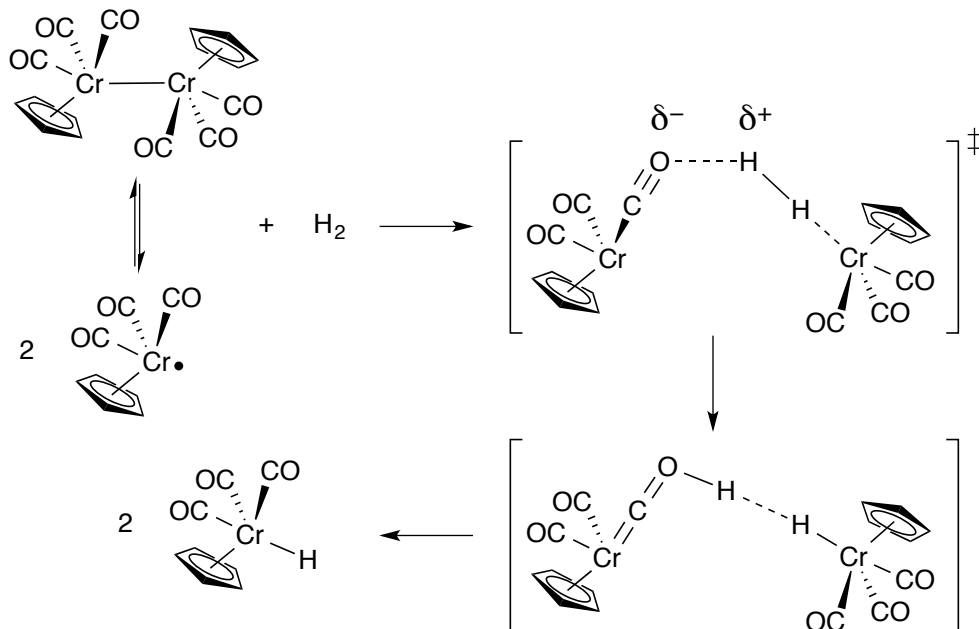


The heterolytic pathway, however, involves an auxiliary base (eq 3.15). Pratt and co-workers have summarized some earlier work on this pathway.<sup>63</sup>



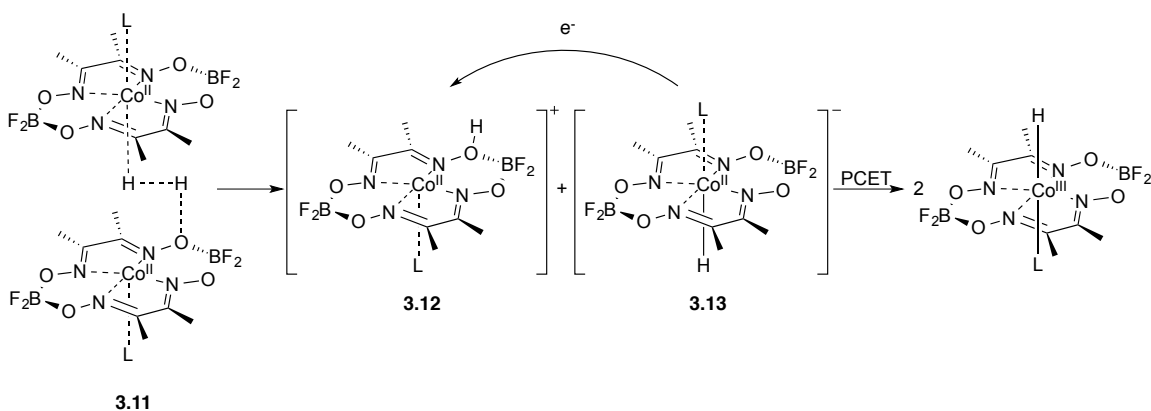
DFT calculations from Dr. Tudor Spataru and Dr. Donald Camaioni (PNNL) suggest a heterolytic pathway, where an oxygen atom of a terminal carbonyl serves as an auxiliary base (Scheme 3.4).<sup>9</sup>

**Scheme 3.4.** Heterolytic Pathway of Dihydrogen Activation by  $\bullet\text{Cr}(\text{CO})_3\text{Cp}$



It seems possible that the oxygen atom in the dmg ligand can also serve as auxiliary base in the  $\text{Co}(\text{dmgBF}_2)_2\text{L}_2$  case, and that a heterolytic cleavage is possible (Scheme 3.5). This mechanism is the microscopic reverse of one proposed by several groups for elimination of  $\text{H}_2$  from cobaloxime hydrides.<sup>15, 17, 18, 21, 22, 64, 65</sup>

**Scheme 3.5.** Heterolytic Pathway of Dihydrogen Activation by  $\text{Co}(\text{dmgBF}_2)_2\text{L}_2$



This mechanism begins with a cofacial  $\text{H}_2$  complex **3.11** related to an  $\text{Ru}_2(\text{H}_2)$  that has been studied by Collman.<sup>66, 67</sup> Complex **3.11** then undergoes heterolytic cleavage to

generate cation **3.12** and anion **3.13**. A proton-coupled electron transfer between **3.12** and **3.13** then gives the desired cobalt hydride species.

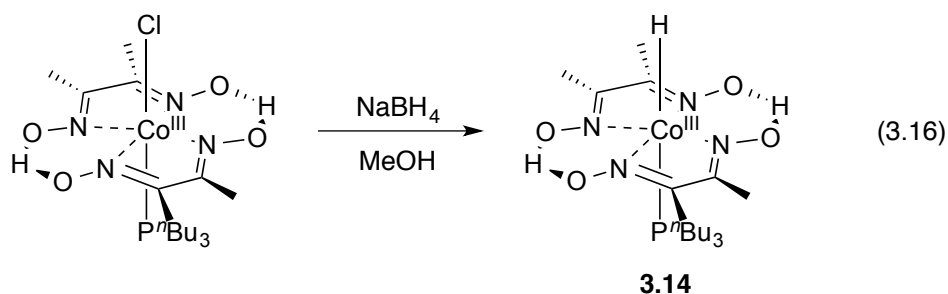
Although the heterolytic mechanism in Scheme 3.5 appears plausible, the homolytic mechanism *cannot* be ruled out since it also follows the rate law in eq 3.3. However, a recent study on cobalt hydride by the Norton group<sup>68</sup> does support the formation of **3.12** (eq 3.17, *vide infra*) that indicates the heterolytic pathway is more likely.

In conclusion, how the cobaloxime activates H<sub>2</sub> remains unclear and needs further studies (probably best by theoretical calculation). We need a better understanding of how metalloradicals cleave H<sub>2</sub>, which will enable us to devise new catalysts for the generation of radicals from olefins/acetylenes and H<sub>2</sub>.

### 3.5 Revisit to the Initially Reported Cobaloxime Hydride

We originally assumed that a cobaloxime hydride was the H• donor that transferred H• to olefins and radicals in our cobalt catalyzed reactions. Often cobaloxime hydrides are thermodynamically unstable and very difficult to observe.<sup>47</sup> In 1971 Schrauzer and co-workers reported the preparation of a cobaloxime hydride HCo(dmgh)<sub>2</sub>(P<sup>n</sup>Bu<sub>3</sub>) (**3.14**) from reduction of ClCo(dmgh)<sub>2</sub>(P<sup>n</sup>Bu<sub>3</sub>) by NaBH<sub>4</sub> (eq 3.16) in MeOH. However, this structure is doubtful because the reported cobalt hydride signal of <sup>1</sup>H NMR at δ 6.0 ppm (vs TMS in *n*-hexane) is much too far downfield for a hydride ligand on a metal center with *d*<sup>6</sup> configuration.<sup>69</sup>

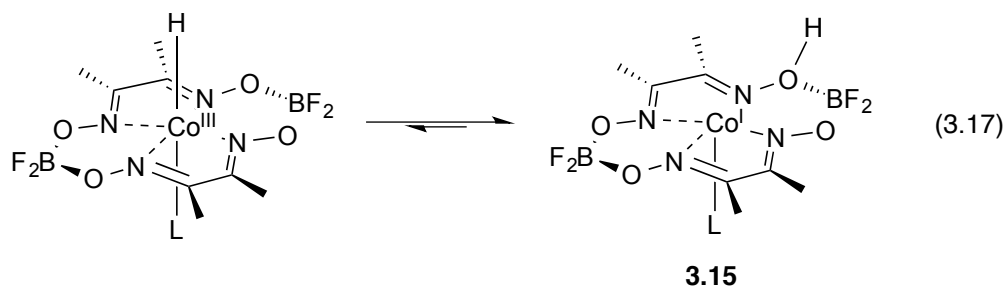




Sun repeated the original procedure and did not observe the same  $^1\text{H}$  NMR that Schrauzer had reported.<sup>70</sup> Sun did obtain a purple complex with a UV-Vis spectrum that varied with temperature and concentration. Sun rationalized this observation by suggesting that  $\text{Co}(\text{dmgH})_2(\text{P}''\text{Bu}_3)$  was in equilibrium with its dimer.

In 2012 Artero and Fontecave predicted from theoretical calculations that the  $^1\text{H}$  NMR of a Co–H resonance in  $\text{HCo}(\text{dmgH})_2(\text{P}''\text{Bu}_3)$  would be upfield of TMS, near  $\delta -5$  ppm.<sup>71</sup> They repeated Schrauzer's procedure and found a signal at  $\delta -5.06$  ppm in  $d_3$ -MeCN. They concluded that  $\text{HCo}(\text{dmgH})_2(\text{P}''\text{Bu}_3)$  could be made but had been mischaracterized.

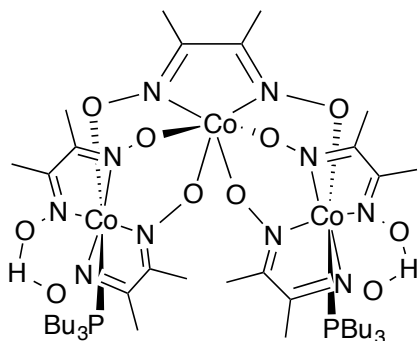
The Norton group (Dr. Deven Estes) attempted to prepare the related hydrides in a different way by treating cobaloximes with high pressures of  $\text{H}_2$ .<sup>68</sup> A broad peak at  $\delta 2.5$  ppm (in  $d_3$ -MeCN) was observed, which disappeared when the  $\text{H}_2$  pressure was released. When the experiment was carried out in solvents with exchangeable deuterium (for instance,  $\text{CD}_3\text{OD}$ ), this peak *did not* appear. Dr. Estes suggested that this peak was the O–H in **3.15**. However, no evidence for a Co–H was ever observed during the high-pressure reaction. Dr. Estes has suggested that the Co–H which may be easily generated under  $\text{H}_2$  pressure; it may quickly tautomerize to **3.15** (eq 3.17).<sup>68</sup>



The Peters group has also repeated the Schrauzer procedure and has agreed that  $\text{HCo}(\text{dmgH})_2(\text{P}^n\text{Bu}_3)$  is not the product of the original reaction.<sup>72</sup> From the reduction they obtained dark-purple crystals (the color of the products Schrauzer and then Sun had obtained). The  $^1\text{H}$  NMR of this product had several broad signals at 25 °C, which significantly sharpened when the sample was cooled to -91 °C. These VT-NMR results imply that this compound is a paramagnetic  $\text{Co}^{\text{II}}$  monomer  $\text{Co}(\text{dmgH})_2(\text{P}^n\text{Bu}_3)$  at room temperature but a dimer at low temperature, which agrees with the earlier suggestion of Sun. More convincingly, they obtained an X-ray quality single crystal of the dimer and found it to have a relatively long Co–Co bond (3.116(2) Å). They confirmed that the product is indeed  $\text{Co}(\text{dmgH})_2(\text{P}^n\text{Bu}_3)$  by adding  $\text{P}^n\text{Bu}_3$  to  $\text{Co}(\text{dmgH})_2(\text{H}_2\text{O})_2$  and obtaining an NMR signal identical with that of product obtained by the previous method. When they treated this isolated dimer with  $\text{H}_2$ , no terminal Co–H signal was observed by either  $^1\text{H}$  NMR or IR. Instead they observed the hydrogenation of ligand, perhaps via the tautomerization in eq 3.17. The Peters group explained the  $\delta$  -5 ppm signal observed by Artero and Fontecave by assigning to a different (not previously observed) compound. A paramagnetic complex is generated if the reduction is not carried out in rigorously air-free conditions. The Peters group obtained a crystal and found it to be a cobalt trimer with two  $\text{Co}^{\text{III}}$  centers and one  $\text{Co}^{\text{II}}$  center. This trimer has all the NMR signals reported

by Artero and Fontecave, including the  $\delta -5$  one that was previously assigned as Co–H (Scheme 3.6).

**Scheme 3.6.** Structure of Paramagnetic Cobalt Trimer



In conclusion, there is no evidence for a stable cobaloxime hydride. It is possible that under  $H_2$  a cobaloxime can be converted to a hydride, but it'll quick transfer  $H^\bullet$  to organic substrates or hydrogenate the cobaloxime ligand if no substrate is present. Both tautomerization and HAT appear to be very fast as is ligand hydrogenation if no external  $H^\bullet$  acceptor is present.

### 3.6 Experiment Details

All manipulations were performed under an argon atmosphere using standard Schlenk or inert atmosphere box techniques. NMR spectra were taken on either a Bruker 300, 400, or 500 MHz spectrometer. IR spectra were taken with a PerkinElmer Spectrum 2000 FT-IR spectrometer. UV-vis spectra were recorded on a Hewlett-Packard spectrophotometer. X-ray diffraction data were collected on a Bruker Apex II diffractometer. Crystal data, data collection, and refinement parameters are summarized in Appendix III. The structures were solved using direct methods and standard difference map techniques and were refined by full matrix least-squares procedures on  $F^2$  with SHELXTL (version

6.1).<sup>73, 74</sup> Benzene and THF were distilled from K/benzophenone ketyl and stored over 3 Å molecular sieves. All other liquids, including benzene-*d*<sub>6</sub>, were dried by distillation from CaH<sub>2</sub> and then deoxygenated by three freeze-pump-thaw cycles and stored under an argon atmosphere.

Cobaloxime complexes Co(dmgbF<sub>2</sub>)<sub>2</sub>(H<sub>2</sub>O)<sub>2</sub> (**3.1**),<sup>56</sup> Co(dmgbF<sub>2</sub>)<sub>2</sub>(MeOH)<sub>2</sub> (**3.8**)<sup>56</sup> and Co(dmgbF<sub>2</sub>)<sub>2</sub>(MeCN)<sub>2</sub> (**3.9**)<sup>18</sup> were synthesized by known procedures. Tris(*p*-*tert*-butylphenyl)methyl radical (**1.13**) was prepared by the process described in the literature.<sup>43, 44</sup>

*Co(dmgbF<sub>2</sub>)<sub>2</sub>(THF)<sub>2</sub> (3.10)*. Diethyl ether (150 mL, O<sub>2</sub> free) was added to a flask containing Co(OAc)<sub>2</sub>·4H<sub>2</sub>O (2.0 g, 8 mmol) and dmgh<sub>2</sub> (1.9 g, 16 mmol), followed by freshly distilled BF<sub>3</sub>·Et<sub>2</sub>O (10 mL, an excess). The mixture was stirred for 6 h under argon. The resulting solid was filtered under argon, washed with ice-cold THF (3 × 5 mL, O<sub>2</sub> free), and dried under vacuum. A red solid product was obtained (3.2 g, 4 mmol, 50% yield). IR (ATR): 2968, 2880, 1615 (C=N), 1438, 1385, 1210, 1164, 1092, 1046, 994, 935, 880, 817, 627, 603, 578, 502, 468 cm<sup>-1</sup>, which includes peaks like those that have been attributed to coordinated THF.<sup>75</sup> UV-vis (C<sub>6</sub>H<sub>6</sub>, 7.6 × 10<sup>-5</sup> M, 1 cm quartz cell): 445 nm [ε = 3.3(2) × 10<sup>3</sup> M<sup>-1</sup> cm<sup>-1</sup>].

**Kinetic Measurements. *Caution!*** Pressure reactions should be handled with care behind a blast shield. Otherwise serious injury may result! All experiments were performed at 300 MHz. In a typical experiment, a stock solution of trityl radical (**1.13**) in

C<sub>6</sub>D<sub>6</sub> was prepared with an internal standard (hexamethylcyclotrisiloxane), along with a stock solution of cobaloxime in C<sub>6</sub>D<sub>6</sub>. Appropriate amounts of the two stock solutions were mixed in a thick-walled J-Young tube in the glovebox, and the tube was sealed and removed from the box. After three freeze-pump-thaw cycles to remove the argon from the solution, hydrogen gas was added until the desired pressure was reached. The tube was allowed to thaw, and its contents were mixed before it was placed in the probe of the NMR (whose controller was already set to the desired temperature, 295 K). A methanol standard was used for temperature calibration. The H• transfer product, tris(*p*-*tert*-butylphenyl)methane (**3.5**), was identified by comparing its <sup>1</sup>H NMR spectrum with that of an authentic sample. The integration of the product methine peak relative to that of the internal standard was recorded as a function of time. Sixteen pulses were used for every kinetic point, with 1 s between pulses. The molar concentration of H<sub>2</sub> in benzene was calculated by Henry's law.<sup>48, 49</sup>

### 3.7 References:

1. Tang, L. H.; Papish, E. T.; Abramo, G. P.; Norton, J. R.; Baik, M. H.; Friesner, R. A.; Rappe, A., Kinetics and Thermodynamics of H• Transfer from ( $\eta^5$ -C<sub>5</sub>R<sub>5</sub>)Cr(CO)<sub>3</sub>H (R = Ph, Me, H) to Methyl Methacrylate and Styrene. *J. Am. Chem. Soc.* **2003**, *125*, 10093-10102; revised: *J. Am. Chem. Soc.*, **2006**, *128*, 11314.
2. Choi, J.; Tang, L. H.; Norton, J. R., Kinetics of Hydrogen Atom Transfer from ( $\eta^5$ -C<sub>5</sub>H<sub>5</sub>)Cr(CO)<sub>3</sub>H to Various Olefins: Influence of Olefin Structure. *J. Am. Chem. Soc.* **2007**, *129*, 234-240.
3. Choi, J.; Pulling, M. E.; Smith, D. M.; Norton, J. R., Unusually Weak Metal-Hydrogen Bonds in HV(CO)<sub>4</sub>(P-P) and Their Effectiveness as H• Donors. *J. Am. Chem. Soc.* **2008**, *130*, 4250-4252.
4. Smith, D. M.; Pulling, M. E.; Norton, J. R., Tin-free and Catalytic Radical Cyclizations. *J. Am. Chem. Soc.* **2007**, *129*, 770-771.
5. Hartung, J.; Pulling, M. E.; Smith, D. M.; Yang, D. X.; Norton, J. R., Initiating Radical Cyclizations by H• Transfer from Transition Metals. *Tetrahedron* **2008**, *64*, 11822-11830.
6. Han, A.; Spataru, T.; Hartung, J.; Li, G.; Norton, J. R., Effect of Double-Bond Substituents on the Rate of Cyclization of  $\alpha$ -Carbomethoxyhex-5-enyl Radicals. *J. Org. Chem.* **2014**, *79*, 1938-1946.
7. Kuo, J. L.; Hartung, J.; Han, A.; Norton, J. R., Direct Generation of Oxygen-Stabilized Radicals by H• Transfer from Transition Metal Hydrides. *J. Am. Chem. Soc.* **2015**, *137*, 1036-1039.
8. Fischer, E. O.; Hafner, W.; Stahl, H. O., Über Cyclopentadienyl-metall-carbonyl-wasserstoffe des Chroms, Molybdäns und Wolframs. *Z. Anorg. Allg. Chem.* **1955**, *282*, 47-62.
9. Norton, J. R.; Spataru, T.; Camaioni, D. M.; Lee, S. J.; Li, G.; Choi, J.; Franz, J. A., Kinetics and Mechanism of the Hydrogenation of the CpCr(CO)<sub>3</sub>/[CpCr(CO)<sub>3</sub>]<sub>2</sub> Equilibrium to CpCr(CO)<sub>3</sub>H. *Organometallics* **2014**, *33*, 2496-2502.
10. Ittel, S. D.; Gridnev, A. A. Initiation of Polymerization by Hydrogen Atom Donation. U.S. Patent 7022792, April 4, 2006.
11. McGinley, C. M.; Relyea, H. A.; van der Donk, W. A., Vitamin B-12 Catalyzed Radical Cyclizations of Arylalkenes. *Synlett* **2006**, 211-214.

12. Weiss, M. E.; Kreis, L. M.; Lauber, A.; Carreira, E. M., Cobalt-Catalyzed Coupling of Alkyl Iodides with Alkenes: Deprotonation of Hydridocobalt Enables Turnover. *Angew. Chem. Int. Ed.* **2011**, *50*, 11125-11128.
13. Dempsey, J. L.; Brunschwig, B. S.; Winkler, J. R.; Gray, H. B., Hydrogen Evolution Catalyzed by Cobaloximes. *Acc. Chem. Res.* **2009**, *42*, 1995-2004.
14. Dempsey, J. L.; Winkler, J. R.; Gray, H. B., Kinetics of Electron Transfer Reactions of H<sub>2</sub> Evolving Cobalt Diglyoxime Catalysts. *J. Am. Chem. Soc.* **2010**, *132*, 1060-1065.
15. Dempsey, J. L.; Winkler, J. R.; Gray, H. B., Mechanism of H<sub>2</sub> Evolution from a Photogenerated Hydridocobaloxime. *J. Am. Chem. Soc.* **2010**, *132*, 16774-16776.
16. Stubbert, B. D.; Peters, J. C.; Gray, H. B., Rapid Water Reduction to H<sub>2</sub> Catalyzed by a Cobalt Bis(iminopyridine) Complex. *J. Am. Chem. Soc.* **2011**, *133*, 18070-18073.
17. Hu, X. L.; Cossairt, B. M.; Brunschwig, B. S.; Lewis, N. S.; Peters, J. C., Electrocatalytic Hydrogen Evolution by Cobalt Difluoroboryl-Diglyoximate Complexes. *Chem. Commun.* **2005**, 4723-4725.
18. Hu, X. L.; Brunschwig, B. S.; Peters, J. C., Electrocatalytic Hydrogen Evolution at Low Overpotentials by Cobalt Macrocyclic Glyoxime and Tetraimine Complexes. *J. Am. Chem. Soc.* **2007**, *129*, 8988-8998.
19. Berben, L. A.; Peters, J. C., Hydrogen Evolution by Cobalt Tetraimine Catalysts Adsorbed on Electrode Surfaces. *Chem. Commun.* **2010**, *46*, 398-400.
20. McCrory, C. C. L.; Uyeda, C.; Peters, J. C., Electrocatalytic Hydrogen Evolution in Acidic Water with Molecular Cobalt Tetraazamacrocycles. *J. Am. Chem. Soc.* **2012**, *134*, 3164-3170.
21. Du, P. W.; Schneider, J.; Luo, G. G.; Brennessel, W. W.; Eisenberg, R., Visible Light-Driven Hydrogen Production from Aqueous Protons Catalyzed by Molecular Cobaloxime Catalysts. *Inorg. Chem.* **2009**, *48*, 4952-4962.
22. McCormick, T. M.; Han, Z. J.; Weinberg, D. J.; Brennessel, W. W.; Holland, P. L.; Eisenberg, R., Impact of Ligand Exchange in Hydrogen Production from Cobaloxime-Containing Photocatalytic Systems. *Inorg. Chem.* **2011**, *50*, 10660-10666.
23. Artero, V.; Chavarot-Kerlidou, M.; Fontecave, M., Splitting Water with Cobalt. *Angew. Chem. Int. Ed.* **2011**, *50*, 7238-7266, and references therein.
24. Zhang, P.; Jacques, P. A.; Chavarot-Kerlidou, M.; Wang, M.; Sun, L. C.; Fontecave, M.; Artero, V., Phosphine Coordination to a Cobalt Diimine-Dioxime

Catalyst Increases Stability during Light-Driven H<sub>2</sub> Production. *Inorg. Chem.* **2012**, *51*, 2115-2120.

25. Zhang, P.; Wang, M.; Dong, J. F.; Li, X. Q.; Wang, F.; Wu, L. Z.; Sun, L. C., Photocatalytic Hydrogen Production from Water by Noble-Metal-Free Molecular Catalyst Systems Containing Rose Bengal and the Cobaloximes of BF<sub>x</sub>-Bridged Oxime Ligands. *J. Phys. Chem. C* **2010**, *114*, 15868-15874.

26. Zhang, P.; Wang, M.; Li, C. X.; Li, X. Q.; Dong, J. F.; Sun, L. C., Photochemical H<sub>2</sub> production with Noble-Metal-Free Molecular Devices Comprising a Porphyrin Photosensitizer and a Cobaloxime Catalyst. *Chem. Commun.* **2010**, *46*, 8806-8808.

27. Dong, J. F.; Wang, M.; Zhang, P.; Yang, S. Q.; Liu, J. Y.; Li, X. Q.; Sun, L. C., Promoting Effect of Electrostatic Interaction between a Cobalt Catalyst and a Xanthene Dye on Visible-Light-Driven Electron Transfer and Hydrogen Production. *J. Phys. Chem. C* **2011**, *115*, 15089-15096.

28. Li, L.; Duan, L. L.; Wen, F. Y.; Li, C.; Wang, M.; Hagfeldt, A.; Sun, L. C., Visible Light Driven Hydrogen Production from a Photo-Active Cathode Based on a Molecular Catalyst and Organic Dye-Sensitized p-Type Nanostructured NiO. *Chem. Commun.* **2012**, *48*, 988-990.

29. Probst, B.; Kolano, C.; Hamm, P.; Alberto, R., An Efficient Homogeneous Intermolecular Rhenium-Based Photocatalytic System for the Production of H<sub>2</sub>. *Inorg. Chem.* **2009**, *48*, 1836-1843.

30. Probst, B.; Rodenberg, A.; Guttentag, M.; Hamm, P.; Alberto, R., A Highly Stable Rhenium-Cobalt System for Photocatalytic H<sub>2</sub> Production: Unraveling the Performance-Limiting Steps. *Inorg. Chem.* **2010**, *49*, 6453-6460.

31. Probst, B.; Guttentag, M.; Rodenberg, A.; Hamm, P.; Alberto, R., Photocatalytic H<sub>2</sub> Production from Water with Rhenium and Cobalt Complexes. *Inorg. Chem.* **2011**, *50*, 3404-3412.

32. Guttentag, M.; Rodenberg, A.; Kopelent, R.; Probst, B.; Buchwalder, C.; Brandstatter, M.; Hamm, P.; Alberto, R., Photocatalytic H<sub>2</sub> Production with a Rhenium/Cobalt System in Water under Acidic Conditions. *Eur. J. Inorg. Chem.* **2012**, 59-64.

33. Szajna-Fuller, E.; Bakac, A., Catalytic Generation of Hydrogen with Titanium Citrate and a Macrocyclic Cobalt Complex. *Eur. J. Inorg. Chem.* **2010**, 2488-2494.

34. Utschig, L. M.; Silver, S. C.; Mulfort, K. L.; Tiede, D. M., Nature-Driven Photochemistry for Catalytic Solar Hydrogen Production: A Photosystem I-Transition Metal Catalyst Hybrid. *J. Am. Chem. Soc.* **2011**, *133*, 16334-16337.



35. Schrauze.Gn; Windgass.Rj, Über Cobaloxime(II) und deren Beziehung zum Vitamin B<sub>12r</sub>. *Chem. Ber.* **1966**, 99, 602-&.
36. Yamaguch.T; Nakayama, M.; Tsumura, T., Effect of Base Strength of Schiff-Bases on Their Catalytic-Hydrogenation with Bis(Dimethylglyoximato) Cobalt(II). *Chem. Lett.* **1972**, 1231-1234.
37. Schrauzer, G. N., The Chemistry of Co(I) Derivatives of Vitamin B<sub>12</sub> and of Related Chelates. *Ann. N. Y. Acad. Sci.* **1969**, 158, 526-539.
38. Yamaguch, T.; Tsumura, T., Effect of Triphenylphosphine on Hydrogenation Reaction of Bis(Dimethylglyoximato)Cobalt(II). *Chem. Lett.* **1973**, 409-412.
39. Simándi, L. I.; Budó-Záhonyi, É.; Szeverényi, Z., Effect of Strong Base on the Activation of Molecular Hydrogen by Pyridinebis(dimethylglyoximato)cobalt(II). *Inorg. Nucl. Chem. Lett.* **1976**, 12, 237-241.
40. Yamaguchi, T.; Miyagawa, R., The Effect of Pyridine on the Hydrogen Absorption Process of Bis(dimethylglyoximato)cobalt(II). *Chem. Lett.* **1978**, 7, 89-92.
41. Simándi, L. I.; Budó-Záhonyi, É.; Szeverényi, Z.; Németh, S., Kinetics and Mechanism of the Activation of Molecular Hydrogen by Bis(dimethylglyoximato)cobalt(II) Derivatives. *J. Chem. Soc., Dalton Trans.* **1980**, 276-283.
42. Simándi, L. I.; Szeverényi, Z.; Budó-Záhonyi, É., Activation of Molecular Hydrogen by Cobaloxime(II) Derivatives. *Inorg. Nucl. Chem. Lett.* **1975**, 11, 773-777.
43. Colle, T. H.; Lewis, E. S., Hydrogen Atom Transfers from Thiophenols to Triarylmethyl Radicals. Rates, Substituent Effects, and Tunnel Effects. *J. Am. Chem. Soc.* **1979**, 101, 1810-1814.
44. Eisenberg, D. C.; Lawrie, C. J. C.; Moody, A. E.; Norton, J. R., Relative Rates of H. Transfer from Transition-Metal Hydrides to Trityl Radicals. *J. Am. Chem. Soc.* **1991**, 113, 4888-4895.
45. Eisenberg, D. C.; Norton, J. R., Hydrogen-Atom Transfer Reactions of Transition-Metal Hydrides. *Isr. J. Chem.* **1991**, 31, 55-66.
46. Rodkin, M. A.; Abramo, G. P.; Darula, K. E.; Ramage, D. L.; Santora, B. P.; Norton, J. R., Isotope Effects on Hydrogen Atom Transfer from Transition Metals to Carbon. *Organometallics* **1999**, 18, 1106-1109.
47. Szeverényi, Z.; Budó-Záhonyi, É.; Simándi, L. I., Autocatalytic Reduction of Pyridinecobaloxime(III) by Molecular Hydrogen. *J. Coord. Chem.* **1980**, 10, 41-45.

48. Zhou, Z. M.; Cheng, Z. M.; Yang, D.; Zhou, X.; Yuan, W. K., Solubility of Hydrogen in Pyrolysis Gasoline. *J. Chem. Eng. Data* **2006**, *51*, 972-976.
49. Krüger, M. B.; Selle, C.; Heller, D.; Baumann, W., Determination of Gas Concentrations in Liquids by Nuclear Magnetic Resonance: Hydrogen in Organic Solvents. *J. Chem. Eng. Data* **2012**, *57*, 1737-1744.
50. Halpern, J.; Pribanic, M., Hydrogenation of Pentacyanocobaltate(II) at High Pressures. *Inorg. Chem.* **1970**, *9*, 2616-2618.
51. Wayland, B. B.; Ba, S. J.; Sherry, A. E., Reactions of H<sub>2</sub> (D<sub>2</sub>) with a Rhodium(II) Metalloradical: Kinetic Evidence for a 4-Centered Transition-State. *Inorg. Chem.* **1992**, *31*, 148-150.
52. Capps, K. B.; Bauer, A.; Kiss, G.; Hoff, C. D., The Rate and Mechanism of Oxidative Addition of H<sub>2</sub> to the •Cr(CO)<sub>3</sub>C<sub>5</sub>Me<sub>5</sub> Radical - generation of a model for reaction of H<sub>2</sub> with the •Co(CO)<sub>4</sub> radical. *J. Organomet. Chem.* **1999**, *586*, 23-30.
53. Roberts, J. A. S.; Franz, J. A.; van der Eide, E. F.; Walter, E. D.; Petersen, J. L.; DuBois, D. L.; Bullock, R. M., Comproportionation of Cationic and Anionic Tungsten Complexes Having an N-Heterocyclic Carbene Ligand To Give the Isolable 17-Electron Tungsten Radical CpW(CO)<sub>2</sub>(IMes)•. *J. Am. Chem. Soc.* **2011**, *133*, 14593-14603.
54. van der Eide, E. F.; Liu, T. B.; Camaioni, D. M.; Walter, E. D.; Bullock, R. M., Facile Thermal W-W Bond Homolysis in the N-Heterocyclic Carbene Containing Tungsten Dimer [CpW(CO)<sub>2</sub>(Ime)]<sub>2</sub>. *Organometallics* **2012**, *31*, 1775-1789.
55. Baffert, C.; Artero, V.; Fontecave, M., Cobaloximes as Functional Models for Hydrogenases. 2. Proton Electroreduction Catalyzed by Difluoroborylbis(dimethylglyoximate)cobalt(II) Complexes in Organic Media. *Inorg. Chem.* **2007**, *46*, 1817-1824.
56. Bakac, A.; Brynildson, M. E.; Espenson, J. H., Characterization of the Structure, Properties, and Reactivity of a Cobalt(II) Macrocyclic Complex. *Inorg. Chem.* **1986**, *25*, 4108-4114.
57. Niklas, J.; Mardis, K. L.; Rakhimov, R. R.; Mulfort, K. L.; Tiede, D. M.; Poluektov, O. G., The Hydrogen Catalyst Cobaloxime: A Multifrequency EPR and DFT Study of Cobaloxime's Electronic Structure. *J. Phys. Chem. B* **2012**, *116*, 2943-2957.
58. Rangel, M.; Leite, A.; Silva, A.; de Castro, B.; Schlindwein, W.; Murphy, L., EPR and XANES Studies of Anaerobic Photolysis of iso-Propilpyridinecobaloxime: Elucidation of the Reactivity of the Co(II) Primary Product. *J. Organomet. Chem.* **2014**, *760*, 11-18.

59. Jensen, F. R.; Kiskis, R. C., Kinetic Differentiation between I<sub>d</sub> and D Mechanisms for Axial Base-Ligand Exchange in Alkyl(Base)Cobaloximes. *J. Am. Chem. Soc.* **1975**, *97*, 5820-5825.
60. Chao, T. H.; Espenson, J. H., Mechanism of Hydrogen Evolution from Hydridocobaloxime. *J. Am. Chem. Soc.* **1978**, *100*, 129-133.
61. Brothers, P. J., Heterolytic Activation of Hydrogen by Transition Metal Complexes. *Prog. Inorg. Chem.* **1981**, *28*, 1-61.
62. Cui, W. H.; Wayland, B. B., Activation of C-H/H-H Bonds by Rhodium(II) Porphyrin Bimetallo-radicals. *J. Am. Chem. Soc.* **2004**, *126*, 8266-8274.
63. Banks, R. G.; Das, P. K.; Hill, H. A. O.; Pratt, J. M.; Williams, R. J. P., Homogeneous Reactions of Hydrogen Compared with Those of Other Gases. *Discuss. Faraday Soc.* **1968**, 80-85.
64. Valdez, C. N.; Dempsey, J. L.; Brunschwig, B. S.; Winkler, J. R.; Gray, H. B., Catalytic Hydrogen Evolution from a Covalently Linked Dicobaloxime. *Proc. Natl. Acad. Sci. U. S. A.* **2012**, *109*, 15589-15593.
65. Solis, B. H.; Hammes-Schiffer, S., Theoretical Analysis of Mechanistic Pathways for Hydrogen Evolution Catalyzed by Cobaloximes. *Inorg. Chem.* **2011**, *50*, 11252-11262.
66. Collman, J. P.; Hutchison, J. E.; Wagenknecht, P. S.; Lewis, N. S.; Lopez, M. A.; Guillard, R., An Unprecedented, Bridged Dihydrogen Complex of a Cofacial Metallodiporphyrin and Its Relevance to the Bimolecular Reductive Elimination of Hydrogen. *J. Am. Chem. Soc.* **1990**, *112*, 8206-8208.
67. Collman, J. P.; Wagenknecht, P. S.; Hutchison, J. E.; Lewis, N. S.; Lopez, M. A.; Guillard, R.; Lher, M.; Bothnerby, A. A.; Mishra, P. K., Dihydrogen Complexes of Metalloporphyrins: Characterization and Catalytic Hydrogen Oxidation Activity. *J. Am. Chem. Soc.* **1992**, *114*, 5654-5664.
68. Estes, D. P.; Grills, D. C.; Norton, J. R., The Reaction of Cobaloximes with Hydrogen: Products and Thermodynamics. *J. Am. Chem. Soc.* **2014**, *136*, 17362-17365.
69. Hartwig, J. F., *Organotransition Metal Chemistry: From Bonding to Catalysis*. 1 ed.; University Science Books: Sausalito, CA, 2010; p 124.
70. Sun, Y. A. *The Anions of C<sub>60</sub> and Its Pyrrolidine Derivatives and B. The Search for Hydridocobaloximes*. Ph.D. Thesis, University of Southern California, Los Angeles, CA, 1997.

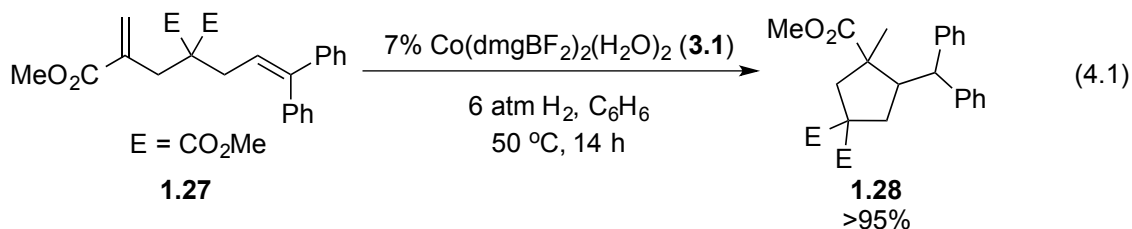
71. Bhattacharjee, A.; Chavarot-Kerlidou, M.; Andreiadis, E. S.; Fontecave, M.; Field, M. J.; Artero, V., Combined Experimental-Theoretical Characterization of the Hydrido-Cobaloxime [HCo(dmgH)<sub>2</sub>(PnBu<sub>3</sub>)]. *Inorg. Chem.* **2012**, *51*, 7087-7093.
72. Lacy, D. C.; Roberts, G. M.; Peters, J. C., The Cobalt Hydride that Never Was: Revisiting Schrauzer's "Hydridocobaloxime". *J. Am. Chem. Soc.* **2015**, *137*, 4860-4864.
73. Sheldrick, G. M. *SHELXTL, An Integrated System for Solving, Refining, and Displaying Crystal Structures from Diffraction Data*, 6.1; University of Göttingen: Göttingen, 1981.
74. Sheldrick, G. M., A Short History of SHELX. *Acta Crystallogr. A* **2008**, *64*, 112-122.
75. Allen, E. A.; Johnson, N. P.; Rosevear, D. T.; Wilkinso.W, Complexes of Rhenium-(IV) and -(V) with Ligands Containing Group VIB Atoms *J. Chem. Soc. A* **1969**, 788-791.

## CHAPTER 4: COBALT-CATALYZED RADICAL REACTIONS INITIATED BY HYDROGEN ATOM TRANSFER<sup>1</sup>

### 4.1 Cobaloxime-Catalyzed Radical Cyclizations

As was discussed in Chapter 3, cobaloximes will generate H• donors under H<sub>2</sub>, which will quickly transfer H• to H• acceptors such as radicals. The 2006 report<sup>1</sup> of chain transfer polymerization catalyzed by cobaloxime **3.1** under H<sub>2</sub> (eq 3.1 in Chapter 3) suggested olefins that could also serve as H• acceptors for the cobaloximes/H<sub>2</sub> system. As the Norton group has reported the radical cyclization of certain diene substrates with HCr(CO)<sub>3</sub>Cp and HV(CO)<sub>4</sub>(P-P),<sup>2-5</sup> it is important to see if the cobaloxime/H<sub>2</sub> system can carry out the same transformation.

This study was initiated by trying to cyclize diene substrate **1.27** with Co(dmgbF<sub>2</sub>)(H<sub>2</sub>O)<sub>2</sub> (**3.1**) under H<sub>2</sub>, since **1.27** has proven to be an ideal substrate with a fast *k*<sub>cyc</sub> (eq 4.1).



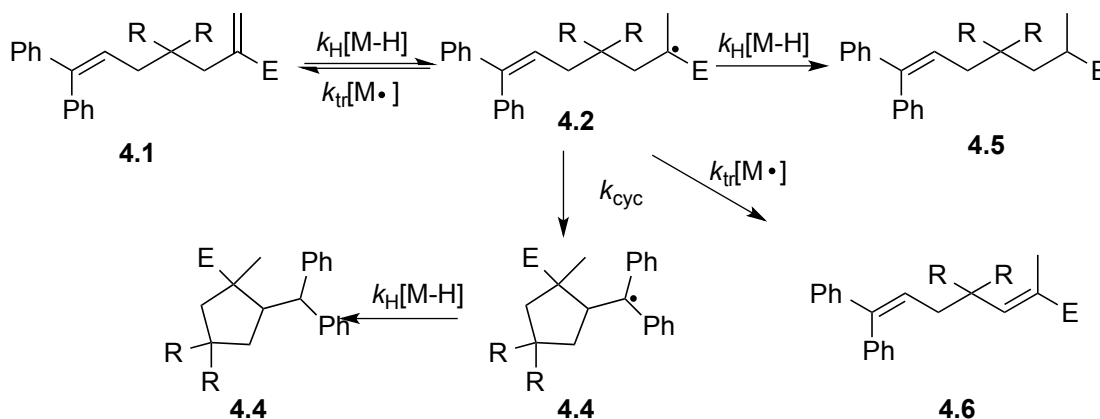
Indeed, with substrate **1.27** quantitative cyclization was observed to **1.28** (eq 4.1); the same result was obtained earlier with catalytic Cr and stoichiometric V hydrides.

We then considered what advantages cobaloximes might offer over our previous catalysts. If the reaction of cobaloxime **3.1** with H<sub>2</sub> is slower than the reaction of the

<sup>1</sup> Part of this work has been published in Li, G.; Han, A.; Pulling, M. E.; Estes, D. P.; Norton, J. R., Evidence for Formation of a Co-H Bond from (H<sub>2</sub>O)<sub>2</sub>Co(dmgbF<sub>2</sub>)<sub>2</sub> under H<sub>2</sub>: Application to Radical Cyclizations. *J. Am. Chem. Soc.* **2012**, *134*, 14662-14665.

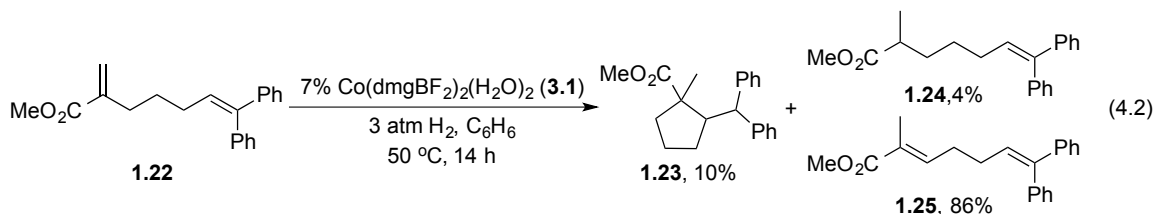
resulting hydride (**3.3**) with our cyclization substrates, the resting state of our catalyst will be  $\text{Co}^{\text{II}}$ , and the concentration of its hydride **3.3** will remain low during the cyclization. The resulting increase in  $[\text{M}\cdot]/[\text{M-H}]$  will change the distribution of isomerized and hydrogenated byproducts (typically **4.5** and **4.6** in Scheme 4.1) that accompany cyclization.

**Scheme 4.1.** How Byproducts Are Formed During Cyclization Reactions



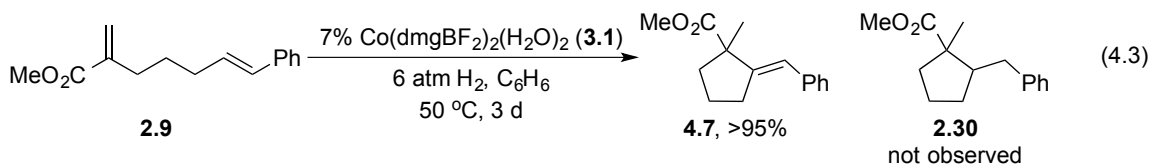
From Scheme 4.1, it is clear that hydrogenation to **4.5** requires an additional M-H, while isomerization to **4.6** requires only  $\text{M}\cdot$  (here  $\text{Co}^{\text{II}}$ ). Thus, the cobalt catalyst should give less hydrogenation to **4.5** and more isomerization to **4.6**.

Indeed, with substrate **1.22** and cobalt catalyst **3.1**, isomerization to **1.25** is the prevailing reaction (eq 4.2). Only traces of the cyclization product **1.23** and the hydrogenation product **1.24** are observed.

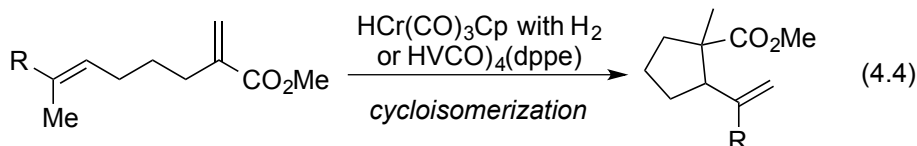


It is clear that in order to achieve a higher cyclization yield, a fast  $k_{\text{cyc}}$  is necessary. To address this kinetic parameter, the diene substrate **2.9** to test the cobaloxime/ $\text{H}_2$  system

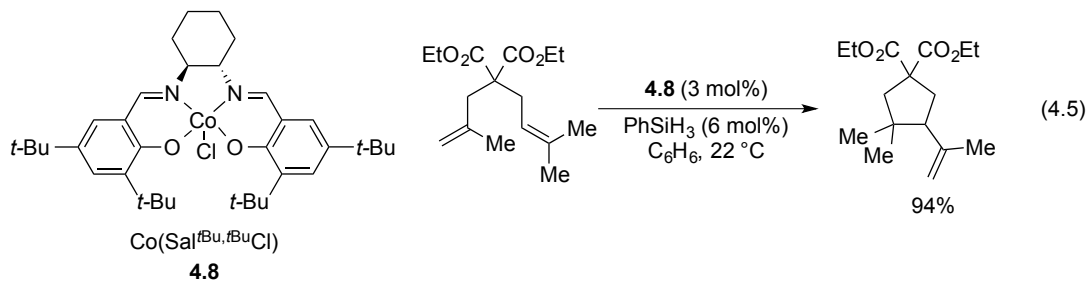
(eq 4.3) because it has only a single phenyl substituent on C6 and is known to cyclize faster (see discussion in Chapter 2). However, instead of generating the “regular” cyclization product **2.30**, the *cycloisomerized* product **4.7** was observed.



The atom economy of this *cycloisomerization* process is nearly ideal.<sup>6-8</sup> In fact, we have already observed examples of cycloisomerization with  $\text{HCr}(\text{CO})_3\text{Cp}$  under  $\text{H}_2$  (eq 4.4, also see eq 2.5 in Chapter 2) and with  $\text{HV}(\text{CO})_4(\text{dppe})^4$  using substrates that contain a methyl substituent on the incipient radical (eq 4.4).



The Shenvi group has reported many additional examples of cycloisomerization recently, using a different cobalt system (**4.8**/ $\text{PhSiH}_3$ , eq 4.5).<sup>9</sup>

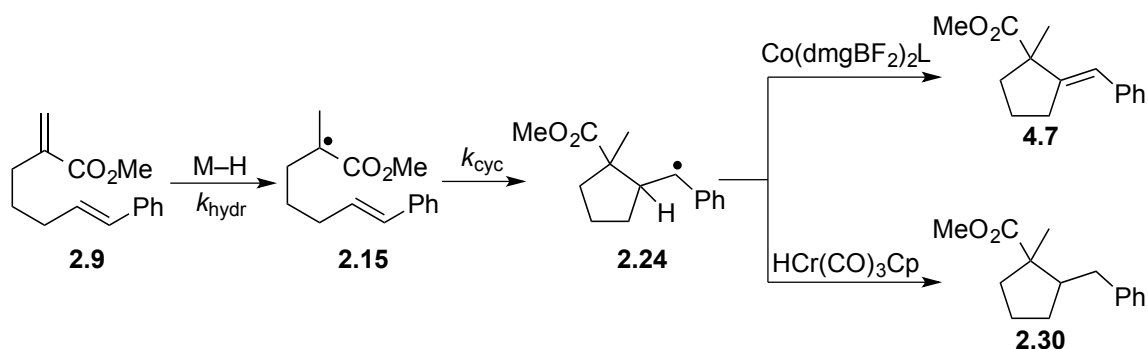


## 4.2 Cyclization vs Cycloisomerization

From the discussion in Chapter 3, in the catalysis of the hydrogenation of trityl radicals by various  $\text{Co}(\text{dmgbF}_2)_2\text{L}_2$  complexes under  $\text{H}_2$  in benzene, the rate-determining step is the activation of  $\text{H}_2$  by the cobaloxime and  $\text{H}_2$ . The active cobalt species is five-

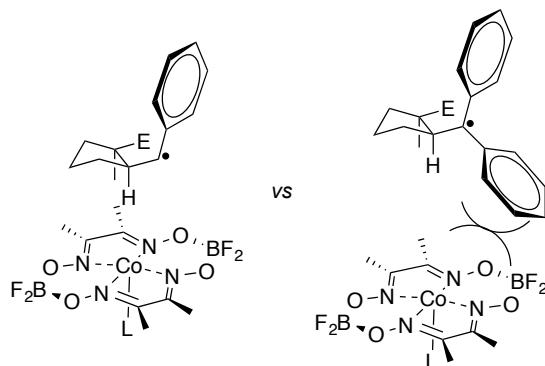
coordinate, with a single axial ligand ( $\text{Co}(\text{dmgBF}_2)_2\text{L}$ ). The resting state of the Co catalytic system is thus a metalloradical  $\text{Co}(\text{dmgBF}_2)_2\text{L}$ . That metalloradical abstracts  $\text{H}\cdot$  from the cyclized radical **2.24** faster than it activates  $\text{H}_2$ , and thus yields the cycloisomerization product **4.7**. On the other hand, the regeneration of  $\text{HCr}(\text{CO})_3\text{Cp}$  by the hydrogenation of  $\cdot\text{Cr}(\text{CO})_3\text{Cp}$  (and its dimer) is faster than  $\text{H}\cdot$  transfer from  $\text{HCr}(\text{CO})_3\text{Cp}$  to most substrates, so the resting state of the Cr catalytic system is the hydride,<sup>10</sup> which will quickly transfer its  $\text{H}\cdot$  to radical **2.24** to generate the “regular” cyclization product **2.30** (Scheme 4.2).

**Scheme 4.2.** Mechanism for the Formation of **4.7** and **2.30** from **2.9**



However, when a substrate with two phenyl substituents (**1.22** or **1.27**) is used, the cyclized radical appears to be too sterically hindered for  $\text{Co}(\text{dmgBF}_2)_2\text{L}$  to abstract  $\text{H}\cdot$  and thus results in a “regular” cyclization product (Scheme 4.3).

**Scheme 4.3.** Steric Effect in Cyclized Radical for  $\text{H}\cdot$  Abstracting





### 4.3 Substrate Scope for Radical Cycloisomerization

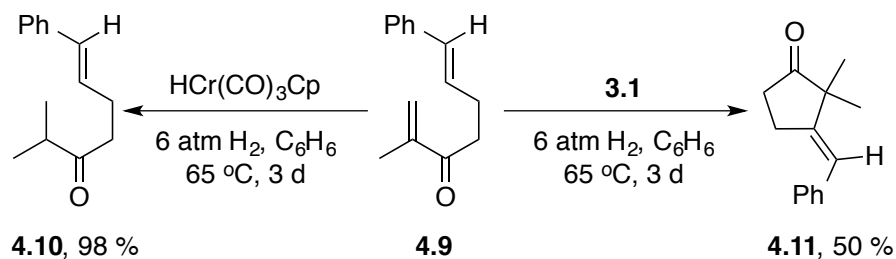
#### 4.3.1 Cycloisomerization via 5-exo Cyclization

According to the discussion in chapter 2, the cyclization of a radical (e.g., radical **4.2** in Scheme 4.1) competes with its hydrogenation and isomerization according to eq 4.6.

$$\frac{\text{cyclized product}}{\text{uncyclized product}} = \frac{k_{\text{cyc}}}{k_{\text{hydr}}[\text{M-H}] + k_{\text{iso}}[\text{M}\bullet]} \quad (4.6)$$

As noted in the section above, the resting state for a Co catalytic system is the metalloradical  $\text{Co}(\text{dmgBF}_2)_2\text{L}$ , which makes concentration of M-H relatively small. Therefore the use of the cobalt catalyst can be advantageous in some cases. The structure of an enone substrate **4.9** eliminates isomerization as a possibility.<sup>11</sup> The Cr catalyst results almost exclusively in hydrogenation to give **4.10**, but the Co catalyst gives substantial cyclization, albeit to the cycloisomerized product **4.11** (Scheme 4.4). The phenyl substituent in **4.9** directs the cyclization to a five-membered ring instead of the six-membered ring reported for the parent radical.<sup>12-15</sup> The Co catalyst does give some hydrogenation (the remaining 50% of substrate **4.9** is converted to **4.10**).

**Scheme 4.4.** Comparison of Cr and Co Catalysts for Cyclization of **4.9**

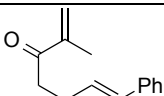
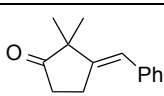
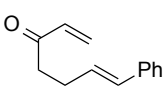
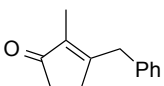
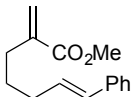
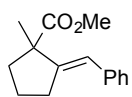
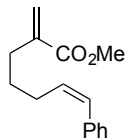
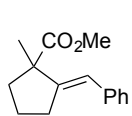
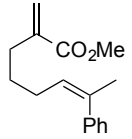
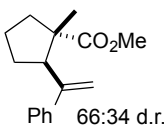
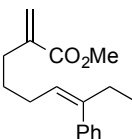
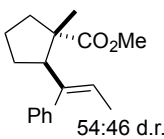
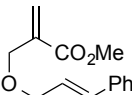
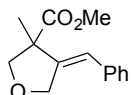
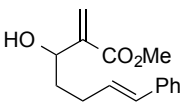
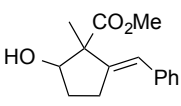
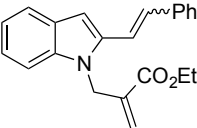
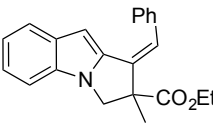
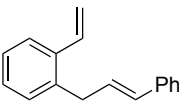
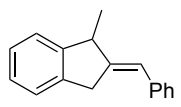


According to the kinetic studies in Chapter 3,  $\text{Co}(\text{dmgBF}_2)_2(\text{THF})_2$  (**3.10**) activates  $\text{H}_2$  faster than  $\text{Co}(\text{dmgBF}_2)_2(\text{H}_2\text{O})_2$  (**3.1**) does. It seemed likely that the reaction in Scheme 4.4 would be faster with **3.10**, and that is proved to be the case (entry 1 in Table 4.1); the yield also improved. A similar result was obtained with the analogous ketone

with no methyl substituent on the  $\alpha$  carbon (entry 2), although the double bond was now able to isomerize to a position within the ring. Better yields were obtained with the acrylate esters in entries 3–8. Making the substituents on C5 and C6 trans to each other slightly improved the yields (entry 3, 4); in agreement with previous observations in Chapter 2. Moderate yields were obtained with the indole derivative in entry 9 and the substituted benzene in entry 10; in both cases the planarity of the aromatic system makes it difficult for the radical to cyclize.<sup>4</sup>

After a substrate cyclizes to a five-membered ring, the radical center moves to C6. A hydrogen atom can be abstracted not only from any suitable substituent on C6 (entries 5 and 6) but also (when there is no suitable substituent on C6) from the sterically hindered C5 (entries 1, 3, 4, 7, and 8–10). Of course these C–H bonds are weakened by the adjacent radical center.<sup>16</sup> Cycloisomerizations of the former type have been reported by Shenvi and co-workers (see eq 4.5 above), but cycloisomerizations of the latter type, forming exocyclic double bonds, are not available from the Co(salen)/PhSiH<sub>3</sub> system. The Co-catalyzed cycloisomerization reaction tolerates an unprotected hydroxyl substituent (entry 8), or a heteroatom in the backbone (entry 7). Heteroatoms are known to increase the rate constant for cyclization,<sup>17</sup> although the cobaloxime system does not require this feature to cyclize substrates in good yield. In contrast, the Co(salen)/PhSiH<sub>3</sub> system seems to require heteroatom acceleration and? the Thorpe-Ingold effect.<sup>9</sup>

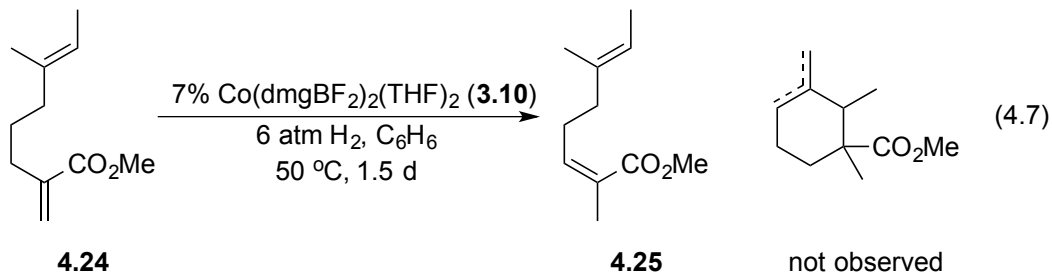
**Table 4.1.** Scope of Cycloisomerizations

entry	substrate		product		yield <sup>a</sup>
1		<b>4.9</b>		<b>4.11</b>	61%
2		<b>4.12</b>		<b>4.13</b>	57%
3		<b>2.9</b>		<b>4.7</b>	>95%
4		<b>2.10</b>		<b>4.7</b>	92%
5		<b>2.11</b>	 66:34 d.r.	<b>2.31</b>	88%
6		<b>4.14</b>	 54:46 d.r.	<b>4.15</b>	95%
7		<b>4.16</b>		<b>4.17</b>	>95%
8		<b>4.18</b>		<b>4.19</b>	90%
9		<b>4.20</b>		<b>4.21</b>	67%
10		<b>4.22</b>		<b>4.23</b>	80%

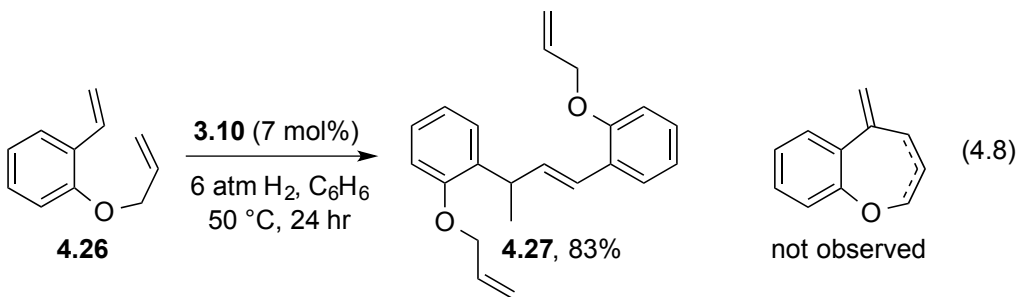
<sup>a</sup>Reaction Conditions: Co(dmgbF<sub>2</sub>)<sub>2</sub>(THF)<sub>2</sub> (**3.10**, 7%), 6 atm H<sub>2</sub>, C<sub>6</sub>H<sub>6</sub> at 50 °C for 1.5 d

#### 4.3.2 Attempts at 6-endo and 7-endo Cycloisomerization

Results in Table 4.1 show that cyclizations are straightforward when five-membered rings are produced,<sup>18, 19</sup> but they become more difficult as  $k_{\text{cyc}}$  decreases.<sup>20</sup> And this has proven to be true. When substrate **4.24** is treated with Cobaloxime/ $\text{H}_2$  system, only isomerization is observed (eq 4.7).



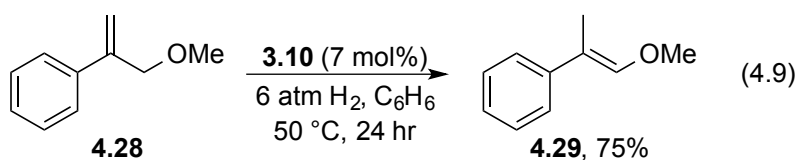
Substrates where  $k_{\text{cyc}}$  is even slower are even more problematic. Although the structure of **4.26** eliminates the possibility of isomerization, and the Co catalyst should minimize hydrogenation, treating **4.26** with **3.10** does not give the anticipated cyclization product, but an 83% yield of the dimer **4.27** (eq 4.8).<sup>21</sup> We can suppress the formation of **4.27** by diluting the reaction ten-fold, in which case we recover only starting material. This indicates that  $k_{\text{cyc}}$  in the 7-endo case is simply too slow.<sup>20, 22</sup>



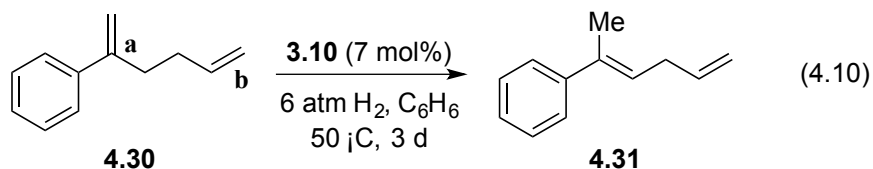
#### 4.4 Cobaloxime-Catalyzed Isomerizations of Olefins

In fact, the isomerization side reaction in a radical cycloisomerization of dienes can be advantageous as an approach to more sterically hindered olefins. Based on the

reported rate constants for HAT from  $\text{HCr(CO)}_3\text{Cp}$  to olefins (see Table 1.1 in Chapter 1), Jonathan Kuo in the Norton group has studied the cobaloxime-catalyzed isomerization of appropriate olefins. For example, allyl ether substrate **4.28** can be isomerized to enol ether **4.29** (eq 4.9) in one day at 50 °C with a 75% isolated yield (only one double bond isomer is observed). Such isomerizations have previously been achieved with strong base (e.g. *n*-BuLi),<sup>23, 24</sup> or transition-metal catalysts that do not contain hydride ligands (e.g.,  $(\text{PPh}_3)_3\text{RhCl}$ ,<sup>25</sup> or  $[\text{Ir}(\text{PCy}_3)]^+$ <sup>26</sup>), and surely with transition-metal hydrides and acids.



With the unconjugated diene **4.30** Jonathan observed the selectivity predicted by the data in Table 1.1, Chapter 1.<sup>27</sup> The 1,1-disubstituted double bond *a*, with one aromatic substituent, is isomerized in preference to the terminal double bond *b* (eq 4.10), producing skipped diene **4.31**. Shenvi and coworkers have isomerized the terminal double bond of 1-decene (a model for double bond *b* in **4.30**) to an internal position at room temperature, suggesting that their system generates a more reactive  $\text{H}^\bullet$  donor.<sup>9</sup>

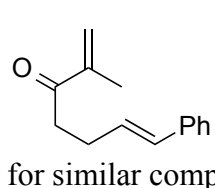


## 4.5 Experiment Details

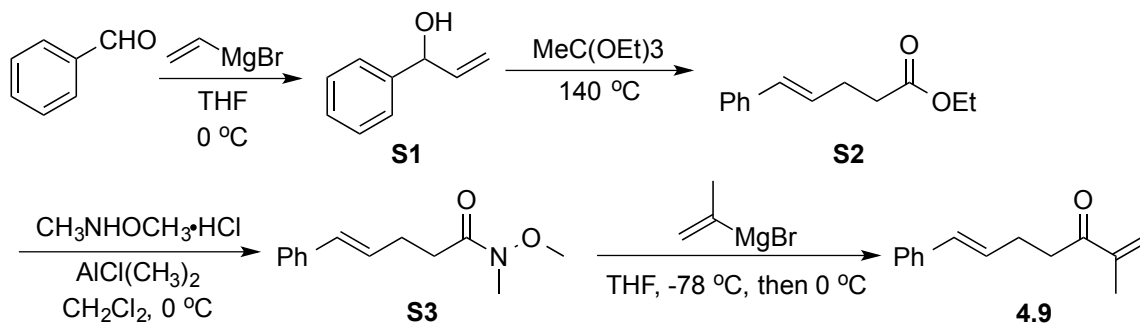
All reactions were carried out under an atmosphere of argon in glassware that had been flame-dried under vacuum and backfilled with argon. High-pressure reactions were

carried out in a Fisher–Porter bottle equipped with a pressure gauge, gas inlet, and pressure release valve. Hexamethylphosphoramide (HMPA) was distilled from  $\text{CaH}_2$ . Deuterated benzene ( $\text{C}_6\text{D}_6$ ) was purified by vacuum transfer from  $\text{CaH}_2$ . THF and benzene ( $\text{C}_6\text{H}_6$ ) were distilled from sodium-benzophenone ketyl.  $\text{Et}_2\text{O}$  and  $\text{CH}_2\text{Cl}_2$  were dried by filtration through alumina. Cobaloximes were synthesized according to procedures described in Chapter 3 and manipulated in an inert argon atmosphere glovebox ( $\text{O}_2 < 1$  ppm). Reaction mixtures involving cobaloximes were all prepared in the glovebox.  $^1\text{H}$  NMR and  $^{13}\text{C}$  NMR spectra were recorded at ambient temperature (298 K) at 500, 400, or 300 MHz and 125, 100, or 75 MHz, respectively. High-resolution mass spectra were acquired (after ionization by EI) by peak matching on a double-focusing magnetic sector instrument.

#### 4.5.1 Synthesis of Diene Substrates

 *(E)*-2-methyl-7-phenylhepta-1,6-dien-3-one (**4.9**). Compound **4.9** was synthesized (with minor revision) according to published procedures for similar compounds (Scheme 4.5).<sup>4</sup>

**Scheme 4.5.** Synthesis of **4.9**



**S1:** To a solution of benzaldehyde (2.12 g, 20 mmol) in dry THF (30 mL) was added vinylmagnesium bromide (1M in THF, 20 mL) at 0 °C dropwise. The reaction was stirred at 0 °C for 2 h. The mixture was then diluted with diethyl ether and quenched with saturated NH<sub>4</sub>Cl solution. The organic layer was separated and washed with water (2 × 20 mL), dried over anhydrous Na<sub>2</sub>SO<sub>4</sub>, filtered, and concentrated *in vacuo*. The residual light yellow oil was used below without further purification. <sup>1</sup>H NMR (400 MHz, CDCl<sub>3</sub>) δ 7.34-7.26 (m, 5H, C<sub>6</sub>H<sub>5</sub>), 6.10-6.02 (m, 1H, -CH=CH<sub>2</sub>), 5.38-5.33 (m, 1H, CH), 5.22-5.19 (m, 2H, -CH=CH<sub>2</sub>).<sup>28</sup>

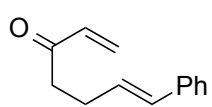
**S2:** A mixture of **S1** (2.63 g, 20 mmol), ethyl orthoacetate (4.86 g, 30 mmol) and propionic acid (0.05 g, 0.7 mmol) was placed in a 100 mL round-bottom flask. The resulting solution was heated to 140 °C for 1 h with an air condenser and short-path distillation head attached. After the ethanol was removed, the temperature was raised to 155 °C and the reaction was refluxed for an additional 5 h. The reaction was then quenched with water (10 mL), and the aqueous phase extracted with diethyl ether (3 × 10 mL). The combined organic layers were dried over Na<sub>2</sub>SO<sub>4</sub>, filtered and concentrated *in vacuo*. The residual red oil was used below without further purification. <sup>1</sup>H NMR (500 MHz, CDCl<sub>3</sub>) δ 7.39-7.19 (m, 5H, C<sub>6</sub>H<sub>5</sub>), 6.44 (dt, *J*<sub>1</sub> = 16 Hz, *J*<sub>2</sub> = 1.5 Hz, 1H, PhCH=CH-), 6.21 (dt, *J* = 16, 6.5, 1H, PhCH=CH-), 4.15 (t, *J* = 7 Hz, 2H, -CH<sub>2</sub>CH<sub>3</sub>), 2.55-2.46 (m, 4H, -CH<sub>2</sub>CH<sub>2</sub>-), 1.26 (t, *J* = 7 Hz, 3H, -CH<sub>2</sub>CH<sub>3</sub>).<sup>29</sup>

**S3:** Dimethylaluminum chloride (1M in hexanes, 10.6 mL) was added to a suspension of N,O-dimethylhydroxylamine hydrochloride (1.03 g, 10.6 mmol) in 90 mL dry CH<sub>2</sub>Cl<sub>2</sub> in a 250 mL Schlenk flask dropwise at 0 °C. The reaction was then warmed to ambient temperature and stirred for 1 h. **S2** (0.714 g, 3.5 mmol) was added to the reaction

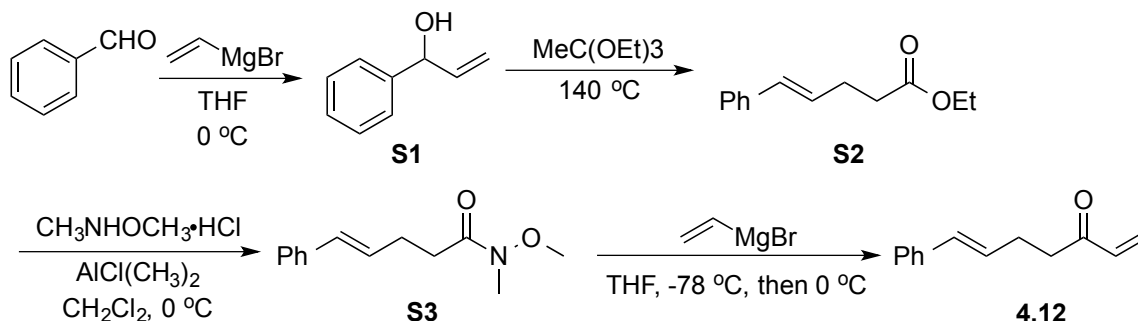
dropwise and the reaction mixture was stirred for another 30 min. Phosphate buffer solution (35 mL, pH = 8) was added to quench the reaction. The aqueous phase was extracted by CH<sub>2</sub>Cl<sub>2</sub> (3 × 20 mL). The organic phases were combined and dried over Na<sub>2</sub>SO<sub>4</sub>, filtered and concentrated *in vacuo*. The residual red oil was used below without further purification. <sup>1</sup>H NMR (400 MHz, CDCl<sub>3</sub>) δ 7.27-7.18 (m, 5H, C<sub>6</sub>H<sub>5</sub>), 6.44 (dt, *J*<sub>1</sub> = 16 Hz, *J*<sub>2</sub> = 1.5 Hz, 1H, PhCH=CH-), 6.26 (dt, *J*<sub>1</sub> = 16 Hz, *J*<sub>2</sub> = 7 Hz, 1H, PhCH=CH-), 3.69 (s, 3H, -OCH<sub>3</sub>), 3.20 (s, 3H, -NCH<sub>3</sub>), 2.62-2.54 (m, 4H, -CH<sub>2</sub>CH<sub>2</sub>-).

**(*E*)-2-methyl-7-phenylhepta-1,6-dien-3-one (4.9):** Isopropenylmagnesium bromide (0.5 M in THF, 14 mL) was added to a solution of **S3** in THF (18 mL) in a 100 mL Schlenk flask dropwise at -78 °C. The reaction was stirred at 0 °C until TLC (ethyl acetate: hexanes = 1: 10) indicated complete consumption of **S3**. Saturated NH<sub>4</sub>Cl solution (30 mL) was then added to quench the reaction. The aqueous phase was extracted with diethyl ether (3 × 20 mL), dried over MgSO<sub>4</sub>, filtered and concentrated *in vacuo*. The crude product was purified by flash chromatography (ethyl acetate: hexanes = 1: 30). The product was obtained as a light yellow oil (680 mg, 3.4 mmol, 97% yield over two steps). <sup>1</sup>H NMR (500 MHz, CDCl<sub>3</sub>) δ 7.34-7.18 (m, 5H, C<sub>6</sub>H<sub>5</sub>), 6.43 (dt, *J*<sub>1</sub> = 16 Hz, *J*<sub>2</sub> = 1.5 Hz, 1H, PhCH=CH-), 6.23 (dt, *J*<sub>1</sub> = 16 Hz, *J*<sub>2</sub> = 7 Hz, 1H, PhCH=CH-), 5.99 (s, 1H, trans -C(-CH<sub>3</sub>)=CH<sub>2</sub>), 5.79 (d, *J* = 1 Hz, 1H, cis -C(-CH<sub>3</sub>)=CH<sub>2</sub>), 2.87 (t, *J* = 7.5 Hz, 2H, -C(=O)-CH<sub>2</sub>CH<sub>2</sub>-), 2.54 (td, *J*<sub>1</sub> = 7 Hz, *J*<sub>2</sub> = 1.5 Hz, 2H, -C(=O)-CH<sub>2</sub>CH<sub>2</sub>-), 1.90 (s, 3H, -CH<sub>3</sub>). <sup>13</sup>C NMR (125 MHz, CDCl<sub>3</sub>) δ 201.1, 144.5, 137.5, 130.6, 129.2, 128.5, 127.0, 126.0, 124.6, 37.1, 27.7, 17.6. IR (neat) 3026, 2926, 1951, 1880, 1804, 1677 (C=O), 1631, 1600, 1493, 1449, 1369, 1091, 966, 935, 745, 694. HRMS (FAB<sup>+</sup>) calculated for C<sub>14</sub>H<sub>16</sub>O [M]<sup>+</sup> 200.1201, found 200.1199.



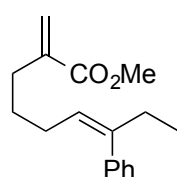

**(E)-7-phenylhepta-1,6-dien-3-one (4.12).** Compound **4.12** was synthesized (with minor revision) according to the procedures for **4.9** (Scheme 4.6).

**Scheme 4.6.** Synthesis of **4.12**



**(E)-7-phenylhepta-1,6-dien-3-one (4.12).** Vinylmagnesium bromide (0.5 M in THF, 14 mL) was added to a solution of **S3** (3.5 mmol) in THF (18 mL) in a 100 mL Schlenk flask dropwise at 0 °C. The reaction was stirred at 0 °C until TLC (ethyl acetate: hexanes = 1: 10) indicated complete consumption of **S3**. Saturated NH<sub>4</sub>Cl solution (30 mL) was then added to quench the reaction. The aqueous phase was extracted with diethyl ether (3 × 20 mL), dried over MgSO<sub>4</sub>, filtered and concentrated *in vacuo*. The crude product was purified by flash chromatography (ethyl acetate: hexanes = 1: 30). The product was obtained as a light yellow oil (595 mg, 3.2 mmol, 92% yield for last step). <sup>1</sup>H NMR (500 MHz, CDCl<sub>3</sub>) δ 7.34-7.19 (m, 5H, C<sub>6</sub>H<sub>5</sub>), 6.43 (d, *J* = 15.5 Hz, 1H, PhCH=CH-), 6.38 (dd, *J*<sub>1</sub> = 17.5, *J*<sub>2</sub> = 10.5 Hz, 1H, -CH=CH<sub>2</sub>), 6.25 (dd, *J*<sub>1</sub> = 17.5, *J*<sub>2</sub> = 1 Hz, 1H, *cis* -CH=CH<sub>2</sub>), 6.22 (dt, *J*<sub>1</sub> = 15.5, *J*<sub>2</sub> = 7.5 Hz, 1H, PhCH=CH-), 5.84 (dd, *J*<sub>1</sub> = 10.5, *J*<sub>2</sub> = 1 Hz, 1H, *trans* -CH=CH<sub>2</sub>), 2.78 (t, *J* = 7.5 Hz, 2H, -CH<sub>2</sub>-C(-R)=O), 2.55 (tdd, *J*<sub>1</sub> = *J*<sub>2</sub> = 7.5 Hz, *J*<sub>3</sub> = 1 Hz, 2H, PhCH=CH-CH<sub>2</sub>-). <sup>13</sup>C NMR (125 MHz, CDCl<sub>3</sub>) δ 199.9, 137.4,

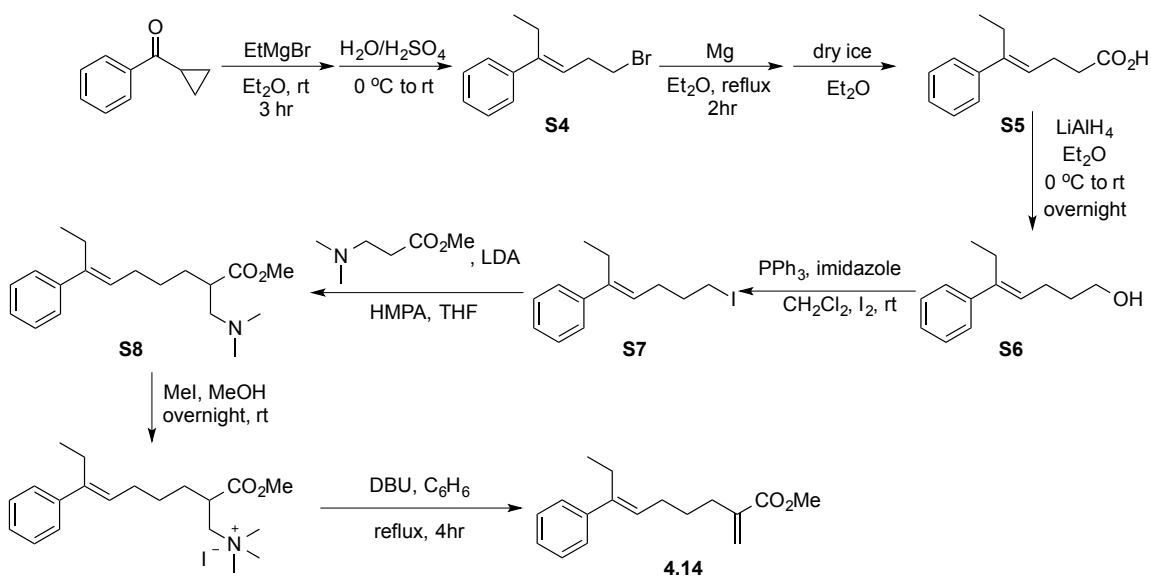
136.5, 130.8, 128.9, 128.5, 128.2, 127.1, 126.0, 39.1, 27.1. IR (neat) 3022, 2924, 2852, 1677 (C=O), 1612, 1493, 1402, 1185, 1100, 968, 745, 693  $\text{cm}^{-1}$ . HRMS (FAB<sup>+</sup>) calculated for  $\text{C}_{13}\text{H}_{14}\text{O}$   $[\text{M}]^+$  186.1045, found 186.1036.



(*E*)-methyl 2-methylene-7-phenylnon-6-enoate (**4.14**). Compound **4.14**

was synthesized according to the procedure in Scheme 4.7.

**Scheme 4.7.** Synthesis of **4.14**



**S4**: Under Ar, EtMgBr (3.0 M in diethyl ether, 3.7 mL) was added dropwise to a solution of cyclopropyl phenyl ketone (1.46 g, 10 mmol) in 10 mL diethyl ether at room temperature. The mixture was stirred for 1 hour at room temperature and cooled down to 0 °C. A mixture of conc.  $\text{H}_2\text{SO}_4$  (1.5 mL) and  $\text{H}_2\text{O}$  (3 mL) was added to the reaction at 0 °C dropwise. The mixture was warmed to room temperature and stirred for 30 min. The aqueous phase was extracted with diethyl ether (3 × 20 mL), dried over  $\text{MgSO}_4$ , filtered and concentrated *in vacuo*. The crude product was used without further purification.  $^1\text{H}$  NMR (400 MHz,  $\text{CDCl}_3$ )  $\delta$  7.36–7.22(m, 5H,  $\text{C}_6\text{H}_5$ ), 5.59 (t,  $J$  = 6.8 Hz, 1H,  $-\text{CH}=\text{C}<$ ),

3.45 (t,  $J = 7.2$  Hz, 2H,  $-\text{CH}_2\text{Br}$ ), 2.78 (td,  $J_1 = 7.2$  Hz,  $J_2 = 6.8$  Hz, 2H,  $-\text{CH}_2-\text{CH}_2\text{Br}$ ), 2.52 (q,  $J = 7.6$  Hz, 2H,  $-\text{CH}_2-\text{CH}_3$ ), 0.99 (t,  $J = 7.6$  Hz, 3H,  $-\text{CH}_3$ ).

**S5:** Under Ar, **S4** was added dropwise to a three-neck flask that contained magnesium (672 mg, 28 mmol) and 50 mL  $\text{Et}_2\text{O}$ . After refluxing for 4 h, the solution was cooled down to room temperature and added to a Schlenk flask that contained excess dry ice. The system was stirred overnight and quenched by 20 mL saturated  $\text{NH}_4\text{Cl}$  solution, followed by 10 mL 1N HCl. The aqueous phase was extracted with diethyl ether ( $3 \times 20$  mL), dried over  $\text{MgSO}_4$ , filtered and concentrated *in vacuo*. The crude product was used without further purification.  $^1\text{H}$  NMR (400 MHz,  $\text{CDCl}_3$ )  $\delta$  7.35–7.23(m, 5H,  $\text{C}_6\text{H}_5$ ), 5.59 (t,  $J = 6.8$  Hz, 1H,  $-\text{CH}=\text{C}<$ ), 2.57–2.49 (m, 6 H,  $-\text{CH}_2-$ ), 0.99 (t,  $J = 7.6$  Hz, 3H,  $-\text{CH}_3$ ).

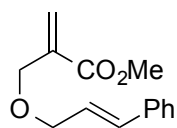
**S6:** Under Ar,  $\text{LiAlH}_4$  (76 mg, 2 mmol) was added to 10 mL  $\text{Et}_2\text{O}$ . The suspension was cooled to 0 °C. To the suspension was added 4 mL of an  $\text{Et}_2\text{O}$  solution of **S5** (372 mg, 1.8 mmol). The reaction was stirred at room temperature overnight. Saturated  $\text{NH}_4\text{Cl}$  solution (30 mL) was then added to quench the reaction. The aqueous phase was extracted with diethyl ether ( $3 \times 20$  mL), dried over  $\text{MgSO}_4$ , filtered and concentrated *in vacuo*. The crude product was used without further purification.  $^1\text{H}$  NMR (400 MHz,  $\text{CDCl}_3$ )  $\delta$  7.36–7.20(m, 5H,  $\text{C}_6\text{H}_5$ ), 5.64 (t,  $J = 7.6$  Hz, 1H,  $-\text{CH}=\text{C}<$ ), 3.72 (t,  $J = 6.4$  Hz, 2H,  $-\text{CH}_2-\text{OH}$ ), 2.53 (dt,  $J_1 = J_2 = 7.6$  Hz, 2H,  $=\text{CH}_2-\text{CH}_2-$ ), 2.31 (q,  $J = 7.6$  Hz, 2H,  $-\text{CH}_2-\text{CH}_3$ ), 1.78–1.71 (m, 2H,  $-\text{CH}_2-\text{CH}_2-\text{CH}_2-$ ), 0.99 (t,  $J = 7.6$  Hz, 3H,  $-\text{CH}_3$ ).

**S7:** Under Ar,  $\text{PPh}_3$  (452 mg, 2.6 mmol) and imidazole (115 mg, 2.6 mmol) was dissolved in 8 mL  $\text{CH}_2\text{Cl}_2$ . At room temperature  $\text{I}_2$  (438 mg, 2.6 mmol) was added to the solution. After stirring at room temperature for 30 min, 4 mL  $\text{CH}_2\text{Cl}_2$  of a solution of **S6** (327 mg, 1.7 mmol) was added to the solution dropwise. The reaction was stirred at room

temperature for 12 h and quenched by 20 mL hexane. The system was filtrated over celite and the filtrate was concentrated *in vacuo*. The crude product was used without further purification.  $^1\text{H}$  NMR (400 MHz,  $\text{CDCl}_3$ )  $\delta$  7.35–7.21(m, 5H,  $\text{C}_6\text{H}_5$ ), 5.56 (t,  $J = 7.6$  Hz, 1H,  $-\text{CH}=\text{C}<$ ), 3.25 (t,  $J = 6.8$  Hz, 2H,  $-\text{CH}_2-\text{I}$ ), 2.55 (dt,  $J_1 = J_2 = 7.6$  Hz, 2H,  $=\text{CH}_2-\text{CH}_2-$ ), 2.33 (q,  $J = 7.2$  Hz, 2H,  $-\text{CH}_2-\text{CH}_3$ ), 1.02-1.95 (m, 2H,  $-\text{CH}_2-\text{CH}_2-\text{CH}_2-$ ), 0.99 (t,  $J = 7.6$  Hz, 3H,  $-\text{CH}_3$ ).

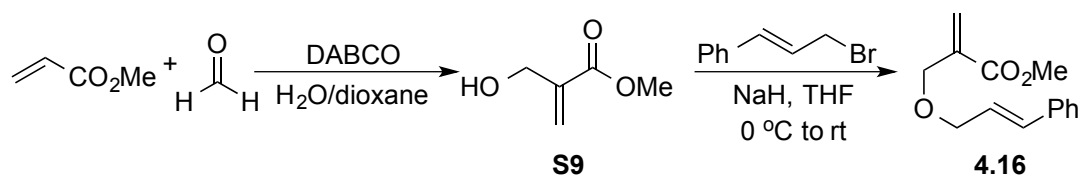
**S8:** To a cooled ( $-78$  °C) solution of diisopropylamine (0.13 mL, 0.9 mmol) in 8 mL THF was added cold ( $-78$  °C) n-BuLi (0.4 mL, 0.88 mmol, 2.2 M in cyclohexane). The mixture was stirred at  $0$  °C for 30 min and was again cooled to  $-78$  °C. A solution of methyl 3-(dimethylamino)propionate (110 mg, 0.8 mmol) in 2 mL of THF was cooled to  $-78$  °C and added to the reaction mixture by cannula over 3 min. After 45 min, a solution of cold ( $-78$  °C) **S7** (210 mg, 0.7 mmol) and hexamethylphosphoramide (HMPA, 0.15 mL, 0.8 mmol) in 2 mL of THF was added to the reaction mixture dropwise by cannula. After stirring at room temperature for 12 h, 10 mL of saturated aqueous  $\text{NH}_4\text{Cl}$  was added. The reaction mixture was extracted with EtOAc (20 mL). The organic layer was washed with  $\text{H}_2\text{O}$  ( $1 \times 20$  mL), saturated aqueous NaCl ( $2 \times 10$  mL), dried over  $\text{Na}_2\text{SO}_4$ , and concentrated *in vacuo*. The crude product was used without further purification.  $^1\text{H}$  NMR (400 MHz,  $\text{CDCl}_3$ )  $\delta$  7.35–7.21(m, 5H,  $\text{C}_6\text{H}_5$ ), 5.56 (t,  $J = 7.2$  Hz, 1H,  $-\text{CH}=\text{C}<$ ), 3.70 (s, 3H,  $-\text{CO}_2\text{CH}_3$ ), 2.67-2.65 (m, 1H,  $>\text{NCH}_2-$ ), 2.64-2.63 (m, 1H,  $>\text{NCH}_2-$ ), 2.49 (q,  $J = 7.2$  Hz,  $-\text{CH}_2\text{CH}_3$ ), 2.22 (s, 6H,  $-\text{N}(\text{CH}_3)_2$ ), 1.64-1.55 (m, 4H,  $-\text{CH}_2-\text{CH}_2-$ ), (t,  $J = 6.8$  Hz, 2H,  $-\text{CH}_2-\text{I}$ ), 2.55 (dt,  $J_1 = J_2 = 7.2$  Hz, 2H,  $=\text{CH}_2-\text{CH}_2-$ ), 1.48-1.42 (m, 1H,  $>\text{CH}-$ ), 0.97 (t,  $J = 7.2$  Hz, 3H,  $-\text{CH}_3$ ).

**(E)-methyl 2-methylene-7-phenylnon-6-enoate (4.14):** To a solution of **S8** (206 mg, 0.7 mmol) in 5 mL MeOH was added iodomethane (0.5 mL, 7 mmol). After 12 h at room temperature, the solution was concentrated *in vacuo* to provide a yellow solid. To a solution of this residue in benzene (5 mL) was added 1,8-diazabicycloundec-7-ene (DBU, 912 mg, 6 mmol). After refluxing for 4 h, H<sub>2</sub>O was added and the reaction mixture was extracted with pentane (3 × 10 mL). The combined organic layers were washed with (1 × 20 mL), saturated aqueous NaCl (2 × 10 mL), dried over Na<sub>2</sub>SO<sub>4</sub> and concentrated *in vacuo*. Purification by flash chromatography (1:10 EtOAc/hexanes) provided the product as a colorless oil (131 mg, 73%, cis:trans = 20:1): <sup>1</sup>H NMR (500 MHz, CDCl<sub>3</sub>) δ 7.36-7.22 (m, 5H, C<sub>6</sub>H<sub>5</sub>), 6.17 (d, *J* = 1 Hz, 1H, cis >C=CH<sub>2</sub>), 5.64 (t, *J* = 7.5 Hz, 1H, -CH=C< ), 5.57 (dt, *J*<sub>1</sub> = *J*<sub>2</sub> = 1 Hz, 1H, trans >C=CH<sub>2</sub>), 3.77 (s, 3H, -CO<sub>2</sub>CH<sub>3</sub>), 2.52 (dt, *J*<sub>1</sub> = *J*<sub>2</sub> = 7.5 Hz, 2H, >CH=CH<sub>2</sub>-), 2.39 (t, *J* = 7.5 Hz, -CH<sub>2</sub>C(CO<sub>2</sub>Me)=CH<sub>2</sub>), 2.24 (q, *J* = 7.5 Hz, 2H, -CH<sub>2</sub>Me), 1.68-1.62 (m, 2H, -CH<sub>2</sub>-CH<sub>2</sub>-CH<sub>2</sub>-), 0.98 (t, *J* = 7.5 Hz, 3H, -CH<sub>2</sub>CH<sub>3</sub>); <sup>13</sup>C NMR (125 MHz, CDCl<sub>3</sub>) δ 167.7, 143.0, 142.0, 140.5, 128.1, 127.6, 126.5, 126.3, 124.7, 51.6, 31.6, 28.6, 27.9, 22.9, 13.6. IR (neat) 2951, 2927, 2856, 1720 (C=O), 1632, 1438, 1270, 1195, 1171, 1141, 941, 817, 760, 697 cm<sup>-1</sup>. HRMS (ASAP<sup>+</sup>) calculated for C<sub>17</sub>H<sub>23</sub>O<sub>2</sub> [M+H]<sup>+</sup> 259.1698, found 259.1709.

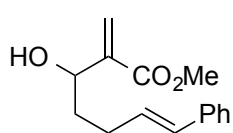


**(E)-methyl 2-((cinnamyloxy)methyl)acrylate (4.16).** Compound **4.16** was synthesized according to the procedure in Scheme 4.8. **S9** was synthesized according to published procedures.<sup>30</sup>

**Scheme 4.8.** Synthesis of **4.16**



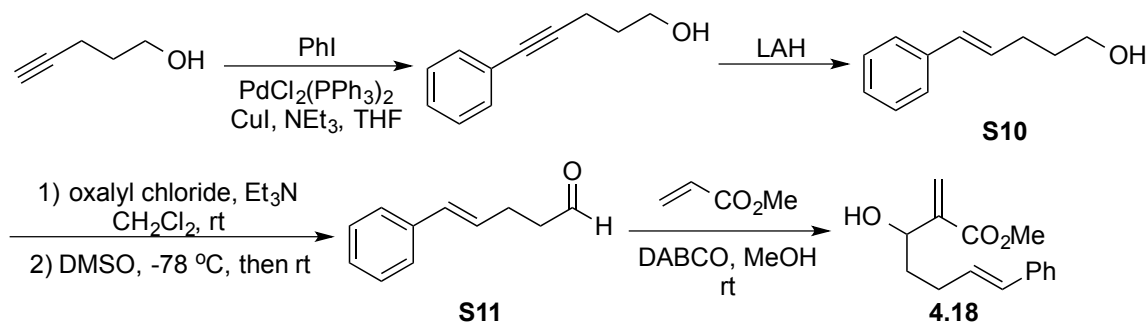
**(E)-methyl 2-((cinnamyloxy)methyl)acrylate (4.16):** Under Ar, sodium hydride (99 mg (60% purity), 2.1 mmol) was added to a solution of **S9** (232 mg, 2 mmol) in THF (15 mL) at 0 °C. The reaction was warmed to room temperature and stirred for 2 h. To the solution was added dropwise a solution of cinnamyl bromide (374 mg, 1.9 mmol) in 3 mL THF. The reaction was stirred overnight until TLC (ethyl acetate: hexanes = 1: 10) indicated complete consumption of cinnamyl bromide. Saturated  $\text{NH}_4\text{Cl}$  solution (30 mL) was then added to quench the reaction. The aqueous phase was extracted with diethyl ether (3  $\times$  20 mL), dried over  $\text{MgSO}_4$ , filtered and concentrated *in vacuo*. The crude product was purified by flash chromatography (ethyl acetate: hexanes = 1: 5). The product was obtained as a light yellow oil (370 mg, 1.6 mmol, 84% yield).  $^1\text{H}$  NMR (500 MHz,  $\text{CDCl}_3$ )  $\delta$  7.40-7.24 (m, 5H,  $\text{C}_6\text{H}_5$ ), 6.63 (d,  $J$  = 16 Hz, 1H  $\text{PhCH=CH-}$ ), 6.33 (d,  $J$  = 2 Hz, 1H, *cis* = $\text{CH}_2$ ), 6.30 (dt,  $J_1$  = 16 Hz,  $J_2$  = 6 Hz, 1H,  $\text{PhCH=CH-}$ ), 5.93 (d,  $J$  = 2 Hz, 1H, *trans* = $\text{CH}_2$ ), 4.26 (s, 2H,  $\text{PhCH=CH-CH}_2\text{-O-CH}_2\text{-}$ ), 4.22 (dd,  $J_1$  = 6 Hz,  $J_2$  = 2 Hz, 2H,  $\text{PhCH=CH-CH}_2\text{-O-}$ ), 3.78 (s, 3H,  $-\text{CO}_2\text{CH}_3$ ).  $^{13}\text{C}$  NMR (125 MHz,  $\text{CDCl}_3$ )  $\delta$  166.3, 137.2, 136.6, 132.6, 128.6, 127.7, 126.5, 126.0, 125.8, 71.4, 68.3, 51.6. IR (neat) 2924, 2852.4, 2361, 1722 (C=O), 1637, 1496, 1439, 1367, 1308, 1277, 1198, 1160, 1113, 966, 817, 745, 693  $\text{cm}^{-1}$ . HRMS (DART) calculated for  $\text{C}_{14}\text{H}_{15}\text{O}_3$   $[\text{M-H}]^-$  231.1021, found 231.0987.



(*E*)-methyl 3-hydroxy-2-methylene-7-phenylhept-6-enoate (**4.18**).

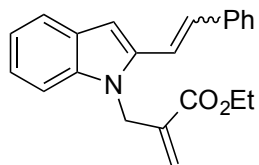
Compound **4.18** was synthesized according to the procedure in Scheme 4.9. **S10**<sup>31</sup> and **S11**<sup>32</sup> are synthesized according to published procedures.

#### Scheme 4.9. Synthesis of **4.18**



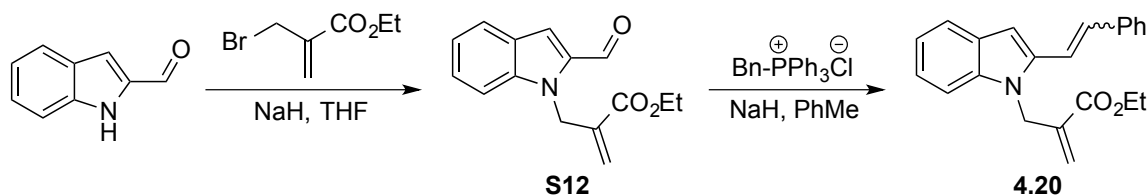
**(*E*)-methyl 3-hydroxy-2-methylene-7-phenylhept-6-enoate (**4.18**):** In a round-bottom flask equipped with a stir bar was placed **S11** (291 mg, 1.8 mmol), methyl methacrylate (235 mg, 2.7 mmol) and 1,4-diazabicyclo[2.2.2]octane (DABCO, 306 mg, 2.7 mmol). Methanol (50  $\mu$ L) methanol was added to the system. The reaction was stirred at room temperature until TLC (ethyl acetate: hexanes = 1: 4) indicated complete consumption of **S11**. The reaction was concentrated *in vacuo* and purified by flash chromatography (ethyl acetate: hexanes = 1: 10). The product was obtained as a light yellow oil (394 mg, 1.6 mmol, 89% yield). <sup>1</sup>H NMR (400 MHz, CDCl<sub>3</sub>)  $\delta$  7.35-7.18 (m, 5H, C<sub>6</sub>H<sub>5</sub>), 4.43 (d, *J* = 16 Hz, 1H, PhCH=CH-), 6.26 (s, 1 H, *cis* =CH<sub>2</sub>), 6.23 (dt, *J*<sub>1</sub> = 16 Hz, *J*<sub>2</sub> = 7 Hz, 1H, PhCH=CH-), 5.83 (s, 1H, *trans* =CH<sub>2</sub>), 3.79 (s, 3H, -CO<sub>2</sub>CH<sub>3</sub>), 2.59 (d, *J* = 4 Hz, 1H, >C(-OH)-H), 2.44-2.27 (m, 2H, =CH-CH<sub>2</sub>-), 1.87-1.81 (m, 2H, =CH-CH<sub>2</sub>-CH<sub>2</sub>-). <sup>13</sup>C NMR (125 MHz, CDCl<sub>3</sub>)  $\delta$  167.0, 142.3, 137.6, 130.5, 129.8, 128.5, 126.9, 126.0, 125.2, 71.2, 51.9, 35.7, 29.3. IR (neat) 3442, 3026, 2951, 2361, 1717, 1630, 1495, 1439, 1287,

1196, 1146, 1071, 964, 819, 744, 693  $\text{cm}^{-1}$ . HRMS ( $\text{FAB}^+$ ) calculated for  $\text{C}_{15}\text{H}_{19}\text{O}_3$   $[\text{M}+\text{H}]^+$  247.1334, found 247.1329.



*Ethyl 2-((2-styryl-1H-indol-1-yl)methyl)acrylate (4.20)*. Compound **4.20** was synthesized according to the procedure in Scheme 4.10.

**Scheme 4.10.** Synthesis of **4.20**

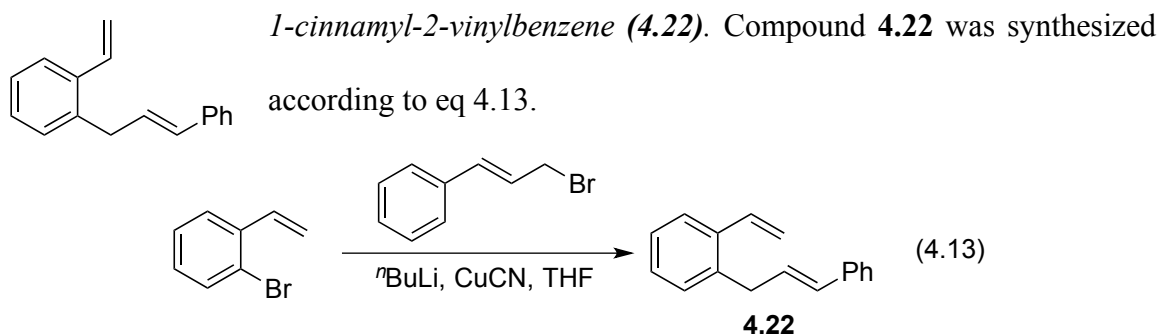


**S12**: Under Ar, sodium hydride (99 mg (60% purity), 2.5 mmol) was added to a solution of indole-2-carboxaldehyde (300 mg, 2 mmol) in THF (25 mL) at 0 °C. The reaction was then warmed to room temperature and stirred for 30 min. To the solution was then added dropwise a solution of ethyl 2-(bromomethyl)acrylate (478 mg, 2.5 mmol) in 5 mL THF. The reaction was stirred overnight until TLC (ethyl acetate: hexanes = 1: 10) indicated complete reaction. Saturated  $\text{NH}_4\text{Cl}$  solution (30 mL) was then added to quench the reaction. The aqueous phase was extracted with diethyl ether ( $3 \times 20$  mL), dried over  $\text{MgSO}_4$ , filtered and concentrated *in vacuo*. The crude product was used without further purification.  $^1\text{H}$  NMR (400 MHz,  $\text{CDCl}_3$ )  $\delta$  9.88 (s, 1H,  $-\text{C}(=\text{O})-\text{H}$ ), 7.43-7.18 (m, 4H,  $\text{C}_6\text{H}_4$ ), 7.33 (s, 1H,  $-\text{C}(\text{=CR}_2)-\text{H}$ ), 6.16 (s, 1H,  $\text{CH}_2=\text{C}(-\text{CO}_2\text{Et})-\text{CH}_2$  cis to  $-\text{CO}_2\text{Et}$ ), 5.47 (s, 2H, indole N- $\text{CH}_2-$ ), 4.83 (s, 1H,  $\text{CH}_2=\text{C}(-\text{CO}_2\text{Et})-\text{CH}_2$  trans to  $-\text{CO}_2\text{Et}$ ), 4.28 (q,  $J = 7.2$  Hz, 2H,  $-\text{CO}_2\text{CH}_2\text{Me}$ ), 1.34 (t,  $J = 7.2$  Hz, 3H,  $-\text{CO}_2\text{CH}_2\text{CH}_3$ ).

**Ethyl 2-((2-styryl-1H-indol-1-yl)methyl)acrylate (4.20)**: Under Ar, sodium hydride (95 mg (60% purity), 2.4 mol) was added to the suspension of benzyltriphenylphosphonium



chloride (926 mg, 2.4 mmol) in toluene (10 mL) at 0 °C. The reaction was then warmed to room temperature and stirred for 1 h. The reaction was cooled to 0 °C, a solution of **S12** in 5 mL toluene was then added dropwise. The reaction was stirred overnight at 80 °C until TLC (ethyl acetate: hexanes = 1: 10) indicated complete reaction. Saturated NH<sub>4</sub>Cl solution (30 mL) was then added to quench the reaction. The aqueous phase was extracted with diethyl ether (3 × 20 mL), dried over MgSO<sub>4</sub>, filtered and concentrated *in vacuo*. The crude product was purified by flash chromatography (ethyl acetate: hexanes = 1: 5). The product was obtained as a yellow solid (trans:cis = 3:1, 629 mg, 1.9 mmol, 79% yield). <sup>1</sup>H NMR (400 MHz, CDCl<sub>3</sub>) δ trans 7.62-6.86 (m, 11H, aryl H's and PhCH=CH-), 6.99 (d, *J* = 16 Hz, 1H, Ph-CH=CH-), 6.86 (s, 1H, =CH<sub>2</sub> cis to -CO<sub>2</sub>Et), 6.22 (s, 1H, =CH<sub>2</sub> trans to -CO<sub>2</sub>Et), 5.09 (s, 2H, N-CH<sub>2</sub>-), 4.31 (q, *J* = 7.2 Hz, 2H, -CO<sub>2</sub>CH<sub>2</sub>Me), 1.35 (t, *J* = 7.2 Hz, 3H, -CO<sub>2</sub>CH<sub>2</sub>CH<sub>3</sub>); δ cis 7.62-6.86 (m, 10H, aryl H's), 6.69 (d, *J* = 12 Hz, 1H, PhCH=CH-), 6.46 (s, 1H, =CH<sub>2</sub> cis to -CO<sub>2</sub>Et), 6.41 (d, *J* = 12 Hz, 1H, Ph-CH=CH-), 6.19 (s, 1H, =CH<sub>2</sub> trans to -CO<sub>2</sub>Et), 4.96 (s, 2H, N-CH<sub>2</sub>-), 4.28 (q, *J* = 7.2 Hz, 2H, -CO<sub>2</sub>CH<sub>2</sub>Me), 1.33 (t, *J* = 7.2 Hz, -CO<sub>2</sub>CH<sub>2</sub>CH<sub>3</sub>). <sup>13</sup>C NMR (125 MHz, CDCl<sub>3</sub>) δ trans 165.62, 138.0, 137.5, 136.9, 136.2, 133.4, 131.4, 128.7, 127.9, 126.5, 125.6, 122.1, 120.5, 120.3, 116.5, 109.3, 99.7, 61.2, 43.5, 14.2; δ cis 165.59, 136.8, 136.6, 136.3, 135.7, 128.6, 128.3, 128.2, 128.0, 127.7, 125.2, 121.9, 120.7, 120.0, 118.4, 109.5, 102.5, 61.1, 53.4, 43.7. IR (neat) 3056, 3027, 2980, 2935, 1707 (C=O), 1634, 1459, 1404, 1370, 1348, 1319, 1297, 1262, 1146, 1133, 1109, 1020, 952, 779, 750, 733, 693, 641, 582, 514, 442 cm<sup>-1</sup>. HRMS (DART) calculated for C<sub>22</sub>H<sub>22</sub>NO<sub>2</sub> [M+H]<sup>+</sup> 332.1651, found 332.1661.

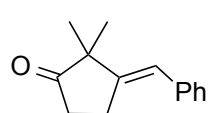


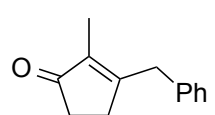
**1-cinnamyl-2-vinylbenzene (4.22)**: To a solution of 2-bromostyrene (121 mg, 0.66 mmol) in 6 mL THF at -78 °C was added *n*BuLi dropwise. The mixture was stirred for 20 min at -78 °C and CuCN (29 mg, 0.33 mmol) was added. The reaction was stirred for 20 mins at -20 °C. The reaction was then cooled down to -78 °C and cinnamyl bromide (116 mg, 0.59 mmol) was added dropwise. The reaction was allowed to warm to room temperature and stirred overnight. Saturated NH<sub>4</sub>Cl solution (10 mL) was added to quench the reaction. The aqueous phase was extracted with diethyl ether (3 × 10 mL), dried over MgSO<sub>4</sub>, filtered and concentrated *in vacuo*. The crude product was purified by flash chromatography (pure hexane). The product was obtained as a colorless oil (96 mg, 0.44 mmol, 74% yield). <sup>1</sup>H NMR (400 MHz, CDCl<sub>3</sub>) δ 7.54-7.19 (m, 9H, aryl Hs), 7.02 (dd, *J*<sub>1</sub> = 17.6 Hz, *J*<sub>2</sub> = 11.2 Hz, 1H, ArCH=CH<sub>2</sub>), 6.36-6.34 (m, 2H, PhCH=CH-), 5.66 (dd, *J*<sub>1</sub> = 17.6 Hz, *J*<sub>2</sub> = 1.6 Hz, 1H, *cis* ArCH=CH<sub>2</sub>), 5.31 (dd, *J*<sub>1</sub> = 11.2 Hz, *J*<sub>2</sub> = 1.6 Hz, 1H, *trans* ArCH=CH<sub>2</sub>), 3.62 (d, *J* = 4.4 Hz, -CH<sub>2</sub>-). <sup>13</sup>C NMR (125 MHz, CDCl<sub>3</sub>) δ 137.5, 137.3, 136.9, 134.5, 131.1, 129.8, 128.8, 128.5, 128.0, 127.1, 126.7, 126.1, 125.9, 115.8, 36.6. IR (neat) 3060, 3026, 2924, 2851, 1626, 1598, 1481, 1448, 1416, 986, 964, 912, 761, 732, 691, 677, 495 cm<sup>-1</sup>. HRMS (FAB<sup>+</sup>) calculated for C<sub>17</sub>H<sub>16</sub> [M]<sup>+</sup> 220.1252, found 220.1244.

#### 4.5.2 Cobaloxime-Catalyzed Radical Cyclizations and Cycloisomerizations of Diene Substrates

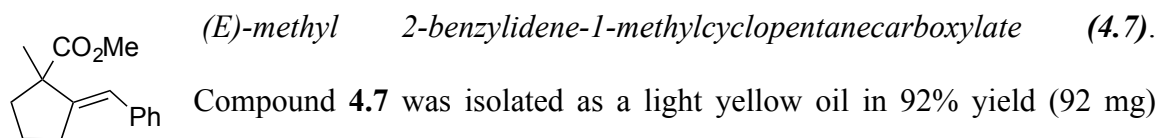
##### General Procedure for Cobaloxime-Mediated Cyclization of Diene Substrates.

To a Fisher-Porter pressure apparatus were added cobaloxime **3.1** or **3.10** (7 mol%) and a C<sub>6</sub>H<sub>6</sub> solution of the substrate (0.1 M) before the apparatus was thoroughly purged with H<sub>2</sub> and pressurized to 6 atm. The reaction was stirred at 50 °C for 1.5-3 d. TLC indicated that no starting materials remained. The reaction mixture was concentrated, and purified by flash chromatography (hexanes: ethyl acetate = 5: 1), affording the cyclized product.

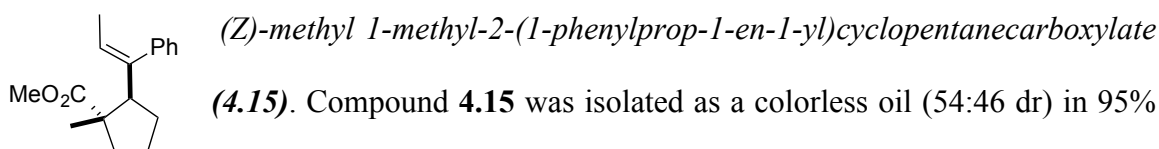
 (*E*)-3-benzylidene-2,2-dimethylcyclopentan-1-one (**4.11**). Compound **4.11** was isolated as a white solid in 61% yield (61 mg) from 100 mg **4.7**. <sup>1</sup>H NMR (500 MHz, C<sub>6</sub>D<sub>6</sub>) δ 7.21–7.07 (m, 5H, C<sub>6</sub>H<sub>5</sub>), 6.22 (t, *J* = 2 Hz, 1H, PhCH=), 2.38 (td, *J*<sub>1</sub> = 7.5 Jz, *J*<sub>2</sub> = 2 Hz, 2H, -C(=O)-CH<sub>2</sub>CH<sub>2</sub>-), 1.94 (t, *J* = 7.5 Hz, 2H, -C(=O)-CH<sub>2</sub>CH<sub>2</sub>-), 1.09 (s, 6H, -CH<sub>3</sub>). <sup>13</sup>C NMR (125 MHz, C<sub>6</sub>D<sub>6</sub>) δ 218.3, 149.4, 137.9, 129.1, 128.5, 126.8, 122.4, 50.0, 35.9, 25.3, 24.8. IR (neat) 2967, 2962, 1744 (C=O), 1492, 1447, 1378, 1292, 1078, 753, 697 cm<sup>-1</sup>. HRMS (FAB<sup>+</sup>) calculated for C<sub>14</sub>H<sub>16</sub>O [M]<sup>+</sup> 200.1201, found 200.1206.

 3-benzyl-2-methylcyclopent-2-enone (**4.13**). Compound **4.13** was isolated as a white solid in 57% yield (57 mg) from 100 mg **4.12**. <sup>1</sup>H NMR (500 MHz, CDCl<sub>3</sub>) δ 7.34–7.15 (m, 5H, C<sub>6</sub>H<sub>5</sub>), 3.74 (s, 2H, PhCH<sub>2</sub>), 2.41–2.39 (m, 2H, -C(=O)-CH<sub>2</sub>CH<sub>2</sub>-), 2.35–2.33 (m, 2H, -C(=O)-CH<sub>2</sub>CH<sub>2</sub>-), 1.83 (t, *J* = 2 Hz, 3H, -CH<sub>3</sub>). <sup>13</sup>C NMR (125 MHz, CDCl<sub>3</sub>) δ 210.1, 171.0, 137.4, 136.6, 128.8, 128.7, 126.8,

37.6, 34.1, 29.1, 8.3. IR (neat) 3029, 2919, 1693 (C=O), 1645, 1495, 1332, 1071, 759, 618 cm<sup>-1</sup>. HRMS (FAB<sup>+</sup>) calculated for C<sub>13</sub>H<sub>15</sub>O [M+H]<sup>+</sup> 187.1123, found 187.1124.

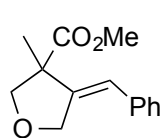


Compound **4.7** was isolated as a light yellow oil in 92% yield (92 mg) from 100 mg **2.10**. <sup>1</sup>H NMR (500 MHz, CDCl<sub>3</sub>) δ 7.33–7.18 (m, 5H, C<sub>6</sub>H<sub>5</sub>), 6.38 (t, *J* = 2.5 Hz, 1H, Ph-CH=C), 3.69 (s, 3H, -C(=O)-OCH<sub>3</sub>), 2.72 (td, *J*<sub>1</sub> = 7 Hz, *J*<sub>2</sub> = 2.5 Hz, 2H, -CH<sub>2</sub>-C(-R)=CHPh), 2.41–2.35 (m, 1H, -CH<sub>2</sub>-CH<sub>2</sub>CH<sub>2</sub>C(-R)=CHPh), 1.98–1.90 (m, 1H, -CH<sub>2</sub>-CH<sub>2</sub>C(-R)=CHPh), 1.82–1.76 (m, 1H, -CH<sub>2</sub>-CH<sub>2</sub>C(-R)=CHPh), 1.65–1.59 (m, 1H, -CH<sub>2</sub>-CH<sub>2</sub>CH<sub>2</sub>C(-R)=CHPh), 1.44 (s, 3H, -CH<sub>3</sub>). <sup>13</sup>C NMR (100 MHz, CDCl<sub>3</sub>) δ 176.9, 149.5, 138.1, 128.4, 128.2, 126.3, 122.7, 54.0, 52.1, 38.2, 32.0, 25.1, 24.6. IR (neat) 2954, 1730 (C=O), 1650, 1493, 1446, 1375, 1266, 1192, 1078, 757, 696 cm<sup>-1</sup>. HRMS (FAB<sup>+</sup>) calculated for C<sub>15</sub>H<sub>18</sub>O<sub>2</sub> [M]<sup>+</sup> 230.1307, found 230.1298.



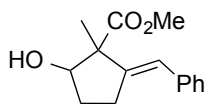
Compound **4.15** was isolated as a colorless oil (54:46 dr) in 95% yield (95 mg) from 100 mg **4.14**. The NMR spectra for the minor diastereomer are reported: <sup>1</sup>H NMR (500 MHz, CDCl<sub>3</sub>) δ 7.29–7.08 (m, 5H, C<sub>6</sub>H<sub>5</sub>), 5.56 (dq, *J*<sub>1</sub> = 7 Hz, *J*<sub>2</sub> = 1.5 Hz, 1H, >C=CH-), 3.07 (s, 3H, -CO<sub>2</sub>CH<sub>3</sub>), 2.15–2.09 (m, 1H, >CH-), 1.91–1.85 (m, 2H, >CH-CH<sub>2</sub>-), 1.78–1.75 (m, 2H, >CH-CH<sub>2</sub>-CH<sub>2</sub>-CH<sub>2</sub>-), 1.55–1.54 (m, 2H, >CH-CH<sub>2</sub>-CH<sub>2</sub>-) 1.53 (d, *J* = 7 Hz, >C=CH-CH<sub>3</sub>), 0.99 (s, 3H, -CH<sub>3</sub>); <sup>13</sup>C NMR (125 MHz, CDCl<sub>3</sub>) δ 178.5, 140.6, 140.2, 129.1, 127.6, 126.3, 122.1, 54.9, 51.2, 50.3, 39.9, 28.6, 22.0, 18.5,

14.6. IR (neat) 2925, 2855, 1728 (C=O), 1441, 1379, 1258, 1193, 1176, 1149, 921, 776, 703  $\text{cm}^{-1}$ . HRMS (ASAP<sup>+</sup>) calculated for  $\text{C}_{17}\text{H}_{23}\text{O}_2$   $[\text{M}+\text{H}]^+$  259.1698, found 259.1698.



*(Z)*-methyl 4-benzylidene-3-methyltetrahydrofuran-3-carboxylate (**4.17**).

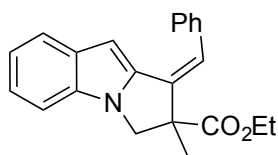
Compound **4.17** was isolated as a colorless oil in 95% yield (95 mg) from 100 mg **4.16**. <sup>1</sup>H NMR (400 MHz,  $\text{CDCl}_3$ )  $\delta$  7.37-7.15 (m, 5H,  $\text{C}_6\text{H}_5$ ), 6.46 (t,  $J = 2.4$  Hz, 1H,  $\text{Ph-CH=}$ ), 4.76 (dd,  $J_1 = 14$  Hz,  $J_2 = 2.4$  Hz, 1H,  $-\text{O-CH}_2-\text{C=}$ ), 4.70 (dd,  $J_1 = 14$  Hz,  $J_2 = 2.4$  Hz, 1H,  $-\text{O-CH}_2-\text{C=}$ ), 4.41 (d,  $J = 8.8$  Hz, 1H,  $-\text{O-CH}_2-\text{C}(-\text{CO}_2\text{Me})$ ), 3.74 (s, 3H,  $-\text{CO}_2\text{CH}_3$ ), 3.66 (d,  $J = 8.8$  Hz, 1H,  $-\text{O-CH}_2-\text{C}(-\text{CO}_2\text{Me})$ ), 1.51 (s, 3H,  $-\text{C}(\text{CO}_2\text{Me})-\text{CH}_3$ ). <sup>13</sup>C NMR (125 MHz,  $\text{CDCl}_3$ )  $\delta$  174.5, 144.3, 136.7, 128.6, 128.2, 127.2, 122.4, 70.7, 53.9, 52.6, 29.7, 22.3. IR (neat) 2951, 2846, 2361, 2336, 1731 (C=O), 1495, 1448, 1272, 1132, 1067, 928, 755, 695  $\text{cm}^{-1}$ . HRMS (FAB<sup>+</sup>) calculated for  $\text{C}_{14}\text{H}_{17}\text{O}_3$   $[\text{M}+\text{H}]^+$  233.1178, found 233.1189.



*(E)*-methyl 2-benzylidene-5-hydroxy-1-methylcyclopentanecarboxylate

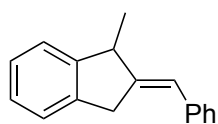
**(4.19)**. Compound **4.19** was isolated as a colorless oil (54:46 dr) in 90% yield (90 mg) from 100 mg **4.18**. <sup>1</sup>H NMR (500 MHz,  $\text{CDCl}_3$ )  $\delta$  major 7.31-7.19 (m, 5H,  $\text{C}_6\text{H}_5$ ), 6.43 (t,  $J = 2.5$  Hz, 1H,  $\text{Ph-CH=}$ ), 4.67 (t,  $J = 7$  Hz, 1H,  $-\text{CH-OH}$ ), 3.72 (s, 3H,  $-\text{CO}_2\text{CH}_3$ ), 2.80-2.76 (m, 1H,  $-\text{CH}_2-\text{C}(-\text{R})=\text{CH-Ph}$ ), 2.67-2.60 (m, 1H,  $-\text{CH}_2-\text{C}(-\text{R})=\text{CH-Ph}$ ), 2.19-2.10 (m, 1H,  $-\text{CH}_2-\text{C-OH}$ ), 1.78-1.72 (m, 1H,  $-\text{CH}_2-\text{C-OH}$ ), 1.40 (s, 3H,  $-\text{C}(\text{CO}_2\text{Me})-\text{CH}_3$ );  $\delta$  minor 7.31-7.19 (m, 5H,  $\text{C}_6\text{H}_5$ ), 6.45 (t,  $J = 2.5$  Hz, 1H,  $\text{Ph-CH=}$ ), 3.95 (t,  $J = 7$  Hz, 1H,  $-\text{CH-OH}$ ), 3.74 (s, 3H,  $-\text{CO}_2\text{CH}_3$ ), 2.94-2.81 (m, 1H,  $-\text{CH}_2-\text{C}(-\text{R})=\text{CH-Ph}$ ), 2.67-2.60 (m, 2H,  $-\text{CH}_2-\text{C}(-\text{R})=\text{CH-Ph}$ ), 2.19-2.10 (m, 2H,  $-\text{CH}_2-\text{C-OH}$ ),

2.04-1.98 (m, 1H, -CH<sub>2</sub>-C-OH), 1.50 (s, 3H, -C(CO<sub>2</sub>Me)-CH<sub>3</sub>). <sup>13</sup>C NMR (125 MHz, CDCl<sub>3</sub>) δ major 175.7, 146.0, 137.5, 128.5, 128.2, 126.5, 124.3, 76.7, 57.9, 52.3, 31.2, 27.9, 16.6; δ minor 175.3, 145.1, 137.5, 128.5, 128.2, 126.6, 124.9, 80.5, 57.4, 52.2, 31.8, 28.2, 23.0. IR (neat) 2926, 2513, 1747 (C=O), 1716 (C=O), 1495, 1456, 1262, 1204, 1123, 1072, 966, 746, 695 cm<sup>-1</sup>. HRMS (FAB<sup>+</sup>) calculated for C<sub>15</sub>H<sub>18</sub>O<sub>3</sub> [M]<sup>+</sup> 246.1256, found 246.1256.



(*Z*)-methyl-1-benzylidene-2-methyl-2,3-dihydro-1H-pyrrolo[1,2-a]indole-2-carboxylate (**4.21**). Compound **4.21** was isolated as a yellow

solid in 67% yield (67 mg) from 100 mg **4.20**. <sup>1</sup>H NMR (500 MHz, CDCl<sub>3</sub>) δ 7.60-7.18 (m, 9H, phenyl H's), 6.66 (s, 1H, indole Hs), 6.48 (s, 1H, Ph-CH=), 4.82 (d, *J* = 13 Hz, 1H, >N-CH<sub>2</sub>-), 4.22 (qd, *J*<sub>1</sub> = 9 Hz, *J*<sub>2</sub> = 1.5 Hz, -CO<sub>2</sub>CH<sub>2</sub>CH<sub>3</sub>), 4.99 (d, *J* = 13 Hz, >N-CH<sub>2</sub>-), 1.75 (s, -CH<sub>3</sub>), 1.24 (t, *J* = 9 Hz, -CO<sub>2</sub>CH<sub>2</sub>CH<sub>3</sub>). <sup>13</sup>C NMR (125 MHz, CDCl<sub>3</sub>) δ 173.8, 139.0, 137.0, 135.9, 133.2, 132.6, 128.42, 128.39, 127.7, 123.9, 122.1, 121.4, 120.1, 109.5, 99.1, 61.7, 57.3, 52.9, 25.2, 14.1. IR (neat) 3055, 3025, 2978, 2928, 2851, 1727 (C=O), 1451, 1379, 1341, 1316, 1264, 1206, 1128, 1113, 1022, 860, 783, 744, 698, 588, 507, 428 cm<sup>-1</sup>. HRMS (FAB<sup>+</sup>) calculated for C<sub>22</sub>H<sub>21</sub>NO<sub>2</sub> [M]<sup>+</sup> 331.1572, found 331.1585.



(*E*)-2-benzylidene-1-methyl-2,3-dihydro-1H-indene (**4.23**).

Compound **4.23** was isolated as a colorless oil in 80% yield (80 mg) from 100 mg **4.22**. <sup>1</sup>H NMR (400 MHz, CDCl<sub>3</sub>) δ 7.39-7.19 (m, 5H, phenyl H's), 6.52 (dt,

$J_1 = J_2 = 2.4$  Hz, PhCH=C<), 4.03-3.92 (m, 3H, -CH<sub>2</sub>- and >CH-CH<sub>3</sub>), 1.50 (d, 3H,  $J = 6.8$  Hz, -CH<sub>3</sub>). <sup>13</sup>C NMR (125 MHz, CDCl<sub>3</sub>)  $\delta$  147.9, 146.5, 141.1, 138.1, 128.3, 128.2, 126.70, 126.65, 126.2, 124.4, 123.6, 122.7, 45.8, 37.4, 21.3. IR (neat) 3023, 2961, 2924, 2866, 2978, 1599, 1481, 1447, 1319, 1200, 1021, 912, 866, 745, 695, 514 cm<sup>-1</sup>. HRMS (FAB<sup>+</sup>) calculated for C<sub>17</sub>H<sub>16</sub> [M]<sup>+</sup> 220.1252, found 220.1244.

## 4.6 References

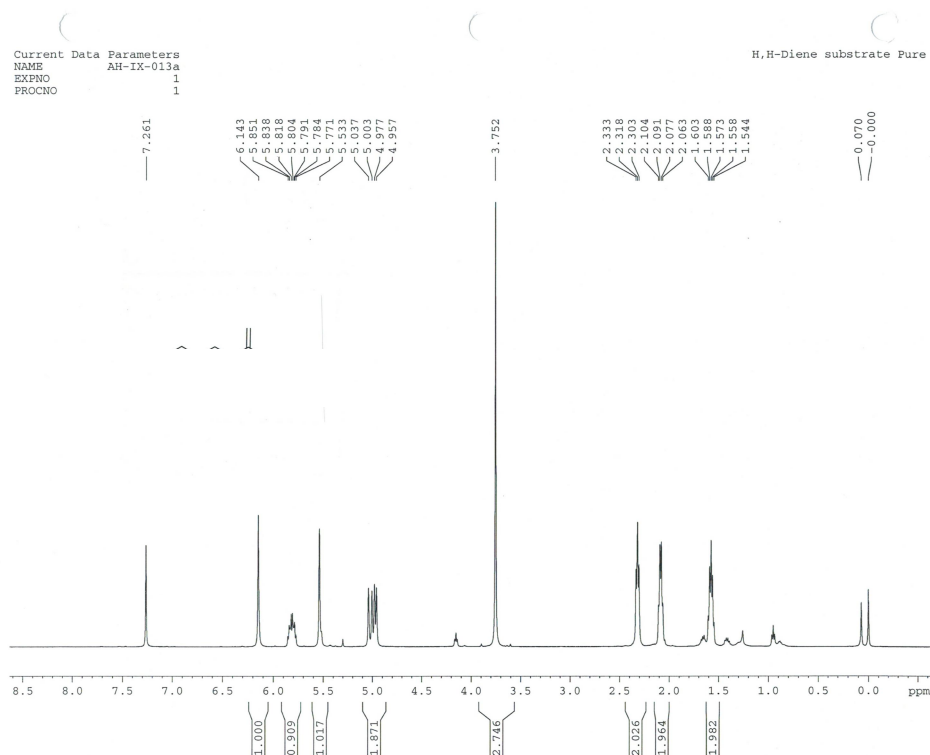
1. Ittel, S. D.; Gridnev, A. A. Initiation of Polymerization by Hydrogen Atom Donation. U.S. Patent 7022792, April 4, 2006.
2. Smith, D. M.; Pulling, M. E.; Norton, J. R., Tin-free and Catalytic Radical Cyclizations. *J. Am. Chem. Soc.* **2007**, *129*, 770-771.
3. Choi, J.; Pulling, M. E.; Smith, D. M.; Norton, J. R., Unusually Weak Metal-Hydrogen Bonds in  $\text{HV}(\text{CO})_4(\text{P-P})$  and Their Effectiveness as  $\text{H}\bullet$  Donors. *J. Am. Chem. Soc.* **2008**, *130*, 4250-4252.
4. Hartung, J.; Pulling, M. E.; Smith, D. M.; Yang, D. X.; Norton, J. R., Initiating Radical Cyclizations by  $\text{H}\bullet$  Transfer from Transition Metals. *Tetrahedron* **2008**, *64*, 11822-11830.
5. Kuo, J. L.; Hartung, J.; Han, A.; Norton, J. R., Direct Generation of Oxygen-Stabilized Radicals by  $\text{H}\bullet$  Transfer from Transition Metal Hydrides. *J. Am. Chem. Soc.* **2015**, *137*, 1036-1039.
6. Widenhoefer, R. A., Synthetic and Mechanistic Studies of the Cycloisomerization and Cyclization/hydrosilylation of Functionalized Dienes Catalyzed by Cationic Palladium(II) Complexes. *Acc. Chem. Res.* **2002**, *35*, 905-913.
7. Trost, B. M., Palladium-Catalyzed Cycloisomerizations of Enynes and Related Reactions. *Acc. Chem. Res.* **1990**, *23*, 34-42.
8. Yamamoto, Y., Transition-Metal-Catalyzed Cycloisomerizations of  $\alpha,\omega$ -Dienes. *Chem. Rev.* **2012**, *112*, 4736-4769.
9. Crossley, S. W. M.; Barabe, F.; Shenvi, R. A., Simple, Chemoselective, Catalytic Olefin Isomerization. *J. Am. Chem. Soc.* **2014**, *136*, 16788-16791.
10. Norton, J. R.; Spataru, T.; Camaioni, D. M.; Lee, S. J.; Li, G.; Choi, J.; Franz, J. A., Kinetics and Mechanism of the Hydrogenation of the  $\text{CpCr}(\text{CO})_3$  /  $[\text{CpCr}(\text{CO})_3]_2$  Equilibrium to  $\text{CpCr}(\text{CO})_3\text{H}$ . *Organometallics* **2014**, *33*, 2496-2502.
11. Such an enone is an attractive substrate because radicals are stabilized by acyl substituents. See: Brocks, J. J.; Beckhaus, H. D.; Beckwith, A. L. J.; Rüchardt, C., Estimation of Bond Dissociation Energies and Radical Stabilization Energies by ESR Spectroscopy. *J. Org. Chem.* **1998**, *63*, 1935-1943.



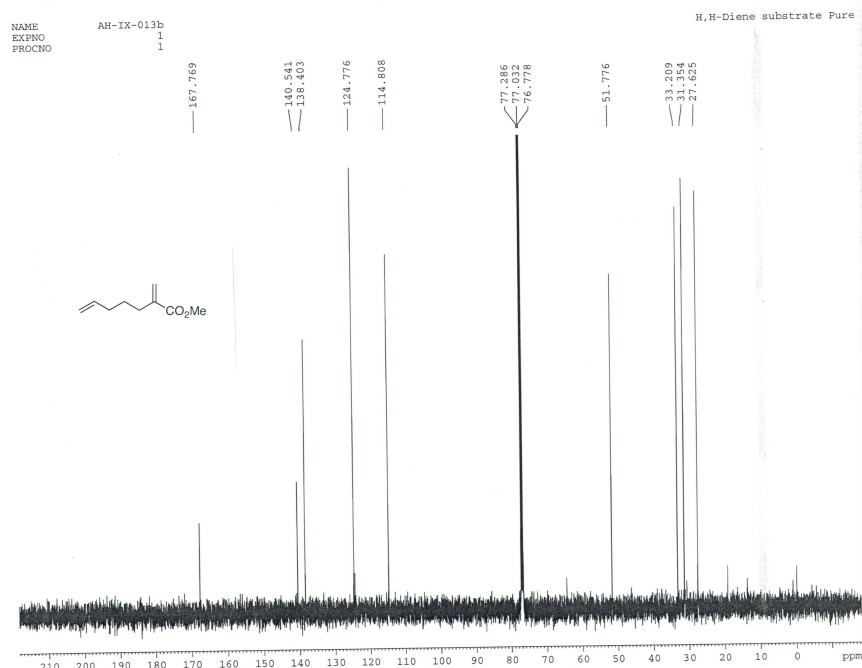
12. Clive, D. L. J.; Cheshire, D. R., On Baldwin Kinetic Barrier against 5-(Enol-endo)-exo-trigonal Closures: a Comparison of Ionic and Analogous Radical Reactions, and a New Synthesis of Cyclopentanones. *J. Chem. Soc., Chem. Comm.* **1987**, 1520-1523.
13. Porter, N. A.; Chang, V. H. T.; Magnin, D. R.; Wright, B. T., Free-Radical Macrocyclization-Transannular Cyclization. *J. Am. Chem. Soc.* **1988**, *110*, 3554-3560.
14. Curran, D. P.; Chang, C. T., Atom Transfer Cyclization Reactions of  $\alpha$ -Iodo Esters, Ketones, and Malonates: Examples of Selective 5-Exo, 6-Endo, 6-Exo, and 7-Endo Ring Closures. *J. Org. Chem.* **1989**, *54*, 3140-3157.
15. Broeker, J. L.; Houk, K. N., MM2 Model for the Intramolecular Additions of Acyl-Substituted Radicals to Alkenes. *J. Org. Chem.* **1991**, *56*, 3651-3655.
16. Blanksby, S. J.; Ellison, G. B., Bond Dissociation Energies of Organic Molecules. *Acc. Chem. Res.* **2003**, *36*, 255-263.
17. Beckwith, A. L. J.; Glover, S. A., Determination of the Rates of Ring-Closure of Oxygen-Containing Analogs of Hex-5-enyl Radical by Kinetic Electron-Spin-Resonance Spectroscopy. *Aust. J. Chem.* **1987**, *40*, 157-173.
18. Beckwith, A. L. J.; Easton, C. J.; Lawrence, T.; Serelis, A. K., Reactions of Methyl-Substituted Hex-5-Enyl and Pent-4-Enyl Radicals. *Aust. J. Chem.* **1983**, *36*, 545-556.
19. Chatgililoglu, C.; Ingold, K. U.; Scaiano, J. C., Rate Constants and Arrhenius Parameters for the Reactions of Primary, Secondary, and Tertiary Alkyl Radicals with Tri-*n*-butyltin Hydride. *J. Am. Chem. Soc.* **1981**, *103*, 7739-7742.
20. Beckwith, A. L. J.; Moad, G., Intramolecular Addition In Hex-5-enyl, Hept-6-enyl, and Oct-7-enyl Radicals. *J. Chem. Soc., Chem. Comm.* **1974**, 472-473.
21. Lo, J. C. L.; Gui, J. H.; Yabe, Y. K.; Pan, C. M.; Baran, P. S., Functionalized Olefin Cross-coupling to Construct Carbon-Carbon Bonds. *Nature* **2014**, *516*, 343-348.
22. Walton, J. C., Unusual Radical Cyclisations. *Top. Curr. Chem.* **2006**, *264*, 163-200.
23. Lunazzi, L.; Ingold, K. U., Electron Paramagnetic Resonance Spectra of Alkylhydrazyl Radicals in Solution. *J. Am. Chem. Soc.* **1974**, *96*, 5558-5560.
24. Evans, D. A.; Andrews, G. C.; Buckwalt, B., Metalated Allylic Ethers as Homoenolate Anion Equivalents. *J. Am. Chem. Soc.* **1974**, *96*, 5560-5561.

25. Aloui, M.; Chambers, D. J.; Cumpstey, I.; Fairbanks, A. J.; Redgrave, A. J.; Seward, C. M. P., Stereoselective 1,2-cis Glycosylation of 2-O-Allyl Protected Thioglycosides. *Chem. Eur. J.* **2002**, *8*, 2608-2621.
26. Nelson, S. G.; Wang, K., Asymmetric Claisen Rearrangements Enabled by Catalytic Asymmetric Di(allyl) Ether Synthesis. *J. Am. Chem. Soc.* **2006**, *128*, 4232-4233.
27. Choi, J.; Tang, L. H.; Norton, J. R., Kinetics of Hydrogen Atom Transfer from ( $\eta^5$ -C<sub>5</sub>H<sub>5</sub>)Cr(CO)<sub>3</sub>H to Various Olefins: Influence of Olefin Structure. *J. Am. Chem. Soc.* **2007**, *129*, 234-240.
28. Zhao, Q. W.; Curran, D. P.; Malacria, M.; Fensterbank, L.; Goddard, J. P.; Lacôte, E., N-Heterocyclic Carbene-Catalyzed Hydrosilylation of Styryl and Propargylic Alcohols with Dihydrosilanes. *Chem. Eur. J.* **2011**, *17*, 9911-9914.
29. Joosten, A.; Lambert, E.; Vasse, J. L.; Szymoniak, J., Diastereoselective Access to trans-2-Substituted Cyclopentylamines. *Org. Lett.* **2010**, *12*, 5128-5131.
30. Guo, Y. J.; Shao, G. A.; Li, L. N.; Wu, W. H.; Li, R. H.; Li, J. J.; Song, J. A.; Qiu, L. Q.; Prashad, M.; Kwong, F. Y., A General Approach to the Synthesis of  $\beta$ 2-Amino Acid Derivatives via Highly Efficient Catalytic Asymmetric Hydrogenation of  $\alpha$ -Aminomethylacrylates. *Adv. Synth. Catal.* **2010**, *352*, 1539-1553.
31. Seiders, J. R.; Wang, L. J.; Floreancig, P. E., Tuning Reactivity and Chemoselectivity in Electron Transfer Initiated Cyclization Reactions: Applications to Carbon-Carbon Bond Formation. *J. Am. Chem. Soc.* **2003**, *125*, 2406-2407.
32. Belanger, G.; Levesque, F.; Paquet, J.; Barbe, G., Competition between Alkenes in Intramolecular Ketene-Alkene [2+2] Cycloaddition: What Does It Take to Win? *J. Org. Chem.* **2005**, *70*, 291-296.

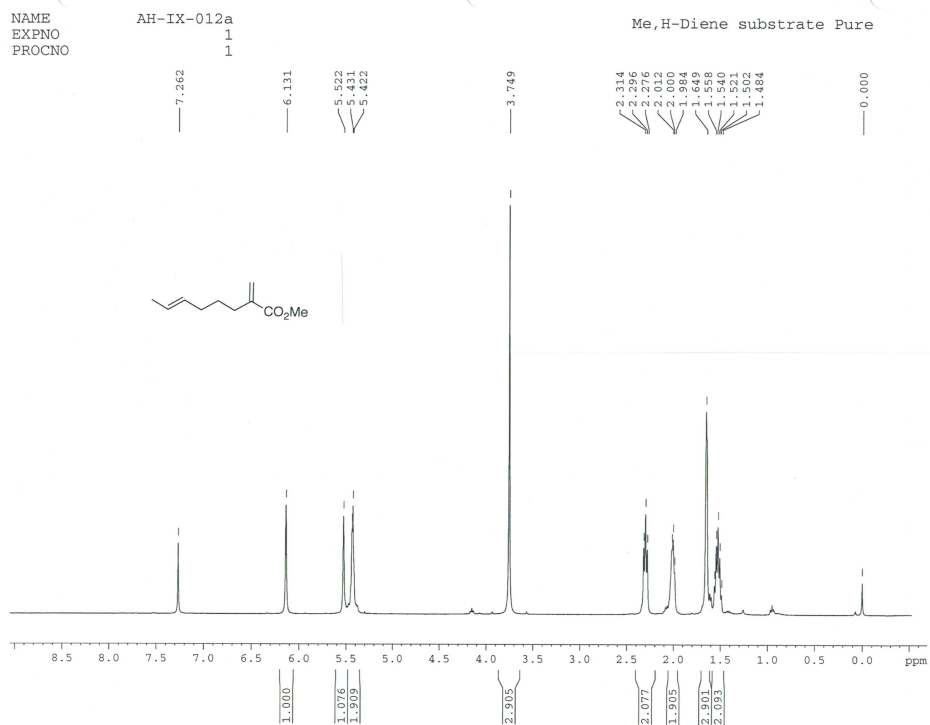
## APPENDIX I: RELEVANT SPECTRAL DATA FOR CHAPTER 2



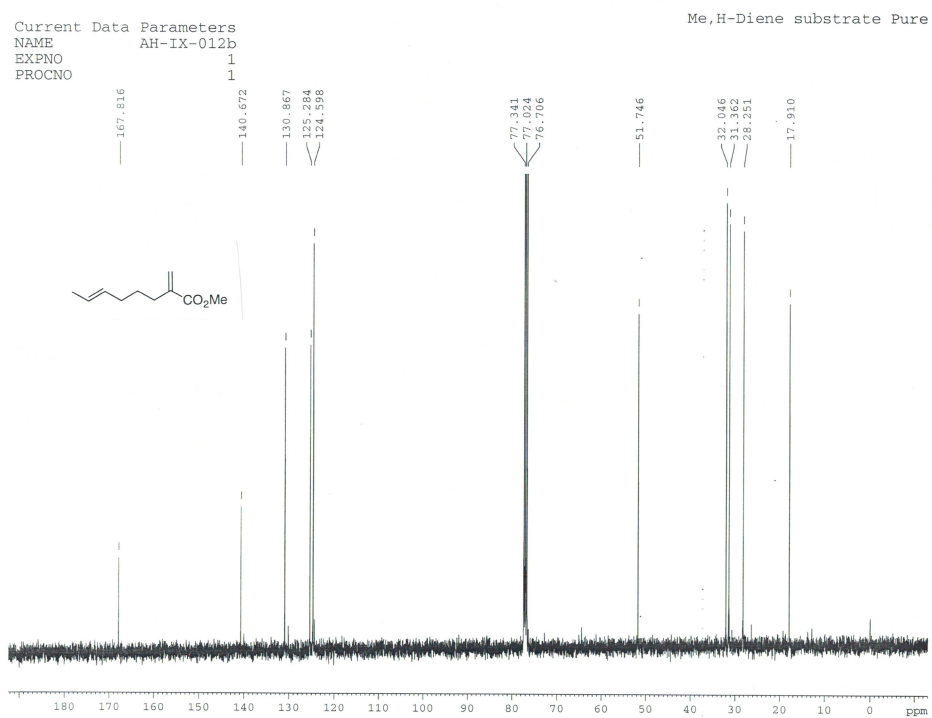
$^1\text{H}$  NMR of Compound 2.6



$^{13}\text{C}$  NMR of Compound 2.6



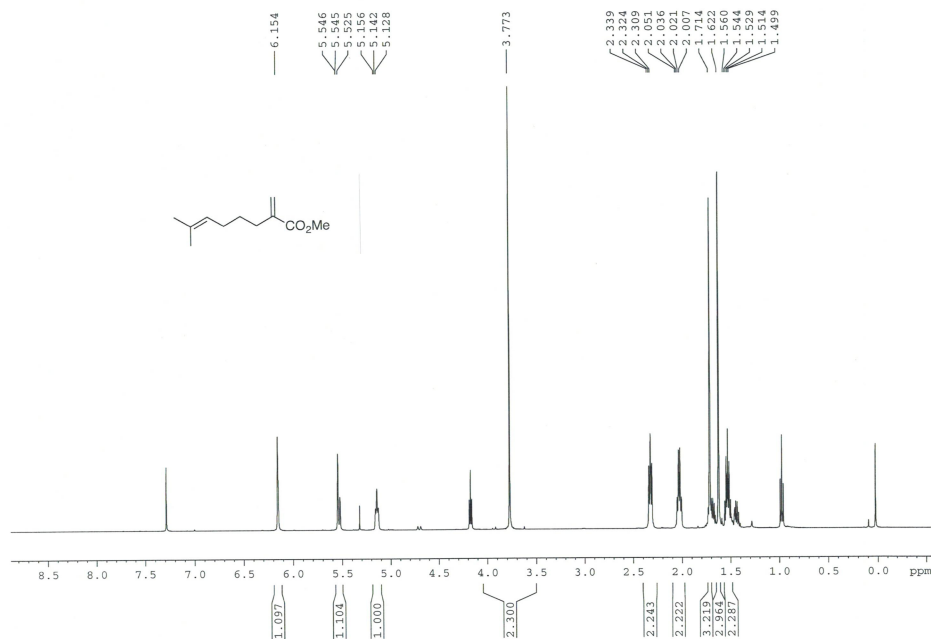
<sup>1</sup>H NMR of Compound 2.7



<sup>13</sup>C NMR of Compound 2.7

Current Data Parameters  
NAME AH-IX-033a  
EXPNO 1  
PROCNO 1

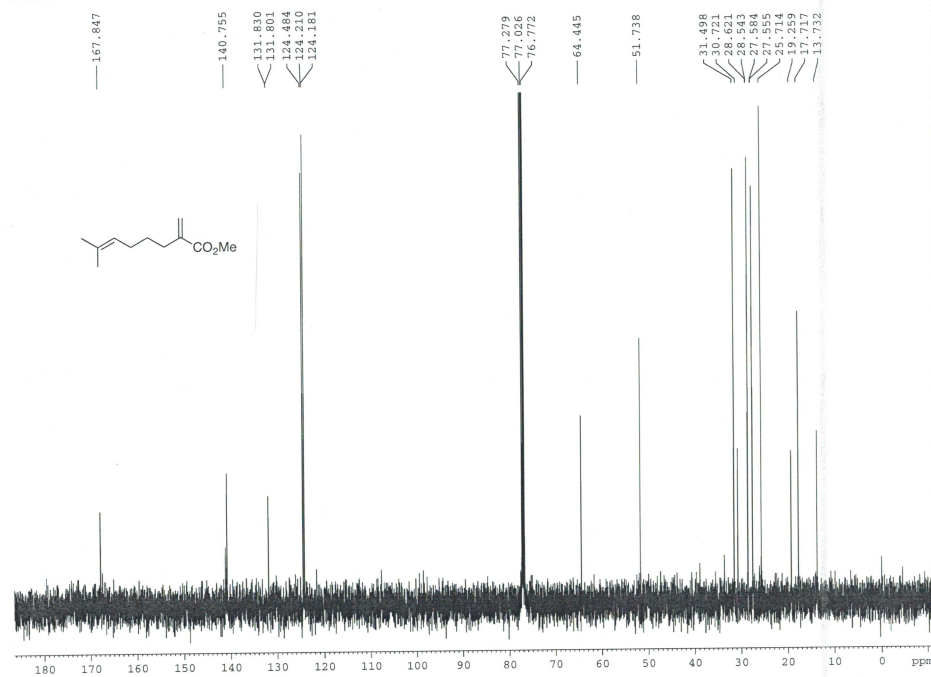
Me,Me-Diene substrate Pure



<sup>1</sup>H NMR of Compound 2.8

NAME AH-IX-033b  
EXPNO 1  
PROCNO 1

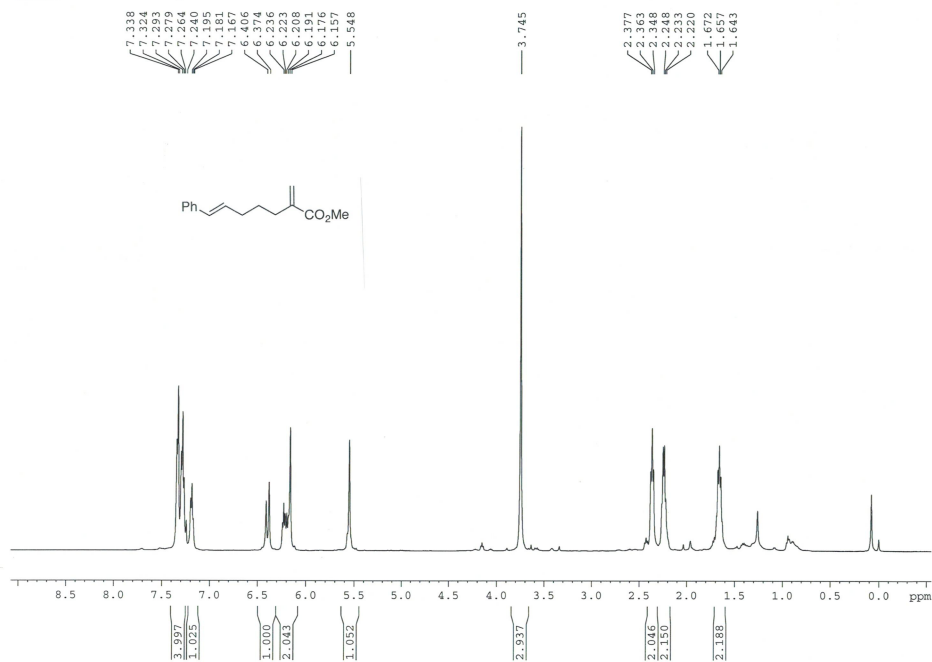
Carbon 13



<sup>13</sup>C NMR of Compound 2.8

Current Data Parameters  
NAME AH-VIII-099a  
EXPNO 1  
PROCNO 1

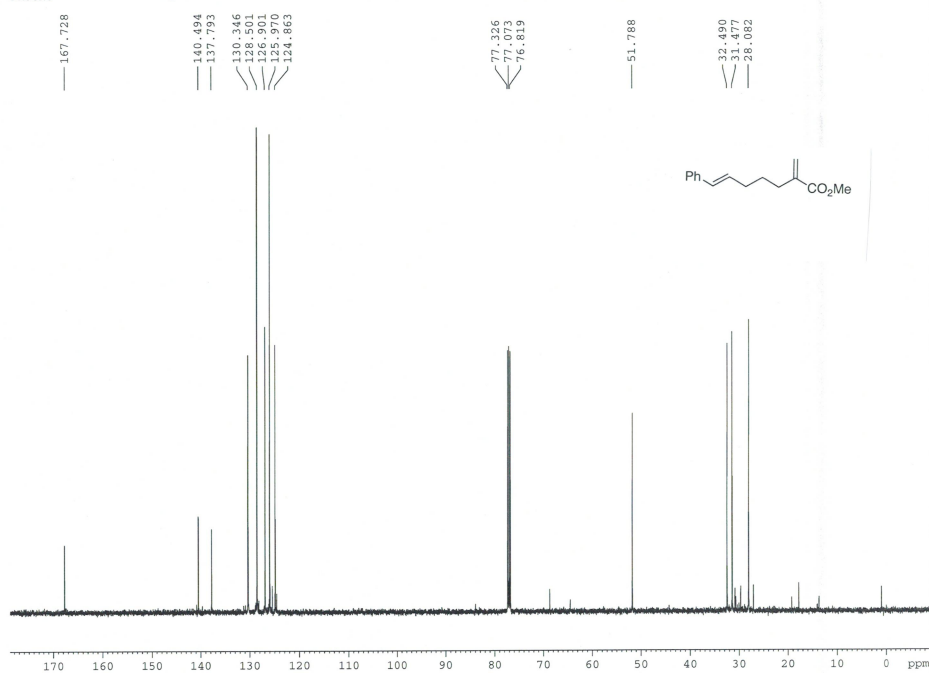
Ph,H-Diene substrate Pure



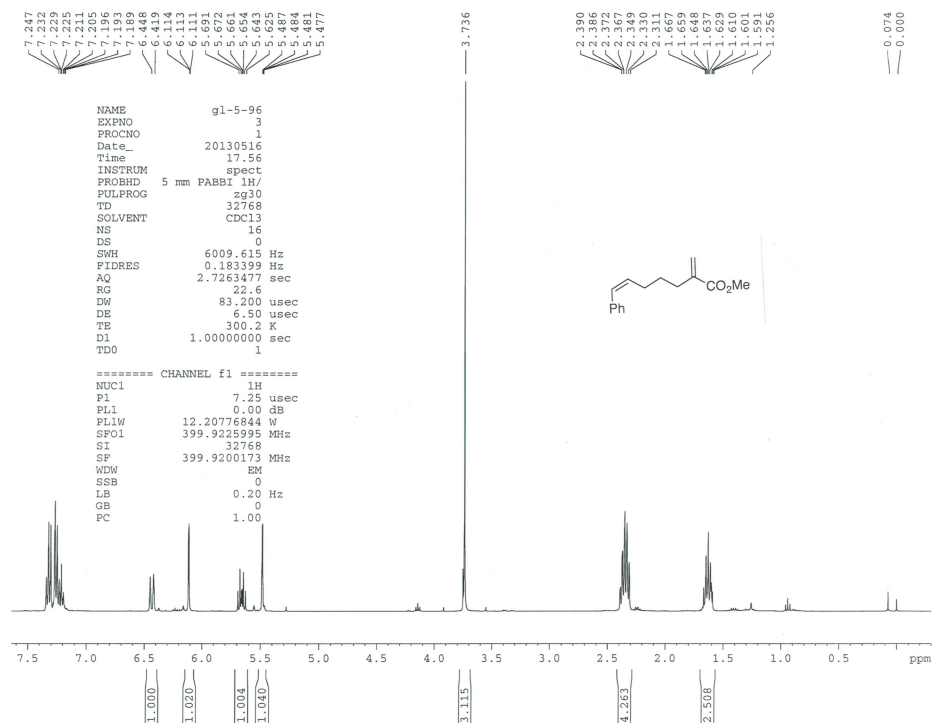
<sup>1</sup>H NMR of Compound 2.9

NAME AH-VIII-099b  
EXPNO 1  
PROCNO 1

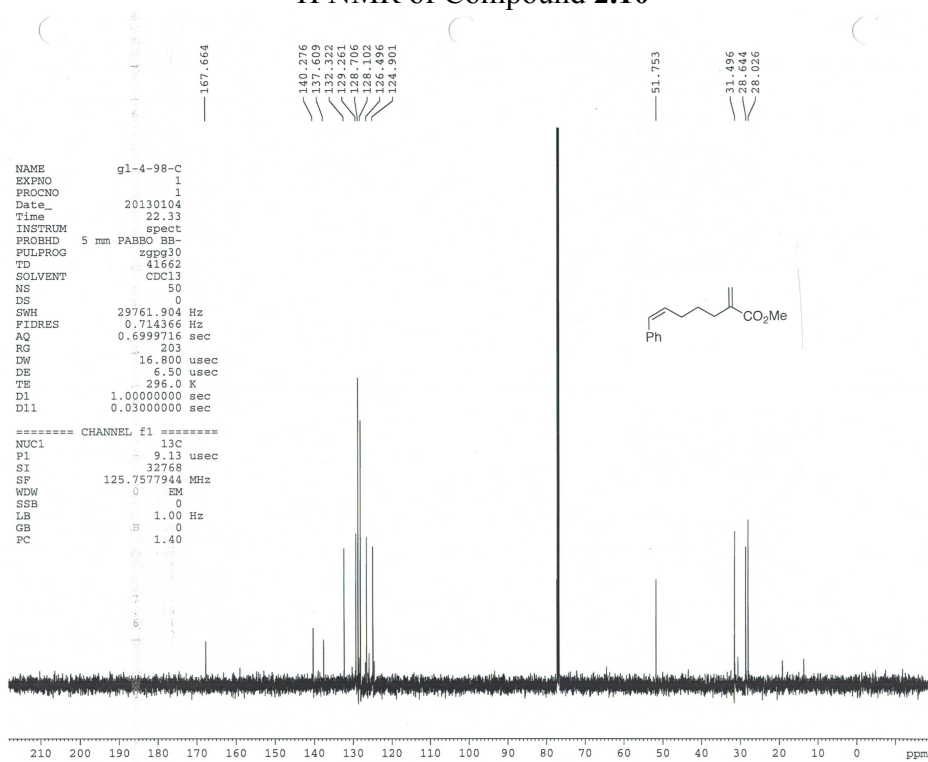
Carbon 13



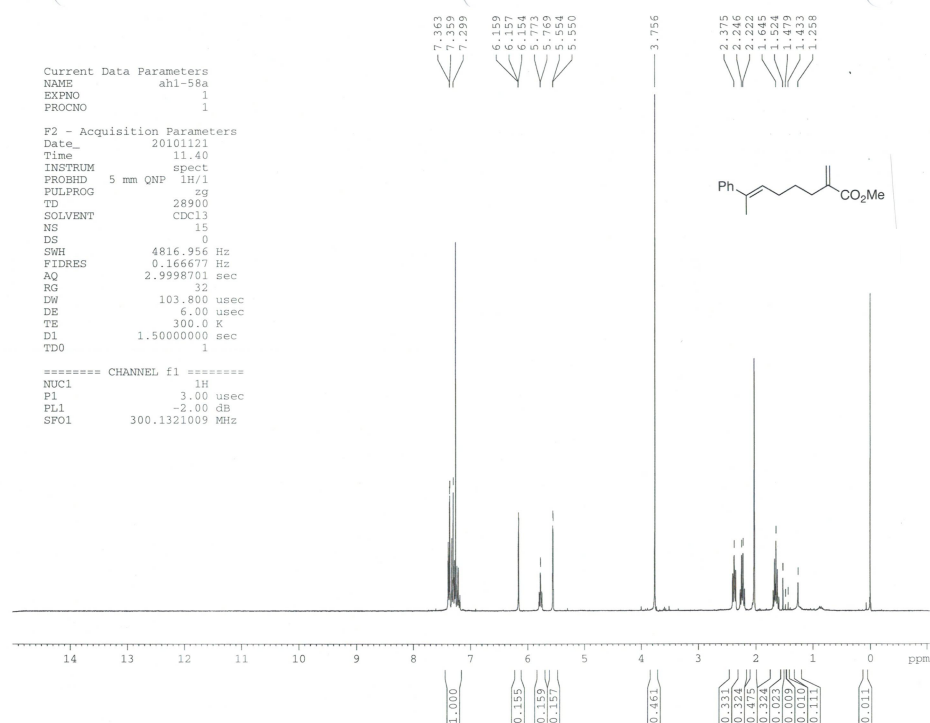
<sup>13</sup>C NMR of Compound 2.9



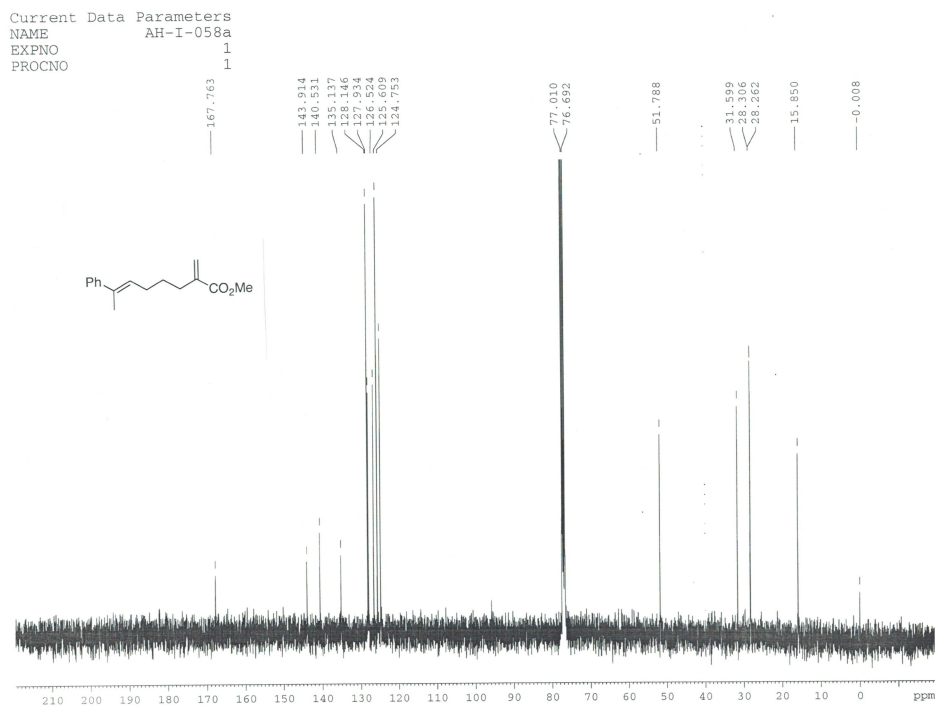
<sup>1</sup>H NMR of Compound 2.10



<sup>13</sup>C NMR of Compound 2.10

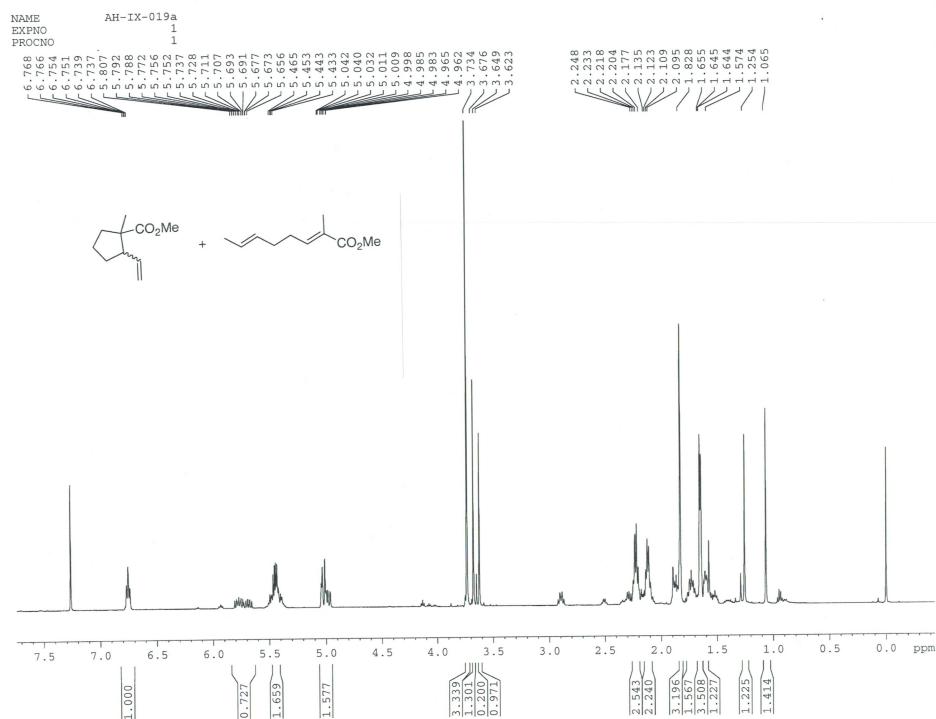


<sup>1</sup>H NMR of Compound 2.11

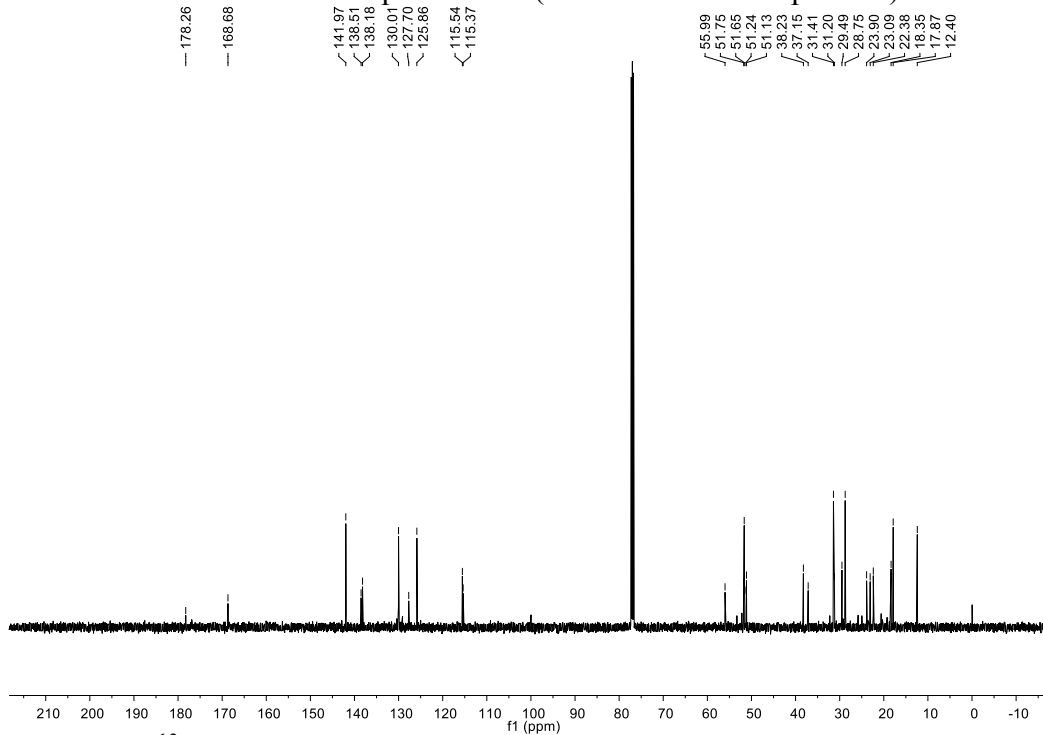


<sup>13</sup>C NMR of Compound 2.11

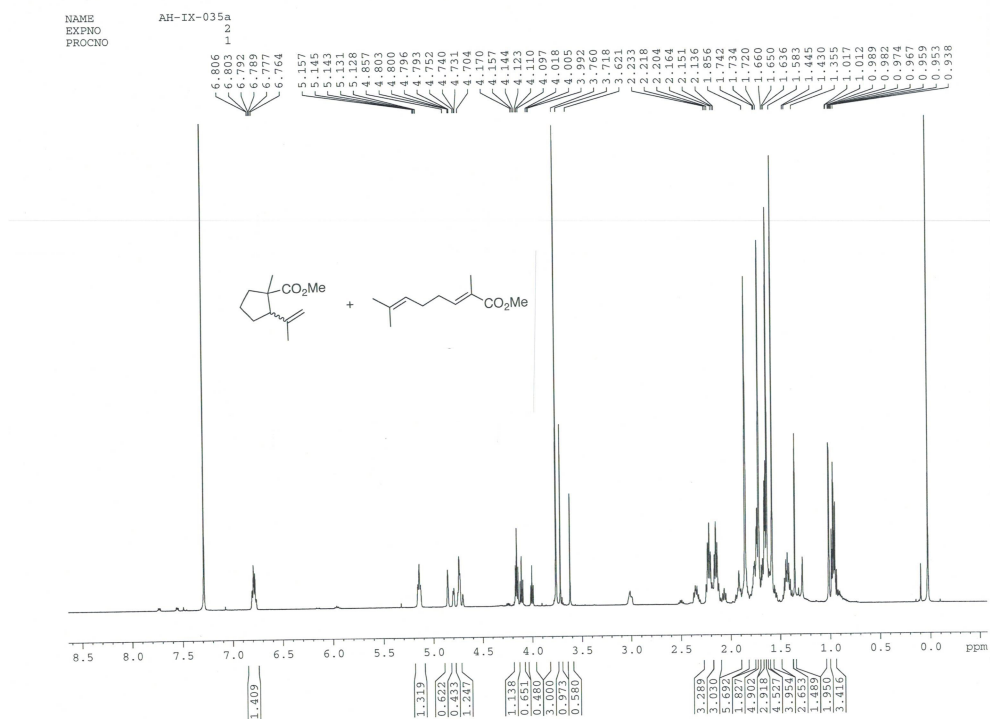




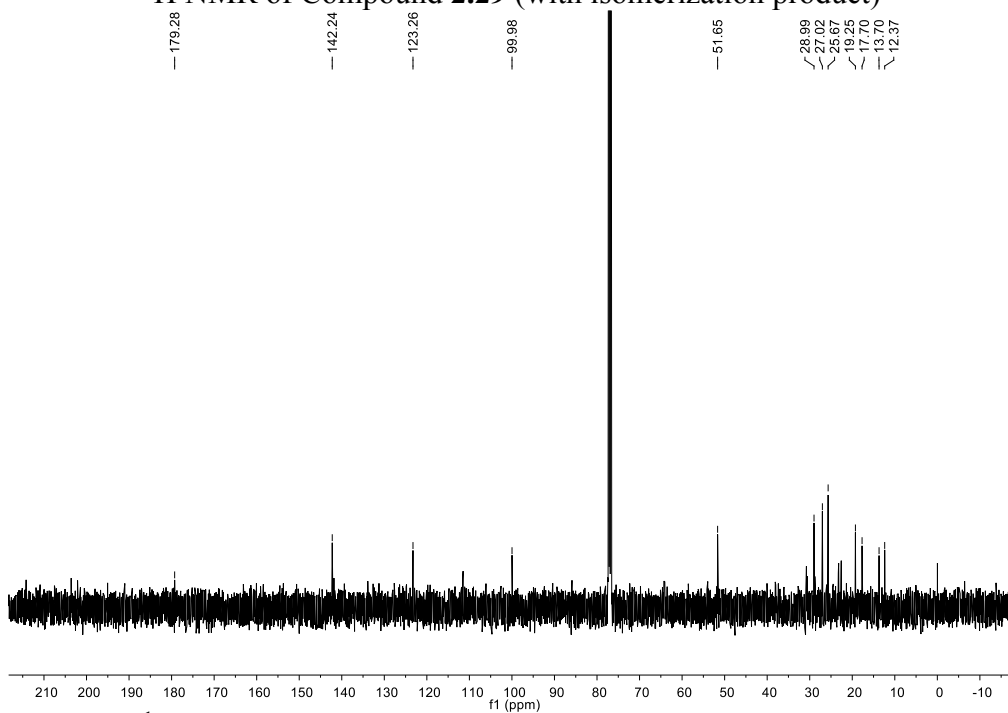
<sup>1</sup>H NMR of Compound **2.28** (with isomerization product)



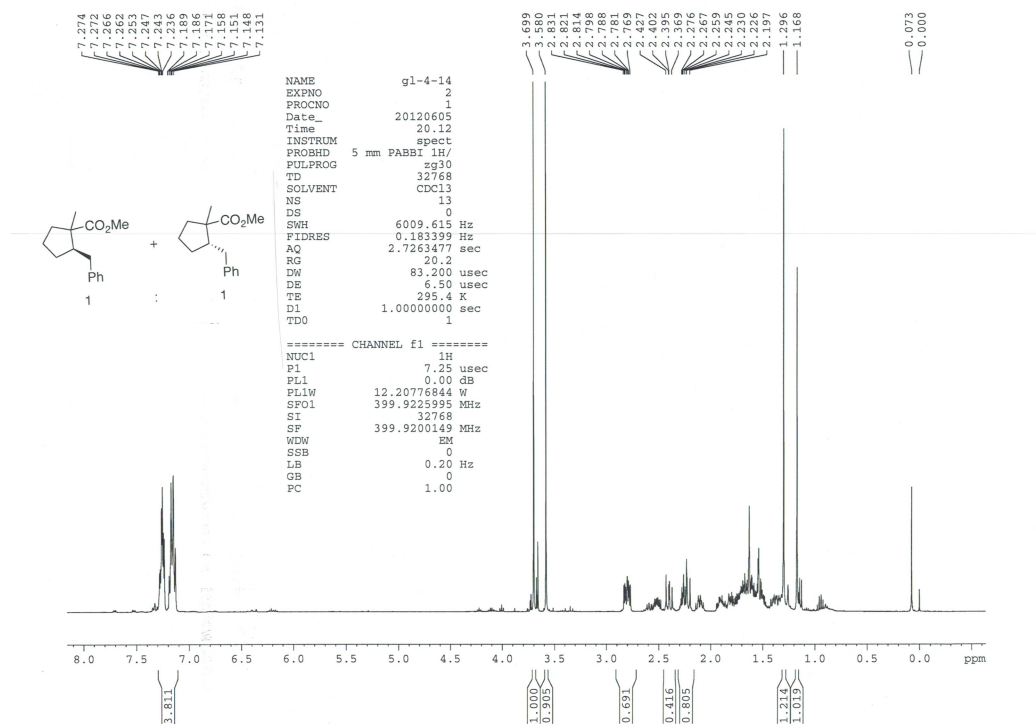
<sup>13</sup>C NMR of Compound **2.28** (with isomerization product)



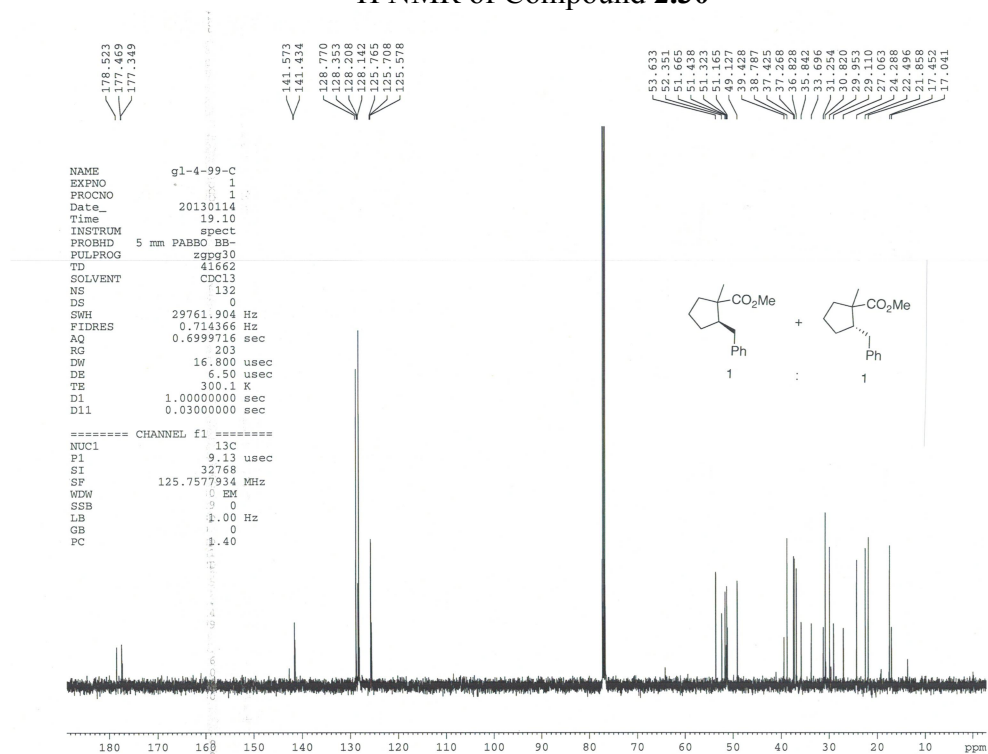
<sup>1</sup>H NMR of Compound **2.29** (with isomerization product)



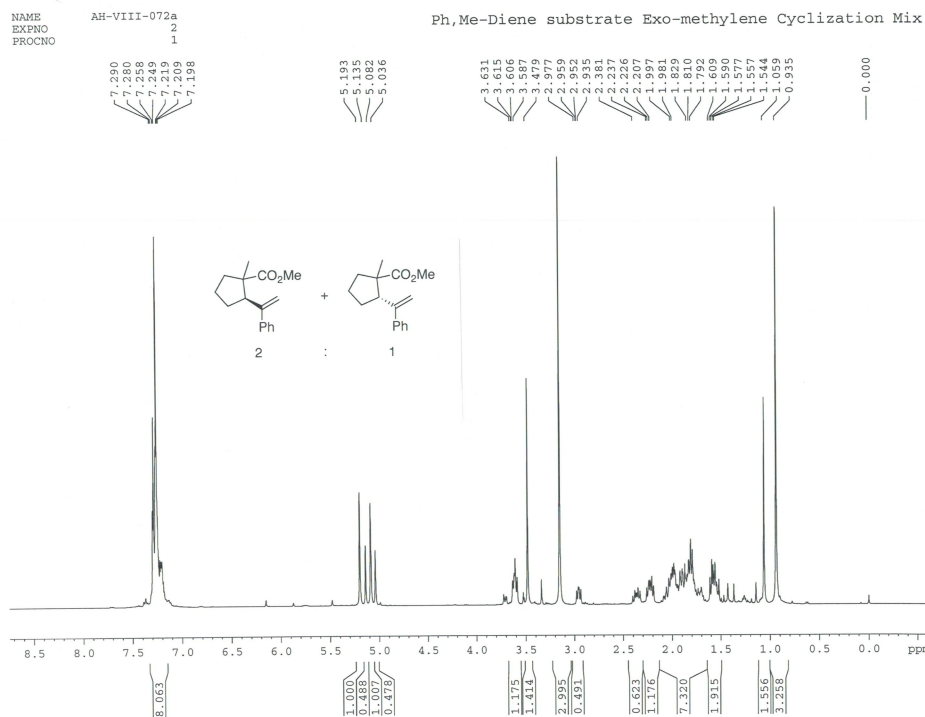
<sup>13</sup>C NMR of Compound **2.29** (with isomerization product)



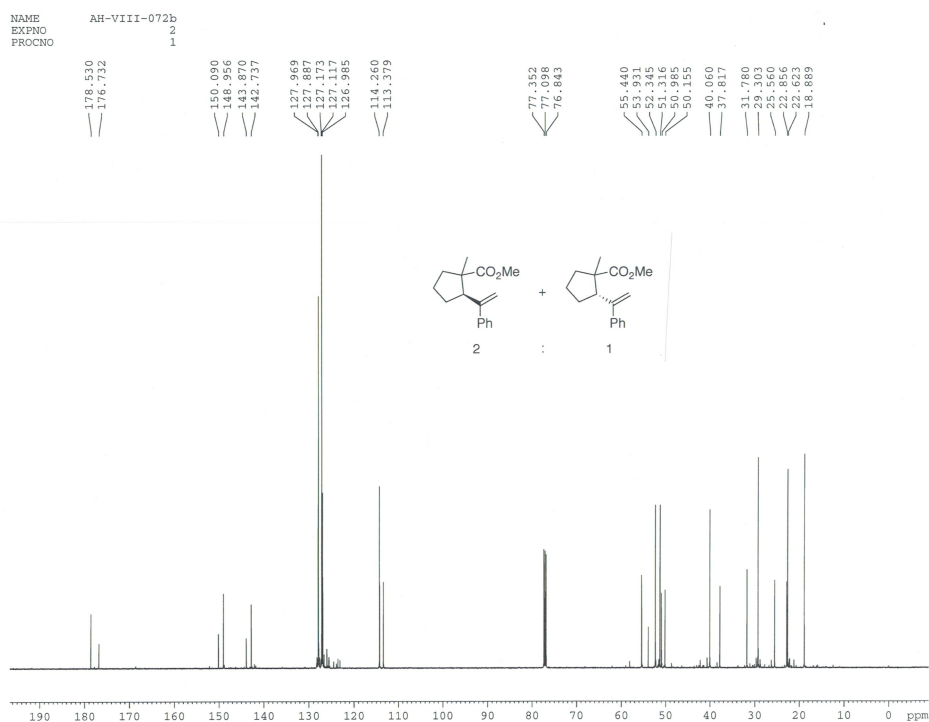
<sup>1</sup>H NMR of Compound 2.30



<sup>13</sup>C NMR of Compound 2.30



<sup>1</sup>H NMR of Compound 2.31



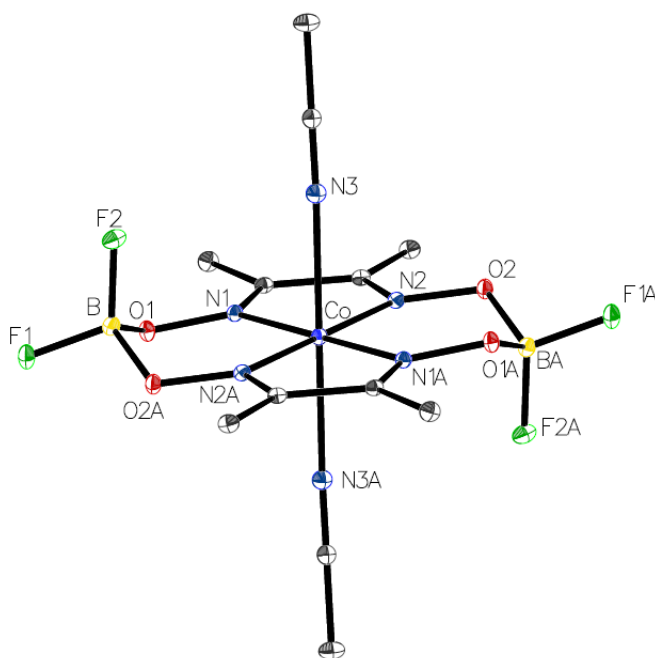
<sup>13</sup>C NMR of Compound 2.31

## **APPENDIX II: CRYSTALLOGRAPHIC DATA AND KINETIC**

### **PROFILES FOR CHAPTER 3**

#### **1. Crystallization Procedures**

**Co(dm $\text{gBF}_2$ ) $_2$ (MeCN) $_2$  (3.9).** A saturated solution of Co(dm $\text{gBF}_2$ ) $_2$ (H $_2$ O) $_2$  in MeCN was layered with ether and allowed to stand overnight after which time large dark crystals were formed. The structural parameters are given in Table S 2.1 below. The thermal ellipsoid diagram shown below, CCDC 998877, contains the supplementary crystallographic data. The cif file can be obtained free of charge from The Cambridge Crystallographic Data Centre via [http://www.ccdc.cam.ac.uk/data\\_request/cif](http://www.ccdc.cam.ac.uk/data_request/cif)



**Co(dm $\text{gBF}_2$ ) $_2$ (THF) $_2$  (3.10).** Hexane vapor was diffused into a THF solution containing Co(dm $\text{gBF}_2$ ) $_2$ (H $_2$ O) $_2$ , which caused the formation of yellow crystals, used for X-ray diffraction. The structural parameters are given in Table S2.1 below. The thermal ellipsoid diagram shown below, CCDC 998878, contains the supplementary crystallographic data. The cif file is included in the supporting information and can also

be obtained free of charge from the Cambridge Crystallographic Data Centre via  
[http://www.ccdc.cam.ac.uk/data\\_request/cif](http://www.ccdc.cam.ac.uk/data_request/cif).

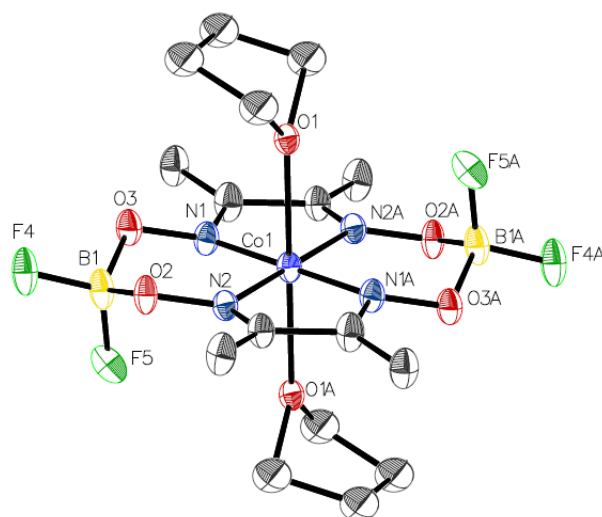


**Table S2.1.** Structural parameters for cobaloxime crystal structures

Structural Parameter	Co(dmgBF <sub>2</sub> ) <sub>2</sub> (CH <sub>3</sub> CN) <sub>2</sub>	Co(dmgBF <sub>2</sub> ) <sub>2</sub> (THF) <sub>2</sub>
Lattice	Monoclinic	Monoclinic
Formula	C <sub>12</sub> H <sub>18</sub> B <sub>2</sub> CoF <sub>4</sub> N <sub>6</sub> O <sub>4</sub>	C <sub>16</sub> H <sub>28</sub> B <sub>2</sub> CoF <sub>4</sub> N <sub>4</sub> O <sub>6</sub>
Formula Weight	466.86	528.97
Space Group	P 2 <sub>1</sub> /c	P 2 <sub>1</sub> /c
a (Å)	8.5877(19)	9.179(8)
b (Å)	11.747(3)	9.762(8)
c (Å)	9.730(2)	15.465(10)
α (°)	90.00	90
β (°)	114.822(3)	126.03(3)
γ (°)	90.00	90
V (Å <sup>3</sup> )	890.88	1120.7(15)
Z	2	2
Temperature (K)	150	150
Radiation (λ, Å)	0.71073	0.71073
ρ (calc.) (g cm <sup>-3</sup> )	1.740	1.568
θ max (deg)	31.00	31.29
μ (Mo Kα) (mm <sup>-1</sup> )	1.039	0.840
no. of data collected	14370	17714
no. of data used	2830	3642
no. of parameters	136	151
R <sub>1</sub> [I > 2σ(I)]	0.0269	0.0886
wR <sub>2</sub> [I > 2σ(I)]	0.0701	0.2670
R <sub>1</sub> [all data]	0.0326	0.1736
wR <sub>2</sub> [all data]	0.0735	0.3346
GOF	1.041	1.047

## 2. Kinetic Profiles

**Figure S2.1.** Plot of [3.5] vs time: [3.1] =  $7.60 \times 10^{-4} \text{ mol}\cdot\text{L}^{-1}$ ) and [1.13]<sub>0</sub> =  $1.02 \times 10^{-2} \text{ mol}\cdot\text{L}^{-1}$  under 1.7 atm (gauge pressure: 10 psi) H<sub>2</sub> in C<sub>6</sub>D<sub>6</sub>. ([H<sub>2</sub>] =  $4.20 \times 10^{-3} \text{ mol}$ ; d[3.5]/dt =  $1.08(2) \times 10^{-3} \text{ mol}\cdot\text{L}^{-1}\cdot\text{h}^{-1}$ )

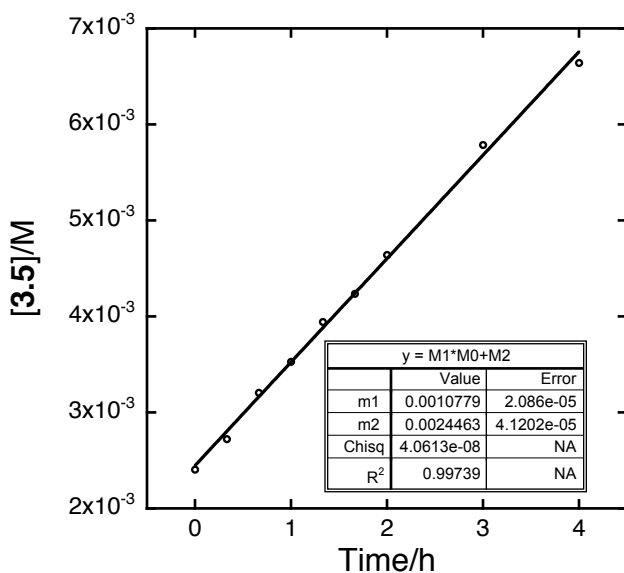


**Figure S2.2.** Plot of [3.5] vs time: [3.1] =  $7.60 \times 10^{-4} \text{ mol}\cdot\text{L}^{-1}$  and [1.13]<sub>0</sub> =  $1.02 \times 10^{-2} \text{ mol}\cdot\text{L}^{-1}$  under 2.0 atm (gauge pressure: 15 psi) H<sub>2</sub> in C<sub>6</sub>D<sub>6</sub>. ([H<sub>2</sub>] =  $5.05 \times 10^{-3} \text{ mol}\cdot\text{L}^{-1}$ ; d[3.5]/dt =  $1.23(2) \times 10^{-3} \text{ mol}\cdot\text{L}^{-1}\cdot\text{h}^{-1}$ )

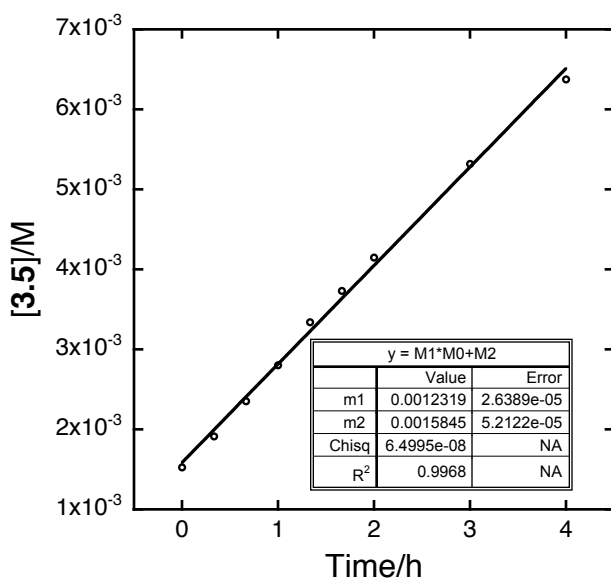


**Figure S2.3.** Plot of [3.5] vs time: [3.1] =  $7.60 \times 10^{-4} \text{ mol}\cdot\text{L}^{-1}$  and [1.13]<sub>0</sub> =  $1.02 \times 10^{-2} \text{ mol}\cdot\text{L}^{-1}$  under 2.4 atm (gauge pressure: 20 psi) H<sub>2</sub> in C<sub>6</sub>D<sub>6</sub>. ([H<sub>2</sub>] =  $5.91 \times 10^{-3} \text{ mol}\cdot\text{L}^{-1}$ ; d[3.5]/dt =  $1.48(1) \times 10^{-3} \text{ mol}\cdot\text{L}^{-1}\cdot\text{h}^{-1}$ )

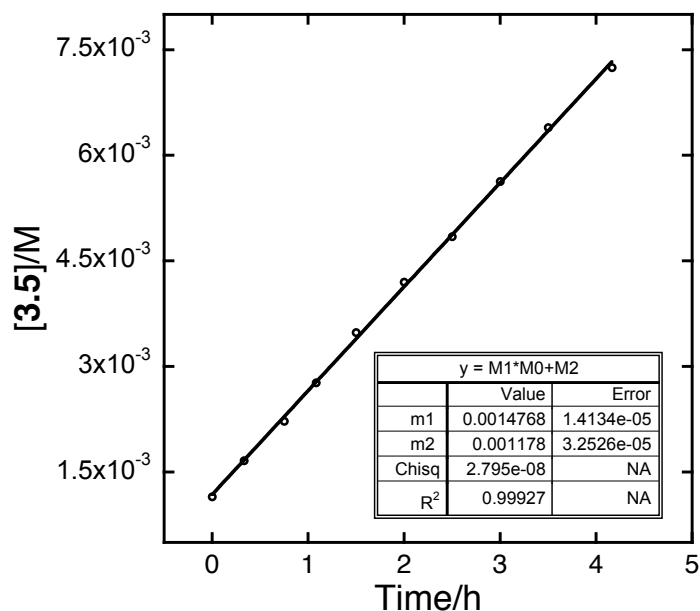


**Figure S2.4.** Plot of [3.5] vs time: [3.1] =  $7.60 \times 10^{-4} \text{ mol}\cdot\text{L}^{-1}$  and [1.13]<sub>0</sub> =  $1.02 \times 10^{-2} \text{ mol}\cdot\text{L}^{-1}$  under 2.7 atm (gauge pressure: 25 psi) H<sub>2</sub> in C<sub>6</sub>D<sub>6</sub>. ([H<sub>2</sub>] =  $6.76 \times 10^{-3} \text{ mol}\cdot\text{L}^{-1}$ ; d[3.5]/dt =  $1.74(5) \times 10^{-3} \text{ mol}\cdot\text{L}^{-1}\cdot\text{h}^{-1}$ )

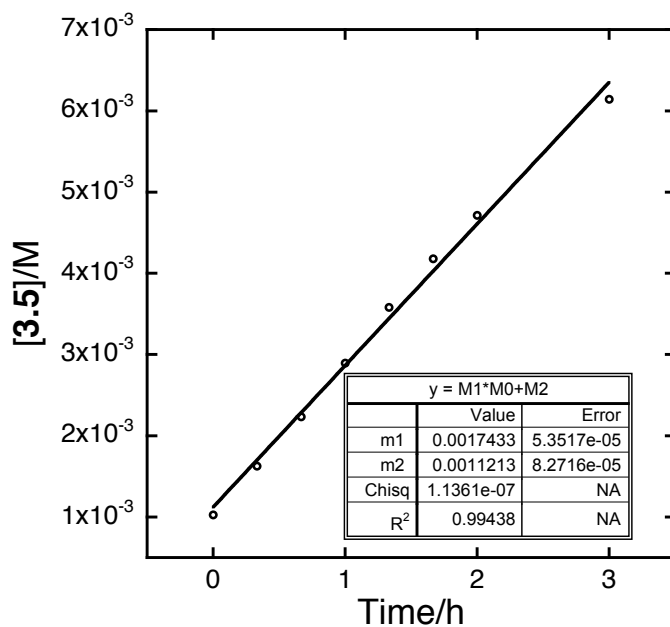




**Figure S2.5.** Plot of [3.5] vs time: [3.1] =  $7.60 \times 10^{-4} \text{ mol}\cdot\text{L}^{-1}$  and [1.13]<sub>0</sub> =  $1.02 \times 10^{-2} \text{ mol}\cdot\text{L}^{-1}$  under 3.0 atm (gauge pressure: 30 psi) H<sub>2</sub> in C<sub>6</sub>D<sub>6</sub>. ([H<sub>2</sub>] =  $7.61 \times 10^{-3} \text{ mol}\cdot\text{L}^{-1}$ ; d[3.5]/dt =  $1.83(2) \times 10^{-3} \text{ mol}\cdot\text{L}^{-1}\cdot\text{h}^{-1}$ )

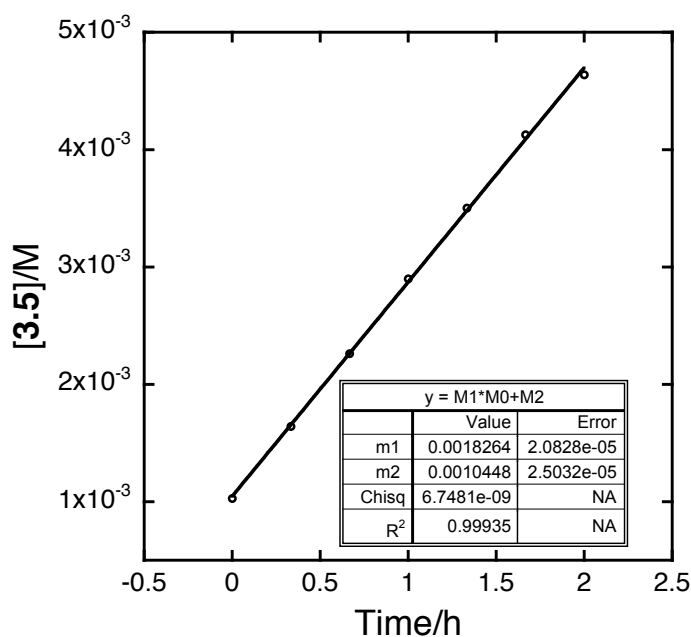


**Figure S2.6.** Plot of [3.5] vs time: [3.1] =  $7.60 \times 10^{-4} \text{ mol}\cdot\text{L}^{-1}$  and [1.13]<sub>0</sub> =  $1.02 \times 10^{-2} \text{ mol}\cdot\text{L}^{-1}$  under 3.4 atm (gauge pressure: 35 psi) H<sub>2</sub> in C<sub>6</sub>D<sub>6</sub>. ([H<sub>2</sub>] =  $8.46 \times 10^{-3} \text{ mol}\cdot\text{L}^{-1}$ ; d[3.5]/dt =  $2.01(2) \times 10^{-3} \text{ mol}\cdot\text{L}^{-1}\cdot\text{h}^{-1}$ )

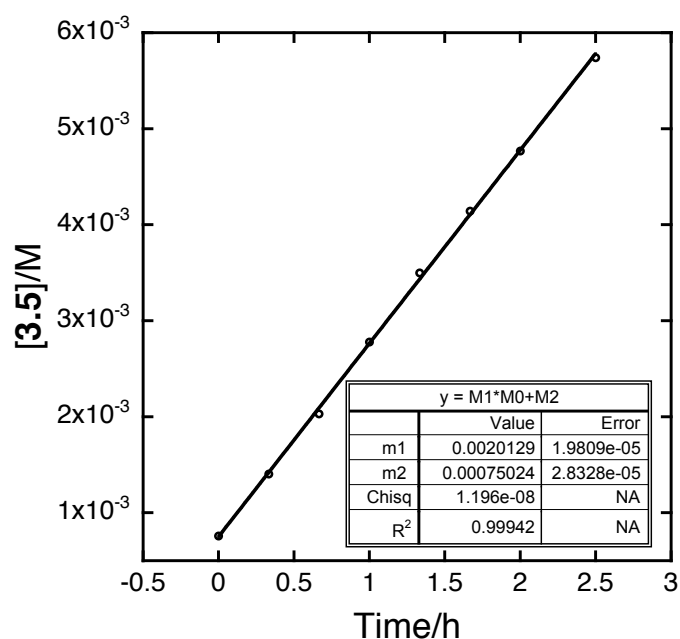


**Figure S2.7.** Plot of  $d[3.5]/dt$  vs  $[H_2]$  at 295 K. ( $k_1 = 108(7) \text{ L}^2\cdot\text{mol}^{-2}\cdot\text{s}^{-1}$ )

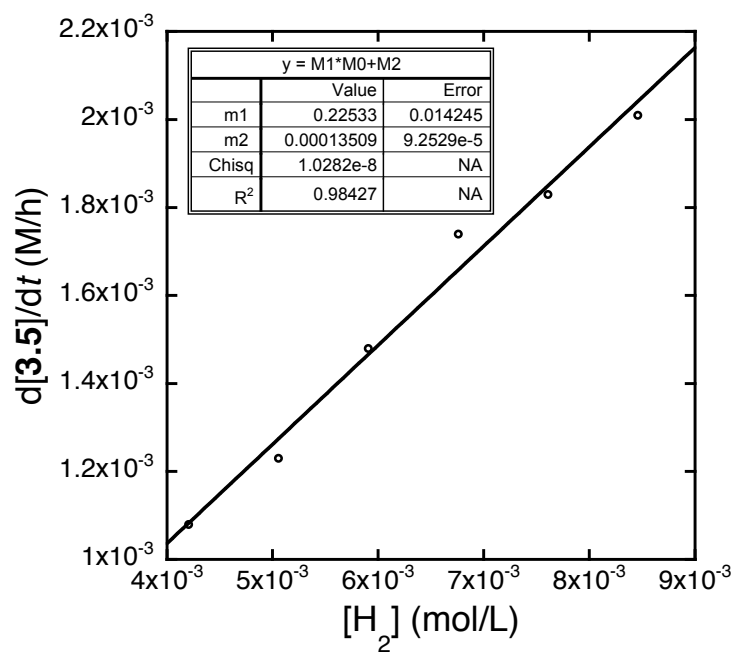


**Figure S2.8.** Plot of  $[3.5]$  vs time:  $[3.1] = 0.23 \times 10^{-4} \text{ mol}\cdot\text{L}^{-1}$  and  $[1.13]_0 = 1.02 \times 10^{-2} \text{ mol}\cdot\text{L}^{-1}$  under 3.0 atm (gauge pressure: 30 psi)  $H_2$  in  $C_6D_6$ . ( $[H_2] = 7.61 \times 10^{-3} \text{ mol}\cdot\text{L}^{-1}$ ;  $d[3.5]/dt = 1.52(2) \times 10^{-4} \text{ mol}\cdot\text{L}^{-1}\cdot\text{h}^{-1}$ )

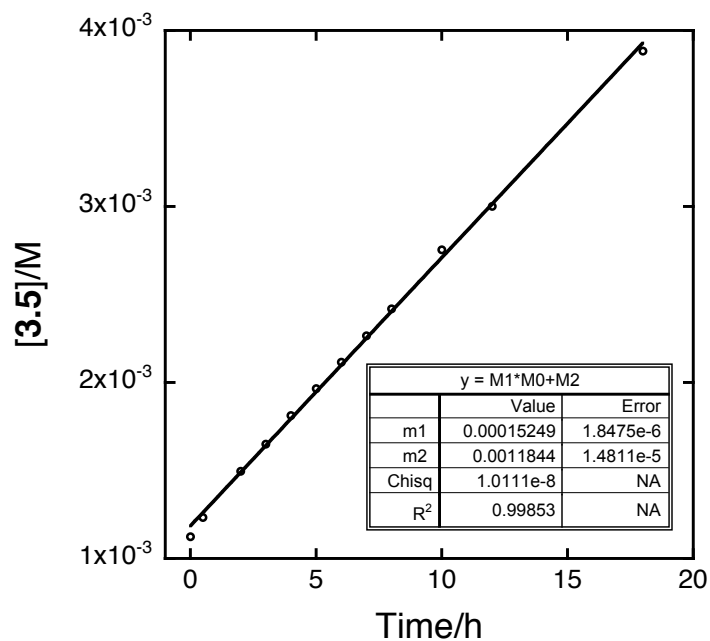


**Figure S2.9.** Plot of  $[3.5]$  vs time:  $[3.1] = 0.48 \times 10^{-4} \text{ mol}\cdot\text{L}^{-1}$  and  $[1.13]_0 = 1.02 \times 10^{-2} \text{ mol}\cdot\text{L}^{-1}$  under 3.0 atm (gauge pressure: 30 psi)  $\text{H}_2$  in  $\text{C}_6\text{D}_6$ . ( $[\text{H}_2] = 7.61 \times 10^{-3} \text{ mol}\cdot\text{L}^{-1}$ ;  $d[3.5]/dt = 1.73(2) \times 10^{-4} \text{ mol}\cdot\text{L}^{-1}\cdot\text{h}^{-1}$ )

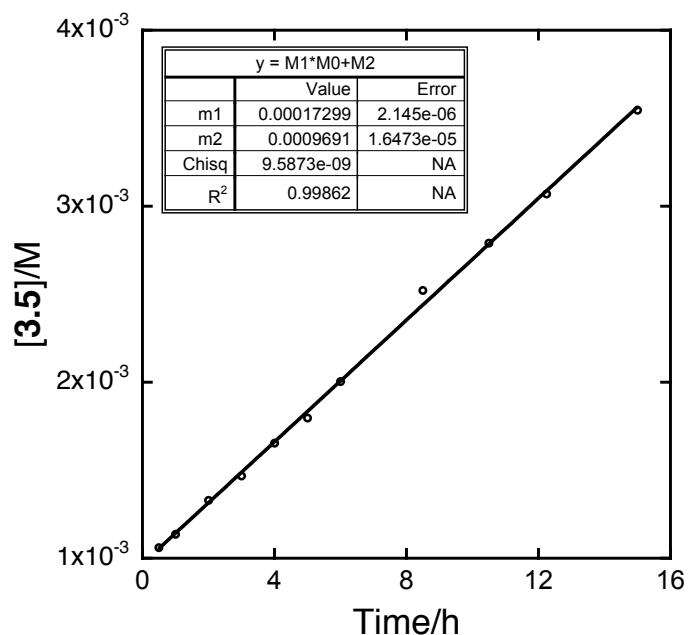


**Figure S2.10.** Plot of  $[3.5]$  vs time:  $[3.1] = 0.95 \times 10^{-4} \text{ mol}\cdot\text{L}^{-1}$  and  $[1.13]_0 = 1.02 \times 10^{-2} \text{ mol}\cdot\text{L}^{-1}$  under 3.0 atm (gauge pressure: 30 psi)  $\text{H}_2$  in  $\text{C}_6\text{D}_6$ . ( $[\text{H}_2] = 7.61 \times 10^{-3} \text{ mol}\cdot\text{L}^{-1}$ ;  $d[3.5]/dt = 2.07(2) \times 10^{-4} \text{ mol}\cdot\text{L}^{-1}\cdot\text{h}^{-1}$ )

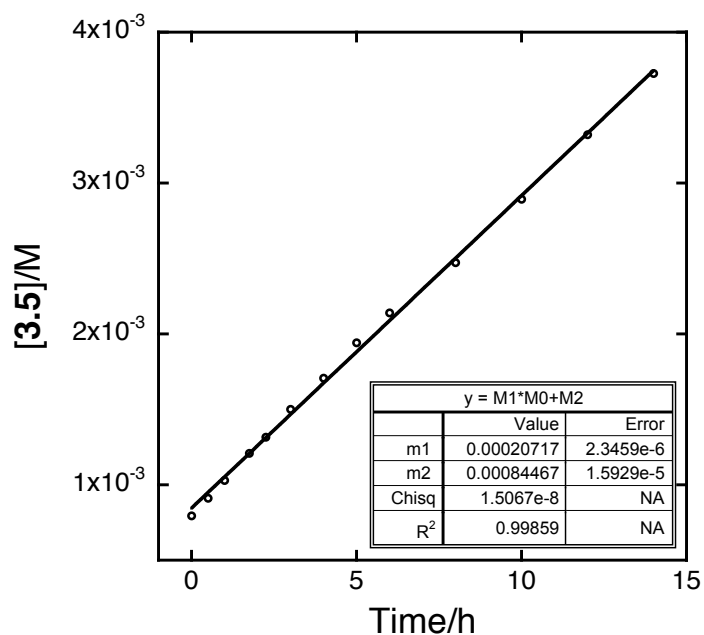


**Figure S2.11.** Plot of [3.5] vs time: [3.1] =  $2.85 \times 10^{-4} \text{ mol}\cdot\text{L}^{-1}$  and [1.13]<sub>0</sub> =  $1.02 \times 10^{-2} \text{ mol}\cdot\text{L}^{-1}$  under 3.0 atm (gauge pressure: 30 psi) H<sub>2</sub> in C<sub>6</sub>D<sub>6</sub>. ([H<sub>2</sub>] =  $7.61 \times 10^{-3} \text{ mol}\cdot\text{L}^{-1}$ ; d[3.5]/dt =  $3.94(7) \times 10^{-4} \text{ mol}\cdot\text{L}^{-1}\cdot\text{h}^{-1}$ )

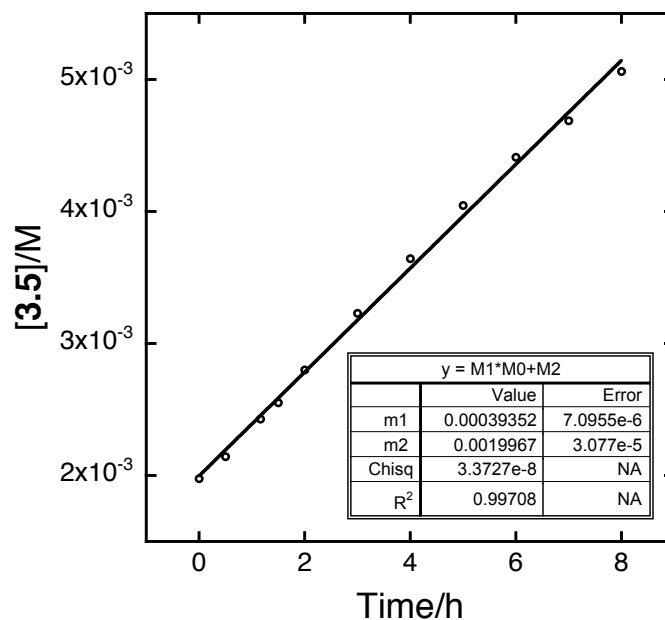


**Figure S2.12.** Plot of [3.5] vs time: [3.1] =  $4.75 \times 10^{-4} \text{ mol}\cdot\text{L}^{-1}$  and [1.13]<sub>0</sub> =  $1.02 \times 10^{-2} \text{ mol}\cdot\text{L}^{-1}$  under 3.0 atm (gauge pressure: 30 psi) H<sub>2</sub> in C<sub>6</sub>D<sub>6</sub>. ([H<sub>2</sub>] =  $7.61 \times 10^{-3} \text{ mol}\cdot\text{L}^{-1}$ ; d[3.5]/dt =  $7.4(2) \times 10^{-4} \text{ mol}\cdot\text{L}^{-1}\cdot\text{h}^{-1}$ )

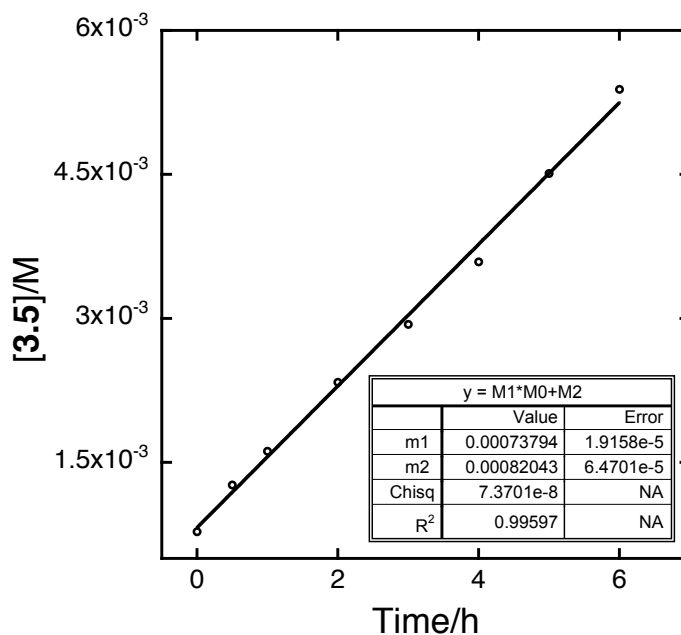


**Figure S2.13.** Plot of  $d[3.5]/dt$  vs  $[3.1]$ . ( $k_1 = 104(3) \text{ L}^2\cdot\text{mol}^{-2}\cdot\text{s}^{-1}$ )

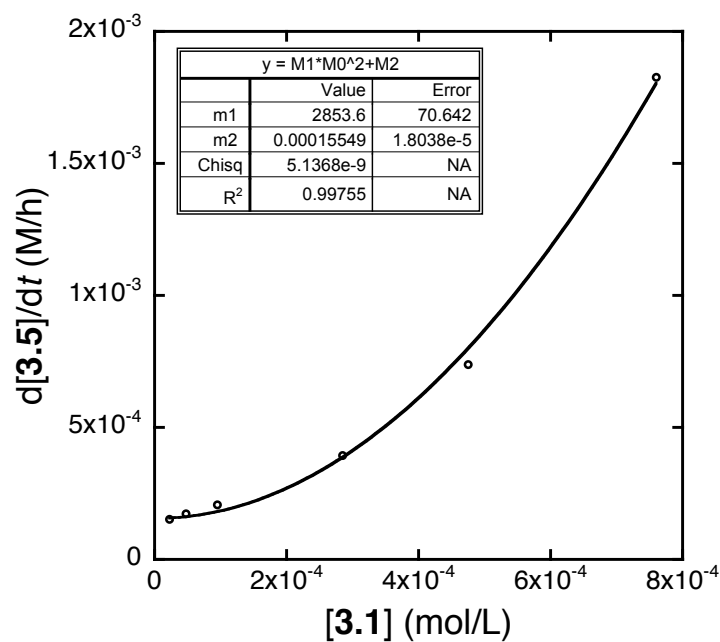


**Figure S2.14.** Plot of  $[3.5]$  vs time:  $[3.1] = 7.60 \times 10^{-4} \text{ mol}\cdot\text{L}^{-1}$  and  $[1.13]_0 = 2.04 \times 10^{-2} \text{ mol}\cdot\text{L}^{-1}$  under 3.0 atm (gauge pressure: 30 psi)  $\text{H}_2$  in  $\text{C}_6\text{D}_6$ . ( $[\text{H}_2] = 7.61 \times 10^{-3} \text{ mol}\cdot\text{L}^{-1}$ ;  $d[3.5]/dt = 1.87(2) \times 10^{-3} \text{ mol}\cdot\text{L}^{-1}\cdot\text{h}^{-1}$ )

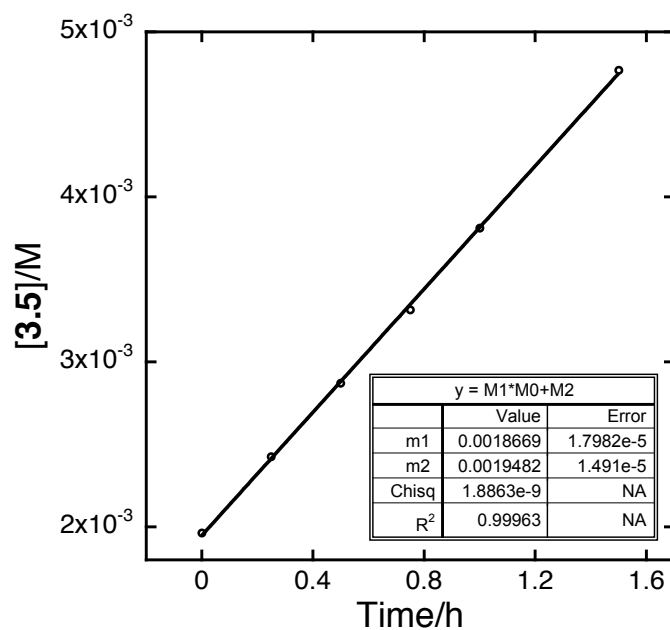


**Figure S2.15.** Plot of [3.5] vs time: [3.1] =  $7.60 \times 10^{-4} \text{ mol}\cdot\text{L}^{-1}$  and [1.13]<sub>0</sub> =  $5.1 \times 10^{-3} \text{ mol}\cdot\text{L}^{-1}$  under 3.0 atm (gauge pressure: 30 psi) H<sub>2</sub> in C<sub>6</sub>D<sub>6</sub>. ([H<sub>2</sub>] =  $7.61 \times 10^{-3} \text{ mol}\cdot\text{L}^{-1}$ ; d[6]/dt =  $1.83(2) \times 10^{-3} \text{ mol}\cdot\text{L}^{-1}\cdot\text{h}^{-1}$ )

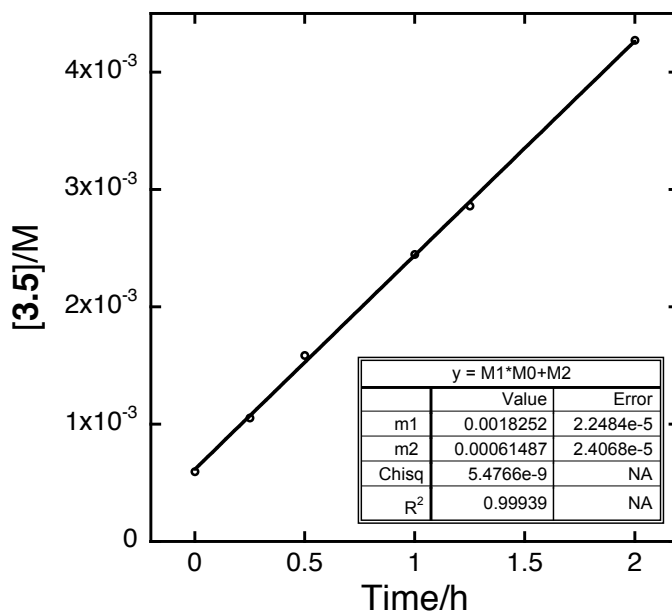


**Figure S2.16.** Plot of [3.7] vs time: [3.1] =  $7.60 \times 10^{-4} \text{ mol}\cdot\text{L}^{-1}$  and [3.6] =  $0.116 \text{ mol}\cdot\text{L}^{-1}$  under 3.0 atm (gauge pressure: 30 psi) H<sub>2</sub> in C<sub>6</sub>D<sub>6</sub>. ([H<sub>2</sub>] =  $7.61 \times 10^{-3} \text{ mol}\cdot\text{L}^{-1}$ ; d[3.7]/dt =  $1.82(2) \times 10^{-3} \text{ mol}\cdot\text{L}^{-1}\cdot\text{h}^{-1}$ )

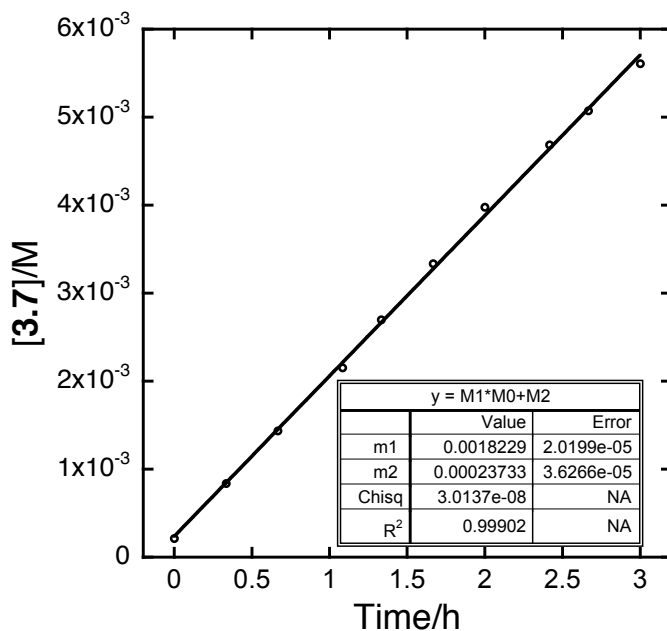


**Figure S2.17.** Comparison of rate of HAT to different  $[1.13]_0$  and  $[3.7]_0$  under same reaction condition ( $[3.1] = 7.60 \times 10^{-4} \text{ mol}\cdot\text{L}^{-1}$ ;  $\text{H}_2$ : 3.0 atm;  $\text{C}_6\text{D}_6$ )

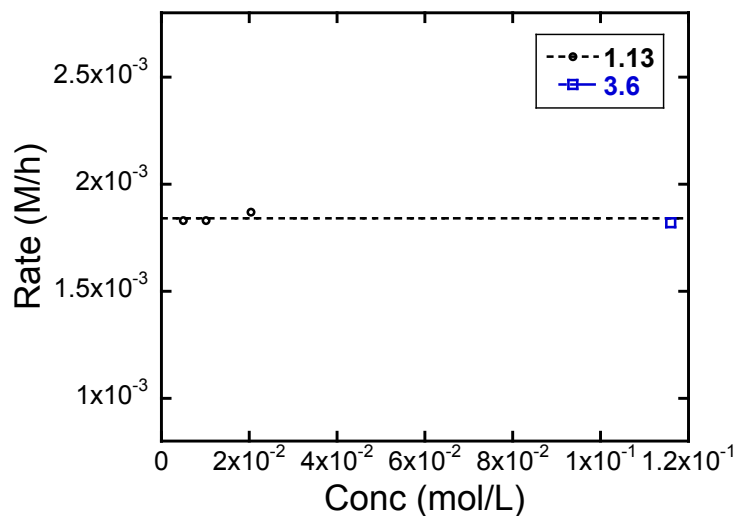


**Figure S2.18.** Plot of  $[3.5]$  vs time:  $[3.10] = 3.80 \times 10^{-4} \text{ mol}\cdot\text{L}^{-1}$  and  $[1.13]_0 = 1.02 \times 10^{-2} \text{ mol}\cdot\text{L}^{-1}$  under 1.7 atm (gauge pressure: 10 psi)  $\text{H}_2$  in  $\text{C}_6\text{D}_6$  at 295 K. ( $[\text{H}_2] = 4.20 \times 10^{-3} \text{ mol}\cdot\text{L}^{-1}$ ;  $d[3.5]/dt = 1.76(5) \times 10^{-3} \text{ mol}\cdot\text{L}^{-1}\cdot\text{h}^{-1}$ )

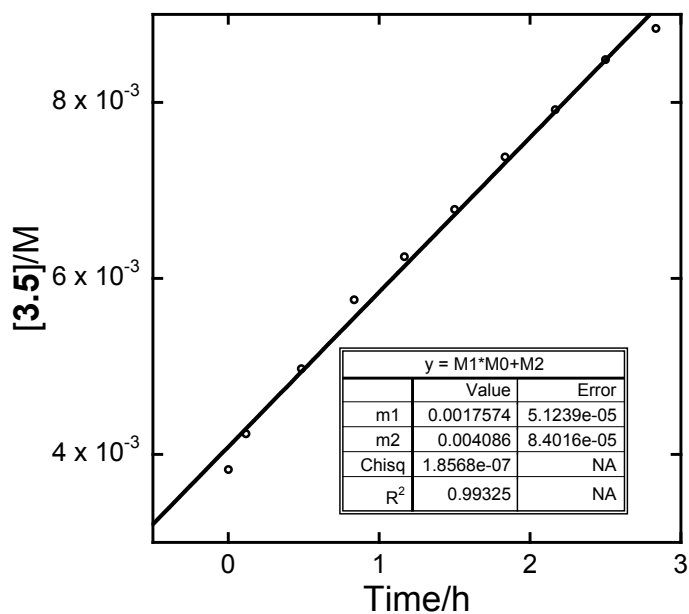


**Figure S2.19.** Plot of [3.5] vs time:  $[3.10] = 3.80 \times 10^{-4} \text{ mol}\cdot\text{L}^{-1}$  and  $[1.13]_0 = 1.02 \times 10^{-2} \text{ mol}\cdot\text{L}^{-1}$  under 2.0 atm (gauge pressure: 15 psi)  $\text{H}_2$  in  $\text{C}_6\text{D}_6$  at 295 K. ( $[\text{H}_2] = 5.05 \times 10^{-3} \text{ mol}\cdot\text{L}^{-1}$ ;  $d[3.5]/dt = 2.28(3) \times 10^{-3} \text{ mol}\cdot\text{L}^{-1}\cdot\text{h}^{-1}$ )

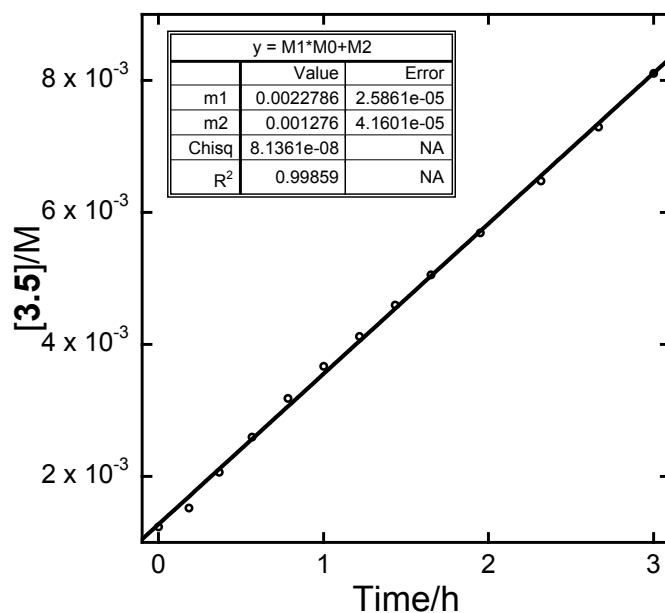


**Figure S2.20.** Plot of [3.5] vs time:  $[3.10] = 3.80 \times 10^{-4} \text{ mol}\cdot\text{L}^{-1}$  and  $[1.13]_0 = 1.02 \times 10^{-2} \text{ mol}\cdot\text{L}^{-1}$  under 2.4 atm (gauge pressure: 20 psi)  $\text{H}_2$  in  $\text{C}_6\text{D}_6$  at 295 K. ( $[\text{H}_2] = 5.91 \times 10^{-3} \text{ mol}\cdot\text{L}^{-1}$ ;  $d[3.5]/dt = 2.60(3) \times 10^{-3} \text{ mol}\cdot\text{L}^{-1}\cdot\text{h}^{-1}$ )

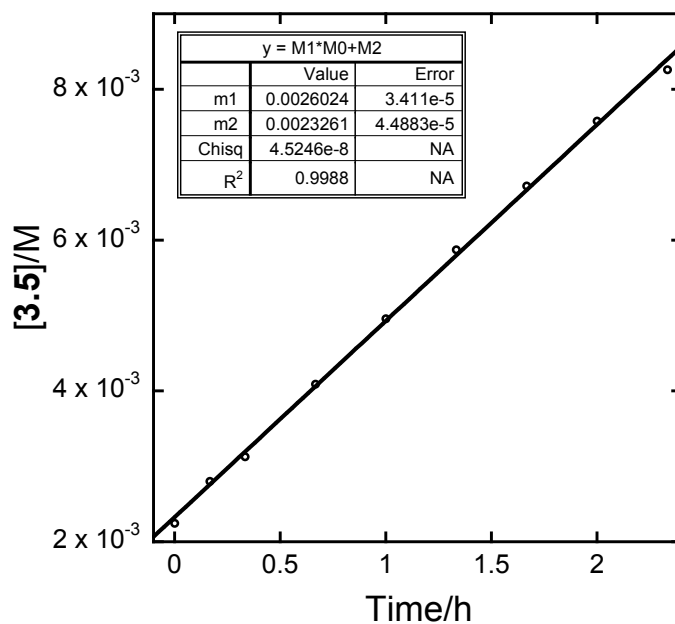




**Figure S2.21.** Plot of [3.5] vs time: [3.10] =  $3.80 \times 10^{-4} \text{ mol}\cdot\text{L}^{-1}$  and [1.13]<sub>0</sub> =  $1.02 \times 10^{-2} \text{ mol}\cdot\text{L}^{-1}$  under 2.7 atm (gauge pressure: 25 psi) H<sub>2</sub> in C<sub>6</sub>D<sub>6</sub> at 295 K. ([H<sub>2</sub>] =  $6.76 \times 10^{-3} \text{ mol}\cdot\text{L}^{-1}$ ; d[3.5]/dt =  $3.13(3) \times 10^{-3} \text{ mol}\cdot\text{L}^{-1}\cdot\text{h}^{-1}$ )

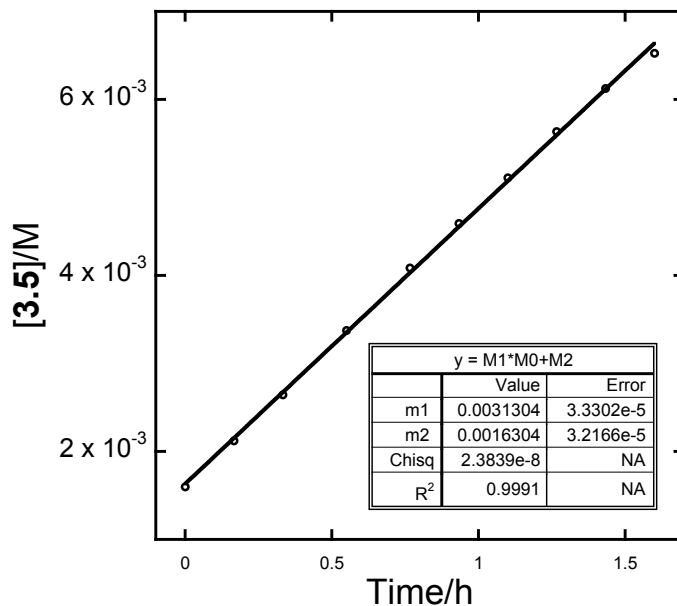


**Figure S2.22.** Plot of [3.5] vs time: [3.10] =  $3.80 \times 10^{-4} \text{ mol}\cdot\text{L}^{-1}$  and [1.13]<sub>0</sub> =  $1.02 \times 10^{-2} \text{ mol}\cdot\text{L}^{-1}$  under 3.0 atm (gauge pressure: 30 psi) H<sub>2</sub> in C<sub>6</sub>D<sub>6</sub> at 295 K. ([H<sub>2</sub>] =  $7.61 \times 10^{-3} \text{ mol}\cdot\text{L}^{-1}$ ; d[3.5]/dt =  $3.7(1) \times 10^{-3} \text{ mol}\cdot\text{L}^{-1}\cdot\text{h}^{-1}$ )

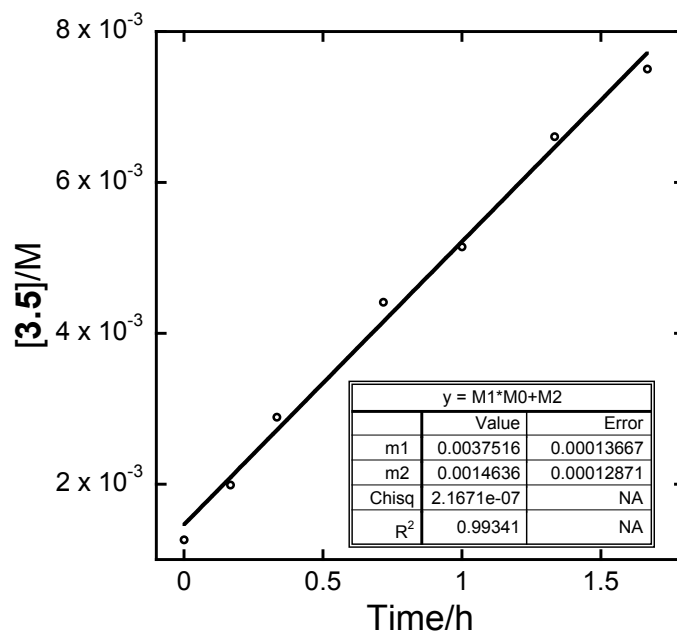


**Figure S2.23.** Plot of  $d[3.5]/dt$  vs  $[H_2]$  at 295 K. ( $k = 1.09(6) \times 10^3 \text{ L}^2 \cdot \text{mol}^{-2} \cdot \text{s}^{-1}$ )

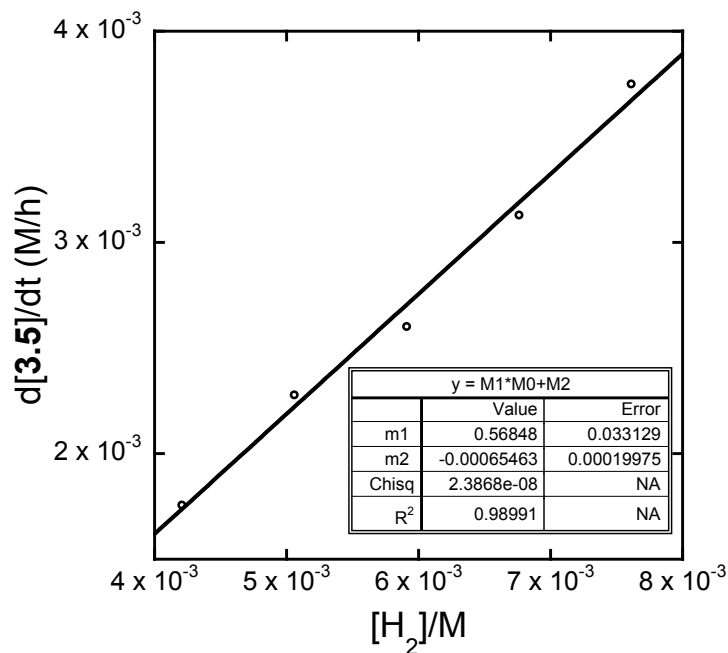


**Figure S2.24.** Plot of  $[3.5]$  vs time:  $[3.10] = 1.90 \times 10^{-4} \text{ mol} \cdot \text{L}^{-1}$  and  $[1.13]_0 = 1.02 \times 10^{-2} \text{ mol} \cdot \text{L}^{-1}$  under 3.0 atm (gauge pressure: 30 psi)  $H_2$  in  $C_6D_6$ . ( $[H_2] = 7.61 \times 10^{-3} \text{ mol} \cdot \text{L}^{-1}$ ;  $d[3.5]/dt = 9.88(9) \times 10^{-4} \text{ mol} \cdot \text{L}^{-1} \cdot \text{h}^{-1}$ )

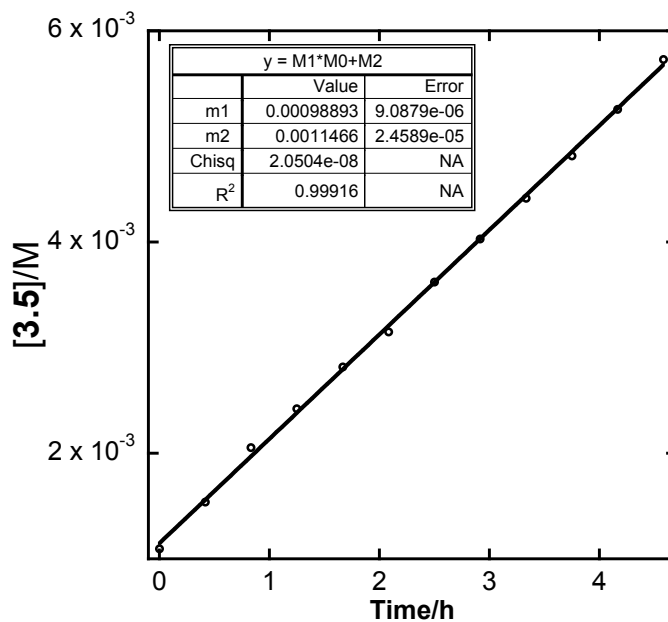


**Figure S2.25.** Plot of [3.5] vs time:  $[3.10] = 2.85 \times 10^{-4} \text{ mol}\cdot\text{L}^{-1}$  and  $[1.13]_0 = 1.02 \times 10^{-2} \text{ mol}\cdot\text{L}^{-1}$  under 3.0 atm (gauge pressure: 30 psi)  $\text{H}_2$  in  $\text{C}_6\text{D}_6$  at 295 K. ( $[\text{H}_2] = 7.61 \times 10^{-3} \text{ mol}\cdot\text{L}^{-1}$ ;  $d[3.5]/dt = 2.21(2) \times 10^{-3} \text{ mol}\cdot\text{L}^{-1}\cdot\text{h}^{-1}$ )

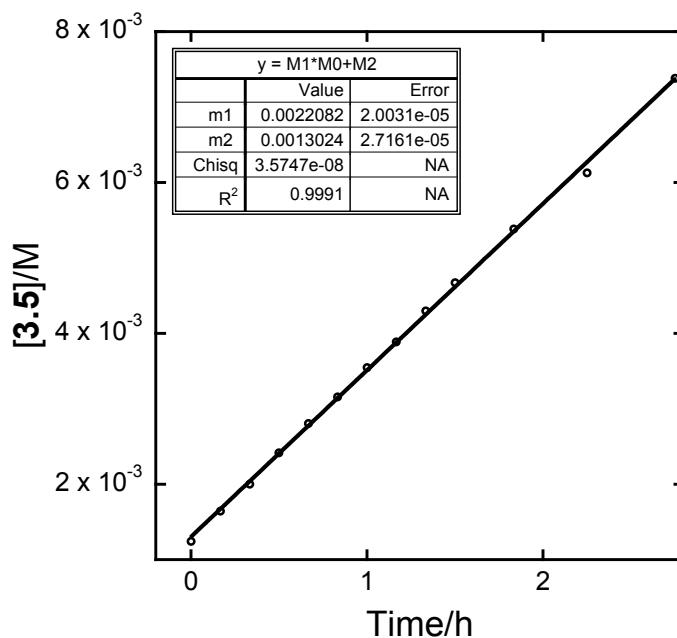


**Figure S2.26.** Plot of [3.5] vs time:  $[3.10] = 4.75 \times 10^{-4} \text{ mol}\cdot\text{L}^{-1}$  and  $[1.13]_0 = 1.02 \times 10^{-2} \text{ mol}\cdot\text{L}^{-1}$  under 3.0 atm (gauge pressure: 30 psi)  $\text{H}_2$  in  $\text{C}_6\text{D}_6$  at 295 K. ( $[\text{H}_2] = 7.61 \times 10^{-3} \text{ mol}\cdot\text{L}^{-1}$ ;  $d[3.5]/dt = 6.2(1) \times 10^{-3} \text{ mol}\cdot\text{L}^{-1}\cdot\text{h}^{-1}$ )

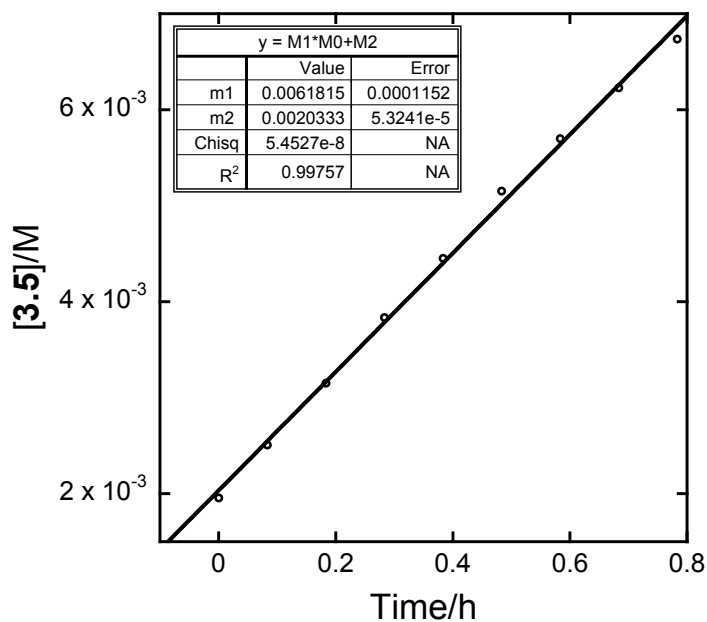


**Figure S2.27.** Plot of [3.5] vs time: [3.10] =  $5.70 \times 10^{-4} \text{ mol}\cdot\text{L}^{-1}$  and [1.13]<sub>0</sub> =  $1.02 \times 10^{-2} \text{ mol}\cdot\text{L}^{-1}$  under 3.0 atm (gauge pressure: 30 psi) H<sub>2</sub> in C<sub>6</sub>D<sub>6</sub> at 295 K. ([H<sub>2</sub>] =  $7.61 \times 10^{-3} \text{ mol}\cdot\text{L}^{-1}$ ; d[3.5]/dt =  $8.8(4) \times 10^{-3} \text{ mol}\cdot\text{L}^{-1}\cdot\text{h}^{-1}$ )

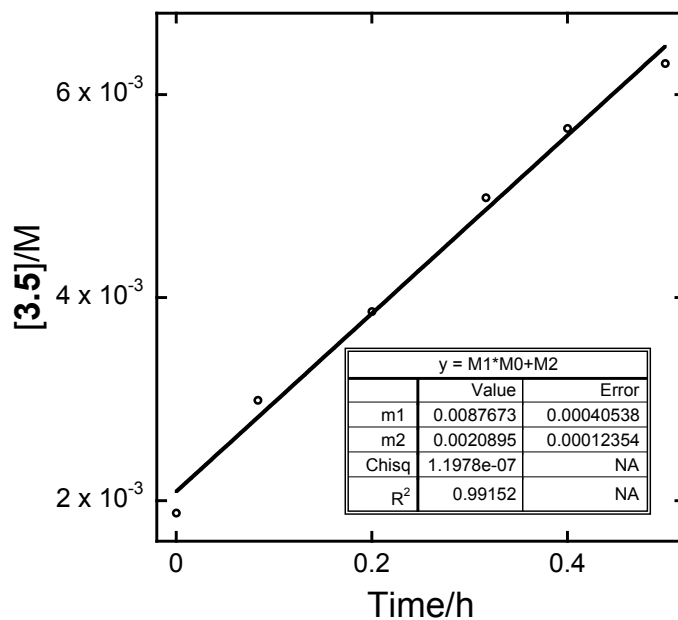


**Figure S2.28.** Plot of d[3.5]/dt vs [3.10] at 295 K. ( $k = 9.9(1) \times 10^2 \text{ L}^2\cdot\text{mol}^{-2}\cdot\text{s}^{-1}$ )

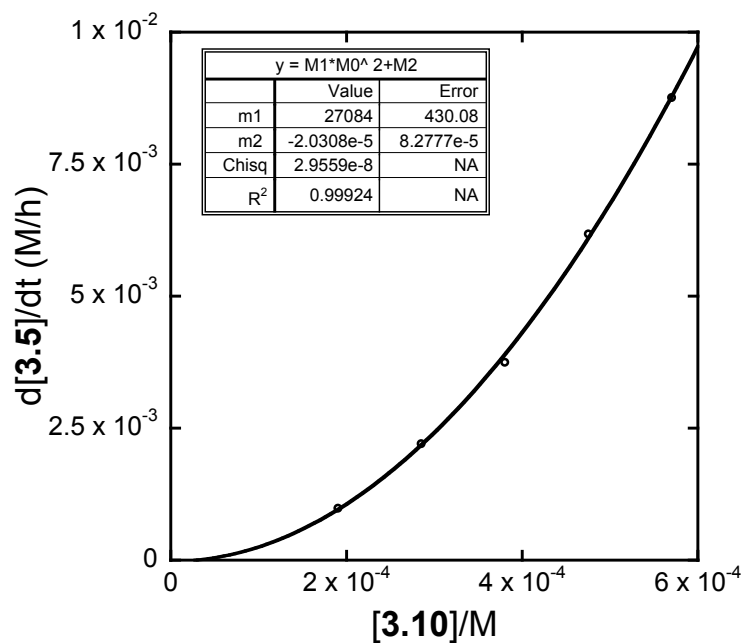


**Figure S2.29.** Plot of [3.5] vs time:  $[3.10] = 3.80 \times 10^{-4} \text{ mol}\cdot\text{L}^{-1}$ ,  $[1.13]_0 = 1.02 \times 10^{-2} \text{ mol}\cdot\text{L}^{-1}$  and  $[\text{THF}] = 3.08 \times 10^{-2} \text{ mol}\cdot\text{L}^{-1}$  under 3.0 atm (gauge pressure: 30 psi)  $\text{H}_2$  in  $\text{C}_6\text{D}_6$  at 295 K. ( $[\text{H}_2] = 7.61 \times 10^{-3} \text{ mol}\cdot\text{L}^{-1}$ ;  $d[3.5]/dt = 3.86(3) \times 10^{-3} \text{ mol}\cdot\text{L}^{-1}\cdot\text{h}^{-1}$ )

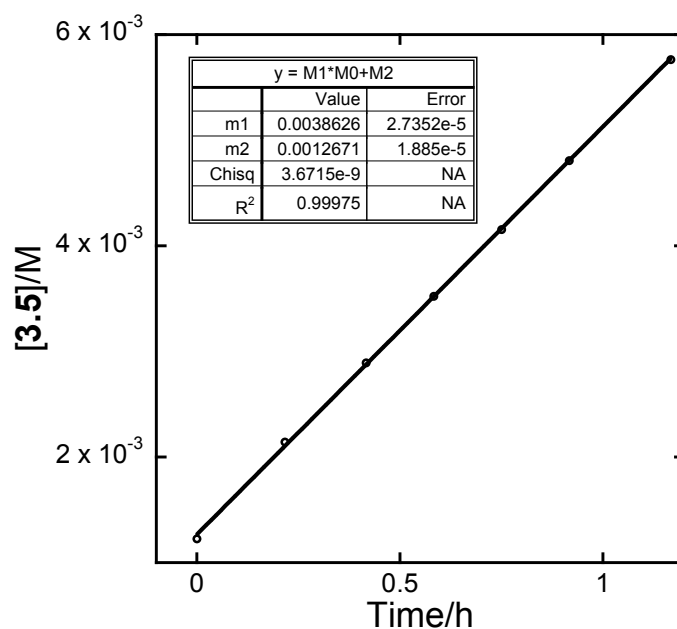


**Figure S2.30.** Plot of [3.5] vs time:  $[3.10] = 3.80 \times 10^{-4} \text{ mol}\cdot\text{L}^{-1}$ ,  $[1.13]_0 = 1.02 \times 10^{-2} \text{ mol}\cdot\text{L}^{-1}$  and  $[\text{THF}] = 6.17 \times 10^{-2} \text{ mol}\cdot\text{L}^{-1}$  under 3.0 atm (gauge pressure: 30 psi)  $\text{H}_2$  in  $\text{C}_6\text{D}_6$  at 295 K. ( $[\text{H}_2] = 7.61 \times 10^{-3} \text{ mol}\cdot\text{L}^{-1}$ ;  $d[3.5]/dt = 3.63(5) \times 10^{-3} \text{ mol}\cdot\text{L}^{-1}\cdot\text{h}^{-1}$ )

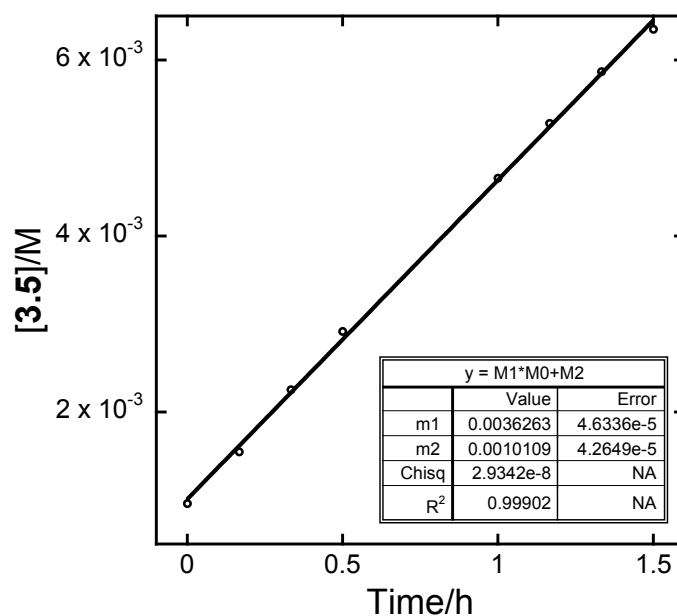


**Figure S2.31.** Plot of **[3.5]** vs time: **[3.10]** =  $3.80 \times 10^{-4} \text{ mol}\cdot\text{L}^{-1}$ , **[1.13]**<sub>0</sub> =  $1.02 \times 10^{-2} \text{ mol}\cdot\text{L}^{-1}$  and **[THF]** =  $9.25 \times 10^{-2} \text{ mol}\cdot\text{L}^{-1}$  under 3.0 atm (gauge pressure: 30 psi) H<sub>2</sub> in C<sub>6</sub>D<sub>6</sub> at 295 K. (**[H<sub>2</sub>]** =  $7.61 \times 10^{-3} \text{ mol}\cdot\text{L}^{-1}$ ; d**[3.5]**/dt =  $3.38(5) \times 10^{-3} \text{ mol}\cdot\text{L}^{-1}\cdot\text{h}^{-1}$ )

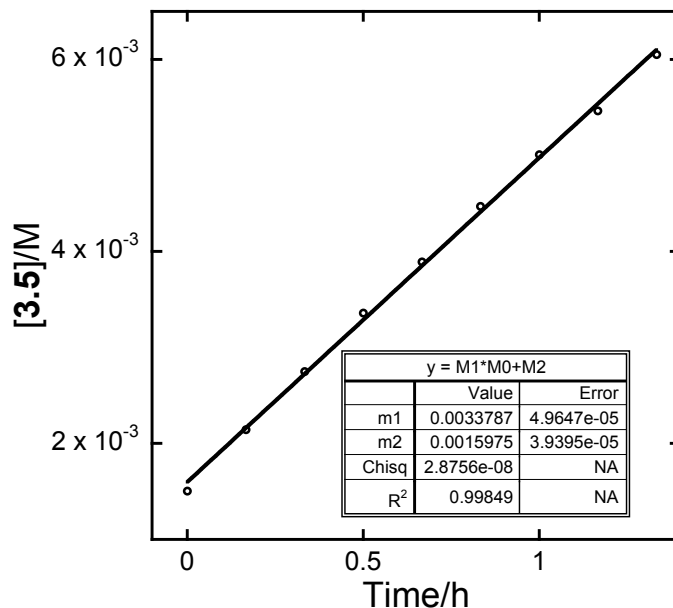


**Figure S2.32.** Plot of **[3.5]** vs time: **[3.10]** =  $3.80 \times 10^{-4} \text{ mol}\cdot\text{L}^{-1}$ , **[1.13]**<sub>0</sub> =  $1.02 \times 10^{-2} \text{ mol}\cdot\text{L}^{-1}$  and **[THF]** =  $1.54 \times 10^{-1} \text{ mol}\cdot\text{L}^{-1}$  under 3.0 atm (gauge pressure: 30 psi) H<sub>2</sub> in C<sub>6</sub>D<sub>6</sub> at 295 K. (**[H<sub>2</sub>]** =  $7.61 \times 10^{-3} \text{ mol}\cdot\text{L}^{-1}$ ; d**[3.35]**/dt =  $3.15(6) \times 10^{-3} \text{ mol}\cdot\text{L}^{-1}\cdot\text{h}^{-1}$ )

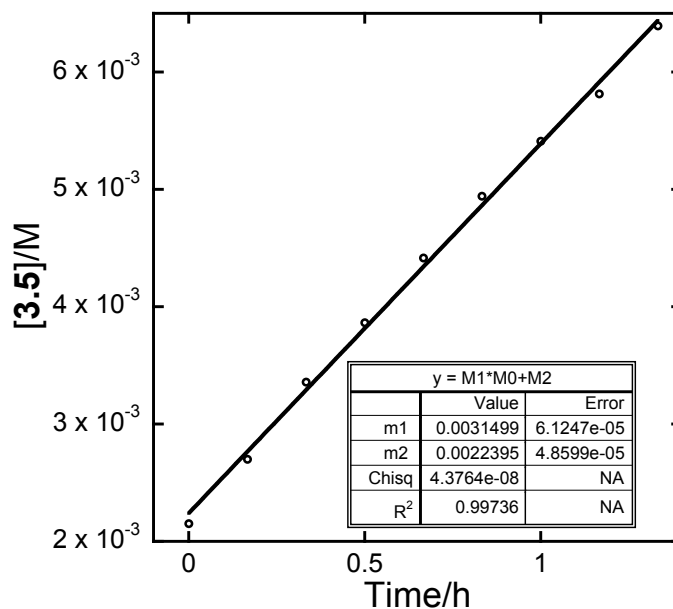


**Figure S2.33.** Plot of [3.5] vs time:  $[3.10] = 3.80 \times 10^{-4} \text{ mol}\cdot\text{L}^{-1}$ ,  $[1.13]_0 = 1.02 \times 10^{-2} \text{ mol}\cdot\text{L}^{-1}$  and  $[\text{THF}] = 3.08 \times 10^{-1} \text{ mol}\cdot\text{L}^{-1}$  under 3.0 atm (gauge pressure: 30 psi)  $\text{H}_2$  in  $\text{C}_6\text{D}_6$  at 295 K. ( $[\text{H}_2] = 7.61 \times 10^{-3} \text{ mol}\cdot\text{L}^{-1}$ ;  $d[3.5]/dt = 2.57(4) \times 10^{-3} \text{ mol}\cdot\text{L}^{-1}\cdot\text{h}^{-1}$ )

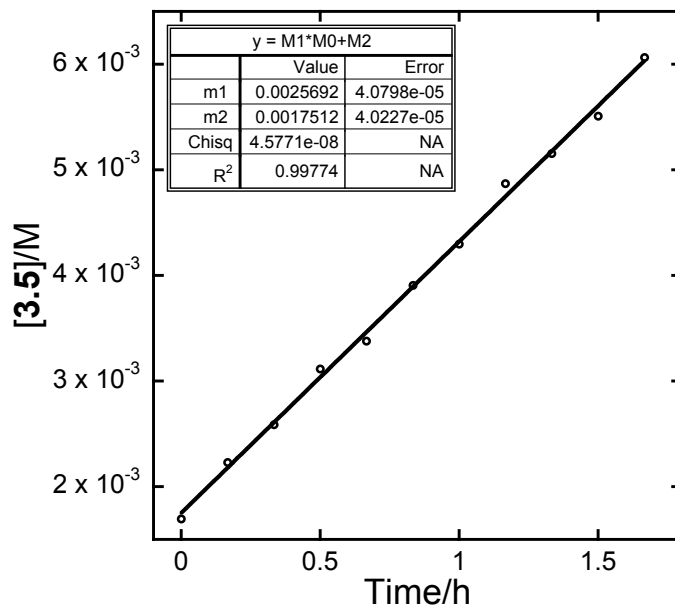


**Figure S2.34.** Plot of [3.5] vs time:  $[3.10] = 3.80 \times 10^{-4} \text{ mol}\cdot\text{L}^{-1}$ ,  $[1.13]_0 = 1.02 \times 10^{-2} \text{ mol}\cdot\text{L}^{-1}$  and  $[\text{THF}] = 4.62 \times 10^{-1} \text{ mol}\cdot\text{L}^{-1}$  under 3.0 atm (gauge pressure: 30 psi)  $\text{H}_2$  in  $\text{C}_6\text{D}_6$  at 295 K. ( $[\text{H}_2] = 7.61 \times 10^{-3} \text{ mol}\cdot\text{L}^{-1}$ ;  $d[3.5]/dt = 2.16(1) \times 10^{-3} \text{ mol}\cdot\text{L}^{-1}\cdot\text{h}^{-1}$ )

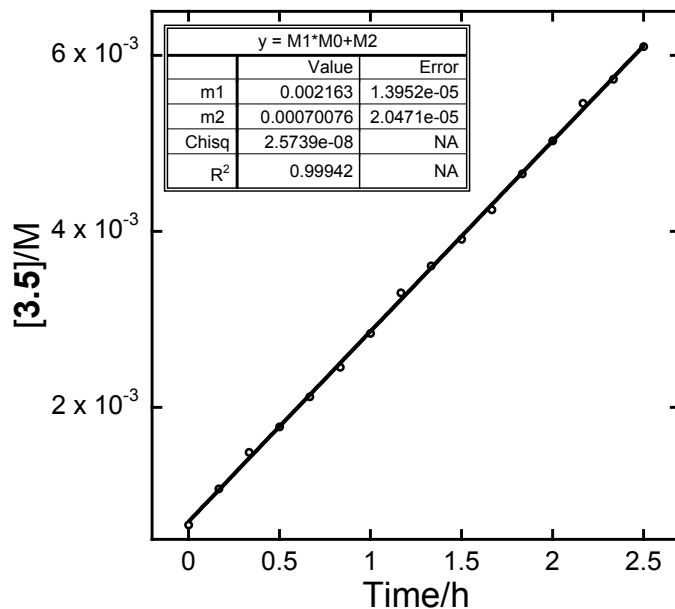


**Figure S2.35.** Plot of [3.5] vs time:  $[3.10] = 3.80 \times 10^{-4} \text{ mol}\cdot\text{L}^{-1}$ ,  $[1.13]_0 = 1.02 \times 10^{-2} \text{ mol}\cdot\text{L}^{-1}$  and  $[\text{THF}] = 6.17 \times 10^{-1} \text{ mol}\cdot\text{L}^{-1}$  under 3.0 atm (gauge pressure: 30 psi)  $\text{H}_2$  in  $\text{C}_6\text{D}_6$  at 295 K. ( $[\text{H}_2] = 7.61 \times 10^{-3} \text{ mol}\cdot\text{L}^{-1}$ ;  $d[3.5]/dt = 1.89(2) \times 10^{-3} \text{ mol}\cdot\text{L}^{-1}\cdot\text{h}^{-1}$ )

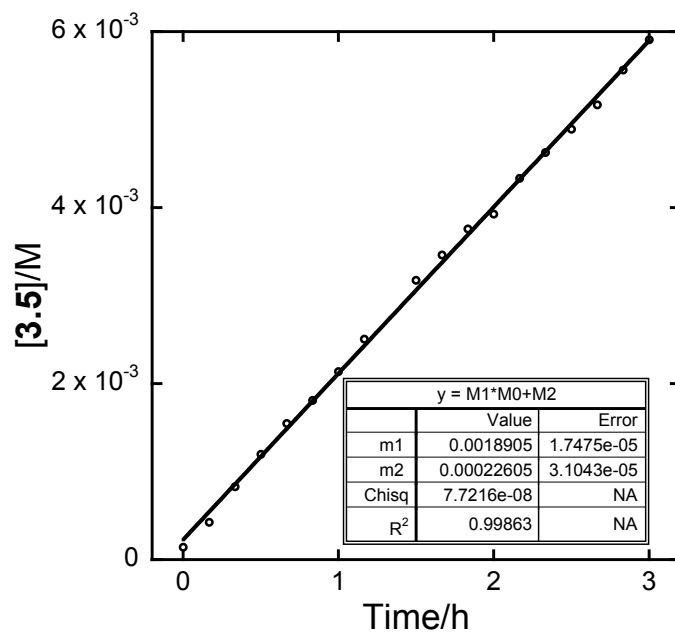


**Figure S2.36.** Plot of  $k$  vs  $[\text{THF}]$  at 295 K. ( $k_1 = 1.02(1) \times 10^3 \text{ L}^2\cdot\text{mol}^{-2}\cdot\text{s}^{-1}$ ,  $K = 1.26(6) \text{ mol}\cdot\text{L}^{-2}$ )

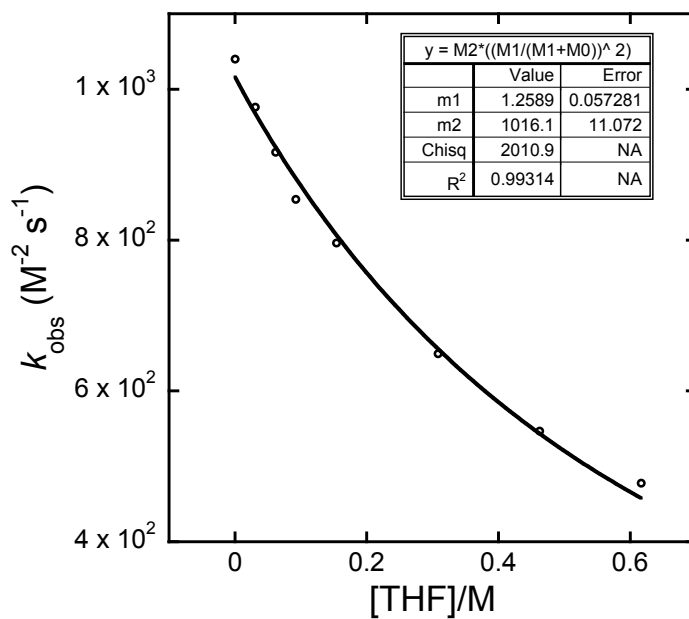




**Figure S2.37.** Plot of [3.5] vs time: [3.8] =  $7.60 \times 10^{-4} \text{ mol}\cdot\text{L}^{-1}$  and [1.13]<sub>0</sub> =  $1.02 \times 10^{-2} \text{ mol}\cdot\text{L}^{-1}$  under 3.0 atm (gauge pressure: 30 psi) H<sub>2</sub> in C<sub>6</sub>D<sub>6</sub> at 295 K. ([H<sub>2</sub>] =  $7.61 \times 10^{-3} \text{ mol}\cdot\text{L}^{-1}$ ; d[3.5]/dt =  $5.4(1) \times 10^{-3} \text{ mol}\cdot\text{L}^{-1}\cdot\text{h}^{-1}$ )

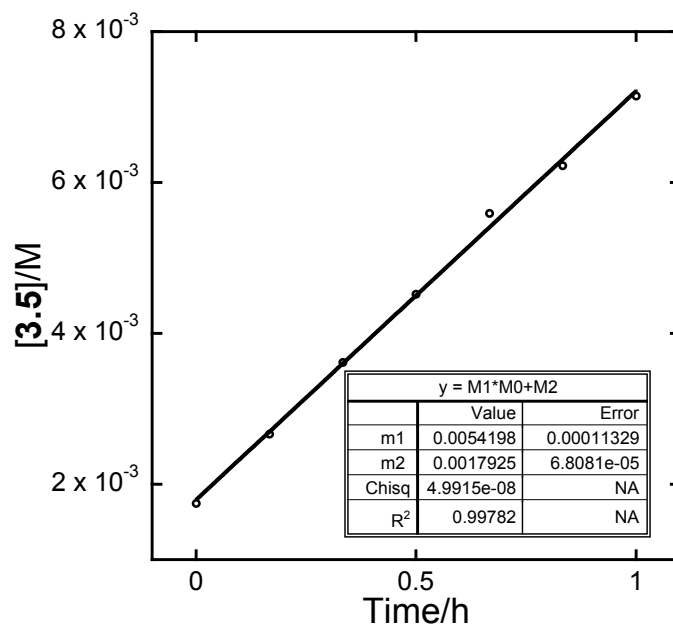


**Figure S2.38.** Plot of [3.5] vs time: [3.8] =  $7.60 \times 10^{-4} \text{ mol}\cdot\text{L}^{-1}$ , [1.13]<sub>0</sub> =  $1.02 \times 10^{-2} \text{ mol}\cdot\text{L}^{-1}$  and [MeOH] =  $3.09 \times 10^{-2} \text{ mol}\cdot\text{L}^{-1}$  under 3.0 atm (gauge pressure: 30 psi) H<sub>2</sub> in C<sub>6</sub>D<sub>6</sub> at 295 K. ([H<sub>2</sub>] =  $7.61 \times 10^{-3} \text{ mol}\cdot\text{L}^{-1}$ ; d[3.5]/dt =  $3.71(9) \times 10^{-3} \text{ mol}\cdot\text{L}^{-1}\cdot\text{h}^{-1}$ )

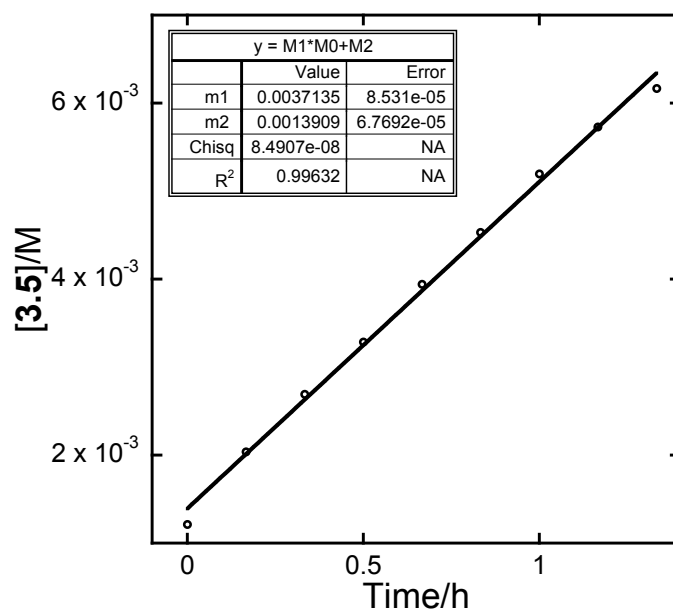


**Figure S2.39.** Plot of [3.5] vs time: [3.8] =  $7.60 \times 10^{-4} \text{ mol}\cdot\text{L}^{-1}$ , [1.13]<sub>0</sub> =  $1.02 \times 10^{-2} \text{ mol}\cdot\text{L}^{-1}$  and [MeOH] =  $6.18 \times 10^{-2} \text{ mol}\cdot\text{L}^{-1}$  under 3.0 atm (gauge pressure: 30 psi) H<sub>2</sub> in C<sub>6</sub>D<sub>6</sub> at 295 K. ([H<sub>2</sub>] =  $7.61 \times 10^{-3} \text{ mol}\cdot\text{L}^{-1}$ ; d[3.5]/dt =  $2.45(4) \times 10^{-3} \text{ mol}\cdot\text{L}^{-1}\cdot\text{h}^{-1}$ )

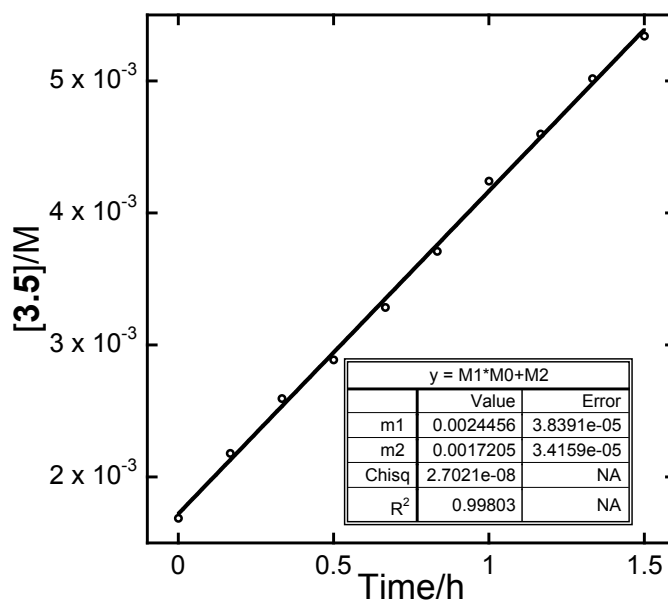


**Figure S2.40.** Plot of [3.5] vs time: [3.8] =  $7.60 \times 10^{-4} \text{ mol}\cdot\text{L}^{-1}$ , [1.13]<sub>0</sub> =  $1.02 \times 10^{-2} \text{ mol}\cdot\text{L}^{-1}$  and [MeOH] =  $9.27 \times 10^{-2} \text{ mol}\cdot\text{L}^{-1}$  under 3.0 atm (gauge pressure: 30 psi) H<sub>2</sub> in C<sub>6</sub>D<sub>6</sub> at 295 K. ([H<sub>2</sub>] =  $7.61 \times 10^{-3} \text{ mol}\cdot\text{L}^{-1}$ ; d[3.5]/dt =  $2.45(4) \times 10^{-3} \text{ mol}\cdot\text{L}^{-1}\cdot\text{h}^{-1}$ )

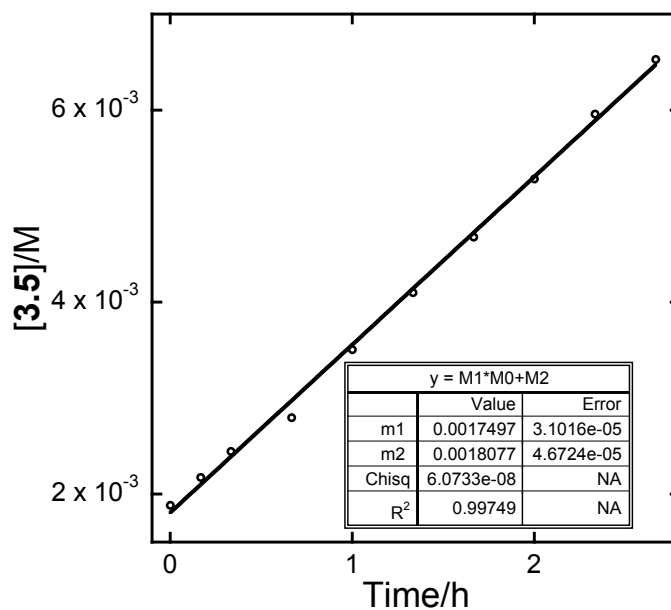


**Figure S2.41.** Plot of [3.5] vs time: [3.8] =  $7.60 \times 10^{-4} \text{ mol}\cdot\text{L}^{-1}$ , [1.13]<sub>0</sub> =  $1.02 \times 10^{-2} \text{ mol}\cdot\text{L}^{-1}$  and [MeOH] =  $1.24 \times 10^{-1} \text{ mol}\cdot\text{L}^{-1}$  under 3.0 atm (gauge pressure: 30 psi) H<sub>2</sub> in C<sub>6</sub>D<sub>6</sub> at 295 K. ([H<sub>2</sub>] =  $7.61 \times 10^{-3} \text{ mol}\cdot\text{L}^{-1}$ ; d[3.5]/dt =  $1.41(3) \times 10^{-3} \text{ mol}\cdot\text{L}^{-1}\cdot\text{h}^{-1}$ )

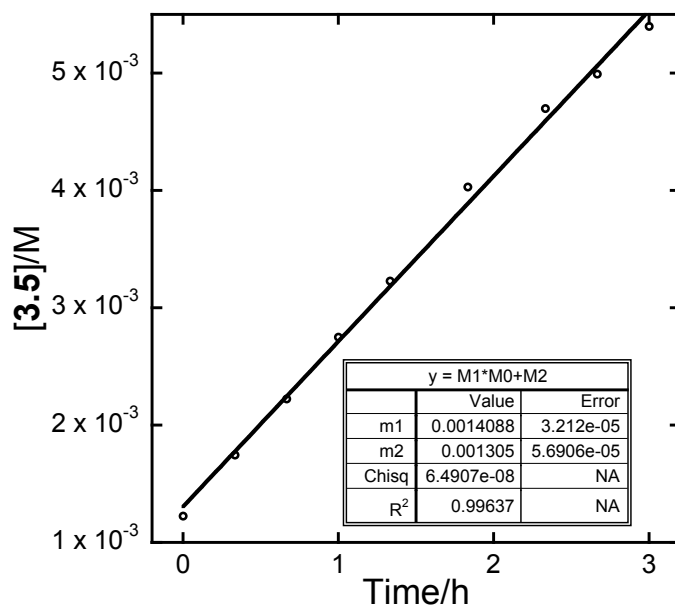


**Figure S2.42.** Plot of  $k$  vs [MeOH] at 295 K. ( $k_1 = 3.46(7) \times 10^2 \text{ L}^2\cdot\text{mol}^{-2}\cdot\text{s}^{-1}$ ,  $K = 1.28(6) \times 10^{-1} \text{ mol}\cdot\text{L}^{-2}$ )

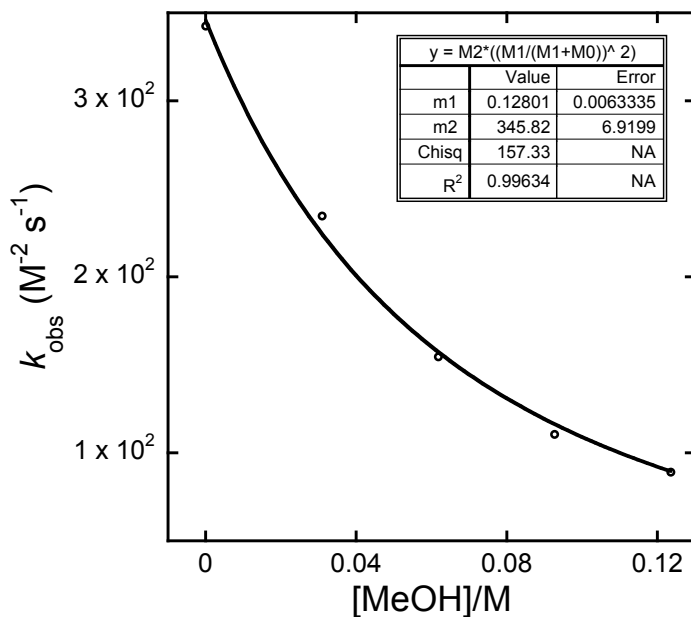


**Figure S2.43.** Plot of [3.5] vs time: [3.1] =  $3.80 \times 10^{-4} \text{ mol}\cdot\text{L}^{-1}$ , [1.13]<sub>0</sub> =  $1.02 \times 10^{-2} \text{ mol}\cdot\text{L}^{-1}$  and [PPh<sub>3</sub>] =  $1.15 \times 10^{-2} \text{ mol}\cdot\text{L}^{-1}$  under 3.0 atm (gauge pressure: 30 psi) H<sub>2</sub> in C<sub>6</sub>D<sub>6</sub> at 323 K. ([H<sub>2</sub>] =  $1.20 \times 10^{-2} \text{ mol}\cdot\text{L}^{-1}$ ; d[3.5]/dt =  $1.05(5) \times 10^{-3} \text{ mol}\cdot\text{L}^{-1}\cdot\text{h}^{-1}$ )

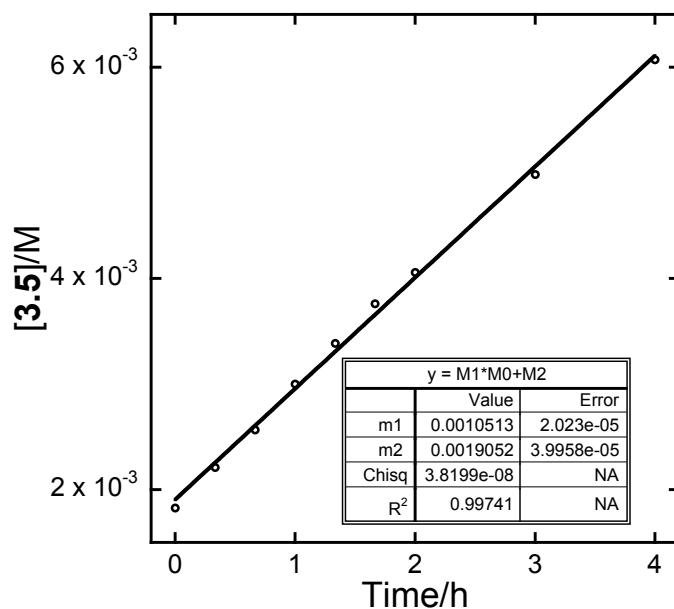


**Figure S2.44.** Plot of [3.5] vs time: [3.1] =  $3.80 \times 10^{-4} \text{ mol}\cdot\text{L}^{-1}$ , [1.13]<sub>0</sub> =  $1.02 \times 10^{-2} \text{ mol}\cdot\text{L}^{-1}$  and [PPh<sub>3</sub>] =  $1.72 \times 10^{-2} \text{ mol}\cdot\text{L}^{-1}$  under 3.0 atm (gauge pressure: 30 psi) H<sub>2</sub> in C<sub>6</sub>D<sub>6</sub> at 323 K. ([H<sub>2</sub>] =  $1.20 \times 10^{-2} \text{ mol}\cdot\text{L}^{-1}$ ; d[3.5]/dt =  $9.5(2) \times 10^{-4} \text{ mol}\cdot\text{L}^{-1}\cdot\text{h}^{-1}$ )

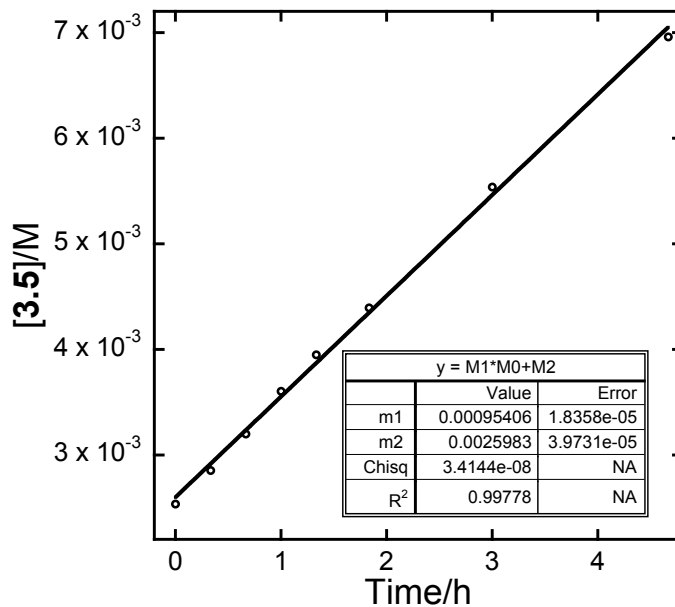


**Figure S2.45.** Plot of [3.5] vs time: [3.1] =  $3.80 \times 10^{-4} \text{ mol}\cdot\text{L}^{-1}$ , [1.13]<sub>0</sub> =  $1.02 \times 10^{-2} \text{ mol}\cdot\text{L}^{-1}$  and [PPh<sub>3</sub>] =  $2.29 \times 10^{-2} \text{ mol}\cdot\text{L}^{-1}$  under 3.0 atm (gauge pressure: 30 psi) H<sub>2</sub> in C<sub>6</sub>D<sub>6</sub> at 323 K. ([H<sub>2</sub>] =  $1.20 \times 10^{-2} \text{ mol}\cdot\text{L}^{-1}$ ; d[3.5]/dt =  $9.2(2) \times 10^{-4} \text{ mol}\cdot\text{L}^{-1}\cdot\text{h}^{-1}$ )

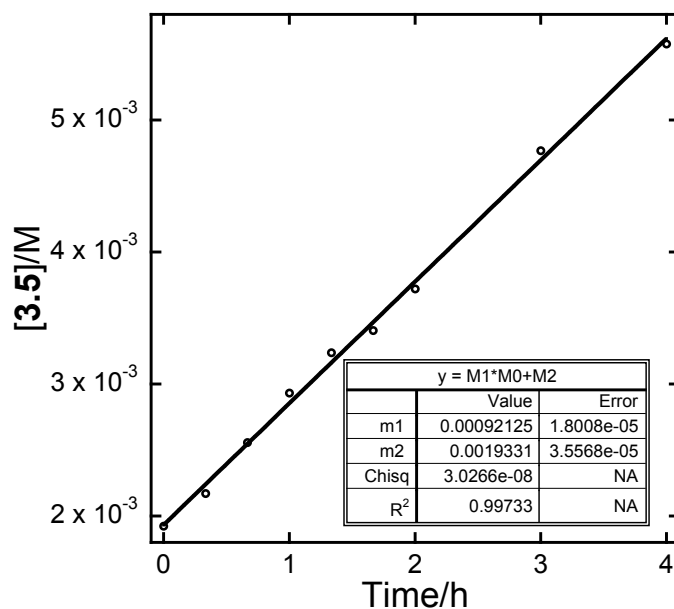


**Figure S2.46.** Plot of [3.5] vs time: [3.1] =  $3.80 \times 10^{-4} \text{ mol}\cdot\text{L}^{-1}$ , [1.13]<sub>0</sub> =  $1.02 \times 10^{-2} \text{ mol}\cdot\text{L}^{-1}$  and [PPh<sub>3</sub>] =  $2.86 \times 10^{-2} \text{ mol}\cdot\text{L}^{-1}$  under 3.0 atm (gauge pressure: 30 psi) H<sub>2</sub> in C<sub>6</sub>D<sub>6</sub> at 323 K. ([H<sub>2</sub>] =  $1.20 \times 10^{-2} \text{ mol}\cdot\text{L}^{-1}$ ; d[3.5]/dt =  $9.7(2) \times 10^{-4} \text{ mol}\cdot\text{L}^{-1}\cdot\text{h}^{-1}$ )

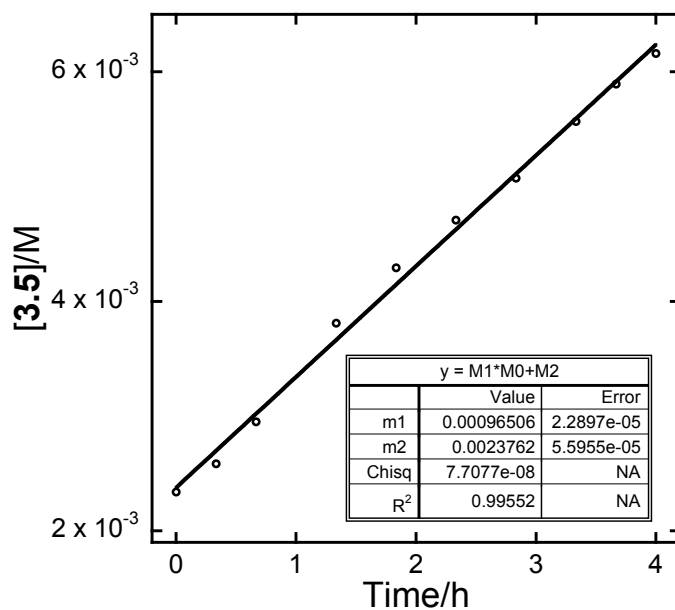


**Figure S2.47.** Plot of  $[3.5]$  vs time:  $[3.10] = 3.80 \times 10^{-4} \text{ mol}\cdot\text{L}^{-1}$ ,  $[1.13]_0 = 1.02 \times 10^{-2} \text{ mol}\cdot\text{L}^{-1}$  and  $[\text{PPh}_3] = 2.29 \times 10^{-2} \text{ mol}\cdot\text{L}^{-1}$  under 3.0 atm (gauge pressure: 30 psi)  $\text{H}_2$  in  $\text{C}_6\text{D}_6$  at 323 K. ( $[\text{H}_2] = 1.20 \times 10^{-2} \text{ mol}\cdot\text{L}^{-1}$ ;  $d[3.5]/dt = 1.00(1) \times 10^{-4} \text{ mol}\cdot\text{L}^{-1}\cdot\text{h}^{-1}$ )

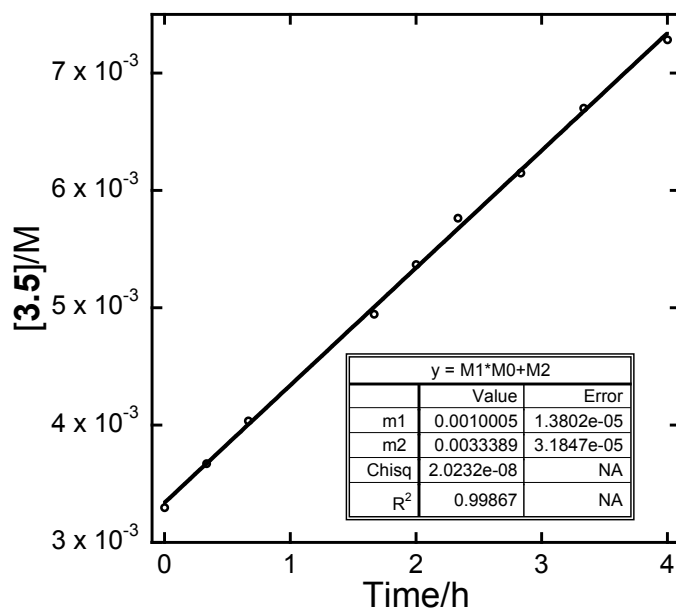


**Figure S2.48.** Plot of  $d[3.5]/dt$  vs  $[\text{Co}(\text{dmgBF}_2)_2(\text{L})_2]$  ( $\text{L} = \text{H}_2\text{O}$ , THF) at 323 K.

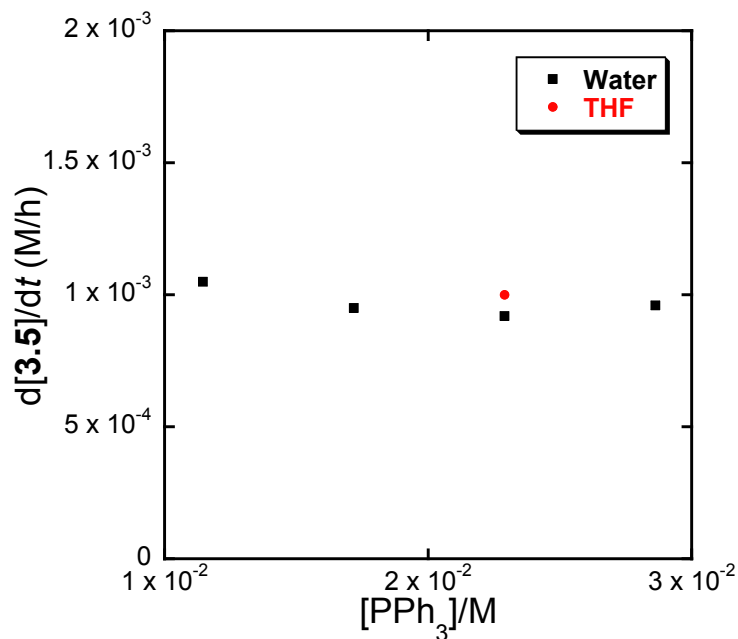


**Figure S2.49.** Plot of [3.5] vs time: [3.1] =  $3.80 \times 10^{-4} \text{ mol}\cdot\text{L}^{-1}$ , [1.13]<sub>0</sub> =  $1.02 \times 10^{-2} \text{ mol}\cdot\text{L}^{-1}$  and [PPh<sub>3</sub>] =  $2.29 \times 10^{-2} \text{ mol}\cdot\text{L}^{-1}$  under 3.0 atm (gauge pressure: 30 psi) H<sub>2</sub> in C<sub>6</sub>D<sub>6</sub> at 318 K. ([H<sub>2</sub>] =  $1.13 \times 10^{-2} \text{ mol}\cdot\text{L}^{-1}$ ; d[3.5]/dt =  $6.44(8) \times 10^{-4} \text{ mol}\cdot\text{L}^{-1}\cdot\text{h}^{-1}$ )

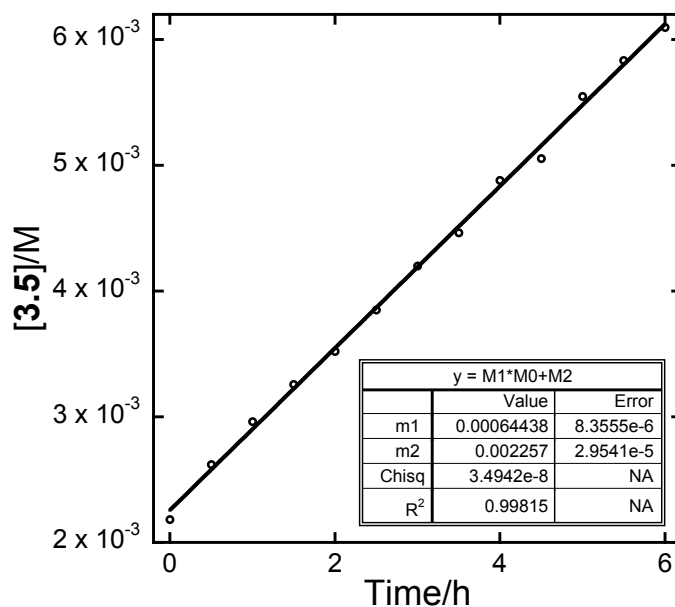


**Figure S2.50.** Plot of [3.5] vs time: [3.1] =  $3.80 \times 10^{-4} \text{ mol}\cdot\text{L}^{-1}$ , [1.13]<sub>0</sub> =  $1.02 \times 10^{-2} \text{ mol}\cdot\text{L}^{-1}$  and [PPh<sub>3</sub>] =  $2.29 \times 10^{-2} \text{ mol}\cdot\text{L}^{-1}$  under 3.0 atm (gauge pressure: 30 psi) H<sub>2</sub> in C<sub>6</sub>D<sub>6</sub> at 328 K. ([H<sub>2</sub>] =  $1.27 \times 10^{-2} \text{ mol}\cdot\text{L}^{-1}$ ; d[3.5]/dt =  $1.15(1) \times 10^{-3} \text{ mol}\cdot\text{L}^{-1}\cdot\text{h}^{-1}$ )

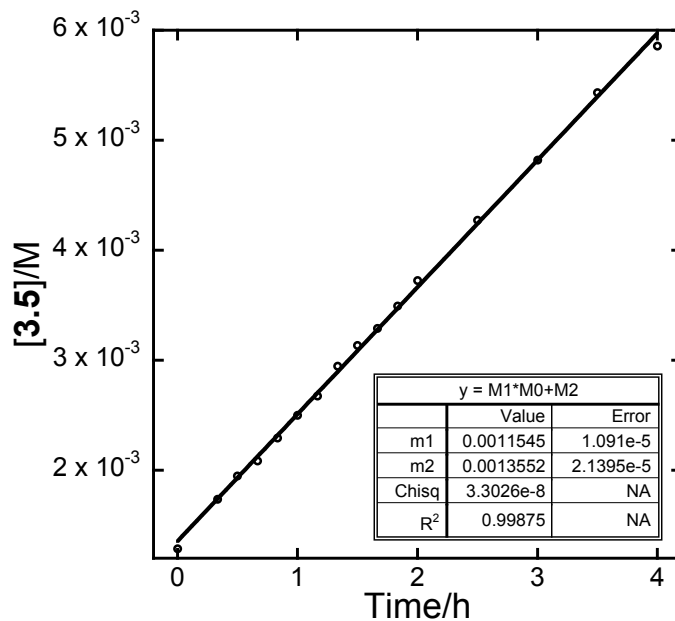


**Figure S2.51.** Plot of [3.5] vs time: [3.1] =  $3.80 \times 10^{-4} \text{ mol}\cdot\text{L}^{-1}$ , [1.13]<sub>0</sub> =  $1.02 \times 10^{-2} \text{ mol}\cdot\text{L}^{-1}$  and [PPh<sub>3</sub>] =  $2.29 \times 10^{-2} \text{ mol}\cdot\text{L}^{-1}$  under 3.0 atm (gauge pressure: 30 psi) H<sub>2</sub> in C<sub>6</sub>D<sub>6</sub> at 333 K. ([H<sub>2</sub>] =  $1.35 \times 10^{-2} \text{ mol}\cdot\text{L}^{-1}$ ; d[3.5]/dt =  $1.49(2) \times 10^{-3} \text{ mol}\cdot\text{L}^{-1}\cdot\text{h}^{-1}$ )

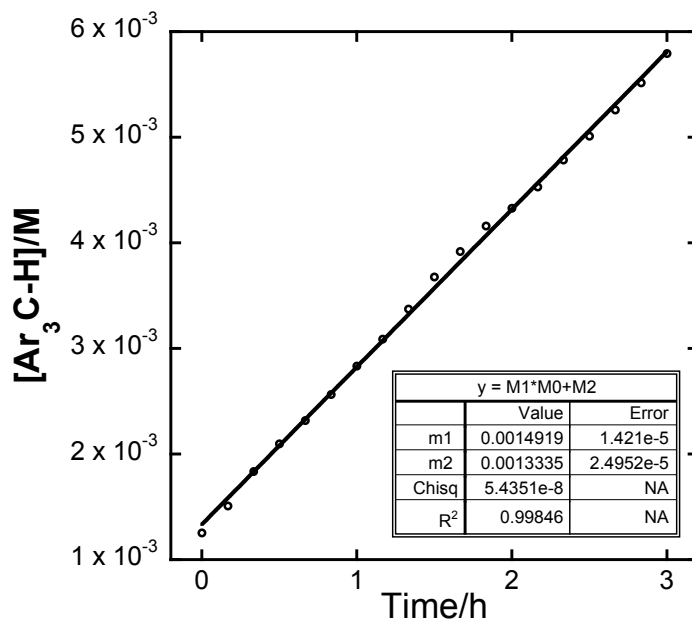
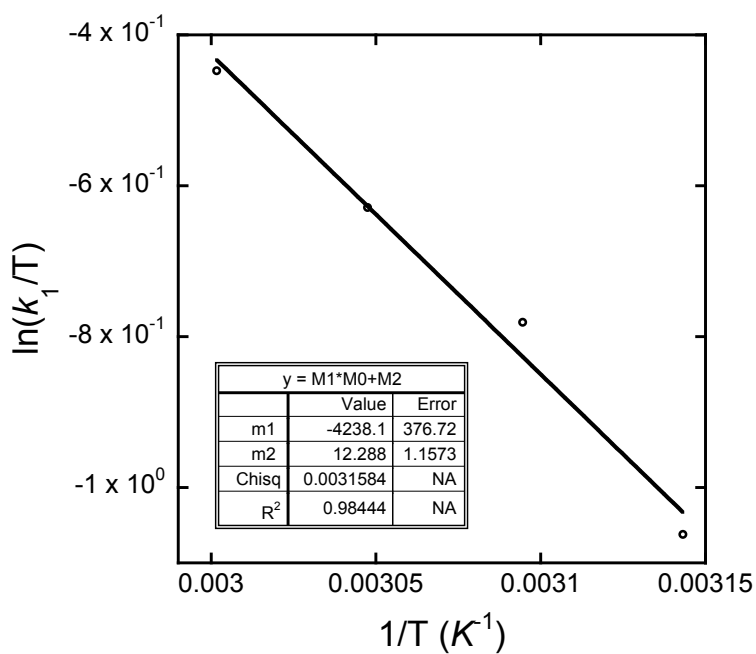


**Figure S2.52.** Eyring Plot of  $\ln(k_1/T)$  vs  $1/T$ . ( $\Delta H^\ddagger = 8(1) \text{ kcal}\cdot\text{mol}^{-1}$ ,  $\Delta S^\ddagger = -23(2) \text{ cal}\cdot\text{mol}^{-1}\cdot\text{K}^{-1}$ )





### 3. Derivation of Rate Law in eq 3.13 from Scheme 3.2

The rate-determining step is reaction 3.11:

$$\frac{d[\mathbf{3.5}]}{dt} = \frac{d[\text{Co-H}]}{dt} = k_{11}[\text{H}_2][\text{LCo}^{\text{II}}]^2$$

From eq 3.10:

$$K = \frac{[\text{L}][\text{LCo}^{\text{II}}]}{[\text{L}_2\text{Co}^{\text{II}}]}$$

where as:

$$[\text{Co}_{\text{Tot}}] = [\text{LCo}^{\text{II}}] + [\text{L}_2\text{Co}^{\text{II}}]$$

Therefore:

$$K = \frac{[\text{L}][\text{LCo}^{\text{II}}]}{[\text{Co}_{\text{Tot}}] - [\text{LCo}^{\text{II}}]}$$

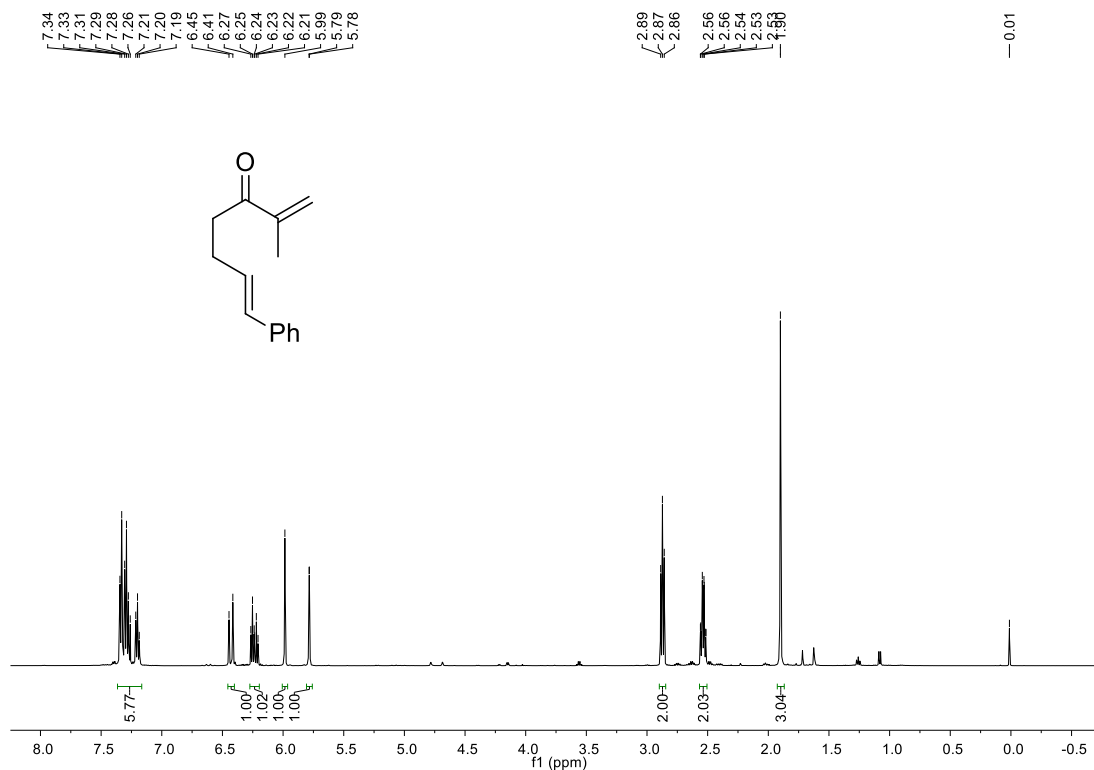
Thus:

$$[\text{LCo}^{\text{II}}] = \frac{K[\text{Co}_{\text{Tot}}]}{K + [\text{L}]}$$

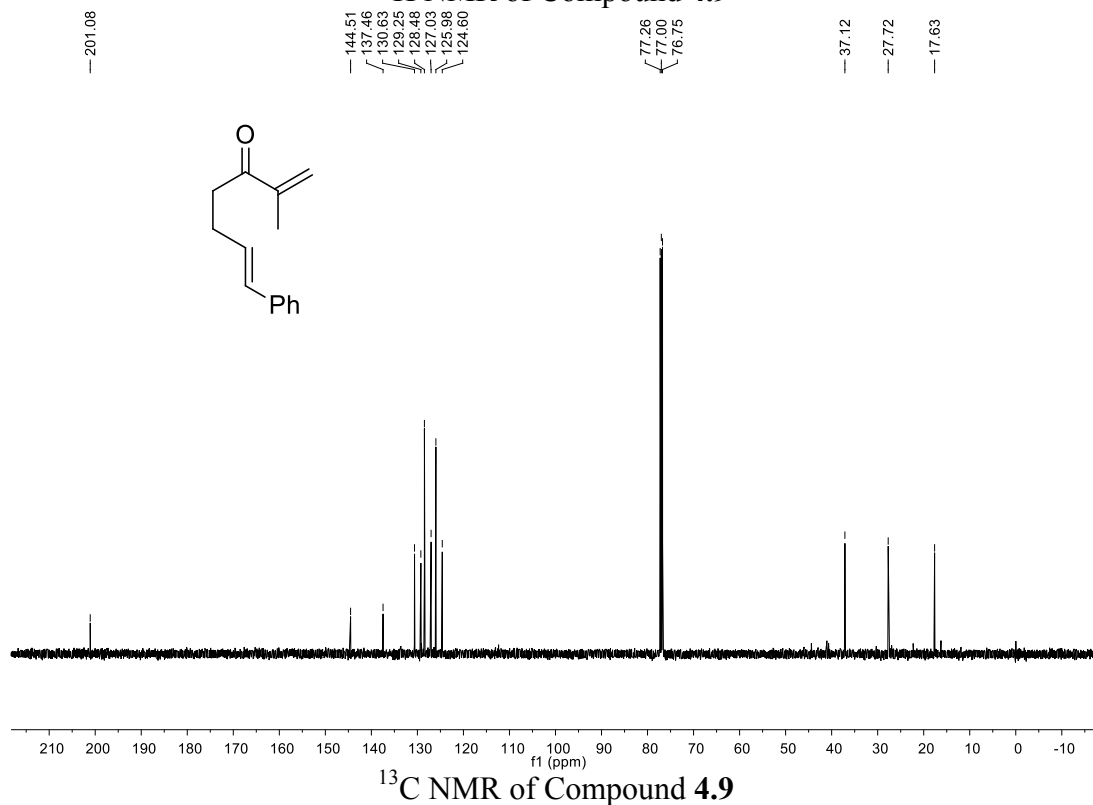
Finally:

$$\frac{d[\mathbf{3.5}]}{dt} = \frac{d[\text{Co-H}]}{dt} = k_{11}[\text{H}_2][\text{LCo}^{\text{II}}]^2 = k_{11}[\text{H}_2]\left(\frac{K[\text{Co}_{\text{Tot}}]}{K + [\text{L}]}\right)^2$$

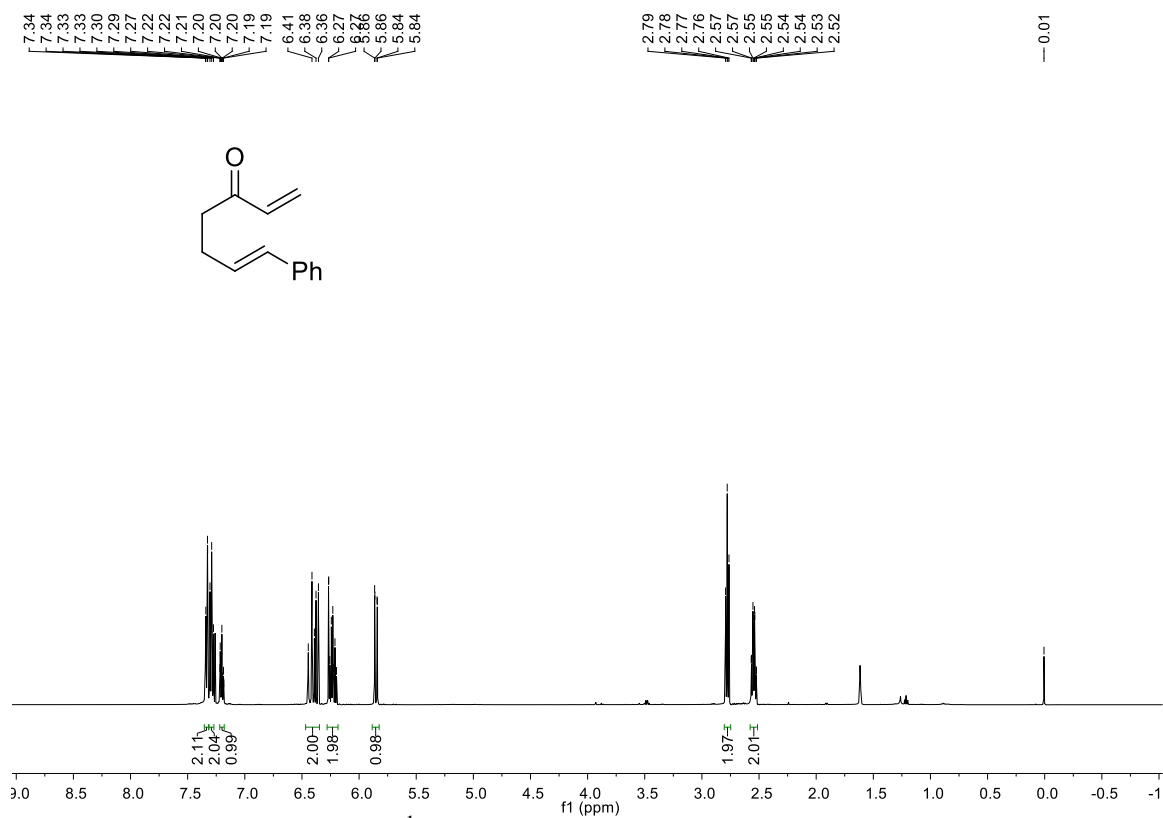
## APPENDIX III: RELEVANT SPECTRAL DATA FOR CHAPTER 4



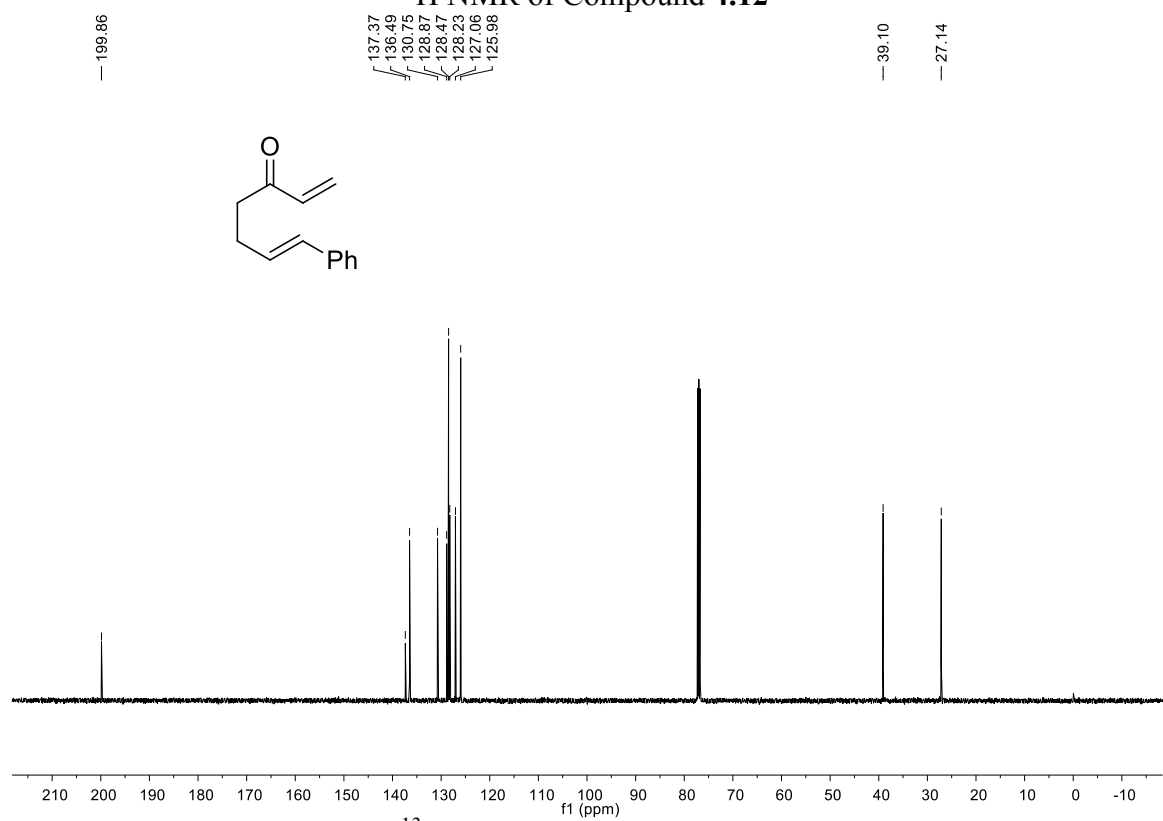
<sup>1</sup>H NMR of Compound 4.9



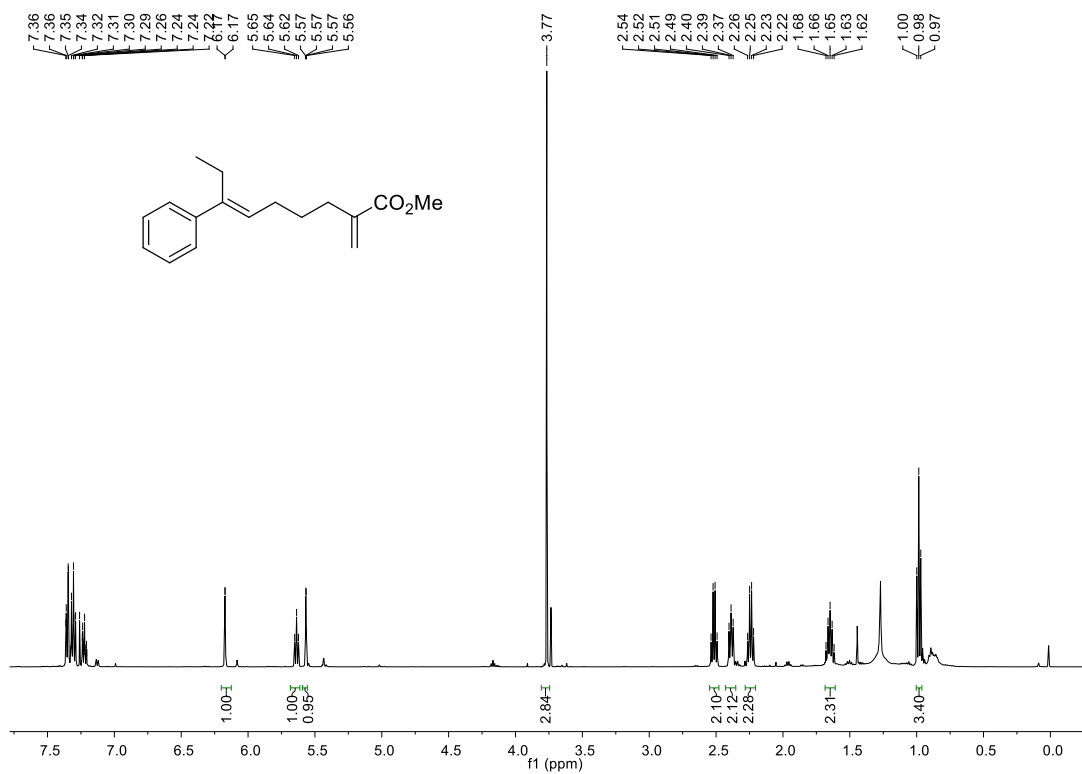
<sup>13</sup>C NMR of Compound 4.9



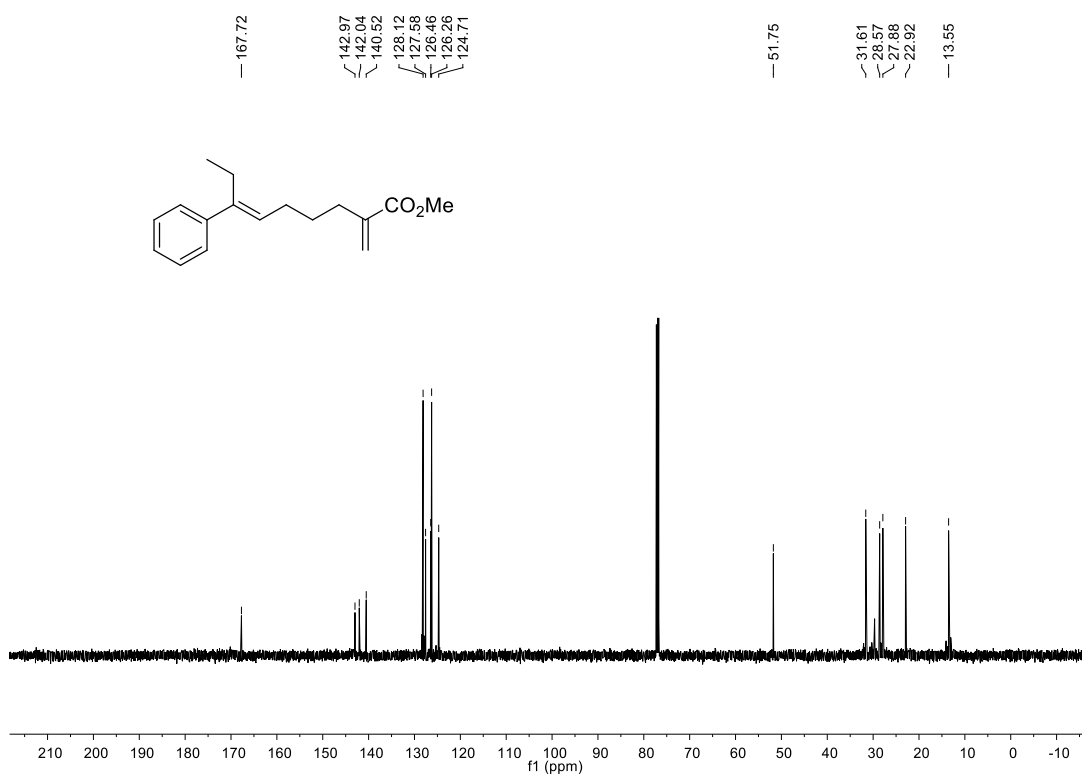
<sup>1</sup>H NMR of Compound 4.12



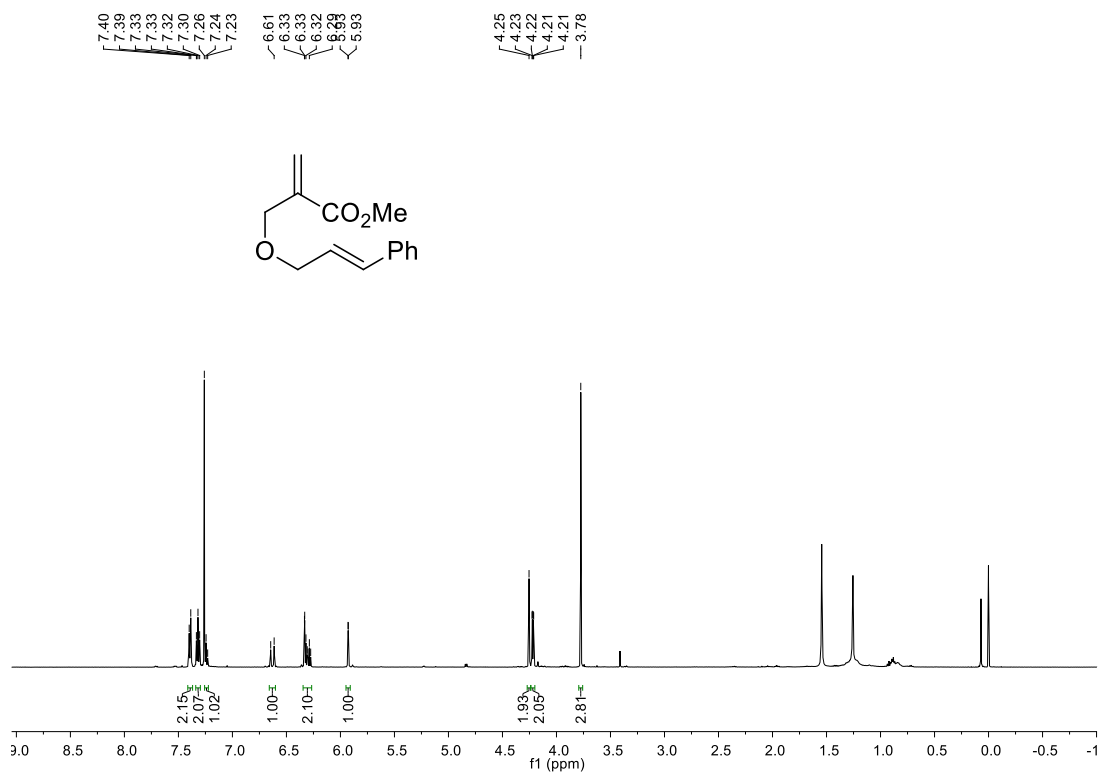
<sup>13</sup>C NMR of Compound 4.12



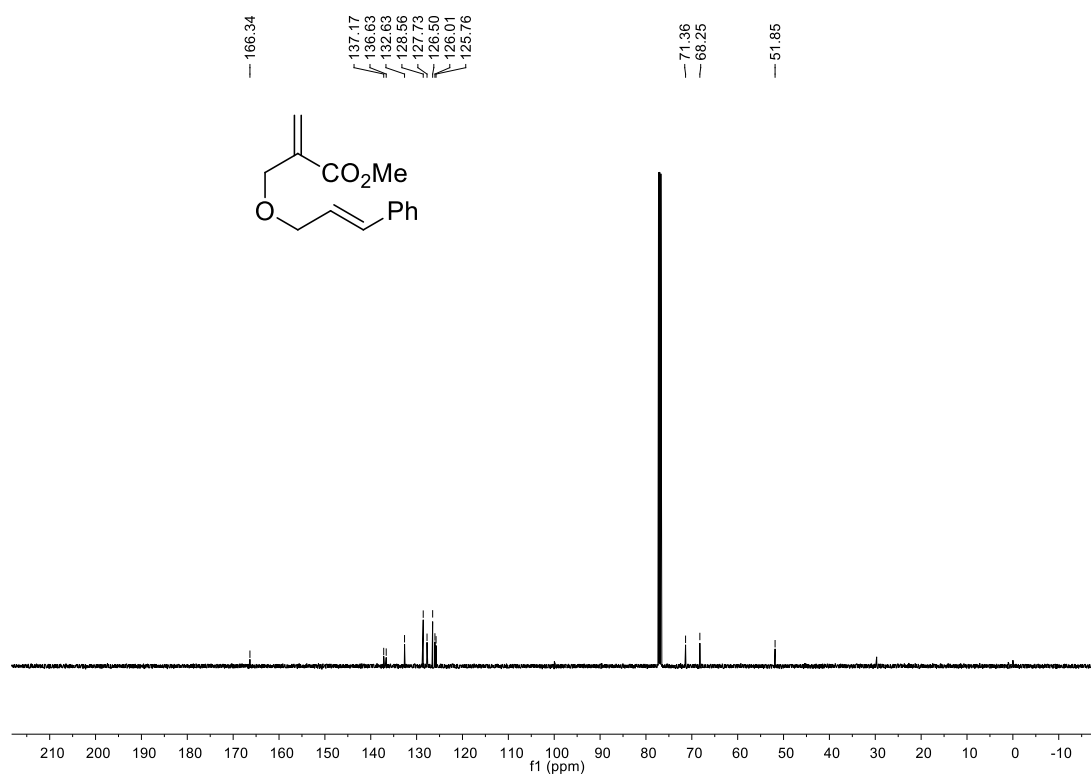
<sup>1</sup>H NMR of Compound 4.14



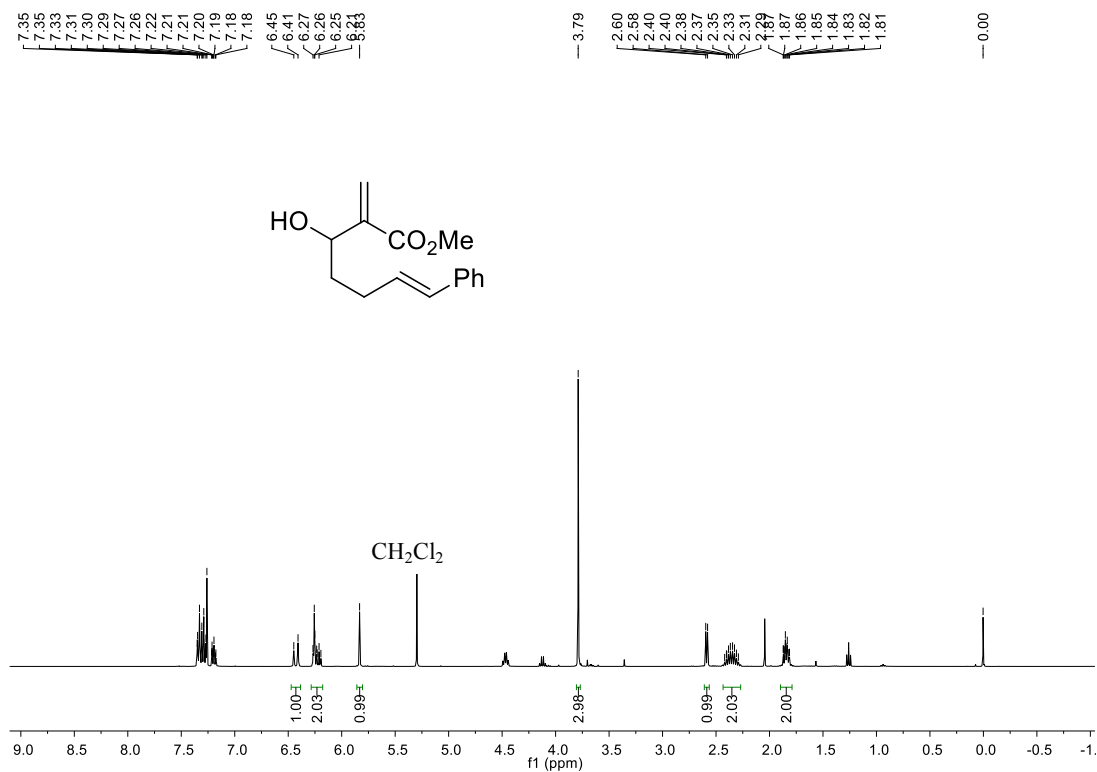
<sup>13</sup>C NMR of Compound 4.14



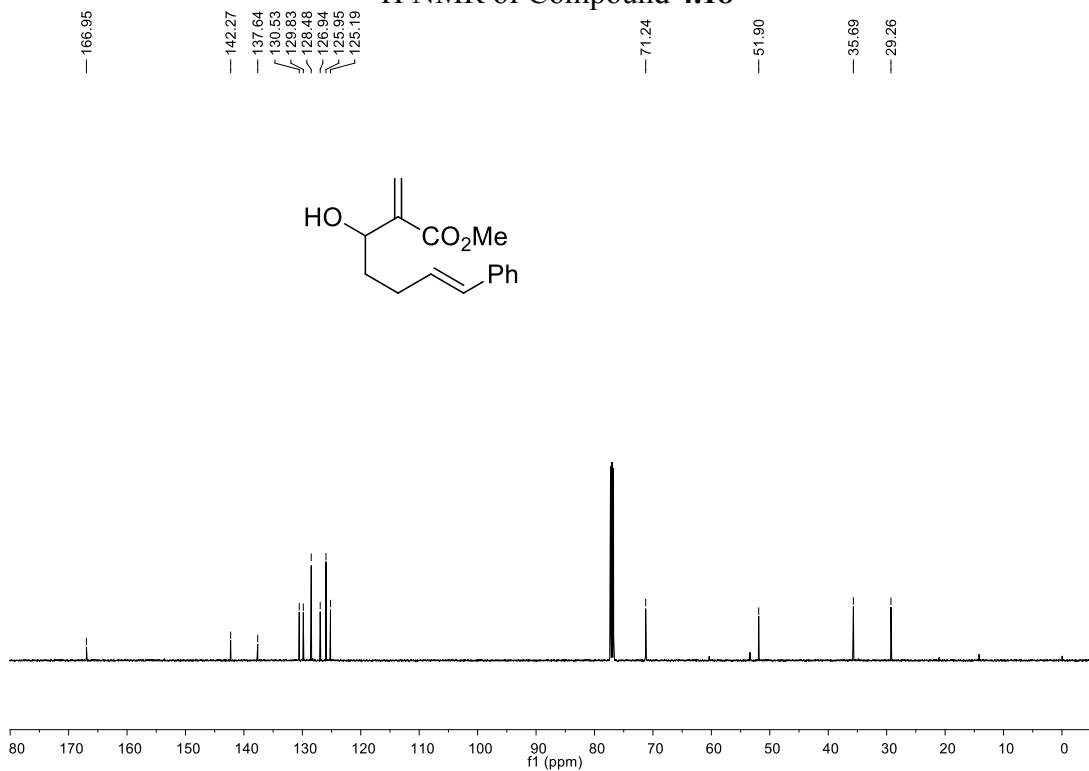
<sup>1</sup>H NMR of Compound 4.16



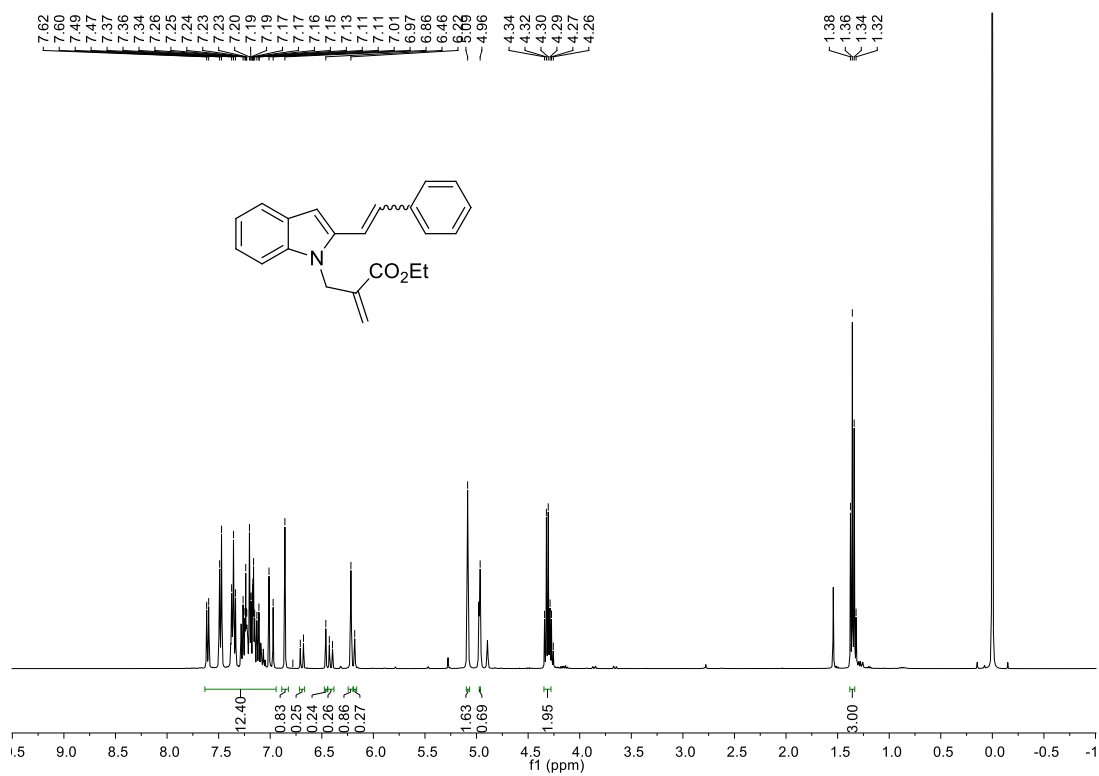
<sup>13</sup>C NMR of Compound 4.16



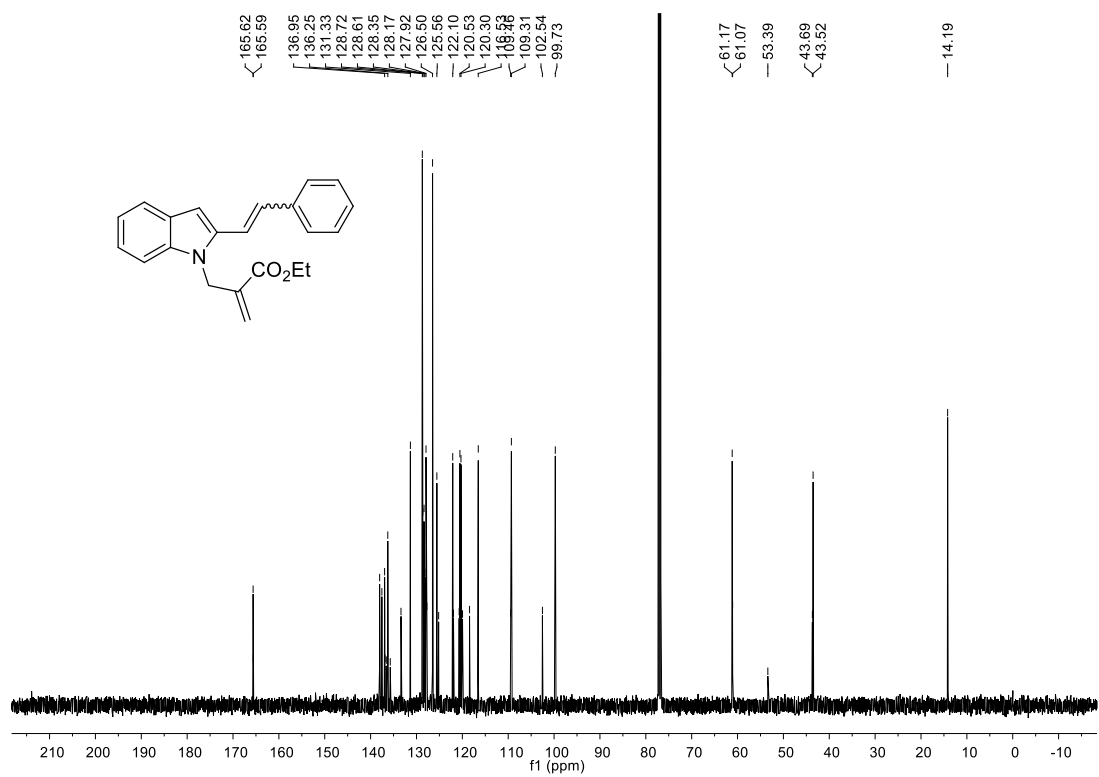
<sup>1</sup>H NMR of Compound 4.18



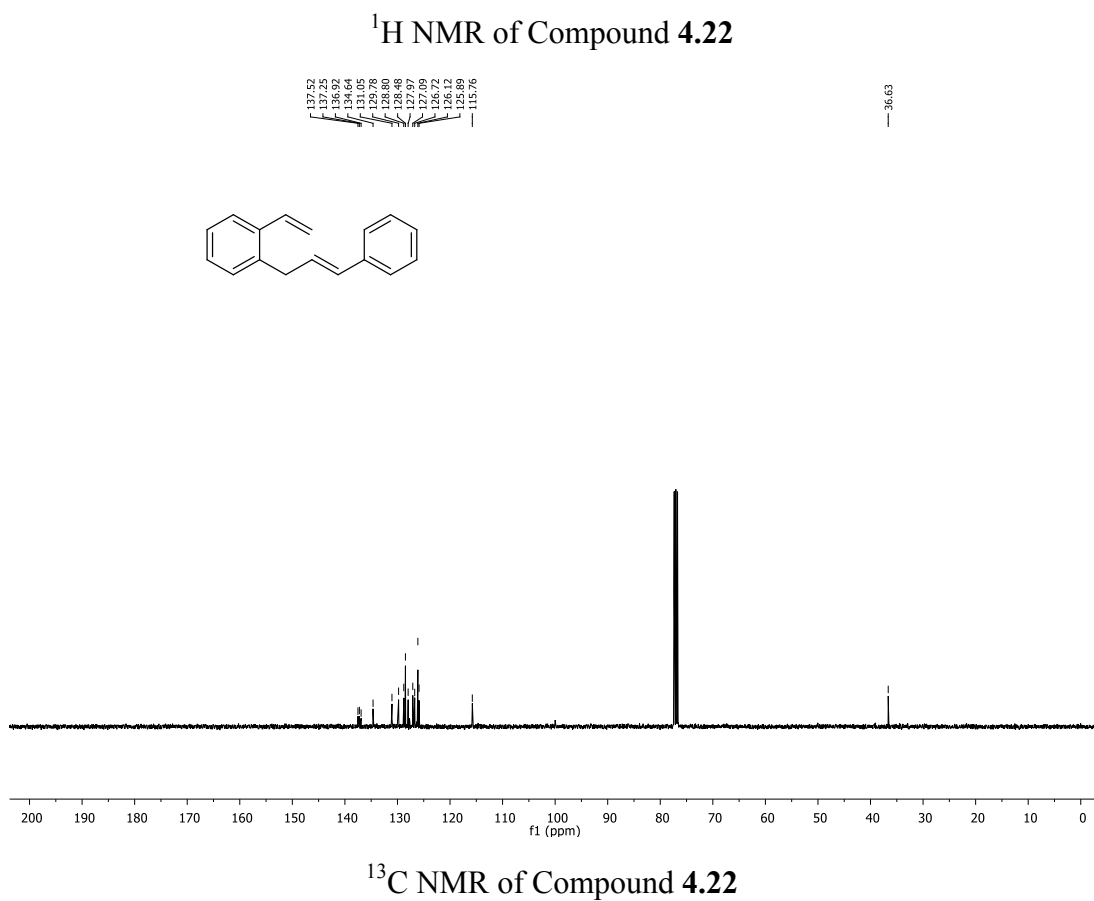
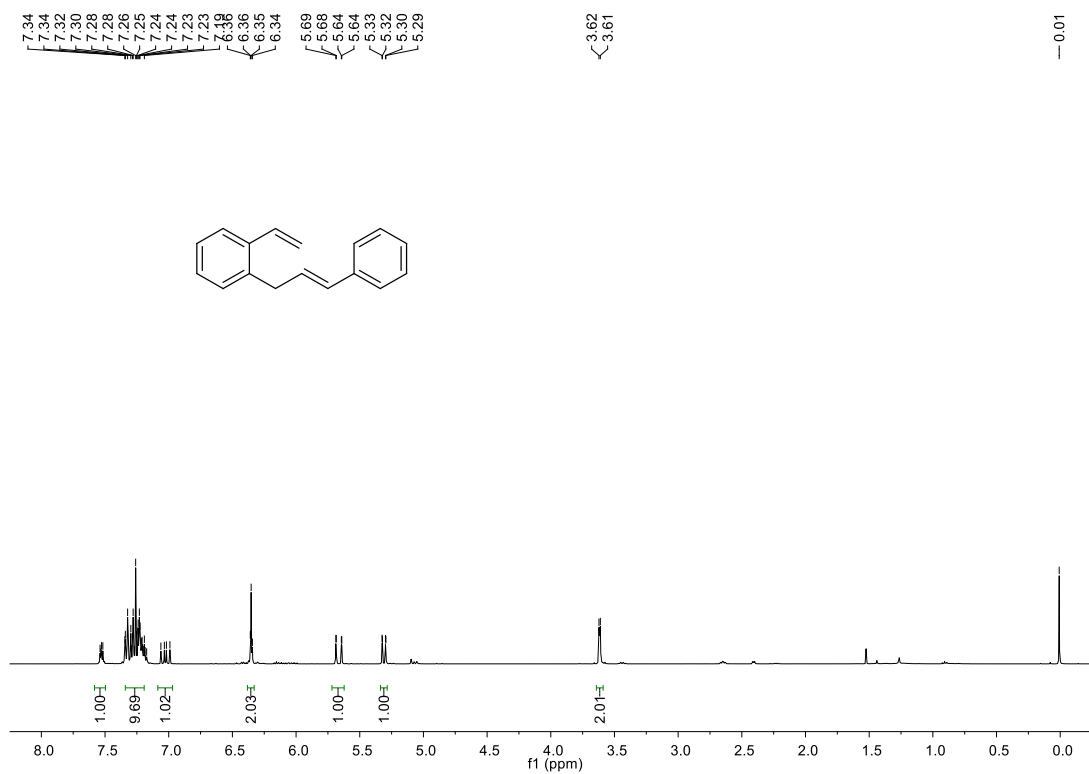
<sup>13</sup>C NMR of Compound 4.18



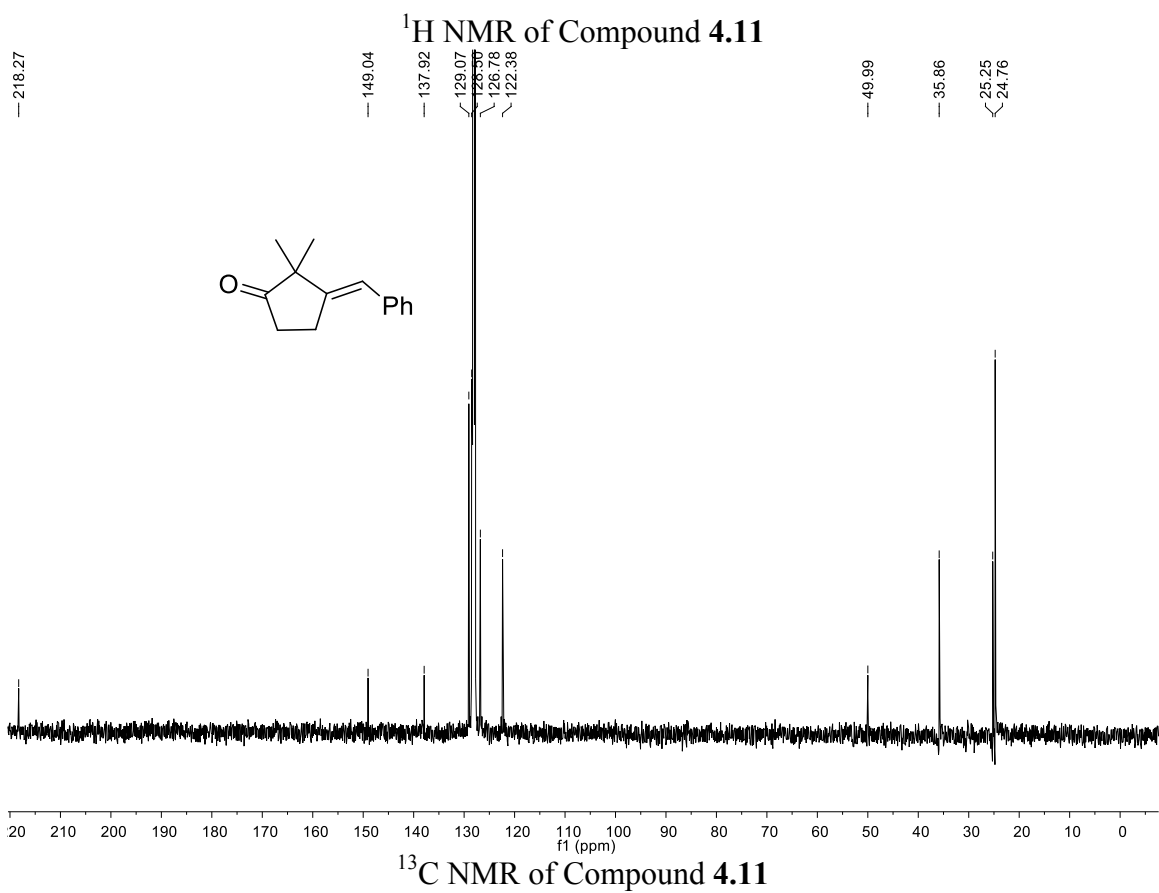
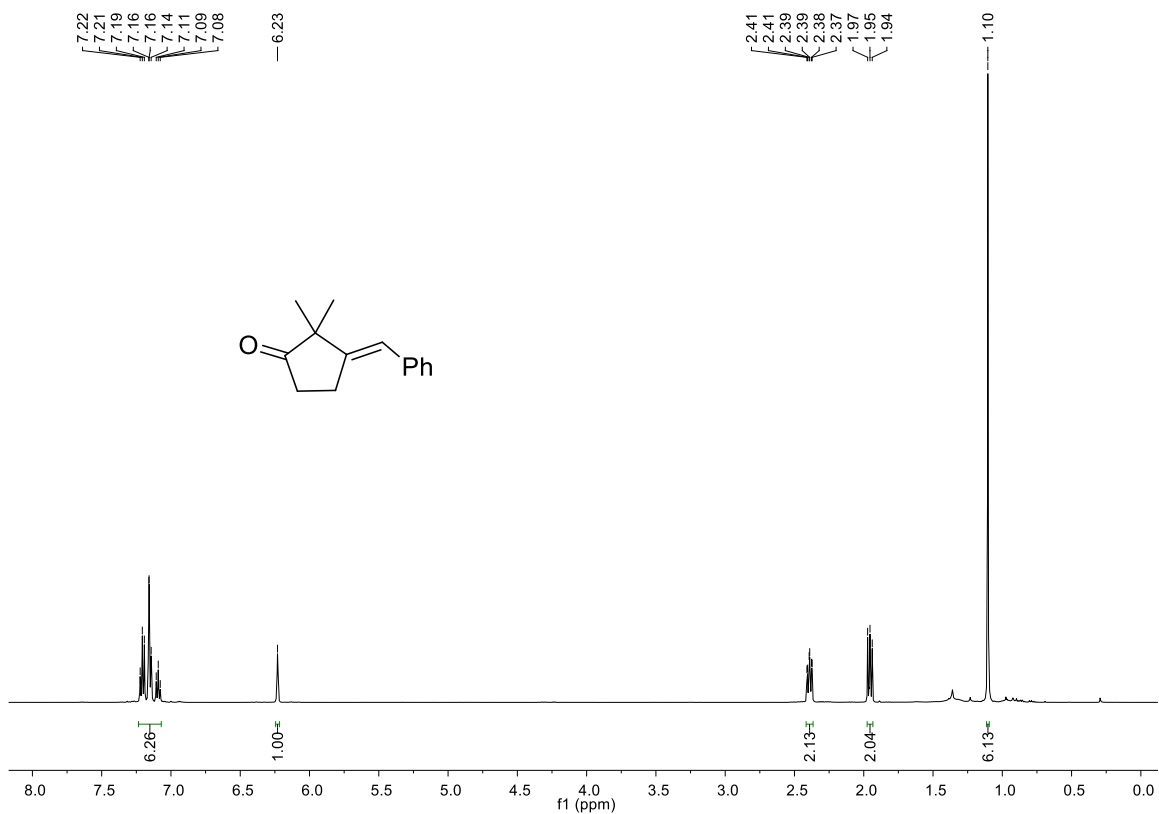
<sup>1</sup>H NMR of Compound 4.20

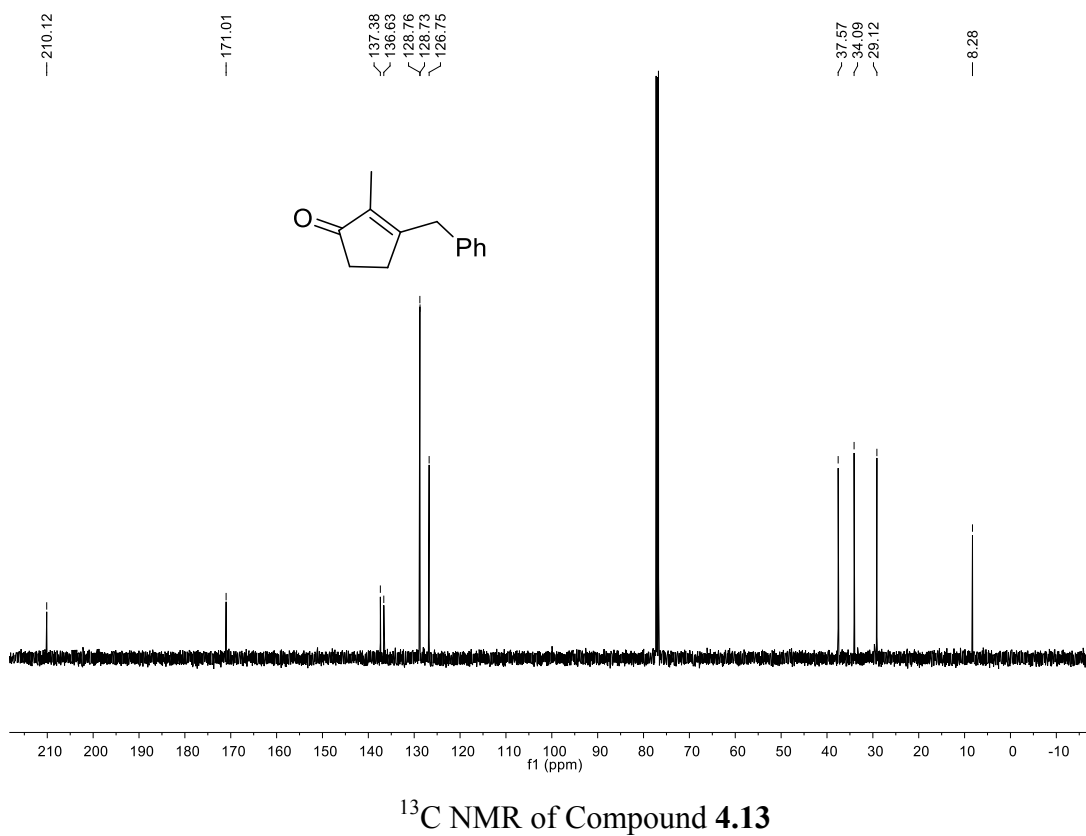
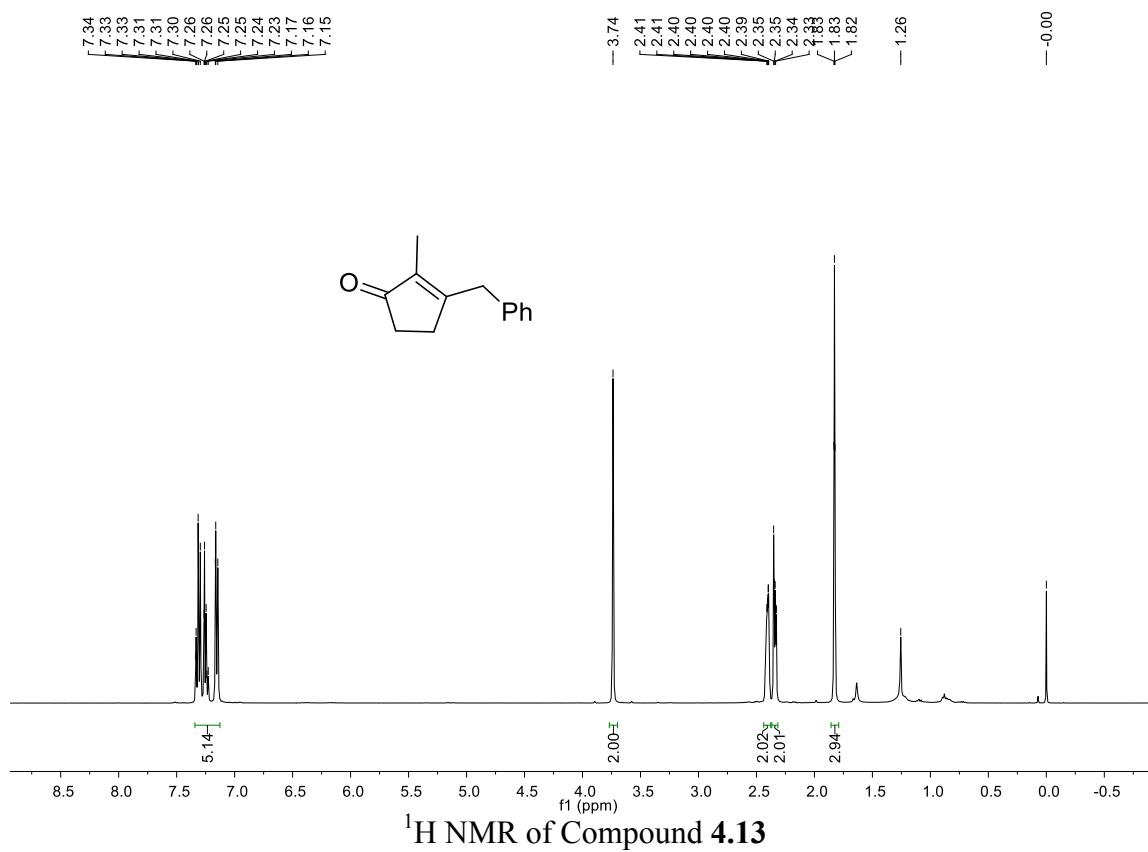


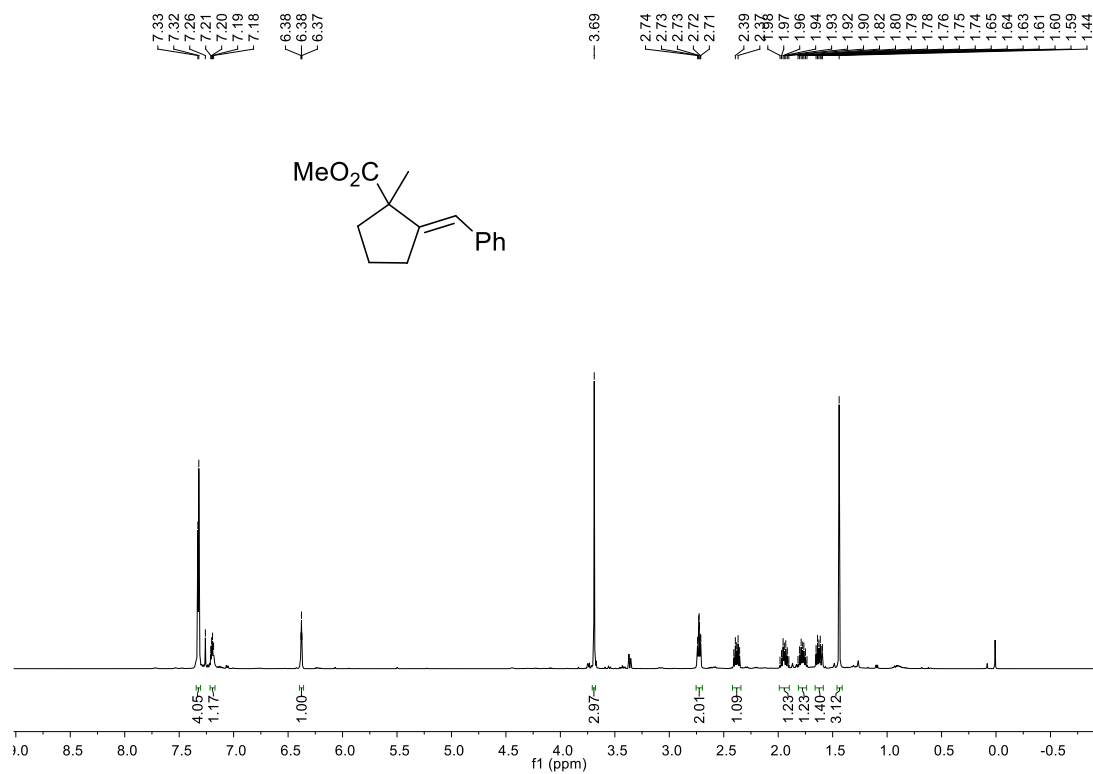
<sup>13</sup>C NMR of Compound 4.20



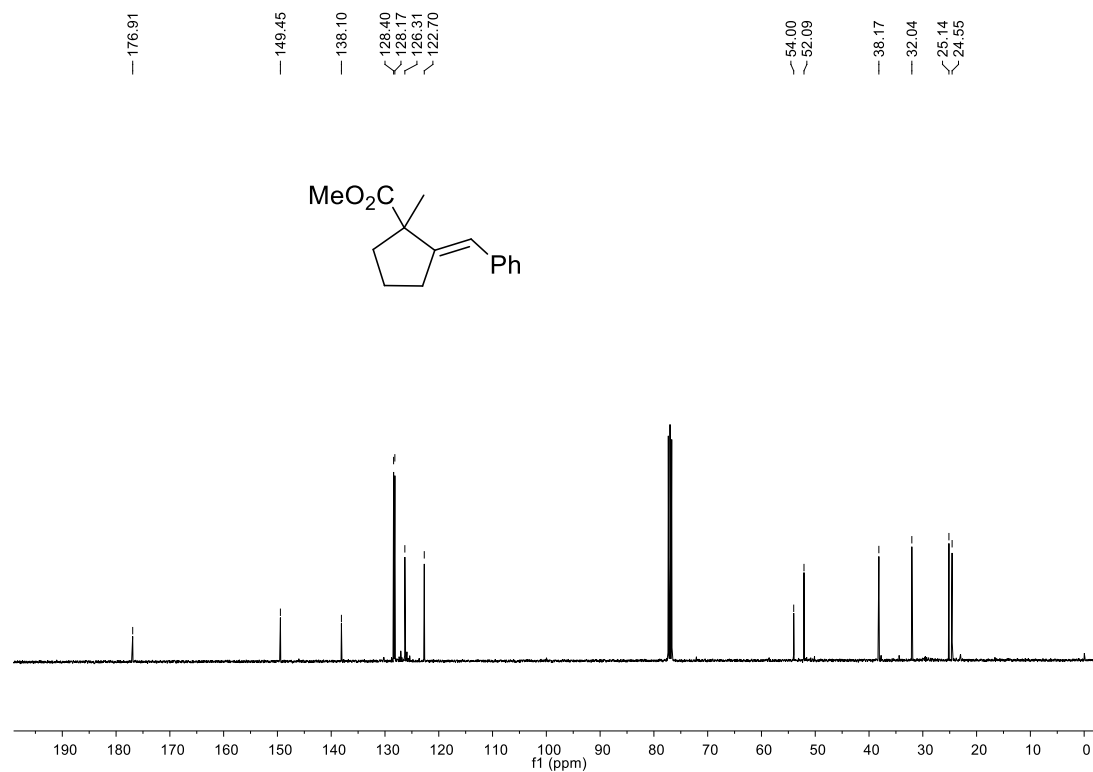




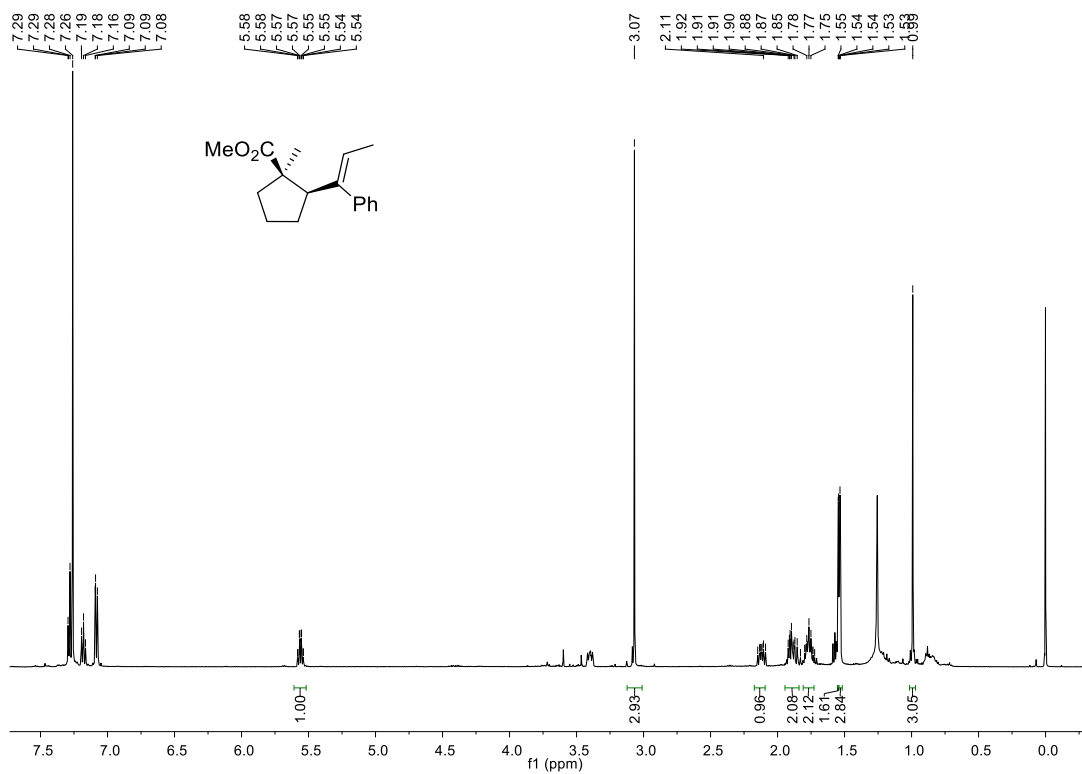




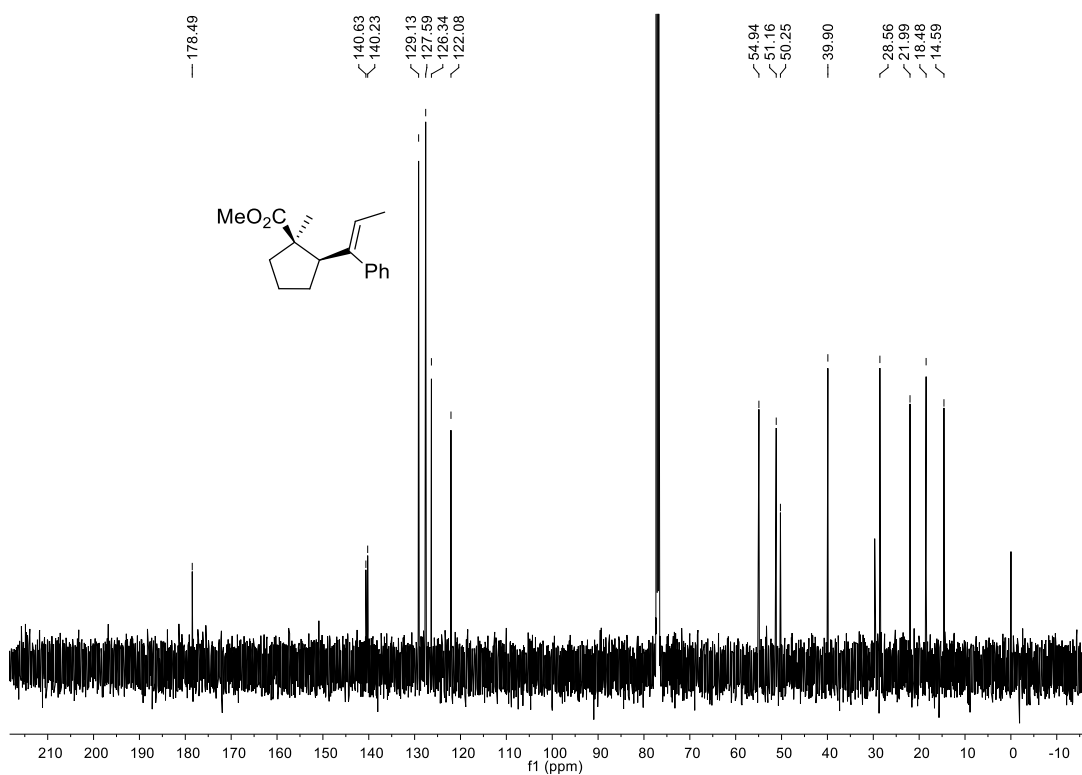
<sup>1</sup>H NMR of Compound 4.7



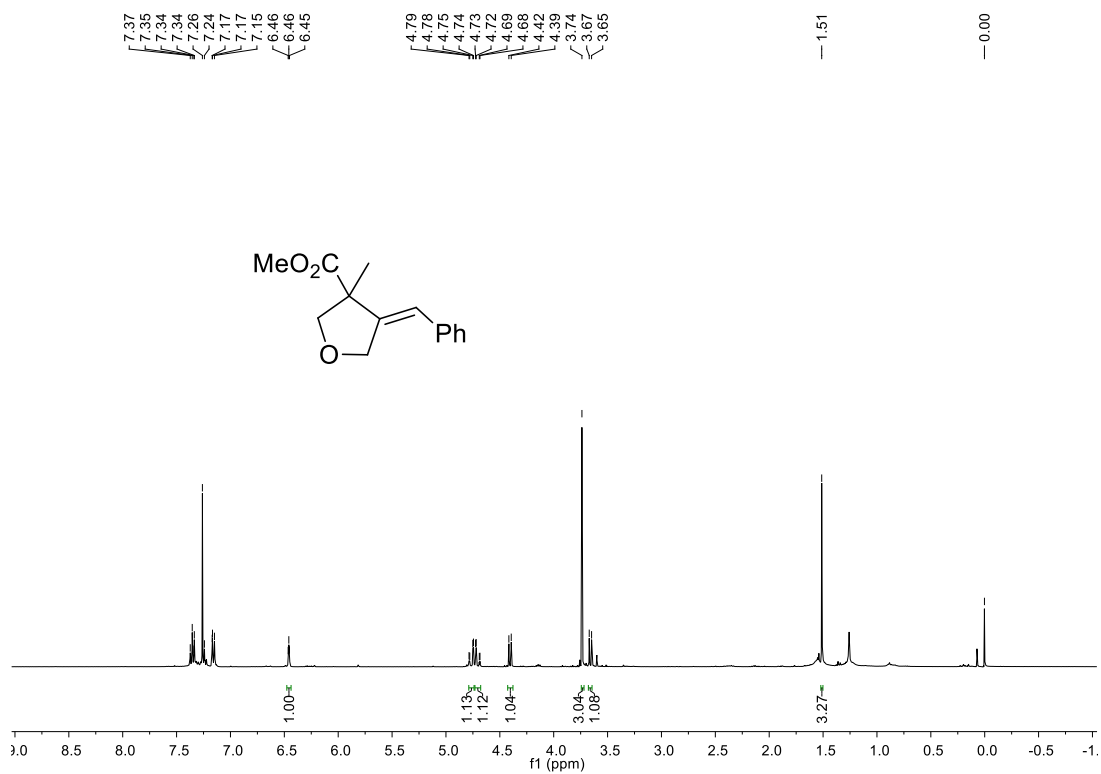
<sup>13</sup>C NMR of Compound 4.7



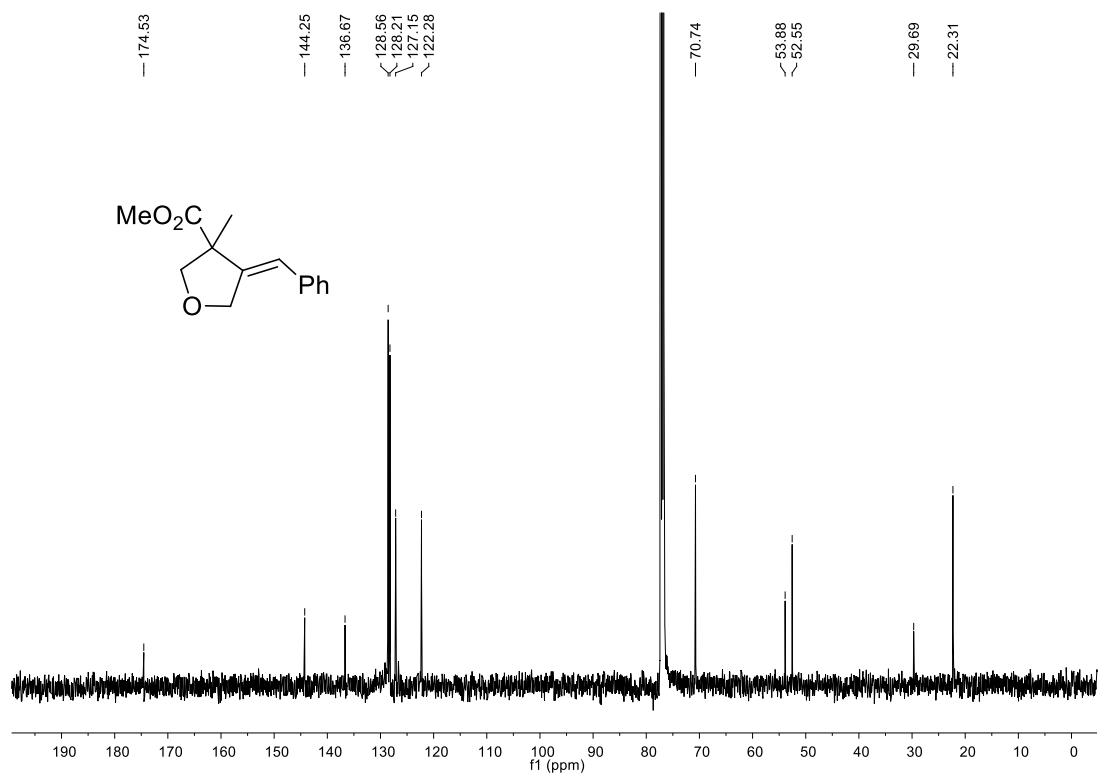
**<sup>1</sup>H NMR of Compound 4.15**



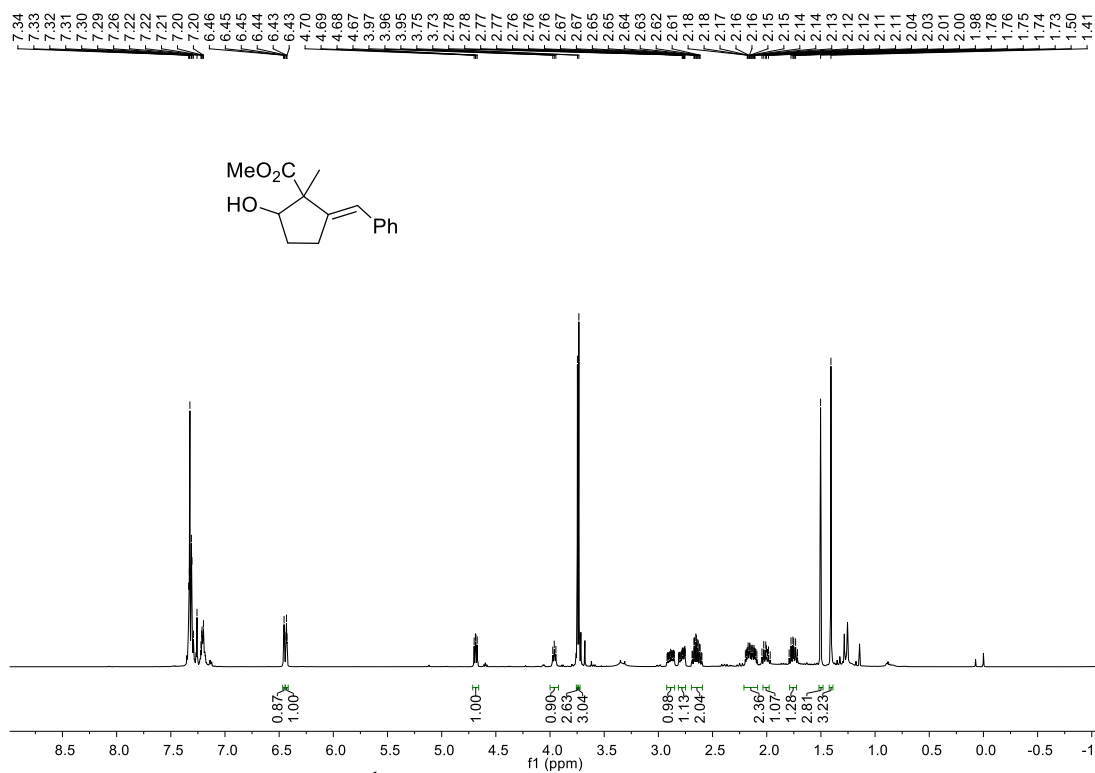
**<sup>13</sup>C NMR of Compound 4.15**



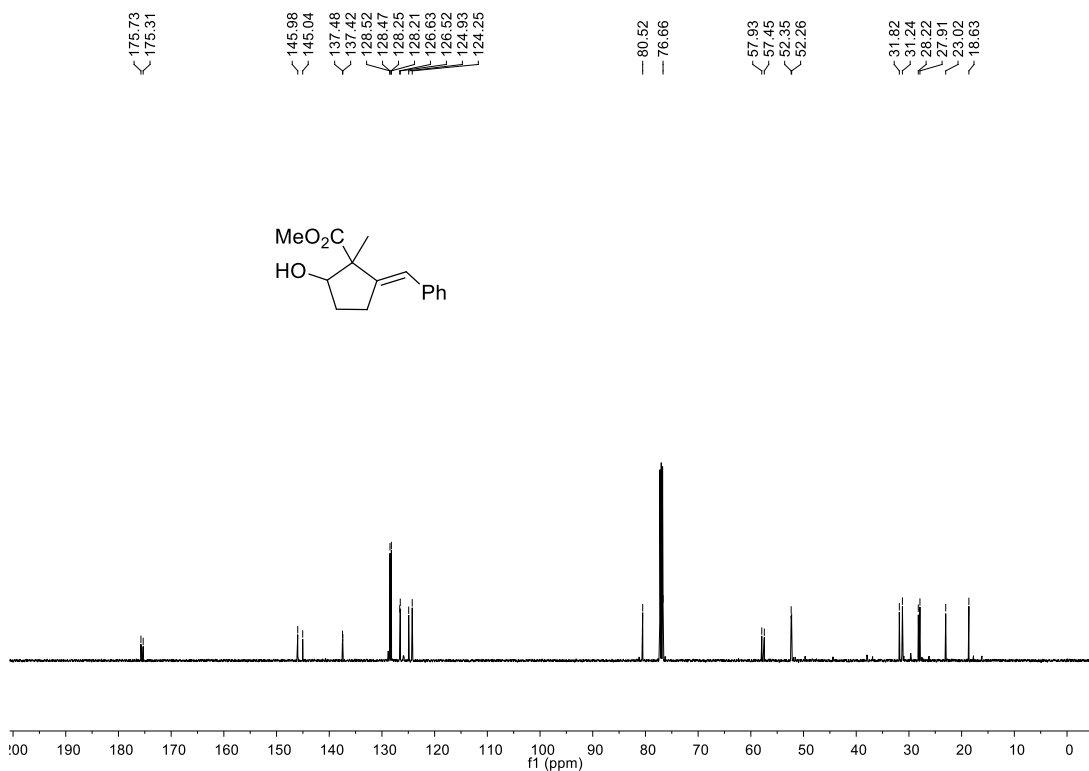
<sup>1</sup>H NMR of Compound 4.17



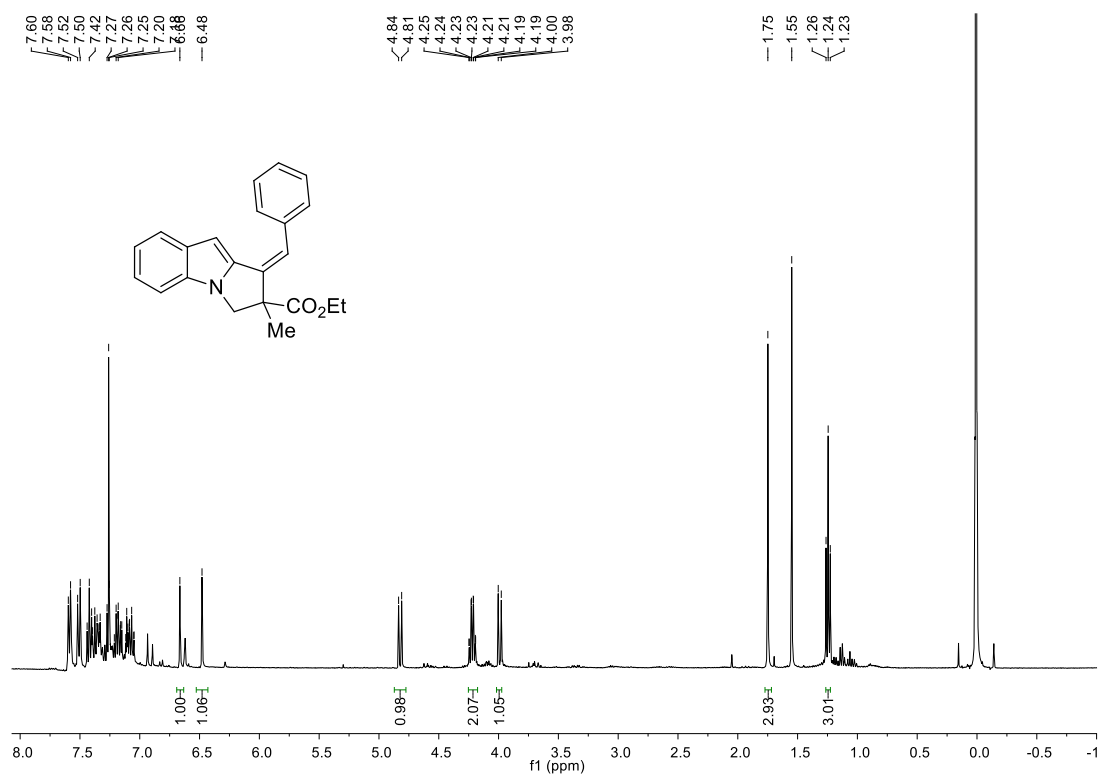
<sup>13</sup>C NMR of Compound 4.17



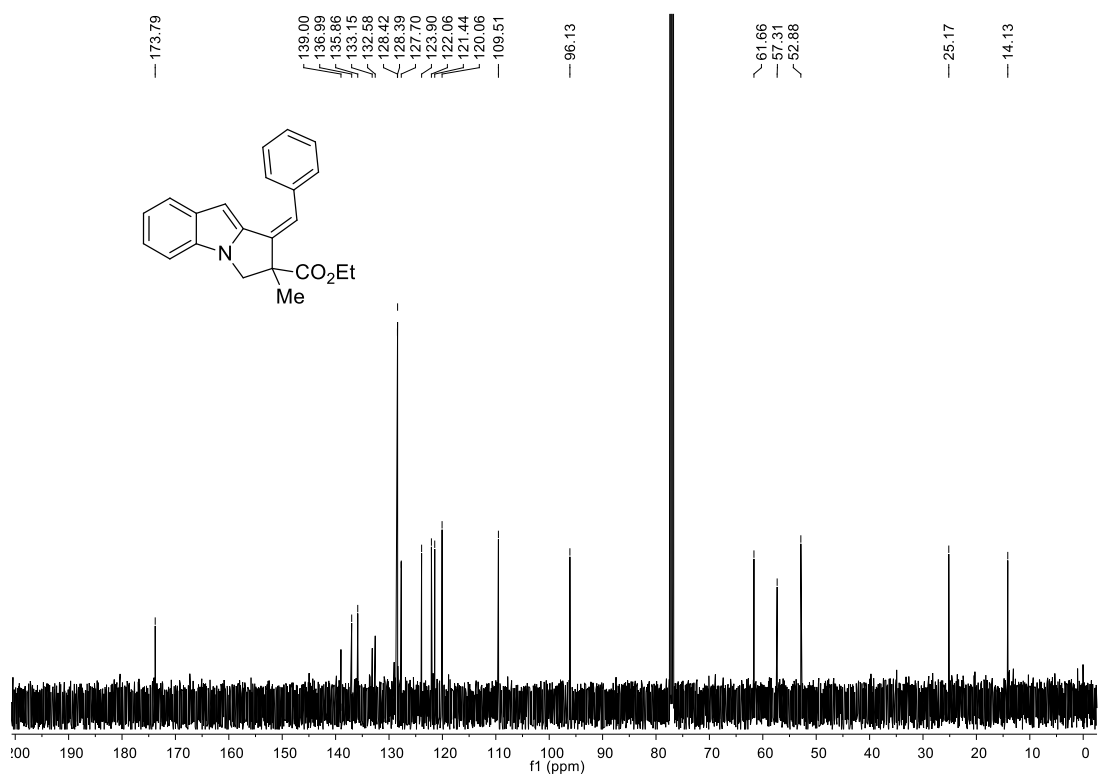
<sup>1</sup>H NMR of Compound 4.19



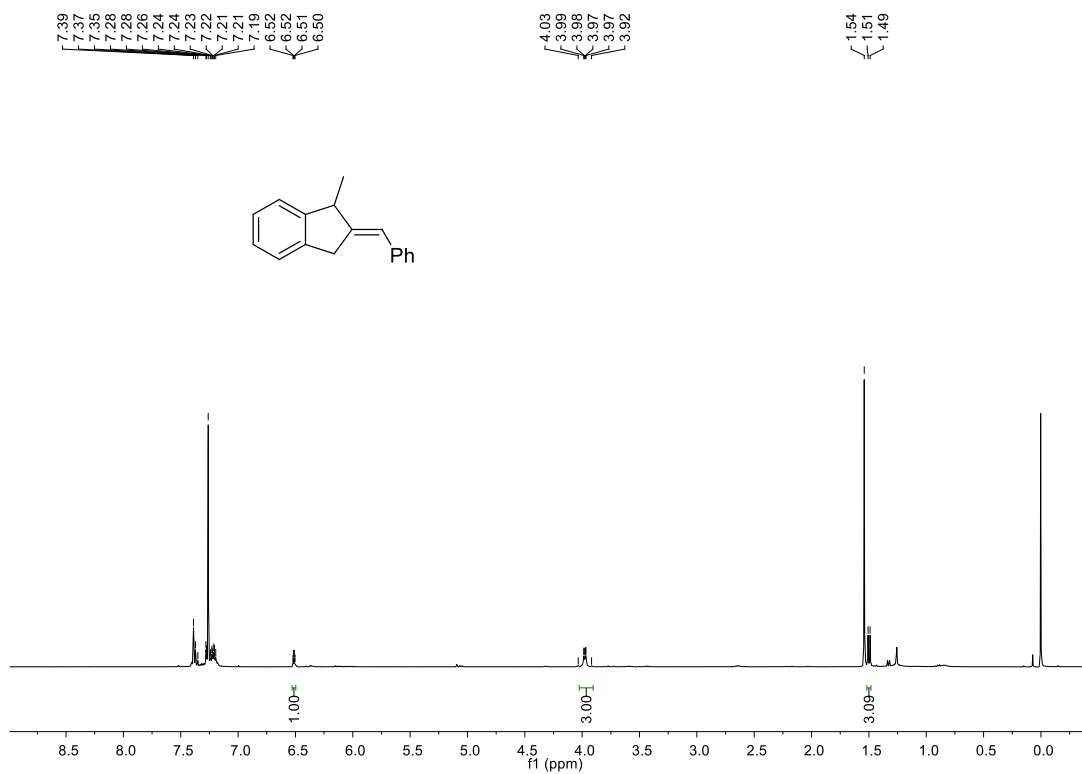
<sup>13</sup>C NMR of Compound 4.19



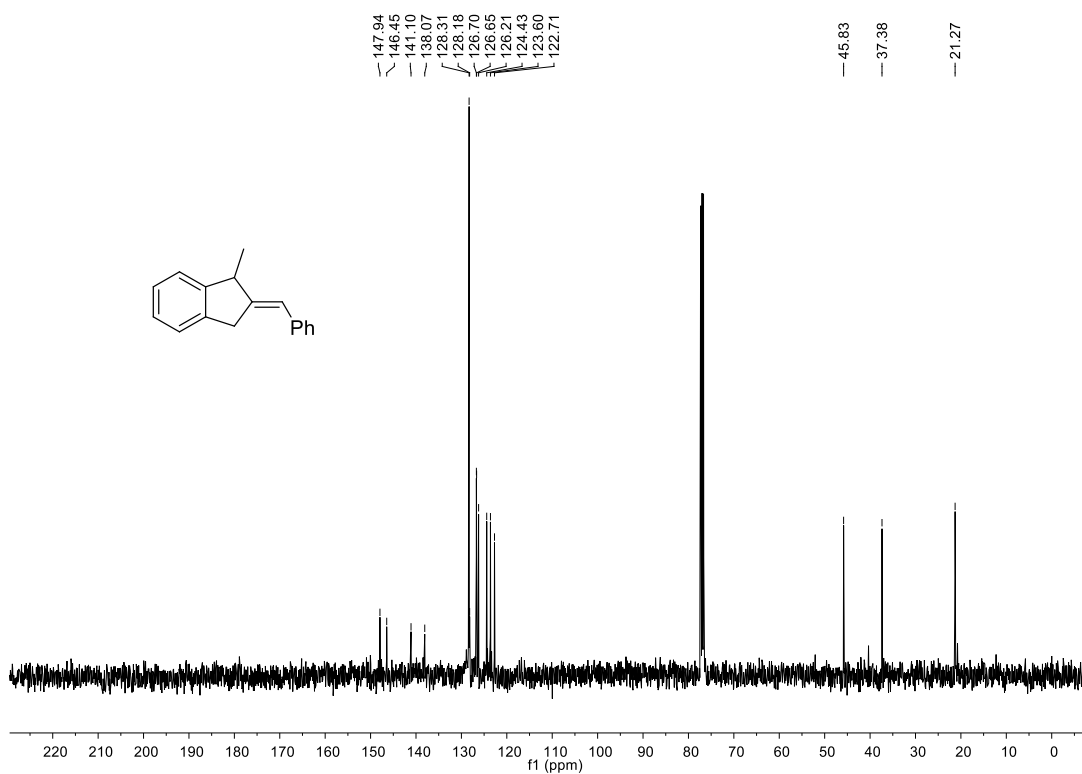
**<sup>1</sup>H NMR of Compound 4.21**



**<sup>13</sup>C NMR of Compound 4.21**



<sup>1</sup>H NMR of Compound 4.23



<sup>13</sup>C NMR of Compound 4.23